AN ABSTRACT OF THE THESIS OF

Sogol Sadat Haddadi for the degree of Master of Science in Civil Engineering presented on June 7, 2017.

Title: Moving Towards Sustainability and Increasing User Safety by Improving Performance of RAP Mixtures and Developing a Network-Level Decision-Making Tool for Pavement Maintenance.

Abstract approved:

_____

Erdem Coleri

Due to a general reduction in pavement program funding levels over the past decade, the current budget is not sufficient to maintain roadways at a high level of service with acceptable roughness levels. Rough roadways with poor ride quality increase drivers' vehicle operating costs (fuel consumption, vehicle maintenance, and tire-wear) and affect road-users' safety. Therefore, current pavement program budget should be more efficiently allocated to road maintenance and rehabilitation. In addition, incorporating high reclaimed asphalt pavement (RAP) into pavement resurfacings reduces the pavement life cycle costs, preserves raw materials, benefits the environment, and provides more money for pavement maintenance programs.

The goal of this study is to develop a network-level decision-making tool to select the most efficient pavement maintenance and rehabilitation strategies to minimize agency and user costs and maximize their benefits. This study also evaluates the effects of different trigger roughness levels, at which the maintenance should be applied, and different treatment methods (1. considering one value for trigger roughness value for all the sections regardless of the traffic levels, and 2. considering different trigger roughness values for sections based on their traffic levels) on user benefits and agency costs. Moreover, to increase RAP content in asphalt mixtures and preserve the long-term durability of the finished asphalt concrete containing RAP, methods of increasing

RAP content (1. Using a softer binder and 2. using high binder content) in asphalt mixtures are investigated.

Results show that available budget level controls the optimal trigger roughness values. Using a lower value for trigger roughness requires a higher budget level and increases user benefits. In addition, this study found that considering one value for trigger roughness for all the sections regardless of their traffic levels is more optimal than considering different values for trigger roughness based on the traffic levels. This study also shows that by using softer binders and higher binder contents, it is possible to increase RAP content in asphalt mixtures without sacrificing performance. In this study, possible combinations of RAP contents, binder contents, and binder grades to achieve acceptable cracking and rutting performance for asphalt mixtures are also suggested.

©Copyright by Sogol Sadat Haddadi
June 7, 2017
All Rights Reserved

Moving Towards Sustainability and Increasing User Safety by Improving Performance of RAP Mixtures and Developing a Network-Level Decision-Making Tool for Pavement Maintenance

by
Sogol Sadat Haddadi

A THESIS

submitted to

Oregon State University

in partial fulfillment of
the requirements for the
degree of

Master of Science

Presented June 7, 2017
Commencement June 2017

Master of Science thesis of Sogol Sadat Haddadi presented on June 7, 2017

APPROVED:

Major Professor, representing Civil Engineering

Head of the School of Civil and Construction Engineering

Dean of the Graduate School

I understand that my thesis will become part of the permanent collection of Oregon State University libraries. My signature below authorizes the release of my thesis to any reader upon request.

Sogol Sadat Haddadi, Author

ACKNOWLEDGEMENTS

I would like to thank my advisor, Professor Erdem Coleri, for his support and expert advice throughout my graduate studies. Being a member of his research team and working under his supervision taught me valuable lessons.

I would also like to express my gratitude to Coleri Research Group for their wonderful collaboration, as well as James Batti for all his help in the laboratory. Shashwath Sreedhar, Blaine Wruck, Yuqi Zhang, Tim Flowerday, Nicholas Kolstad, John Paul Morton, Andrew Johnson, Natasha Anisimova, Matthew Haynes, Jawad Qassem, and Sunny Lewis contributed in different parts of this project. Without their passionate participations, this research project could not have been successfully conducted.

I would like to express my acknowledgment to the Oregon Department of Transportation (ODOT) and the Pacific Northwest Transportation Consortium (PacTrans) for funding this research. Also, a special thank you to the members of the ODOT Project Technical Advisory Committee for their advice and assistance, to Terri Zahler from McCall Oil for providing asphalt binders, and to Mike Miller from Oldcastle Materials for providing aggregates and RAP materials used in this study.

Finally, I am also indebted to my mother, Zahra, my older sister, Nazgol, and my life teammate, Faraz, for their unfailing support and motivation during the hardest times. This accomplishment would not have been possible without them.

CONTRIBUTION OF AUTHORS

Shashwath Sreedhar assisted with testing the samples and writing the literature review for the first manuscript. Shashwath also mixed and compacted all the samples prepared in the laboratory. He had a huge role in making the first research successful. Tim Flowerday, Nicholas Kolstad, John, Paul Morton, Andrew Johnson, Natasha Anisimova, Matthew Haynes, Jawad Qassem, and Sunny Lewis were responsible for sieving, batching, and measuring the theoretical maximum specific gravity of samples. Blaine Wruck conducted all the analysis presented in section 3.5 and developed the GIS map. Blaine also helped write the introduction for the first manuscript and the literature review for the second manuscript.

TABLE OF CONTENTS

Page

1. CHAPTER 1 – INTRODUCTION 1

2. CHAPTER 2 - BINDER-GRADE BUMPING AND HIGH BINDER CONTENT TO IMPROVE PERFORMANCE OF RAP MIXTURES 4

2.1 INTRODUCTION 5

2.1.1 Major research products developed in this study 7

2.1.2 Key objectives of this study 7

2.1.3 Organization of the report 8

2.2 LITERATURE REVIEW 9

2.2.1 Strategies to increase RAP/RAS content 9

2.2.2 Mix design procedure 22

2.2.3 Field performance of RAP-RAS mixtures 23

2.2.4 Economic and environmental benefits of using RAP/RAS mixtures 25

2.2.5 Summary 29

2.3 EXPERIMENTAL DESIGN, MATERIALS, AND SAMPLE PREPARATION 32

2.3.1 Experimental plan 32

2.3.2 Materials 33

2.3.3 Sample preparation 36

2.4 TEST METHODS 40

2.4.1 Semi-circular bend (SCB) test 40

2.4.2 Dynamic modulus test 47

2.4.3 Flow number test 48

2.5 RESULTS AND DISCUSSION 52

2.5.1 Semi-circular bend test 52

2.5.2 Flow number test 56

2.5.3 Dynamic modulus test 59

TABLE OF CONTENT (Continued)

Page

2.5.4 Summary of test results....75
2.5.5 Regression modeling and Monte Carlo simulations to determine asphalt mixtures with high rutting and cracking performance....84
2.6 SUMMARY AND CONCLUSIONS....96
2.7 FUTURE STUDY....98
2.8 ACKNOWLEDGMENTS....99
2.9 REFERENCES....100
3. CHAPTER 3 - A NETWORK-LEVEL DECISION-MAKING TOOL FOR PAVEMENT MAINTENANCE AND USER SAFETY....106
3.1 INTRODUCTION....107
3.1.1 Key objectives of this study....108
3.1.2 Organization of the report....108
3.2 LITERATURE REVIEW....110
3.2.1 Pavement roughness....110
3.2.2 Effects of roughness on vehicle operating costs....111
3.2.3 Effect of roughness on user safety....117
3.2.4 Pavement life cycle assessment....119
3.2.5 Decision-making tools....125
3.3 RESEARCH METHODOLOGY....132
3.3.1 Analysis of framework – code development....132
3.3.2 Steps followed for model development....135
3.3.3 Methodology of finding the trigger IRI by considering user safety, user cost benefits, and agency costs....147
3.4 RESULTS AND DISCUSSION....149
3.4.1 One value for trigger IRI....149
3.4.2 Different trigger IRI values based on traffic levels....150
3.4.3 Optimal trigger IRI according to the available budget....151
3.5 INTEGRATION OF THE DEVELOPED DECISION-MAKING TOOL WITH GEOGRAPHIC INFORMATION SYSTEMS (GIS)....155

TABLE OF CONTENT (Continued)

Page

3.6 SUMMARY AND CONCLUSIONS 163
3.7 FUTURE STUDY 164
3.8 SUGGESTED IMPLEMENTATION STRATEGY 165
3.9 ACKNOWLEDGMENTS 166
3.10 REFERENCES 167

4. CHAPTER 4 – CONCLUSION 171

5. BIBLIOGRAPHY 173

APPENDICES 183

LIST OF FIGURES

Figure Page

Figure 2.1. Map of U.S. states with increased RAP use since 2007 (Copeland 2011).10

Figure 2.2. Map of U.S. states using RAP contents of 25% or greater in various HMA layers (Copeland 2011) 10

Figure 2.3. Wheel-tracking test results: (a) District 1 (b) District 5 (Aurangzeb et al. 2012) 12

Figure 2.4. Plot of beam fatigue test results for RAP experimental sections (West et al. 2009) 14

Figure 2.5. Mix design process involving RAP (Newcomb et al. 2007) 22

Figure 2.6. RAP aggregate gradations 35

Figure 2.7. Viscosity-temperature line for binder grade of PG 58-34 36

Figure 2.8. Target, extracted RAP, and stockpiled aggregate gradations.....37

Figure 2.9. Cutting and notching procedure for SCB sample preparation.....41

Figure 2.10. SCB loading set up and test.....42

Figure 2.11. Load versus displacement (P-u) curve (AASHTO TP 105-13).....43

Figure 2.12. Illustration of load-displacement curve and slope at inflection point (m) (Ozer et al. 2016) 46

Figure 2.13. Illustration of load-displacement curve of ductile and brittle mixtures ...47

Figure 2.14. Relationship between permanent strain and load cycles in FN test (Biligiri et al. 2007) 49

Figure 2.15. Flexibility index for mixtures with different RAP contents (30% and 40%), binder grades (PG 58-34, PG 64-22, and PG 76-22), and binder contents (6%, 6.4%, and 6.8%).....53

Figure 2.16. Fracture energy for mixtures with different RAP contents (30% and 40%), binder grades (PG 58-34, PG 64-22, and PG 76-22), and binder contents (6%, 6.4%, and 6.8%).....54

LIST OF FIGURES (Continued)

Figure Page

Figure 2.17. Secant stiffness for mixtures with different RAP contents (30% and 40%), binder grades (PG 58-34, PG 64-22, and PG 76-22), and binder contents (6%, 6.4%, and 6.8%) 55

Figure 2.18. Fracture toughness for mixtures with different RAP contents (30% and 40%), binder grades (PG 58-34, PG 64-22, and PG 76-22), and binder contents (6%, 6.4%, and 6.8%) 56

Figure 2.19. Flow number of the mixtures with different RAP contents (30% and 40%), binder grade of PG 58-34, and different binder contents (6%, 6.4%, and 6.8%) .57

Figure 2.20. Flow number of the mixtures with different RAP contents (30% and 40%), binder grade of PG 64-22, and different binder contents (6%, 6.4%, and 6.8%) .58

Figure 2.21. Flow number of the mixtures with different RAP contents (30% and 40%), binder grade of PG 76-22, and different binder contents (6%, 6.4%, and 6.8%) .58

Figure 2.22. Average flow number of the mixtures for all the combinations of RAP contents, binder contents, and binder grades 59

Figure 2.23. Master curves of dynamic modulus for the mixtures with different RAP contents (30% and 40%), binder grade of PG 58-34, and different binder contents (6%, 6.4%, and 6.8%) 60

Figure 2.24. Master curves of dynamic modulus for the mixtures with different RAP contents (30% and 40%), binder grade of PG 64-22, and different binder contents (6%, 6.4%, and 6.8%) 61

Figure 2.25. Master curves of dynamic modulus for the mixtures with different RAP contents (30% and 40%), binder grade of PG 76-22, and different binder contents (6%, 6.4%, and 6.8%) 61

Figure 2.26. Master curves of dynamic modulus for the mixtures with different RAP contents (30% and 40%), different binder grades (PG 58-34, PG 64-22, and PG 76-22), and 6% binder content 62

Figure 2.27. Master curves of dynamic modulus for the mixtures with different RAP contents (30% and 40%), different binder grades (PG 58-34, PG 64-22, and PG 76-22), and 6.4% binder content 63

LIST OF FIGURES (Continued)

Figure Page

Figure 2.28. Master curves of dynamic modulus for the mixtures with different RAP contents (30% and 40%), different binder grades (PG 58-34, PG 64-22, and PG 76-22), and 6.8% binder content 63

Figure 2.29. Dynamic modulus of the mixtures at 4 ºC and 0.1 Hz and all the combinations of RAP contents, binder contents, and binder grades.....65

Figure 2.30. Dynamic modulus of the mixtures at 4 ºC and 10 Hz and all the combinations of RAP contents, binder contents, and binder grades.....66

Figure 2.31. Dynamic modulus of the mixtures at 20 ºC and 0.1 Hz and all the combinations of RAP contents, binder contents, and binder grades.....67

Figure 2.32. Dynamic modulus of the mixtures at 20 ºC and 10 Hz and all the combinations of RAP contents, binder contents, and binder grades.....68

Figure 2.33. Dynamic modulus of the mixtures at 40 ºC and 0.1 Hz and all the combinations of RAP contents, binder contents, and binder grades.....69

Figure 2.34. Dynamic modulus of the mixtures at 40 ºC and 10 Hz and all the combinations of RAP contents, binder contents, and binder grades.....70

Figure 2.35. Master curves of phase angles for the mixtures with different RAP contents (30% and 40%), binder grade of PG 58-34, and different binder contents (6%, 6.4%, and 6.8%).....71

Figure 2.36. Master curves of phase angles for the mixtures with different RAP contents (30% and 40%), binder grade of PG 64-22, and different binder contents (6%, 6.4%, and 6.8%).....72

Figure 2.37. Master curves of phase angles for the mixtures with different RAP contents (30% and 40%), binder grade of PG 76-22, and different binder contents (6%, 6.4%, and 6.8%).....73

Figure 2.38. Master curves of phase angles for the mixtures with different RAP contents (30% and 40%), different binder grades of (PG 58-34, PG 64-22, and PG 76-22), and 6% binder content 74

Figure 2.39. Master curves of phase angles for the mixtures with different RAP contents (30% and 40%), different binder grades of (PG 58-34, PG 64-22, and PG 76-22), and 6.4% binder content 74

LIST OF FIGURES (Continued)

Figure Page

Figure 2.40. Master curves of phase angles for the mixtures with different RAP contents (30% and 40%), different binder grades of (PG 58-34, PG 64-22, and PG 76-22), and 6.8% binder content 75

Figure 2.41. Flexibility index and flow number (numbers on each bar) of the mixtures with different RAP contents (30% and 40%), binder grades (PG 58-34, PG 64-22, and PG 76-22), and binder contents (6.0%, 6.4%, and 6.8%) 76

Figure 2.42. Dynamic modulus of mixtures at 40 ºC and 10 Hz versus flow number for all the combinations of RAP content, binder content, and binder grades.....77

Figure 2.43. Dynamic modulus of mixtures at 40 ºC and 10 Hz versus flexibility index for all the combinations of RAP content, binder content, and binder grades 78

Figure 2.44. Dynamic modulus of mixtures at 40 ºC and 0.1 Hz versus flow number for all the combinations of RAP content, binder content, and binder grades.....78

Figure 2.45. Dynamic modulus of mixtures at 40 ºC and 0.1 Hz versus flexibility index for all the combinations of RAP content, binder content, and binder grades 79

Figure 2.46. Dynamic modulus of mixtures at 20 ºC and 10 Hz versus flow number for all the combinations of RAP content, binder content, and binder grades.....80

Figure 2.47. Dynamic modulus of mixtures at 20 ºC and 10 Hz versus flexibility index for all the combinations of RAP content, binder content, and binder grades 80

Figure 2.48. Dynamic modulus of mixtures at 20 ºC and 0.1 Hz versus flow number for all the combinations of RAP content, binder content, and binder grades.....81

Figure 2.49. Dynamic modulus of mixtures at 20 ºC and 0.1 Hz versus flexibility index for all the combinations of RAP content, binder content, and binder grades 81

Figure 2.50. Dynamic modulus of mixtures at 4 ºC and 10 Hz versus flow number for all the combinations of RAP content, binder content, and binder grades.....82

Figure 2.51. Dynamic modulus of mixtures at 4 ºC and 10 Hz versus flexibility index for all the combinations of RAP content, binder content, and binder grades 82

Figure 2.52. Dynamic modulus of mixtures at 4 ºC and 0.1 Hz versus flow number for all the combinations of RAP content, binder content, and binder grades.....83

LIST OF FIGURES (Continued)

Figure Page

Figure 2.53. Dynamic modulus of mixtures at 4 ºC and 0.1 Hz versus flexibility index for all the combinations of RAP content, binder content, and binder grades 83

Figure 2.54. Correlation between FI and FN 84

Figure 2.55. ln(FI) for each combination of RAP content, binder content, and binder grade.....87

Figure 2.56. Residual plots for the regression model correlating ln(FI) with RAP content, binder content, and binder grade 88

Figure 2.57. ln(FN) for each combination of RAP content, binder content, and binder grade.....90

Figure 2.58. Residual plots for the regression model correlating ln(FN) with RAP content, binder content, and binder grade 91

Figure 2.59. Predicted FI and FN for different RAP contents, binder contents, and binder grades 93

Figure 3.1. PSR rating (Pavement Interactive 2017) 110

Figure 3.2. IRI roughness scale (Pavement Interactive 2017) 111

Figure 3.3. Effect of pavement condition on truck health (Mitchell 2000) 113

Figure 3.4. Relation between road accident rate and road roughness (Tighe et al. 2000) 118

Figure 3.5. Phases and components of the pavement life-cycle (Santero et al. 2011)120

Figure 3.6. System enters the steady state at the time of the first resurfacing(Li and Madanat, 2002) 126

Figure 3.7. Effect of budget on trigger roughness values (Sathaye and Madanat 2011) 128

Figure 3.8. Effect of budget on network-level optimal costs (Sathaye and Madanat 2011) 129

LIST OF FIGURES (Continued)

Figure Page

Figure 3.9. Optimal preservation strategies for three overlay systems without considering the traffic growth (Zhang et al. 2010) 131

Figure 3.10. Flowchart of procedure to develop the decision-making tool (MATLAB code).....134

Figure 3.11. Example of AADTT versus year for a section in Washington where chip seal is the last treatment (WA-C350-DGAC-CS).....137

Figure 3.12. Annually collected IRI of the last treatment versus year of the last treatment for all the sections in Oregon 138

Figure 3.13. Example of performance equation of IRI versus year for a section in Washington where chip seal is the last treatment (WA-C350-DGAC-CS).....139

Figure 3.14. Example of the approach for obtaining the frequency of resurfacing and treating for the CA-0504-DGAC section 141

Figure 3.15. Average price per unit tonne of DGAC versus quantity per project 143

Figure 3.16. Illustration of user benefits for a section in Washington where chip seal is the last treatment (WA-C350-DGAC-CS).....145

Figure 3.17. Illustration of efficient frontier curve for 7 sections of this study.....146

Figure 3.18. Optimal trigger IRI for different traffic levels (Madanat 2014).....148

Figure 3.19. Efficient frontier curve for different values of trigger IRI regardless of traffic levels 150

Figure 3.20. Efficient frontier curve for different values of trigger IRI by considering traffic levels 151

Figure 3.21. Illustration of finding optimal IRI for different budget levels 152

Figure 3.22. Illustration of optimal IRI for different budget levels and efficient frontier curve for different values of trigger IRI by considering traffic levels.....153

Figure 3.23. Optimal trigger IRI versus agency costs (budget).....154

Figure 3.24. Map of Oregon highway network with LTPP sections shown.....157

LIST OF FIGURES (Continued)

Figure Page

Figure 3.25. Close-up view of Oregon LTPP section with clipped line data 158

Figure 3.26. Efficient Frontier Curve for Oregon at an IRI value of 170 inches/mile159

Figure 3.27. Efficient Frontier Curve for Idaho at an IRI value of 170 inches/mile ..160

Figure 3.28. Flowchart for GIS Methodology 161

LIST OF TABLES

Table Page

Table 2.1. Mixture properties....19

Table 2.2. Experimental plan....33

Table 2.3. RAP aggregate gradations....34

Table 2.4. Target, extracted RAP, and stockpiled aggregate gradations....37

Table 2.5. Minimum average FN requirement for different traffic levels (AASHTO TP 79-13)....50

Table 2.6. Independent and dependent variables used for regression models....85

Table 2.7. ANOVA table for the regression model correlating FI test results with RAP content, binder grade, and binder content....86

Table 2.8. ANOVA table for the regression model correlating FN test results with RAP content, binder grade, and binder content....86

Table 2.9. Independent variables and their ranges for FI and FN predictions....92

Table 2.10. Suggested strategies - Mixtures with FN greater than 740 and FI greater than 10....94

Table 1.1. Baseline costs (cents per mile) (Barnes and Langworthy 2004)....114

Table 1.2. Costs with city driving conditions (cents per mile) (Barnes and Langworthy 2004)....115

Table 1.3. Costs for poor pavement quality (cents per mile) (Barnes and Langworthy 2004)....115

Table 3.4. Increase in user costs for passenger cars and pickup trucks due to pavement roughness (Islam and Buttlar 2012)....116

Table 3.5. User benefits, available budget, and B/C ratios of 7 sections....146

Table 3.6. Suggested optimal trigger IRI for different budget levels....154

Table 3.7. Attribute table for Oregon LTPP sections with MATLAB outputs, benefit-to-cost ratios and ranking....157

LIST OF APPENDICES

Appendix Page

APPENDIX A: GRADATION AND BINDER CONTENT OF RAP.....184

APPENDIX B: TEMPERATURE CURVES FOR VIRGIN BINDERS.....186

APPENDIX C: THEORETICAL MAXIMUM SPECIFIC GRAVITIES 192

APPENDIX D: ONE EXAMPLE OF BATCHING.....194

APPENDIX E: SEMI-CIRCULAR BEND TEST RESULTS.....196

APPENDIX F: EXAMPLE OF DATA GENERATED BY UTM DEVICE FOR DYNAMIC MODULUS TEST AND DEVELOPING THE MASTER CURVES ...200

APPENDIX G: FLOW NUMBER TEST RESULTS 206

APPENDIX H: PAVEMENT HISTORY AND STRUCTURES FOR EACH SECTION 207

LIST OF APPENDIX FIGURES

Figure Page

Figure A 1. RAP aggregate gradation....184

Figure A 2. Binder content and theoretical maximum specific gravity (Gmm) of RAP 185

Figure B 1. Temperature curve of PG 58-34 binder....187

Figure B 2. Temperature curve of PG 64-22 binder....187

Figure B 3. Temperature curve of PG 76-22 binder....188

Figure B 4. PG 58-34 binder properties....189

Figure B 5. PG 64-22 binder properties....190

Figure B 6. PG 76-22 binder properties....191

Figure E 1. An example of output SCB test of the sample with 30% RAP content, 6% binder content, and PG 58-34 binder grade....196

Figure F 1. An example of output dynamic modulus test of mixture with 30% RAP content, 6% binder content, and PG 58-34 binder grade....200

Figure F 2. Dynamic modulus of the mixture with 30% RAP content, 6% binder content, and PG 58-34 binder grade at different temperatures and frequencies....202

Figure F 3. An example of procedure of creating master curve 203

Figure F 4. An example of the master curve of dynamic modulus for the mixture with 30% RAP content, 6% binder content, and PG 58-34 binder grade....204

Figure F 5. Shift factor curve of the mixture with 30% RAP content, 6% binder content, and PG 58-34 binder grade....204

Figure F 6. An example of the master curve of phase angle for the mixture with 30% RAP content, 6% binder content, and PG 58-34 binder grade....205

Figure G 1. An example of flow number test output data for the sample with 30% RAP content, 6% binder content, and PG 58-34 binder grade....206

LIST OF APPENDIX TABLES

Table Page

Table B 1. Mixing and compaction temperatures of PG 76-22 binder.....186

Table B 2. Mixing and compaction temperatures of PG 64-22 binder.....186

Table B 3. Mixing and compaction temperatures of PG 58-34 binder.....186

Table C 1. Theoretical maximum specific of the mixtures with 30% RAP content, binder contents of 6%, 6.4%, and 6.8%, and binder grades of PG 58-34, PG 64-22, and PG 76-22 192

Table C 2. Theoretical maximum specific of the mixtures with 40% RAP content, binder contents of 6%, 6.4%, and 6.8%, and binder grades of PG 58-34, PG 64-22, and PG 76-22 193

Table D 1. Quantity of coarse, medium, and fine aggregates and RAP materials for the mixture with 30% RAP, 6% binder content, and binder grade of PG 58-34.....194

Table D 2. Quantity of binder, RAP materials, and total aggregates for the the mixture with 30% RAP, 6% binder content, and binder grade of PG 58-34 195

Table E 1. SCB output parameters of the mixtures with RAP contents of 30% and 40%, binder contents of 6%, 6.4%, and 6.8%, and binder grade of PG 58-34 197

Table E 2. SCB output parameters of the mixtures with RAP contents of 30% and 40%, binder contents of 6%, 6.4%, and 6.8%, and binder grade of PG 64-22 198

Table E 3. SCB output parameters of the mixtures with RAP contents of 30% and 40%, binder contents of 6%, 6.4%, and 6.8%, and binder grade of PG 76-22 199

Table F 1. VMA and VFA of the mixture with 30% RAP content, 6% binder content, and PG 58-34 binder grade 201

Table F 2. Dynamic modulus and phase angles of mixture with 30% RAP content, 6% binder content, and PG 58-34 binder grade at different temperatures and frequencies.... 201

Table H 1. Pavement history for all.....207

1. CHAPTER 1 – INTRODUCTION

2012 Pavement Condition Report released by the Oregon Department of Transportation (2013) reported that pavement program funding levels have decreased around 30% over the past decade. Current pavement funding levels allow for pavement resurfacing and treatment every 30 years or longer. However, pavement resurfacings commonly last between 10 to 20 years (ODOT 2013) depending on the treatment types and thicknesses. Thus, substandard pavement conditions with high roughness levels are expected in the future. According to a report by a National Transportation Research Group (TRIP) (2015), more than 28 percent of U.S. roadways (interstates, freeways, and arterial routes) are in substandard conditions with high roughness levels. Rough roadways provide poor ride quality for drivers and increase vehicle operating costs in terms of vehicle maintenance, fuel consumption, and tire-wear (Chatti and Zabaar 2012; Mitchell 2000; Barnes and Langworthy 2004; Islam and Buttlar 2012).

A general reduction in pavement program funding levels created a need for low cost yet effective alternative ways to rehabilitate, preserve, and maintain roadway network in Oregon. The impacts of road roughness on vehicle operating costs should also be considered in pavement maintenance strategies, along with other important factors such as agency costs. Therefore, a network-level decision-making software should be developed to be able to recommend the most efficient maintenance and rehabilitation strategies by minimizing user and agency costs and maximizing their benefits.

In addition, using recycled highway construction materials in pavement resurfacings and treatments reduces the pavement life cycle costs, conserves natural resources, and protects the environment (Willis 2015; Lee et al. 2011). Andreen et al. (2011) found that a saving of $40.87 per ton was realized by using Recycled Asphalt Pavement (RAP) in Hot Mix Asphalt (HMA), with most of these savings coming from reducing energy consumption at the HMA plant. Reducing asphalt mixture costs by using higher percentages of RAP will allow agencies to maintain and rehabilitate more roadway sections and reduce network-level roughness levels. Consequently,

vehicle operating costs will decrease and road user comforts will increase by treating pavements at higher levels of service.

Although using RAP is beneficial in many aspects, asphalt pavements with high RAP contents are more susceptible to cracking. Aged binder in RAP makes asphalt pavements more brittle and creates long-term durability problems (Bennert et al. 2014). Using softer virgin binder grade (binder-grade bumping) and higher virgin binder content improve cracking performance of pavements with high amounts of RAP (Bennert et al. 2014; Aurangzeb et al. 2012; Li et al. 2008; West et al. 2009). However, careful considerations are required in designing asphalt pavements with high RAP. Softer virgin binder grade and higher binder content make pavements more resistant to cracking, but more susceptible to permanent deformation. Hence, a balance of the combination of RAP content, binder content, and binder grade should be considered in the mix design.

Pavement roughness and rutting (deformation on roadways) directly affect drivers' safety. Roughness levels influence user driving habits, steering control, and vehicle handling characteristics. Consequently, pavement roughness affects single-vehicles and multiple-vehicles accident rates (Anastasopoulos et al. 2008; Bester 2003; Tighe et al. 2000). On the other hand, not only can rutting impact driving quality by increasing pavement roughness levels, but also it can lead to hydroplaning in rainy days and reduce skid resistance (Guo et al. 2014; Sha 2008). To reduce the safety problems associated with pavement roughness and rutting, mixtures with high RAP contents should be carefully designed.

This study aims to develop a network-level decision-making tool for budget allocation to road maintenance and rehabilitation. The effects of pavement roughness and trigger roughness level (a value for roughness indicating failure of the pavement) on user and agency costs are evaluated. Moreover, strategies to modify asphalt mixtures with high RAP contents are investigated to make roadways safer with less frequent need for resurfacings.

This thesis consists of two manuscripts which are two separate papers with a related topic. The first manuscript is discussed in Chapter 2 and evaluates the effects of binder-grade bumping and

high virgin binder content on cracking and rutting performance of asphalt mixtures with high RAP contents. Chapter 3 presents the second manuscript and discusses the development of a network-level decision-making tool to select the most efficient pavement maintenance and rehabilitation strategies. In addition, to extend the utility of the network-level decision-making tool developed in this study, a prototype GIS map is created using ArcGIS.

2. CHAPTER 2 - BINDER-GRADE BUMPING AND HIGH BINDER CONTENT TO IMPROVE PERFORMANCE OF RAP MIXTURES

Sogol Sadat Haddadi[1]; Erdem Coleri[2]; and Shashwath Sreedhar[3]

Abstract: Recycling highway construction materials and minimizing the use of virgin materials can reduce the pavement life cycle costs, improve highway network condition, conserve natural resources, and protect the environment. Although the recycling of asphalt pavements is beneficial in most cases by reducing the need for virgin materials and construction costs, asphalt pavements with high RAP contents should be carefully designed to avoid premature cracking. This study evaluates the effects of binder-grade bumping and high virgin binder content on cracking and rutting performance of asphalt mixtures. These two strategies were determined to be effective in improving cracking performance. Semi-circular bend tests, dynamic modulus tests, and flow number tests were conducted on prepared samples in laboratory to assess their cracking and rutting performance with two RAP contents (30% and 40%), three binder contents (6%, 6.4%, and 6.8%), and three binder grades (PG 58-34, PG 64-22, and PG 76-22). As RAP content increases, binder content decreases, and a stiffer binder is used, asphalt mixtures get more susceptible to cracking and more resistant to rutting. A balance of the combination of these variables should be considered in the mix design. In this study, possible combinations of RAP content, binder content, and binder grade to produce asphalt mixtures with high cracking and rutting performances were suggested.

Keywords: reclaimed asphalt pavement (RAP), binder grade bumping, high binder content, rutting performance, cracking performance, flow number test, dynamic modulus test, semi-circular bend test.

---

[1] Graduate Research Assistant, School of Civil and Construction Engineering, Oregon State University, 101 Kearney Hall, Corvallis, OR, USA, 97331, Email: haddadis@oregonstate.edu.

[2] Assistant Professor, School of Civil and Construction Engineering, Oregon State University, 101 Kearney Hall, Corvallis, OR, USA, 97331, Tel: (541) 737-0944, Email: erdem.coleri@oregonstate.edu.

[3] Graduate Research Assistant, School of Civil and Construction Engineering, Oregon State University, 101 Kearney Hall, Corvallis, OR, USA, 97331, Email: mahmouai@oregonstate.edu.

2.1 INTRODUCTION

Reclaimed Asphalt Pavement (RAP) and Reclaimed Asphalt Shingles (RAS) have inherent value as recycled construction materials. Using RAP and RAS as a supplement for virgin aggregate and binder in Hot Mix Asphalt (HMA) has significant merit for conserving raw materials, reducing mixture costs, and reaching sustainability goals. The major goal of this study is to investigate methods of increasing the RAP content in HMA mixtures beyond the current threshold in order to displace a maximum amount of virgin materials while still preserving the long-term durability of the finished asphalt concrete.

The use of RAP/RAS in the United States became widespread after the 1970s oil embargo that drove up the cost of petroleum products, although asphalt recycling existed to some degree prior to this event. Following the oil embargo, many state DOTs permanently adopted the use of RAP/RAS in their mix designs. Although a sharp reduction in oil prices has recently been observed, depletion of readily available oil reserves is expected to increase the cost of oil and petroleum products in the long run. More strict regulations for new rock mines are also expected to increase the cost of aggregates (Willis et al. 2012). These phenomena necessitate a more proactive approach to increase the recycled content used in HMA paving.

Looking forward, the use of high RAP/RAS mixtures will help the asphalt pavement industry to become more energy independent, more sustainable, and more profitable while promoting environmental stewardship within all pavement agencies. Even as oil prices rise and fall, efforts to increase the use of RAP/RAS should not be discontinued. This practice can help to establish a notion of sustainability in pavement engineering.

A benefit of conserving virgin binder and aggregates is creating economic savings. Reducing the amount of virgin asphalt binder and aggregates used in HMA mixes has direct cost-saving potential. Willis et al. (2012) suggested that supplementing 50% RAP/RAS into HMA mixes can save agencies up to 35% on the cost of raw materials in asphalt paving projects. In 2014, the use of RAP/RAS on U.S. roads displaced 20M barrels of oil and 68M tons of aggregate (Hansen and Copeland 2014). This resulted in a savings of $2.8B based on binder cost of $550/ton and aggregate cost of $9.50/ton, according to a study by National Asphalt Pavement Association

(NAPA) (Hansen and Copeland 2014). This evidence is testament to the ability of RAP/RAS use to provide economic benefits to federal and state transportation agencies.

Saving money by using more recycled content also means that agencies will have more money to allocate toward pavement improvement projects. This means that more roads can be maintained at higher levels of service. This is conducive to user comfort and vehicle operating cost (VOC) savings (mostly fuel consumption), as pavement roughness is a major factor in VOCs.

The primary concern when using high RAP mixes lies in the altered long-term durability properties of HMA mixtures. The dilemma is finding a way to use higher RAP contents in HMA without compromising any long-term durability. Aged binder in RAP is less ductile than virgin binder and gives rise to failure under repeated high axle loads and thermal effects. The placed high-RAP asphalt concrete mix becomes very brittle and is highly susceptible to fatigue cracking. Ideally, a high RAP content HMA mix should exhibit comparable or better strength and durability as compared to conventional non-RAP mixtures.

Another concern on the percentage of RAP that can be used stems from the variability of this material. When RAP is milled off an old surface, it might be mixed in with original pavement materials, as well as maintenance treatments such as patches and chip seals. Due to this variability, agencies tend to limit the percentage RAP that can be used in new mixtures. The way RAP materials are stockpiled can also have ramifications; i.e. when a stockpile includes more homogeneous RAP, a higher percentage is allowed compared to stockpiles with RAP containing more maintenance treatment materials (Copeland 2011).

According to the NAPA (Hansen and Copeland 2014), asphalt pavement is the most recycled material in the U.S. On average, a RAP content of 19.6% by weight was reported for U.S. state DOT HMA mixes with only 0.1M tons landfilled (Hansen and Copeland 2014) while the current upper bound on recycled content in HMA mixes for several state DOTs was reported to be around 30%, although proportions range from state to state. In states where virgin aggregate is scarcer, a higher RAP content might be used. Climate also dictates the limit of recycled content to some degree since thermal cracking is a major concern for mixes with high RAP content.

Abroad, RAP is being utilized in a similar manner. Japan has delved into the use of RAP and have reported the successful use of mixes containing up to 51% RAP without any compromise on durability (Hansen and Copeland 2014). However, it should be noted that truck weights and axle loads in Japan are significantly lower than the U.S., which prevents any direct performance comparisons. European countries also make use of RAP to achieve sustainability targets, but use far less recycled content as compared to the U.S. (World Highways 2013).

With the many variables and potential consequences associated with using high RAP/RAS contents in HMA, there is a need for a way to evaluate changes in the lifespan and sustainability of the pavement. Life Cycle Analysis (LCA) is a useful tool in identifying economic and environmental benefits of using RAP/RAS in large-scale projects. LCA considers each component of a project in terms of functional units. Having a unit cost analysis helps to identify where the majority of a project's resources are utilized and provides a measure of their effectiveness. Analyzing HMA mix design in this way will allow engineers to pinpoint areas where significant savings are opportune. LCA takes into account the environmental impacts of all components of a project to yield a comprehensive analysis of the project's environmental footprint. These types of analyses can be useful to identify factors that are critical to achieve organizational sustainability goals.

2.1.1 Major research products developed in this study

The major research products developed in this study are as follows:

- Recommended RAP content, binder content, and binder grade for new asphalt pavement construction;
- Strategies to increase RAP content by increasing binder content and/or using softer binder;
- A software to analyze the data produced by semi-circular bend (SCB) test; and
- A software to analyze the data produced by flow number test.

2.1.2 Key objectives of this study

The main objectives of this study are to:

- Investigate methods of increasing the RAP content in HMA mixtures beyond the current threshold in order to displace a maximum amount of virgin materials while still preserving the long-term durability of the finished asphalt concrete;
- Compare cracking performance of asphalt mixtures with different RAP contents (30% and 40%), binder contents (6%, 6.4%, and 6.8%), and binder grades (PG 58-34, PG 64-22, and PG 76-22) by conducting SCB and dynamic modulus (DM) Tests.
- Compare rutting performance of asphalt mixtures, same mixtures produced for cracking tests, by conducting flow number (FN) Tests.
- Develop linear regression models correlating flexibility index (FI) and flow number (FN) with RAP content, binder content, and binder grade.
- Suggest possible combinations of RAP contents, binder contents, and binder grades for mix design.

2.1.3 Organization of the chapter

This chapter is organized as follows:

In this thesis, this introductory chapter is followed by the literature review. Chapter 2.3 provides information about the experimental plan and material source used for this study. Information about test methods including SCB, DM, and FN tests, to evaluate cracking and rutting performance of prepared mixtures with different RAP contents, binder contents, and binder grades are presented in Chapter 2.4. Chapter 2.5 presents the results of SCB and DM tests that were conducted to quantify the cracking and elastic modulus of the prepared asphalt mixtures, respectively. FN test results characterizing the rutting performance of asphalt mixtures are also provided in Chapter 2.5. The impact of RAP contents, binder contents, and binder grades on performance are also discussed in this Chapter. Summary and conclusions are presented in Chapter 2.6. Finally, future recommendations are discussed in Chapter 2.7.

2.2 LITERATURE REVIEW

2.2.1 Strategies to increase RAP/RAS content

Due to ever growing demand of asphalt pavement materials and limited supply of aggregate and asphalt binder, using RAP in HMA mixtures started to create significant benefits. For this reason, agencies are interested in finding ways to increase the RAP content of HMA mixtures. Prior to the introduction of the Superpave® method, RAP was frequently used by different state DOTs. Superpave® did not really provide a thorough method for using RAP in HMA mixtures (Copeland 2011) while it encouraged agencies to use RAP in asphalt mixtures. Moreover, due to high content of fines in RAP stockpiles and high variability in RAP, most DOTs refused to implement higher RAP percentages in their paving operations. As a result, the RAP content threshold was capped at 15 percent in the past. But in the late 2000s, a notable increase in binder costs brought about major interest in using higher percentage of RAP as a more cost-effective option in HMA paving. Therefore, a basis for allowing pavement designers to use a higher percentage of RAP was needed, as state DOTs were requesting more structured guidelines for using higher RAP contents. As it can be seen in Figure 2.1 and Figure 2.2, there is a growing interest of using higher RAP content in the U.S. Figure 2.1 shows the increased RAP use in the U.S. by comparing the amount of RAP used prior to and after 2007. Figure 2.2 shows the current use of RAP contents of 25 percent and above for all U.S. states.

The primary concern when using high RAP/RAS mixes lies in the altered long-term durability properties of HMA mixtures. The dilemma is finding a way to use higher RAP contents in HMA without compromising any long-term durability. Major concerns result from higher cracking susceptibility due to stiffer RAP mix. Regarding these concerns, the following strategies were generally suggested in the literature to increase the RAP content without compromising the cracking resistance (Bennert et al. 2014):

1. Softer virgin binder grade (binder-grade bumping);
2. Increased binder content;
3. Recycling agents;
4. Polymer and rubber modifiers; and
5. Warm mix asphalt

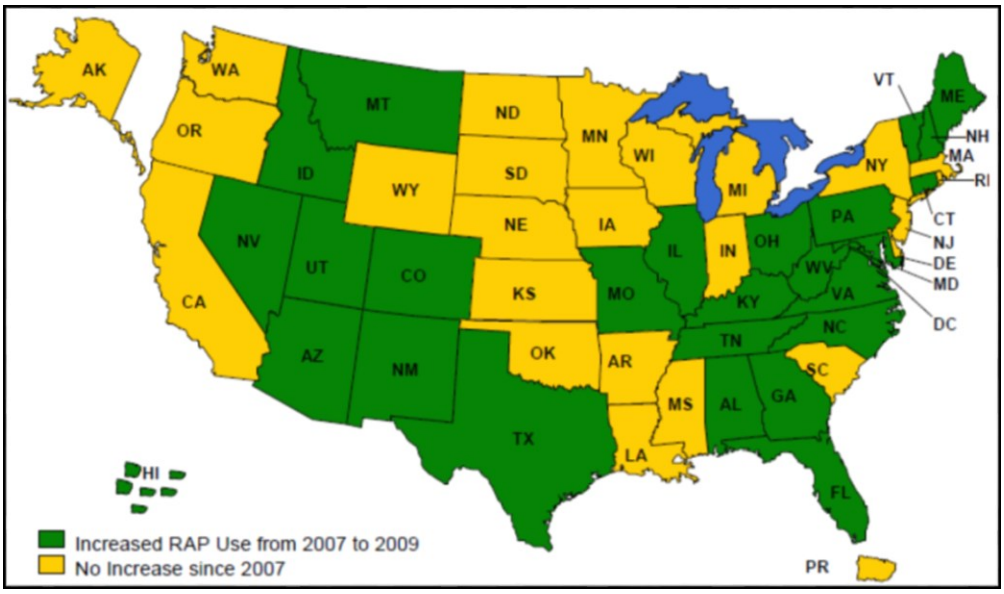

Figure 2.1. Map of U.S. states with increased RAP use since 2007 (Copeland 2011)

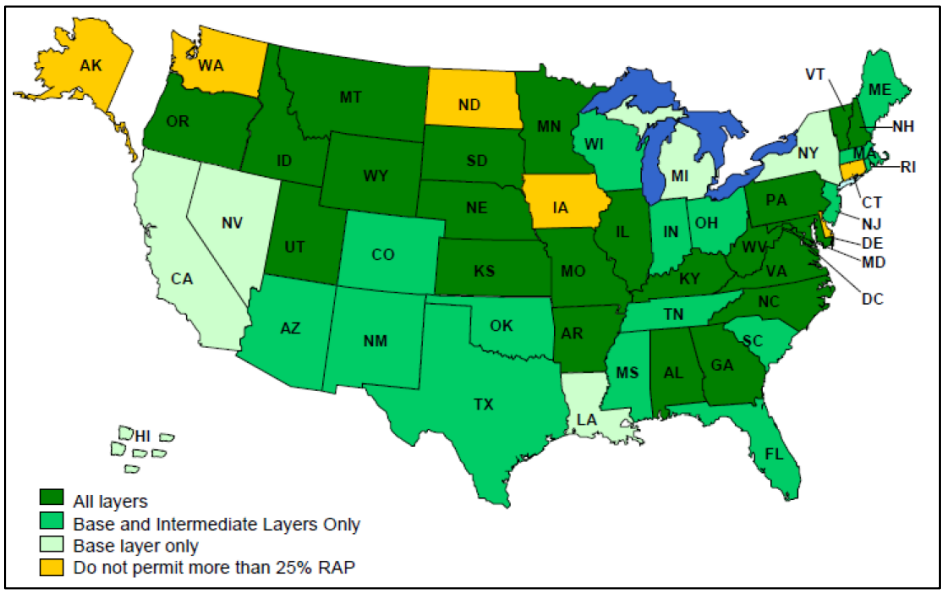

Figure 2.2. Map of U.S. states using RAP contents of 25% or greater in various HMA layers (Copeland 2011)

2.2.1.1 Binder-grade bumping

With the increasing global awareness to achieve sustainable practices in pavement construction, the necessity to use higher percentages of RAP in asphalt mixtures is gaining more attention. One of the strategies identified to be effective in increasing RAP/RAS content is binder grade bumping. Binder grade bumping refers to decreasing high binder PG grade by one or two grades while double-bumped grade means decreasing high and low binder grades by one grade.

Aurangzeb et al. (2012) carried out a study with an objective to quantify the impact of binder-grade bumping on the performance of high RAP asphalt mixtures. The virgin aggregates and RAP were obtained from two districts of Illinois Department of Transportation. In order to assess the effect of binder grade bumping on the performance of RAP mixtures, PG 58-22 and PG 58-28 binders were used. Eight asphalt mixtures were prepared, four for each of the two districts. The four mixtures for each district consisted of a control mix (no RAP), a mix with 30% RAP, a mix with 40% RAP, and a mix with 50% RAP. Wheel-tracking and beam fatigue tests were carried out on these asphalt mixtures. The findings from this study are as follows:

- Although there was a viscoelastic softening effect of binder grade bumping on mixtures, the mixtures with the softest binder had a smaller rut depth than the control mixture as show in the Figure 2.3. It was also observed that the addition of RAP improved the rutting resistance of asphalt mixtures.
- In general, single grade bumping improved the fatigue behavior of asphalt mixtures. However, double-grade bumping did not show any significant improvement as compared to single-grade bumping.

Li et al. (2008) investigated the effect of binder grade on RAP performance by conducting dynamic modulus and semi-circular bend (SCB) fracture tests. Two different RAP sources, three RAP contents (0%, 20%, and 40%), and two different asphalt binder grades (PG 58-28 and PG 58-34) were used for sample preparation. Based on the dynamic modulus tests, it was concluded that softer binder (PG 58-34) provides higher fracture resistance and increases fatigue life. West et al. (2012) investigated the performance of four sections with surface layers containing 45% RAP and different virgin binder grades (PG 52-28, PG 67-22 and PG 76-22). After a total of 20 million

ESALs, mixes with softer binders showed better cracking performance than the mixes with stiffer binders. This result suggested that using binder-grade bumping can be an effective strategy to improve cracking performance of high RAP mixes. The NCAT laboratory study conducted by Willis et al. (2012) concluded that binder-grade bumping along with a 0.3% increase in binder content significantly improved the cracking performance of 50% RAP mixes.

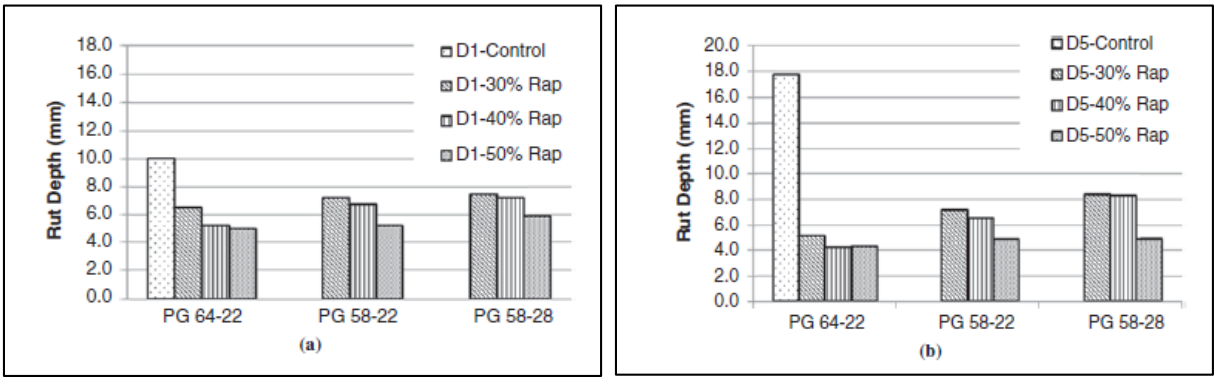

Figure 2.3. Wheel-tracking test results: (a) District 1 (b) District 5 (Aurangzeb et al. 2012)

2.2.1.2 High binder content

One of the major drawbacks of using higher RAP content is the increased stiffness of the mixture which in turn reduces the fatigue performance. This problem can potentially be overcome by increasing the ductility of the mix by increasing the binder content. A study conducted by West et al. (2009) investigated the performance of two sections with 20% RAP, four sections with 45% RAP, and one control section with no RAP at the National Center for Asphalt Technology (NCAT) test track. RAP sections were constructed with 50 mm thick overlays in 2006. Sections with 20% RAP had asphalt mixes with 5.6% binder content with PG 76-22 and PG 67-22 binders. The binder content for the sections with 45% RAP was 5.0% with PG 52-28, PG 67-22, PG 76-22, and PG 76-22 plus 1.5% Sasobit binders. The control section consisted of 5.8% asphalt binder with the PG 67-22.

After 24 months (9.4 million ESALs), rutting was measured with scanning laser rut-bar, cracking was measured by weekly visual inspections, and roughness was measured by using inertial profiler technology (AASHTO R 43-07). International Roughness Index (IRI) was almost equal for all

segments except for the control section and the section with 20% RAP and PG 67-22 binder, which had higher IRI levels. Moreover, rut depths were the greatest for the section with 20% RAP and PG 67-22 followed by the section with virgin binder. Minor cracks with low severity were observed at 45% RAP section with PG 76-22 plus Sasobit (reflection cracks) and 20% RAP section with PG 76-22 (top-down cracks). Other segments did not show any cracking. According to Asphalt Pavement Analyzer (APA) rutting test results, mixes with softer asphalt binders and higher VFA showed higher rutting. Furthermore, results from dynamic modulus tests illustrated that mixtures with stiffer binder and higher percentage of RAP had higher dynamic moduli.

The beam fatigue test was also conducted (AASHTO T 321-07) on long-term aged samples. Results are shown in Figure 2.4. Sections with 45% RAP asphalt mixes exhibited significantly lower fatigue resistance than the 20% RAP sections and the sections without RAP due to the lower effective binder content. The design binder content for the 45% RAP mixes was 5% while the effective binder content for the final mix was expected to be higher as a result of the blending of virgin binder with the RAP binder. However, significantly lower fatigue resistance for the 45% RAP mixes suggested that RAP and virgin binders were not completely blended. Although the 45% RAP mixes with softer binders (PG 52-28 and PG 67-22) have higher fatigue resistance than the stiffer ones (PG 76-22 and PG 76-22 with Sasobit), the effect of binder grade on the fatigue test results was not significant when compared with the effect of effective binder content. It was concluded that the effect of binder-grade bumping becomes less influential as RAP content of the mix increases.

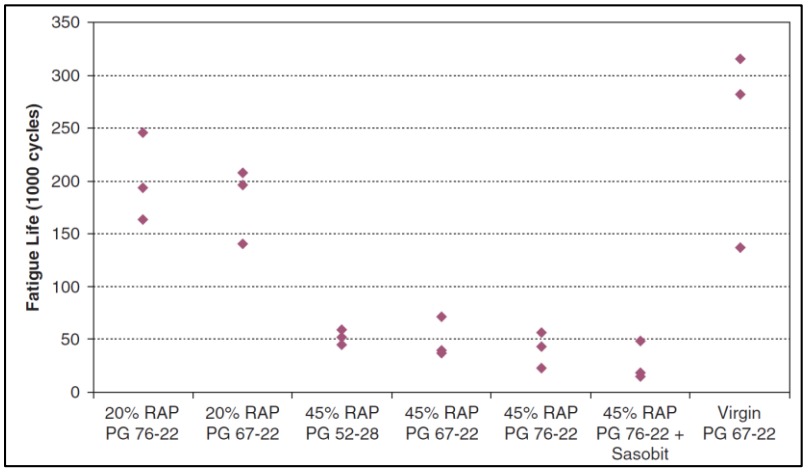

Figure 2.4. Plot of beam fatigue test results for RAP experimental sections (West et al. 2009)

2.2.1.3 Recycling agent

For mixtures with higher percentage of RAP and RAS, one of the strategies for improving the resistance to cracking is using recycling agents such as rejuvenators and softening agents. While softening agents, such as slurry oil and lube stock, can reduce binder viscosity, rejuvenators are used to create chemical reactions in the binder phase to improve its physical properties. The conventional method for softening the hardened aged binder in RAP is using virgin binder. In addition, rejuvenators can be used to reduce the viscosity of RAP mixtures (Tran et al. 2012; Zaumanis et al. 2013). Since adding rejuvenator to the mixture containing RAP has some uncertainties, including inadequate blending between rejuvenator and recycled binder and the required reaction time, it is not widely used. However, selecting a proper amount of rejuvenator, ensuring appropriate mixing, and allowing the required reaction time to occur offset these uncertainties and improve the crack resistance of mixtures (Tran et al. 2012).

Rejuvenators restore the physical and chemical properties of aged binder and reduce the viscosity of the mix (Roberts et al. 1996). They encompass high amounts of maltene components (napthenic and polar aromatic fractions) that can be used to replace the maltenes lost due to binder aging during the construction and use phases. Maltenes incorporated into the RAP mix are expected to reduce the viscosity of the aged and hardened recycled binder (Terrel and Epps 1989). Diffusion of rejuvenators into recycled binder is crucial and consists of four main steps: 1) RAP aggregates are covered with rejuvenator; 2) rejuvenator penetrates to the aged binder layer around the

aggregates and softens the binder (at this step the amount of raw rejuvenator decreases); 3) the rejuvenator penetrates further into the inner layer of the binder which softens the inner layer of the binder while viscosity of binder in outer layer gradually increases; 4) the equilibrium of viscosity is reached in the layers of the recycled binder. The rejuvenator diffuses further into the layer of aged binder during mixing, construction, and use phases of the pavement life cycle (Carpenter and Wolosick 1980).

Tran et al. (2012) evaluated the effect of rejuvenators on HMA mixtures containing high percentages of RAP and RAS. In this study, a mix with no RAP or RAS (control mix), two 50% RAP mixtures with and without rejuvenator, and two 20% RAP plus 5% RAS mixtures with and without rejuvenator were prepared using Cyclogen L rejuvenator and virgin binder with PG 67-22. Dynamic shear rheometer (DSR) and bending beam rheometer (BBR) tests were conducted on extracted RAP binder with different percentages of rejuvenators to determine the optimum amount of rejuvenator required to reach the performance properties of mix with PG 67-22 binder. In the first stage, the optimum amount of rejuvenator was determined to be around 12% of the total recycled binder. In the second stage, mixtures were blended with optimum percentage of rejuvenator and tested to determine Tensile Strength Ratio (TSR) to evaluate moisture susceptibility, dynamic modulus test for mixture stiffness, energy ratio test (resilient modulus, creep compliance, and indirect tensile tests) for resistance to top-down cracking, indirect tensile test (IDT) for resistance to low temperature cracking, modified Overlay Tester (OT) for resistance to reflective cracking, and Asphalt Pavement Analyzer (APA) for rutting resistance. Results illustrated that rejuvenator decreased the mixture stiffness, improved all four fracture properties from the energy ratio test, improved low temperature performance of mixture, and increased resistance to rutting (the improvement against rutting was not significant). It was concluded that using rejuvenator for high amount of recycled binder could be an effective method for enhancing the binder properties.

Shen et al. (2007) compared properties of mixtures containing RAP and rejuvenator against mixtures with a softer binder instead of a rejuvenator. Amounts of rejuvenators for mixtures were determined by blending charts of RAP binders with rejuvenators which were established through dynamic shear rheometer and bending beam rheometer tests (considering the properties of binder

with PG 64-22). Ten mixtures with RAP (five with rejuvenator and five without rejuvenator) and two mixtures without RAP (control mixtures) were designed and tested to evaluate the impact of rejuvenators and softer binders on mix performance. Several asphalt samples with RAP contents up to 48 percent, one oil type rejuvenator, and virgin binders with PG 64-22 and PG 52-28 were prepared. Indirect tensile strength and APA tests were conducted for evaluating the moisture susceptibility and rutting properties of mixtures. This study showed that the RAP content could be increased by up to 10% more in mixtures using rejuvenators with PG 64-22 virgin binder as compared to mixtures containing the softer PG 52-28 binder. It was concluded that blending charts were proper tools to estimate the rejuvenator contents. Furthermore, mixtures with rejuvenators illustrated better mechanical and rutting properties than mixtures containing softer binder.

A study by Oliveira et al. (2013) used motor oil as a rejuvenator to evaluate the properties of mixtures containing 100% RAP. Using penetration grade, softening point, and dynamic viscosity tests, the optimum amount of rejuvenator required to increase penetration grade from 10/20 to 20/30 was estimated to be around 5%. Conventional control HMA mixtures were produced with 5.1% binder content and a binder classified as 35/50 penetration grade. Water sensitivity (by conducting indirect tensile strength tests with dry and wet samples), permanent deformation (using wheel tracking test), stiffness modulus (using four-point bending beam test), and fatigue cracking tests were conducted on control HMA and 100% RAP mixtures to assess their properties. Test results showed that 100% RAP mixtures are more resistant to moisture than the control mix. Fatigue cracking and rut resistance of 100% RAP mixes were also higher than the control mix. It was concluded that high performance 100% RAP mixes can be produced by providing appropriate storing and production conditions.

2.2.1.4 Combining RAP/RAS with warm mix asphalt (WMA)

The workability and compactibility of HMA with high RAP content have always been a challenge to control (Petersen 1984). Aged, stiffened RAP binder can cause problems during mixing and construction. Using Warm-Mix Additives (WMA) is a strategy to mitigate problems brought on by using high percentages of RAP in asphalt pavements. Below are summaries of studies looking at the effects of WMA on RAP mixes.

Tao and Mallick (2009) evaluated the impact of using two types of WMA (Sasobit H8 and Advera zeolite) on the workability, density, seismic modulus (tested at 0ºC, 26.7ºC, and 50ºC) and strength (by conducting indirect tensile strength) of 100% RAP mixes. One RAP source with 6% asphalt binder content was used in this study. Sasobit H8 (1.5%, 2.0%, and 5.0% by weight of total asphalt binder) and Advera zeolite (0.3%, 0.5%, and 0.7% by weight of total mix) were mixed with RAP and compacted with a standard gyratory compactor (SGC) at 125ºC. Mixes with Sasobit H8 additives exhibited higher bulk specific gravity (BSG) after compaction as compared to the control mix with 100% RAP and no additives. The mix with 0.3% Advera zeolite also had a higher BSG than the control mix. This trend resulted from increased compactibility due to added WMA. However, the mixes with 0.5% and 0.7% of Advera zeolite had lower BSG than the control. It was indicated that lower BSG is a result of excessive volume expansion at higher additive contents created by water vapor. The workability of the mixes were tested by using a torque tester after adding 2.0% Sasobit H8 and 0.5% Advera zeolite to the mixes. The mixes showed greater workability than the control mix at 110ºC and less workability at 80ºC. This study showed that both WMAs had a stiffening effect on the mix at low temperatures. Moreover, mixes with WMA had a higher seismic modulus than the control mix at all temperatures.

A study carried out by Mallick et al. (2008) investigated the feasibility of preparing 75% RAP mixtures with WMA (Sasobit H8) to determine whether these mixes met standard specifications. Table 2.1 summarizes the properties of the mixtures prepared in this study. Samples were tested for BSG, indirect tensile strength at -10 ºC, rutting resistance (using the asphalt paver analyzer test), and seismic modulus at 0 ºC, 25 ºC, and 40 ºC. This study showed that Sasobit H8 increased compactibility and enhanced workability of the mix. It was concluded that preparing mixtures with 75% RAP with air void contents similar to mixtures without RAP was possible. The control mix had the highest indirect tensile strength, whereas the mixture with WMA and PG 42-42 asphalt binder showed the lowest indirect tensile strength. Adding Sasobit H8 to the mixtures resulted in a tensile strength increase for the same binder performance grade. Rut depths were least for the mixture without WMA and PG 52-28 binder and greatest for the mixture with WMA and PG 42-42 binder. All rut depths were less than 4 mm due to stiffness brought on by the high RAP content in the mixtures. The seismic modulus test showed that stiffness of the RAP mixes with the softest

binder and Sasobit H8 were close to the control mixture at all the test temperatures. Mallick et al. (2008) stated that it is possible to prepare 75% RAP mixes with the same air void content as mixes without RAP at lower temperatures.

In a study conducted by Zhao et al. (2012), rutting resistance, fatigue resistance, and moisture susceptibility of WMA and HMA mixes containing different amounts of RAP were evaluated. The WMA mixtures were produced with a foaming technology at 0%, 30%, 40%, and 50% RAP contents. Standard HMA mixtures, as control mixes, contained 0% and 30% RAP. Rutting resistance was tested with the asphalt pavement analyzer (APA) rutting test and Hamburg wheel-tracking test. Results illustrated that rutting resistance was improved by adding more RAP to the mixtures. This improvement was more significant for WMA-RAP mixtures than HMA-RAP mixtures. Moisture susceptibility was tested with the tensile strength ratio (TSR) test. Mixtures containing RAP showed less moisture susceptibility than mixtures without RAP. This trend was observed in both WMA and HMA mixtures. However, WMA mixtures had lower TSR than HMA mixtures, indicating that moisture susceptibility is a concern for WMA mixtures. Fatigue performance was tested with Superpave IDT (including resilient modulus, creep, and indirect tensile strength tests) and beam fatigue tests. According to beam fatigue test results, adding more RAP to the WMA samples increased fatigue cracking performance. On the other hand, for mixes without WMA, increased RAP content reduced fatigue life. It is worth noting that increasing the RAP content in WMA mixtures increased the energy ratio (ER) values and fracture resistance of the WMA mixtures, leading to longer fatigue life.

Table 2.1. Mixture properties

	Control mix	Mix 1	Mix 2	Mix 3	Mix 4
RAP content	0%	75%	75%	75%	75%
WMA type	NA	NA	Sasobit H8	Sasobit H8	NA
WMA content[1]	0%	0%	1.5%	1.5%	0%
Virgin binder grade	PG 64-28	PG 52-28	PG 52-28	PG 42-42	PG 42-42
Virgin binder content	4.7%	1.5%	1.5%	1.5%	1.5%
Compaction temperature	150 ºC	135 ºC	125 ºC	125 ºC	125 ºC
Number of prepared samples	18	18	18	18	2

Note: [1]WMA content is by weight of total asphalt binder.

2.2.1.5 Modification of RAP/RAS mixtures

Modification of RAP/RAS mixes with crumb rubber and polymer improves the mechanical characteristics of HMAs and allows the use of higher RAP/RAS contents. Although polymer and rubber modification increase the cost of asphalt mixes, increased RAP content can offset the high cost of modified binders. Below are studies that investigated the effects of modification on mixes with high RAP contents.

Hajj et al. (2009) investigated the impact of three sources of RAP in three contents (0%, 15%, and 30%) on the mechanical characteristics of the mixtures. Two different types of binders (PG 64-22 and PG 64-28NV[4] polymer-modified) were used for preparing laboratory mixtures. Fatigue beam tests were conducted at different strain levels to evaluate the cracking resistance of prepared mixes. This study showed that polymer-modified mixtures had greater fatigue performance than unmodified mixtures regardless of RAP content. While polymer-modified mixtures containing

[4] NV indicated that the binder grading showed additional toughness and ductility for virgin and RTFO aged binder at 40ºF besides the standard Superpave binder testing requirements.

RAP had lower fatigue resistance than polymer-modified mixtures without RAP, they showed higher fatigue resistance than unmodified mixtures without RAP. This study concluded that using RAP with polymer modification could enhance the fatigue performance of mixtures and offset the increased costs of using these modifications when life cycle cost analysis (LCCA) is used to evaluate the cost effectiveness for the design period.

A study conducted by West et al. (2009) investigated the performance of two sections with 20% RAP with PG 76-22 and PG 67-22 asphalt binders, four sections with 45% RAP with PG 52-28, PG 67-22, PG 76-22, and PG 76-22 binder with 1.5% Sasobit warm-mix additive, and one control section with PG 67-22 asphalt binder and no RAP at the National Center for Asphalt Technology (NCAT) test track. The field study showed that the 45% RAP sections with softer binders were compacted easier than the sections with polymer-modified binders. It was also observed that adding Sasobit to modified binders did not improve compactibility. Moreover, conducting indirect tensile tests (IDT) to estimate creep compliance, fracture energy, and resilient modulus showed that polymer modification was effective in increasing the energy ratio and reducing the potential for top-down cracking.

Xiao et al. (2007) assessed the rutting performance of crumb rubber-modified RAP mixtures. Two rubber types (Ambient and Cryogenic), four rubber contents (0%, 5%, 10%, and 15% by weight of virgin binder), and three rubber sizes were selected for preparing RAP mixtures from two RAP sources with different contents (0%, 15%, 25%, and 30% for one RAP source and 0%, 15%, and 38% for the other). Wet and dry Indirect Tensile Strength (ITS) tests and Asphalt Pavement Analyzer (APA) rutting tests were conducted with the prepared samples. This study concluded that higher percentages of RAP reduced the rut depth and increased the ITS and stiffness values. On the other hand, increasing the rubber content decreased the ITS value and creep stiffness. Moreover, this study showed that the effect of rubber size on rutting performance was insignificant. In general, crumb rubber reduced air voids and improved rutting performance.

Influence of crumb rubber size and type on RAP mixture properties were investigated in the study carried out by Xiao et al. (2009). This study used three rubber sizes and two rubber types (ambient and cryogenic) in the samples with 25% RAP and virgin binder with PG 64-22. Indirect tensile

strength tests (ITS) for moisture susceptibility, resilient modulus tests, and the flexural bending beam fatigue tests were conducted to evaluate the performance of asphalt mixes. It was concluded that using crumb rubber as a modifier in RAP mixtures could reduce the need for adding virgin binder and increase the moisture resistance by increasing the Tensile Strength Ratio (TSR). In general, using RAP and crumb rubber increased the resilient modulus at different temperatures. However, as the size of crumb rubber increased, resilient modulus decreased regardless of rubber types. Addition of crumb rubber improved the fatigue performance of mixtures as the rubber size increased. However, it should be noted that increased rubber size can create compaction problems during construction.

Mohammad et al. (2011) conducted a study on evaluating the crumb rubber effect on high RAP content mixtures. Six different mixtures were prepared: 1) HMA mixture with PG 64-22 binder; 2) HMA mixture with SBS polymer-modified asphalt binder classified as PG 70-22M[5]; 3) HMA mixture with SBS polymer-modified asphalt binder classified as PG 76-22M; 4) HMA mixture with crumb rubber modified binder (wet process) graded as PG 76-22; 5) mixture with 15% RAP and SBS polymer-modified asphalt binder classified as PG 76-22M; and 6) mixture with dry blending 40% RAP, crumb rubber additives, and PG 64-22 binder. Moisture resistance, rutting performance, and cracking resistance were evaluated using a modified Lottman test, loaded -wheel tracking test, flow number test, dynamic modulus test, semi-circular bend test, and dissipated creep strain energy test. The results of this study showed that adding crumb rubber additives led to softening the blended asphalt binder. Moreover, rubber modified mixture with high RAP content showed adequate moisture resistance. However, the mixture with no RAP content and rubber modified binder failed in moisture resistance test. SBS modified mixture with PG 76-22M binder and rubber modified mixture with high RAP content ranked first and last in fracture energy, respectively, whereas they both showed adequate performance in permanent deformation. It was concluded that these results could be due to the properties of asphalt binder with PG 64-22 and the high RAP content.

[5] M: Modified

In summary, polymer-modification was observed to improve fatigue cracking resistance of high RAP mixes. For this reason, polymer modification can be an effective strategy to increase RAP content of asphalt mixes. However, life cycle cost analyses and performance modeling should be used to evaluate the cost effectiveness of using polymer modification in RAP mixes. It is prudent to note that the studies focusing on the use of rubber modification to improve cracking performance of RAP mixtures did not suggest any significant improvement in performance created by the use of crumb rubber.

2.2.2 Mix design procedure

The mix design procedures involving RAP mixtures are similar to that of conventional asphalt mixtures. However, the RAP materials should meet the typical aggregate gradation and quality specifications in order to be mixed with the virgin materials. After separating aggregate and binder in the RAP, the aggregates are tested for gradation and quality. McDaniel and Anderson (2001) suggest that the PG binder grade can remain the same when less than 15% RAP is used in HMA. It is suggested to lower the PG binder grade by one grade when 15-25% RAP is used in the mixture. When using more than 25% of RAP, it is suggested to use the blending chart to determine the amount of RAP and PG binder grade that should be used in the mixture. The mix design process is summarized in Figure 2.5.

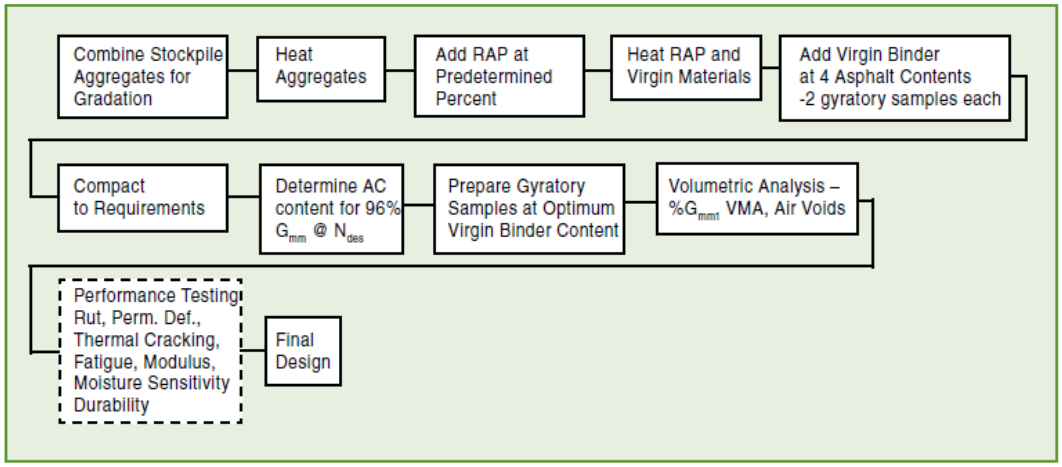

Figure 2.5. Mix design process involving RAP (Newcomb et al. 2007)

2.2.3 Field performance of RAP-RAS mixtures

As a result of using aged recycled material from different sources, there are uncertainties associated with the fatigue and rutting performance of reclaimed asphalt pavements. Although laboratory experiments show acceptable performance for RAP and RAS mixtures when compared with conventional HMA mixes, field performance should be taken into account to evaluate the short and long term performance of mixtures containing RAP and RAS. Studies evaluating the field performance of RAP and RAS mixtures are summarized below.

The Louisiana Department of Transportation (Paul 1996) constructed five roadway sections with RAP mixes between the years 1978-1981. The purpose was to compare the performance of these sections with and without RAP (in 5 sites) over a five-year period. RAP mixes and control mixes (without RAP) had identical properties including gradation, binder content, and compaction. The analysis included evaluation of pavement condition ratings, serviceability, structural properties and mixture and binder properties. Serviceability of the pavements was measured using pavement condition ratings based on the Mays Ride Meter (MRM). The Dynamic Deflection Determination System (Dynaflect) was used to evaluate the structural properties of the pavements. Cores were taken from each site to determine binder content and gradation. The results of this study showed that there were no significant differences in pavement condition ratings, recovered asphalt binder characteristics or structural properties of the pavements with RAP contents ranging from 20 to 50 percent and the conventional HMA mixtures. However, sections with RAP experienced slightly more cracking than the control pavements.

Eighteen states in the U.S. conducted overlay rehabilitation, known as the Specific Pavement Study 5 (SPS-5), between 1989 and 1998 for the purpose of comparing long-term performance of mixes without RAP to mixes containing 30% RAP. Each project consisted of eight test sections: a control section without an asphalt overlay and 7 other sections with overlay thicknesses ranging from 50 to 125 mm, both milled and not milled, and with and without RAP pavements. West et al. (2011) measured the International Roughness Index (IRI), rutting, fatigue cracking, longitudinal cracking, transverse cracking, block cracking, and raveling of these sections to evaluate the performance of mixes with and without RAP. The results showed that performance of pavements

with RAP was very close to the in-situ performance of pavements constructed without any RAP. However, RAP mixtures showed slightly more longitudinal and transverse cracking.

Carvalho et al. (2010) collected performance data from 18 SPS-5 sites 8 to 17 years after rehabilitation. The purpose of the study was to evaluate the short-term and long-term in-situ performances of RAP mixes by considering the effects of overlay thickness, environmental factors, and surface conditions. In general, there were no statistically significant differences in overall performance of overlays with or without RAP. Only 22% of the pavements without RAP showed greater performance in fatigue cracking while the remaining 78% had fatigue cracking performance equal to the mixes containing RAP. Moreover, pavements without RAP showed slightly better performance when thinner overlays were used. As the thickness increased, overlays with and without RAP exhibited no discernable difference in cracking performance. Results from falling-weight deflectometer (FWD) tests, a non-destructive field test conducted to determine pavement layer stiffnesses, also pointed out equal structural performance for HMA overlays with and without RAP.

Williams and Shaidur (2015) investigated the causes of early cracking by evaluating the cracking performance of 10 sections (6 with top-down cracking and 4 without top-down cracks) within the state of Oregon highway system. These sections had RAP contents ranging from 0% to 30%. FWD tests and dynamic core penetrometer (DCP) tests were conducted to evaluate the structural performance. Cores from cracked and uncracked sections were taken for laboratory investigations. Dynamic modulus tests and indirect tensile (IDT) tests were performed at different frequencies on the samples extracted from the field. Binders were extracted from the cores and tested by dynamic shear rheometer (DSR) tests and bending beam rheometer (BBR) tests to indicate their performance properties. Cracked sections exhibited a higher dynamic modulus, stiffer binder (with higher complex shear modulus) and lower indirect tensile strength. In general, cracked sections showed higher variability in measured indirect tensile strength, air void contents, and mix densities. It can be concluded that variability is a major cause of top-down cracking and decreased fatigue cracking resistance. Since the RAP mixtures are more prone to variability due to use of RAP from different sources and problems associated with blending the RAP and virgin materials, it is expected that RAP mixtures are more susceptible to top-down fatigue cracking.

Based on the aforementioned studies, cracking is the most critical distress in RAP mixtures during the design life. Since distresses (top-down cracking and rutting) are generally confined to the upper layers for well-constructed thick asphalt pavement structures, removal of top one or two layers and replacing them with thin asphalt overlays (thinlays) was determined to be a cost-effective strategy to preserve and/or improve highway network condition (Newcomb 2009). Therefore, using thin overlays and chip seals on top of the reclaimed asphalt pavements could increase the long-term durability of RAP sections and reduce the aging rate of pavement surface.

2.2.4 Economic and environmental benefits of using RAP/RAS mixtures

Analyzing the benefits and drawbacks of using high RAP mixes should be done by considering economic, societal and environmental factors and quantifying them in terms of monetary costs and environmental impacts. Life Cycle Assessment (LCA) procedures are fast becoming the best way to accomplish this for pavements. An agency that uses LCA can select specific performance indicators to focus in their project that will help reduce the cost and environmental impact of asphalt paving with high RAP/RAS mixes. The key components of LCA for pavements consider material production, construction, maintenance and rehabilitation, vehicle operating costs (VOC) during the use phase and recycling.

One aspect of LCA more specific to economic costs and benefits is Life Cycle Cost Analysis (LCCA). LCCA can be used to deal specifically with changes in asphalt mix costs that result from the use of high RAP mixes, which could include reduced virgin binder use or increased maintenance frequency. LCCA is most crucial for large projects where significant savings can be made.

Construction energy use is a portion of the LCA that allows the analyst to study the effects of resource and labor-oriented energy use and emissions on the environmental cost of the project. Since pavement maintenance frequency ultimately controls the level of service of the roadway and directly impacts vehicle operating costs, the cost of deferred maintenance reflects directly in the analysis. It is worth noting, however, that more data needs to be obtained from asphalt mixing plants concerning the difference in energy use and emissions in procurement of mixes using high

RAP contents versus conventional HMA mixes. Costs associated with roughness related excess fuel consumption from vehicles over the lifespan of the pavement can be considered, but may require data acquisition from pavement and tire experts in order to formulate an analysis subcategory (UC 2014). Economic savings brought on by using RAP will allow DOTs to maintain roads more often and reduce network level pavement roughness which will translate to lower user costs.

An example of using LCA for evaluating RAP comes in a recent study by Aurangzeb et al. (2013), where a 50% RAP mix was used to investigate environmental and cost savings as compared to a standard HMA mix. This study focused on the binder course only and considered impacts based on greenhouse gas (GHG) emissions and energy use. The study used a hybrid LCA, meaning that it encompassed environmental impact factors from traditional LCAs as well as cost-based factors from typical life cycle costs analysis (LCCA). Societal impacts were not considered here, but if they were of importance, they ought to be considered early on in the analysis so that any areas that need improvement can be changed before the project is too far along. In the study by Aurangzeb et al. (2013), it was found that using 50% RAP in a HMA mix can reduce the feedstock energy, or embodied energy of asphalt binder, by as much as 40%. The construction phase turns out to be a very small portion of the embodied energy or global warming potential of a high RAP paving project, with only 6-8% of global warming potential attributed to this phase (Aurangzeb et al. 2013). Overall, it was found that the material procurement phase yielded the most energy savings and GHG emission reduction of all phases considered in this LCA, based on data obtained from an asphalt plant who participated in the study (Aurangzeb et al. 2013). In the study by Aurangzeb et al. (2013), it was realized that the LCA did not accurately quantify the conservation of resources brought on by using a high RAP mix. There needs to be more attention paid to this area by pavement engineers in charge of creating the LCA.

A study from the University of Texas at Austin asserts that using RAP may not be equally viable in all cases, and can sometimes incur more costs due to decreased maintenance intervals. The objective of the study by Aguiar-Moya et al. (2011) was to examine the long term cost effectiveness of using RAP mixtures according to service life, as well as cracking susceptibility and rate. An additional goal was to show that LCCA is the best way to analyze these factors.

Aguiar-Moya et al. (2011) asserts that RAP usage should be decided on a case-by-case basis, as the effective use of RAP could vary between regions or for different RAP contents. Augiar-Moya et al. (2011) suggested to develop regional deterioration models for RAP mixes in different lift thicknesses and RAP contents in order to have an index of RAP durability. The Aguiar-Moya et al. (2011) study utilized data from the FHWA LTPP SPS-5 experiment in Texas to quantify benefits and drawbacks of RAP use. However, it is worth noting that this experiment is outdated in comparison to the recent evolution of RAP use in state DOTs, so more long-term RAP mix durability data needs to be obtained. In general, the finding of this study was that although RAP helps to mitigate rutting failure, it does give rise to a higher degree of cracking failure that occurs in a shorter amount of time. Aguiar-Moya et al. (2011) suggested using lower PG grade virgin binder to help to combat cracking and preserve the durability of the finished pavement. Aguiar-Moya et al. (2011) also suggested that more research be put into studying high RAP mixes that utilize fractioned RAP as well as RAS.

Andreen et al. (2011) investigated the cost effectiveness of using RAP in HMA paving, as base rock, and as a dust suppression method on gravel roads. Andreen et al. (2011) used a "means equal comparison", basing savings per ton of RAP utilized, to analyze the cost effectiveness of RAP in these three applications. In HMA paving, materials transport and virgin materials displaced were selected as LCA impact categories. Andreen et al. (2011) found that a saving of $40.87 per ton was realized when using RAP in HMA, with most of these savings coming from reducing energy consumption at the HMA plant. This was the most significant of all savings between RAP use on gravel roads, as base rock, and in HMA paving. Andreen et al. (2011) indicated that calculated savings will increase with increasing RAP content. Andreen et al. (2011) also mentioned that normalizing the savings on a per ton of RAP basis was the key to simplifying the analysis.

A study by the National Taiwan University examined the environmental benefits of using RAP in HMA mixes. Lee et al. (2011) used the PaLATE LCA tool in conjunction with energy use and CO_2 emission data obtained from HMA plants and binder manufacturers to investigate the potential for RAP to reduce CO_2 production and energy consumption in HMA paving. The study was based on a comparison to a conventional HMA mix cradle-to-grave analysis. Using CO_2 emissions and energy use as the performance indicators in the LCA, Lee et al. (2011) found that

by using a mix with 30% RAP, approximately 84% less CO_2 is emitted and 80% less energy is used based on a cradle-to-grave analysis of the RAP mix and its components, with most of these savings attributed to the re-use of asphalt and the displaced virgin materials that would otherwise comprise the mix. Lee et al. (2011) suggests that the environmental impact can further be reduced if energy saving measures and odor control devices are implemented at the HMA plants. Lee et al. (2011) indicated that RAP HMA mixes are indeed cost effective to use if the RAP mix can achieve 80-90% of the service pavement life of conventional HMA mix. Lee et al. (2011) further indicated that the performance and durability of RAP mixes can be increased if recycling agents or additives are used to mitigate cracking failure.

A National Center for Asphalt Technology (NCAT) study investigated the sustainability of using RAP HMA mixes using the Roadprint LCA software tool. Using the NCAT test track in Alabama as a case, this study by Willis (2015) quantified the benefits of using RAP using a triple bottom-line methodology, focusing on environmental, economic and societal benefits. Willis (2015) used a basis of CO_2 equivalents to analyze the emissions reduction of RAP use and chose to focus on two phases of pavement life in the LCA: materials and construction/production. Willis (2015) chose to study using RAP on its own, using RAP in conjunction with Warm Mix Asphalt (WMA), and using RAP combined with locally sourced materials to conduct the analysis. Willis (2015) found that utilizing recycled asphalt resulted in a 9-26% energy savings and a 5-29% reduction in CO_2 emissions when using RAP alone. A 19-42% energy savings and a 6-39% reduction in CO_2 emissions were realized when using RAP along with locally sourced materials. Finally, focusing on impact reduction at the asphalt plant, Willis (2015) found that 12-17% less energy was used and 6-9% less CO_2 was emitted when using RAP along with the WMA technique. In general, Willis (2015) found that it is most sustainable to use RAP in conjunction with locally sourced materials in order to reduce embodied energy brought on by materials transport. Willis (2015) did not obtain economic or societal results, as a LCCA is most useful for those aspects.

LCA is a powerful impact estimation tool, but it still has a few caveats and can become quite complicated for broad projects that encompass many different road types or performance indicators. In order for it to be useful in pavement engineering, it is important to keep industry professionals and decision makers in the loop on how LCA works and how it can help firms and

agencies analyze costs and environmental impacts accurately. Additionally, if this tool is to be used on an international scale, then significant standardization must be implemented to make the LCA relevant to all regions of the world. This will require collaboration from pavement agencies internationally to create a LCA tool that encompasses a wide enough perspective to account for regional needs.

2.2.5 Summary

A review of literature indicated that significant economic and environmental benefits can be achieved by using RAP/RAS in asphalt mixes. In the study by Aurangzeb et al. (2013), it was found that using 50% RAP in a HMA mix can reduce the feedstock energy, or embodied energy of asphalt binder, by as much as 40%. Andreen et al. (2011) found that a saving of $40.87 per ton was realized when using RAP in HMA, most of these savings coming from reducing energy consumption at the HMA plant. Lee et al. (2011) found that by using a mix with 30% RAP, approximately 84% less CO_2 is emitted and 80% less energy is used while Willis (2015) found that utilizing recycled asphalt resulted in a 9-26% energy savings and a 5-29% reduction in CO_2 emissions. Lee et al. (2011) also indicated that RAP HMA mixes are indeed cost effective to use if the RAP mix can achieve 80-90% of the service pavement life of conventional HMA mix. Findings of these research studies emphasize the importance of increasing RAP/RAS contents in asphalt mixes.

Several studies in the literature focused on developing strategies to increase the RAP content without compromising the cracking resistance. Aurangzeb et al. (2012) carried out a study with an objective to quantify the impact of binder-grade bumping on the performance of high RAP asphalt mixtures. Results of the study showed that in general, single grade bumping improved the fatigue behavior of asphalt mixtures. However, double-grade bumping did not show any significant improvement as compared to single-grade bumping. West et al. (2009) investigated the impact of binder-grade bumping and increased binder content on cracking performance of high RAP mixes. It was concluded that the effect of binder grade on the fatigue test results was not significant when compared with the effect of effective binder content. Thus, West et al. (2009) suggested the use of increased binder content as a strategy to improve cracking resistance of RAP/RAS mixtures. The NCAT laboratory study conducted by Willis et al. (2012) concluded that binder-grade bumping

along with a 0.3% increase in binder content significantly improved the cracking performance of 50% RAP mixes.

One of the strategies for improving the resistance to cracking is using recycling agents such as rejuvenators and softening agents. Tran et al. (2012) evaluated the effect of rejuvenators on HMA mixtures containing high percentages of RAP and RAS. It was concluded that using rejuvenator for high amount of recycled binder could be an effective method for enhancing the binder properties. Shen et al. (2007) compared properties of mixtures containing RAP and rejuvenator against mixtures with a softer binder instead of a rejuvenator. Ten mixtures with RAP (five with rejuvenator and five without rejuvenator) and two mixtures without RAP (control mixtures) were designed and tested to evaluate the impact of rejuvenators and softer binders on mix performance. It was concluded that mixtures with rejuvenators illustrated better mechanical and rutting properties than mixtures containing softer binder.

The workability and compactibility of HMA with high RAP content has always been a challenge to control (Petersen 1984). Aged, stiffened RAP binder can cause problems during mixing and construction. Using WMA is a strategy to mitigate problems brought on by using high percentages of RAP in asphalt pavements. In a study conducted by Zhao et al. (2012), rutting resistance, fatigue resistance, and moisture susceptibility of WMA and HMA mixes containing different amounts of RAP were evaluated. Mixtures containing RAP showed less moisture susceptibility than mixtures without RAP. This trend was observed in both WMA and HMA mixtures. However, WMA mixtures had lower TSR than HMA mixtures, indicating that moisture susceptibility is a concern for WMA mixtures. According to beam fatigue test results, adding more RAP to the WMA samples increased fatigue cracking performance. On the other hand, for mixes without WMA, increased RAP content reduced fatigue life.

Modification of RAP/RAS mixes with crumb rubber and polymer improves the mechanical characteristics of HMAs and allows the use of higher RAP/RAS contents. Several studies in the literature investigated the effects of modification on mixes with high RAP contents. In summary, polymer-modification was observed to improve fatigue cracking resistance of high RAP mixes. For this reason, polymer modification can be an effective strategy to increase RAP content of

asphalt mixes. However, life cycle cost analyses and performance modeling should be used to evaluate the cost effectiveness of using polymer modification in RAP mixes. It should be noted that the studies focusing on the use of rubber modification to improve cracking performance of RAP mixtures did not suggest any significant improvement in performance created by the use of crumb rubber.

This research study quantifies the performance benefits of using binder-grade bumping and increased binder content strategies in RAP/RAS mixture production in Oregon. Although increased binder content and binder-grade bumping were generally suggested to be effective strategies to improve cracking performance of RAP/RAS mixtures according to several research studies, the impact of increased asphalt mix cost on overall life-cycle costs should be evaluated. The most effective strategies for different climate regions and traffic levels in Oregon needs to be determined by mechanistic-empirical procedures. Binder-grade bumping and high binder content strategies are expected to increase the RAP/RAS content in asphalt mixtures, reduce the life-cycle cost, improve the cracking performance, and encourage the widespread use of high RAP/RAS asphalt mixtures in Oregon.

2.3 EXPERIMENTAL DESIGN, MATERIALS, AND SAMPLE PREPARATION

After preparing the experimental plan for sample preparation and testing, the following process is followed to prepare samples for testing. The following procedure is discussed in the next sections in detail.

1. Material sampling: 8 barrels of coarse, 7 barrels of medium, and 7 barrels of fine aggregates were sampled for this study. Wet-sieve and dry-sieve analysis were performed on one sample from each barrel to determine the gradation of each stockpiled aggregate.
2. Ignition oven test (AASHTO T 30-10) was conducted on the sampled RAP materials to find the RAP binder content and aggregate gradations;
3. Theoretical maximum specific gravity (G_{mm}) of each combination of RAP content, binder content, and binder grade was measured;
4. Batching sheets were developed, and samples were batched to achieve 7% air content, target gradation, and the corresponding measured G_{mm};
5. Samples were mixed and compacted in the laboratory;
6. The air contents were measured for all the samples after compaction; and
7. Prepared samples were cut for SCB, DM, and FN tests.

2.3.1 Experimental plan

This section summarizes the experimental plan followed in this study. The goal is to find the effects of changing binder content, RAP content, and binder grade on cracking and rutting performance of asphalt mixtures with high RAP contents. Therefore, samples with different binder content, binder grade, and RAP content were prepared while other variables including air-void content, gradation, and sample dimensions were kept the same for all the samples. Mix properties and experimental plan are given as follows:

SCB, DM, and FN tests were conducted on samples with two RAP contents (30% and 40%), three binder contents (6%, 6.4%, and 6.8%), and three binder grades (PG58-34, PG64-22, and PG76-22). Since DM test is a non-destructive test (low strain level), the same samples prepared for DM tests were used for FN tests to compare the rutting resistance of HMA mixtures. Table 2.2 shows the experimental plan followed in this study.

Table 2.2. Experimental plan

Test type	Binder content	RAP content	Binder grade	Temp.[2]	Air-void content	Repl.[3]	Total tests
SCB	6.0% 6.4% 6.8%	30% 40%	PG 58-34 PG 64-22 PG 76-22	25 ºC	7%	4	72
Dynamic Modulus	6.0% 6.4% 6.8%	30% 40%	PG 58-34 PG 64-22 PG 76-22	1 run[1]	7%	2	36
Flow Number	6.0% 6.4% 6.8%	30% 40%	PG 58-34 PG 64-22 PG 76-22	54.7 ºC	7%	2	36

Note: [1]Samples were tested at temperatures of 4 ºC, 20 ºC, and 40 ºC and the loading frequencies of 0.1, 0.5, 1, 5, and 10 Hz. A loading frequency of 0.01 Hz was also used for 40 ºC tests.
[2]Temp. = Temperature.
[3]Repl. = Replicate.

2.3.2 Materials

This section provides information about virgin binders, virgin aggregates, and RAP aggregates used in this study. All the materials were obtained from local producers.

2.3.2.1 Aggregates

This study intends to evaluate the effects of binder content, RAP content, and binder grade on cracking performance of asphalt mixtures. Therefore, to determine the effects of these variables on performance, gradation was kept constant for all the samples. Virgin aggregates were donated by Old Castle Materials from the River Bend Sand and Gravel Company in Salem, Oregon. The virgin aggregates were delivered in three gradations, namely coarse (1/2" to #4), medium (#4 to #8), and fine (#8 to zero). To determine the gradation of each stockpiled aggregate, wet-sieve and dry-sieve analysis were performed on multiple samples of each stockpile following AASHTO T 27-11. Aggregate gradations are presented in Section 2.3.3.1.

2.3.2.2 Recycled asphalt pavement (RAP)

RAP material was also provided by Old Castle Materials from the River Bend Sand and Gravel Company in Salem, Oregon. Gradation, binder content, and theoretical maximum specific gravity

(G_{mm}) of RAP materials were provided by Old Castle. AASHTO T 308-10 was followed for binder extraction and RAP binder content measurements. The quantity of binder in RAP materials was determined as 6.22%. AASHTO T 30-10 was followed to determine the gradation of extracted RAP aggregates. For five samples of RAP materials, RAP aggregates were extracted, and their gradations were determined, as shown in Table 2.3. Then, to get the final RAP aggregate gradation, percent passing #200 sieve is reduced by 1 percent. This correction is applied due to the aggregate breakdown in ignition oven test (AASHTO T 30-10). Average and final gradation of RAP aggregates are presented in Table 2.3 and Figure 2.6. Detailed information about the RAP gradation, binder content, and theoretical specific gravity are given in Appendix A.

Table 2.3. RAP aggregate gradations

Stockpile	Sample 1	Sample 2	Sample 3	Sample 4	Sample 5	Average	Final Gradation
Sieve Size	Percentage Passing						
3/4"	100	100	100	100	100	100.0	100.0
1/2"	98.0	97.6	98.8	98.5	98.5	98.3	98.3
3/8"	88.3	87.5	87.7	90.8	87.1	88.3	88.3
1/4"	70.8	69.0	73.0	75.2	68.5	71.3	71.4
#4	61.3	60.2	63.9	65.6	58.4	61.9	62.0
#8	44.1	42.5	46.7	47.3	40.1	44.1	44.1
#16	31.1	30.1	33.6	33.6	27.3	31.1	31.1
#30	23.4	22.2	25.7	24.7	20.5	23.3	23.3
#50	17.1	16.5	18.7	18.2	15.2	17.1	17.1
#100	12.9	12.4	13.9	13.5	11.7	12.9	12.9
#200	9.6	9.2	10.2	9.6	8.6	9.4	8.4

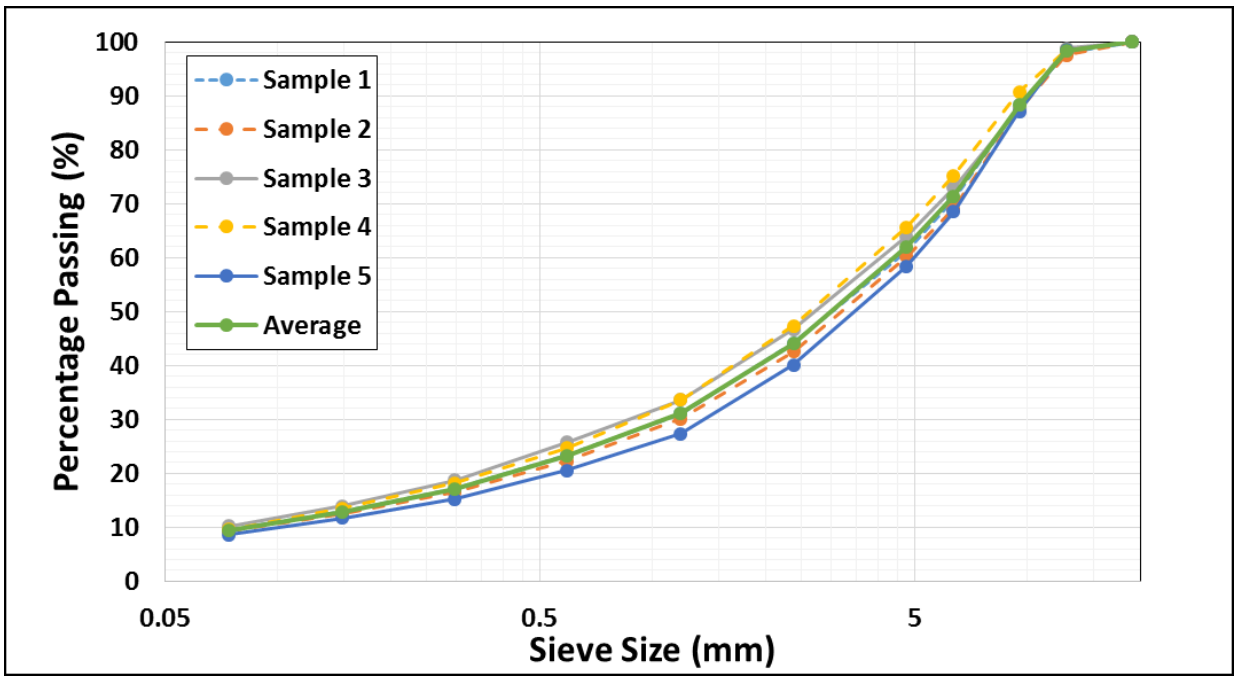

Figure 2.6. RAP aggregate gradations

2.3.2.3 Binders

McCall Oil and Chemical Corporation in Portland, Oregon (McCall) provided the virgin binders with different binder grades (PG 58-34, PG 64-22, and PG76-22) for this study. Temperature curves, mixing temperatures, and compaction temperatures were provided by McCall as well. Appendix B shows the temperature curves and binder properties for each binder grade. Laboratory mixing and compaction temperatures were estimated by using the viscosity-temperature lines given in Appendix B. An example of the viscosity-temperature line for binder grade of PG 58-34 is presented in Figure 2.7. The Asphalt Institute (2016) suggested that mixing and compaction temperatures can be determined where the viscosity is within the range of 0.17 ± 0.02 Pa-s and 0.28 ± 0.03 Pa-s, respectively. To create the viscosity-temperature line, rotational viscosity should be measured at 135 ºC and 165 ºC following the procedure described in AASHTO T 316-11.

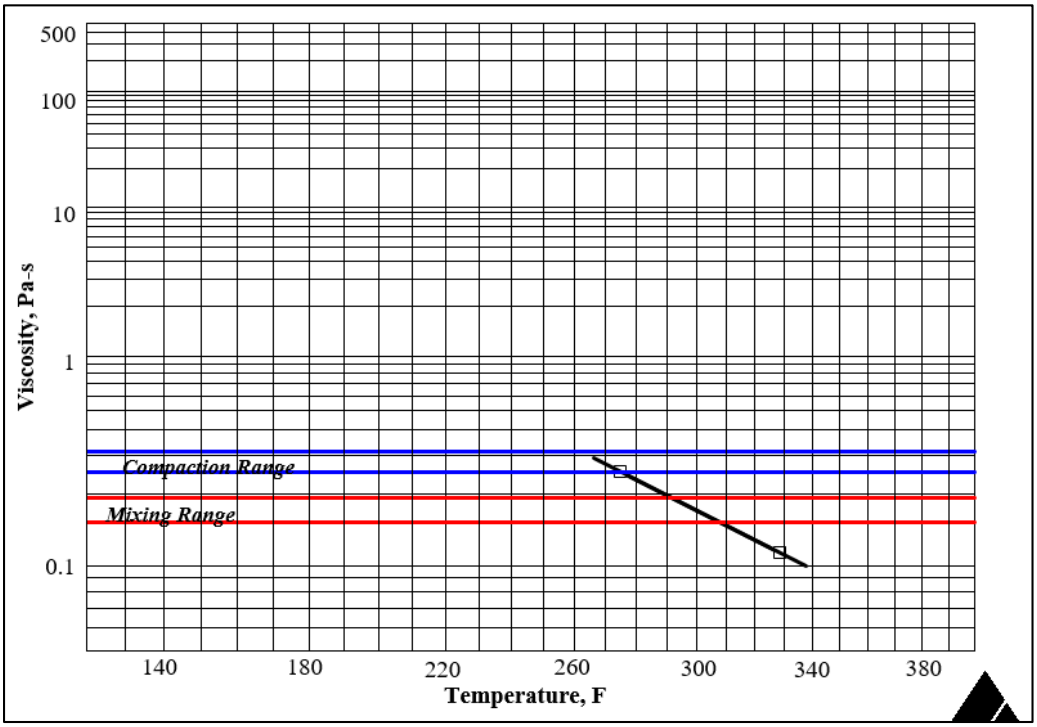

Figure 2.7. Viscosity-temperature line for binder grade of PG 58-34

Asphalt mixtures were prepared with three binder contents (6%, 6.4%, and 6.8%) in this study. These binder contents are the percentage of the total binder by the weight of the mix, and they include the recycled binder as well. In this study, it was assumed that all the RAP binder was completely blended with the virgin binder (100 % blending).

2.3.3 Sample preparation

2.3.3.1 Target gradations

Target gradation was obtained from an ODOT level 4 dense-graded mix design. All the mixes were designed based on the target gradation. Target gradation and the gradations of virgin aggregates and extracted RAP aggregates are presented in Table 2.4 and Figure 2.8.

Table 2.4. Target, extracted RAP, and stockpiled aggregate gradations

Sieve Size	Percentage Passing				
Stockpile	Coarse	Medium	Fine	RAP	Target Gradation
3/4"	100.0	100.0	100.0	100.0	100
1/2"	95.8	100.0	100.0	98.3	98
3/8"	53.1	98.2	100.0	88.3	83
1/4"	21.9	64.9	100.0	71.3	59
#4	13.2	38.0	99.9	61.9	49
#8	2.3	3.3	83.3	44.1	31
#16	1.3	1.3	55.1	31.1	22
#30	1.2	1.2	35.8	23.3	16
#50	1.1	1.1	23.7	17.1	11
#100	1.1	1.1	15.6	12.9	8
#200	0.9	1.0	10.7	8.4	6.3
pan	0	0	0	0	0

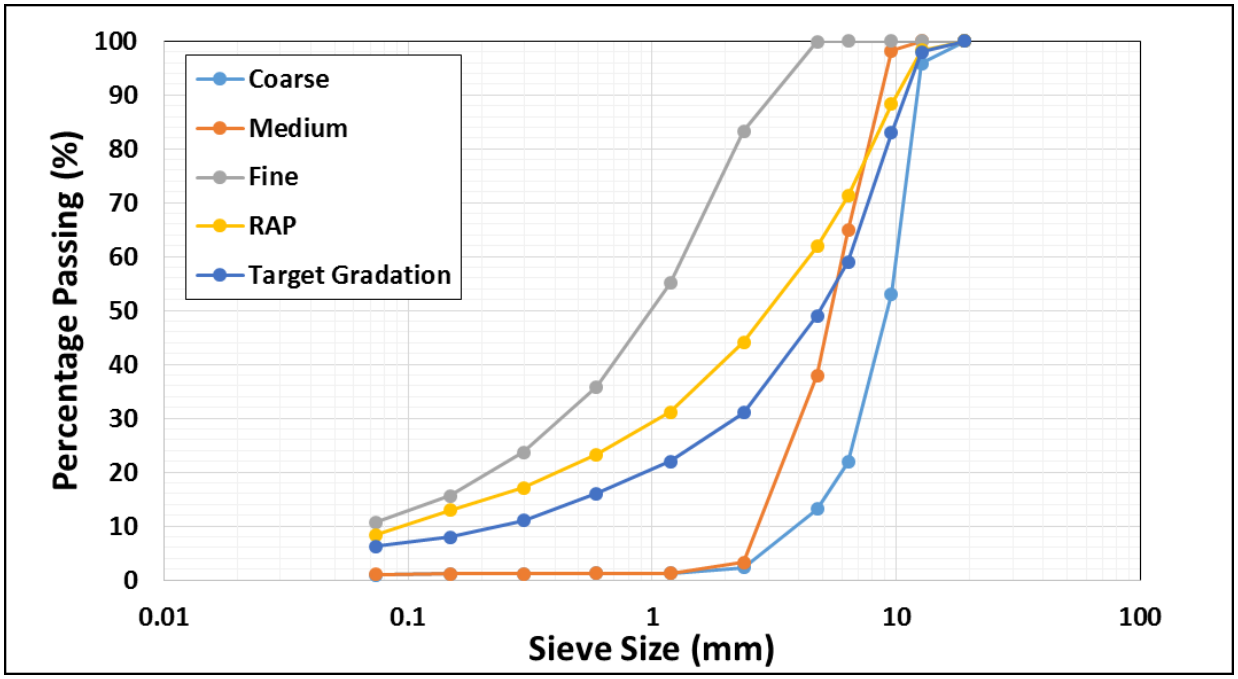

Figure 2.8. Target, extracted RAP, and stockpiled aggregate gradations

2.3.3.2 Batching

After measuring the gradations of virgin and RAP aggregates, three replicates of each combination of RAP content, binder content, and binder grade were mixed according to AASHTO T 312-12 and their G_{mm} were measured following the procedure described in AASHTO T 209-12. All the measured theoretical maximum specific gravities are presented in Appendix C. Then, aggregates were batched to meet the final gradation to reach 7% air content. To find the percentage of coarse, medium, fine, and RAP aggregates, optimization was conducted with Excel Solver 2013. Having G_{mm}, bulk specific gravity (G_{mb}) of samples required to reach 7% air-void content were calculated using Equation 2.3.1. G_{mb} is the density of asphalt mixture divided by the density of water at 23-^{o}C (Pavement Interactive 2017) (Equation 2.3.2). The total volume of the samples was calculated by knowing the dimensions of the compacted sample. Then, the total mass of samples was calculated using Equation 2.3.3. Mass of aggregates and binders were determined afterwards, and samples were batched for mixing and compaction. An example of batching calculation is shown in Appendix D.

$$\text{air voids (\%)} = \frac{G_{mm} - G_{mb}}{G_{mm}} * 100 \qquad \textbf{2.3.1}$$

$$G_{mb} = \frac{\text{mass per unit volume of asphalt mixture}}{\text{density of water}} \qquad \textbf{2.3.2}$$

$$\text{total mass of sample} = \text{density of water} * G_{mb} * \text{volume of sample} \qquad \textbf{2.3.3}$$

2.3.3.3 Mixing and compaction

Batched samples were mixed and compacted using AASHTO T 312-12 procedure. Before mixing, aggregates were kept in the oven at 10 ^{o}C higher than the mixing temperature, RAP materials were kept at 110 ^{o}C (Mcdaniel and Anderson 2001), and binder was kept at the mixing temperature for 2 hours. After mixing, prepared loose mixtures were kept in the oven for 4 hours at 135 ^{o}C (AASHTO R 30-10) to simulate short-term aging. The goal of short-term aging is to simulate the aging and binder absorption that occurs during mixing phase of the production process. Then the

aged loose asphalt mixtures were kept in the oven for 2 more hours at the compaction temperature prior to compaction.

2.3.3.4 Air content

All the samples were prepared for the target 7% air content. Air-void contents were measured for all the samples after compaction. To find the air contents, G_{mb} of the samples were measured after compaction by following AASHTO T 166-12. Then air voids were determined by using Equation 2.3.1. All the air contents should be within 7%±1%. In this study, all the samples met the requirement for air content while majority of the samples had air-void contents within 7%±0.5%.

2.4 TEST METHODS

Test methods followed in this study (for SCB, DM, and FN tests) to evaluate cracking and rutting performance of prepared asphalt mixtures with different RAP contents, binder contents, and binder grades are presented in this Chapter.

2.4.1 Semi-circular bend (SCB) test

SCB tests were conducted in this study to determine cracking performance of asphalt mixtures. Test method for evaluating cracking performance of asphalt concrete at intermediate temperatures developed by Wu et al. (2005) was followed.

2.4.1.1 Sample preparation

130 mm tall samples were compacted in the laboratory according to AASHTO T 312-12. Two samples with the thicknesses of 57 ± 2 mm were cut from each gyratory compacted sample using a high-accuracy saw (Figure 2.9a). Then the circular samples (cores) were cut into two identical halves (Figure 2.9b) using a special jig designed and developed at Oregon State University (OSU).

Wu et al. (2005) suggested testing samples with different notch depths (25.4 mm, 31.8 mm, and 38.0 mm). However, Ozer et al. (2016) and Nsengiyumva (2015) showed that reducing the notch depth reduces the variability. For this reason, in this study, a 15 mm notch depth is selected for sample preparation. A notch along the axis of symmetry of each half was created with the table saw using another special cutting jig developed at OSU (Figure 2.9c). Notch depth was 15 ± 0.5-mm in length and 3 mm wide.

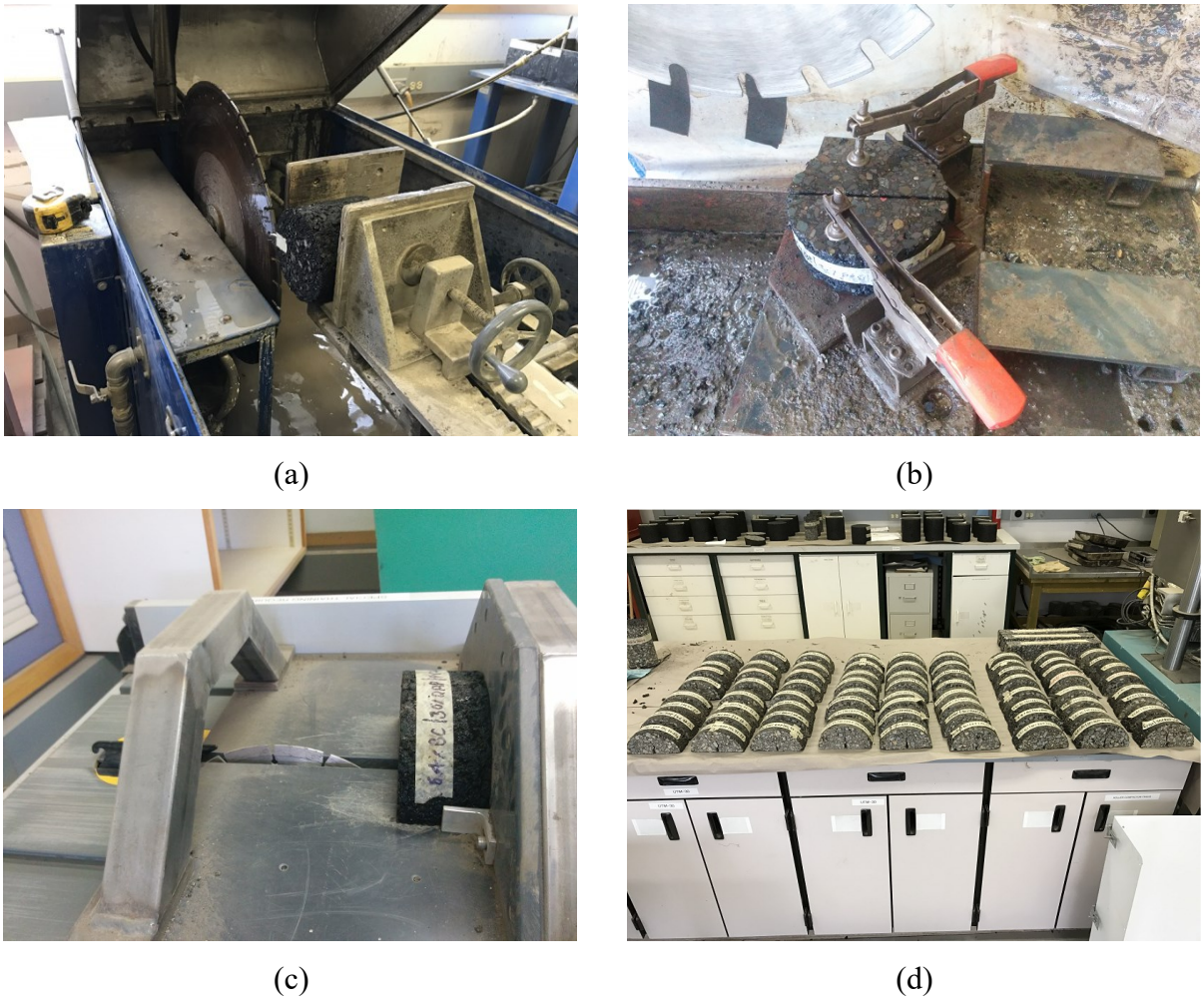

(a) (b)

(c) (d)

Figure 2.9. Cutting and notching procedure for SCB sample preparation.

2.4.1.2 Testing

Tests were conducted at 25 ºC with a displacement rate of 0.5 mm/min (AASHTO TP 105-13). Samples were kept in the chamber at the testing temperature for conditioning the day before being tested. The flat side of semi-circular samples was placed on two rollers (Figure 2.10). As vertical load with constant displacement rate is applied on the samples, applied load is measured (AASHTO TP 105-13). The test stops when the load drops below 0.5 kN. Fracture energy (G_f), fracture toughness (K_{IC}), secant stiffness (S), and flexibility index (FI) are the testing parameters obtained from this test. Procedures followed to calculate these test parameters are given in the next section.

Figure 2.10. SCB loading set up and test

2.4.1.3 Parameters obtained from SCB tests

This section describes the parameters obtained from SCB test results (displacement vs. load curves) including fracture energy (G_f), fracture toughness (K_{IC}), secant stiffness (S), and flexibility index (FI). The most effective parameter to identify the effects of RAP content, binder content, and PG grade on cracking resistance was also determined. Moreover, a MATLAB (2016) code and a stand-alone software were developed. Developed software takes the raw test data, processes it, and calculates all these parameters.

- **Fracture Energy (G_f)**

Fracture energy (G_f) is obtained by dividing the work of fracture (W_f) by the ligament area (A_{lig} in Equation 2.4.1). As the G_f increases, the work required for crack initiation and propagation increases. Therefore, asphalt mixtures with higher G_f values are expected to show higher resistance to cracking (Ozer et al. 2016). Work of fracture is the area under load versus displacement (P-u) curve (Figure 2.11). The test stops when the load drops below 0.5 kN. The remainder of the curve is extrapolated to estimate the area under the tail part of the P-u curve. W_f is the sum of the area under the curve obtained from the test (W) and the extrapolated tail part (W_{tail}) as it is shown in Figure 2.11.

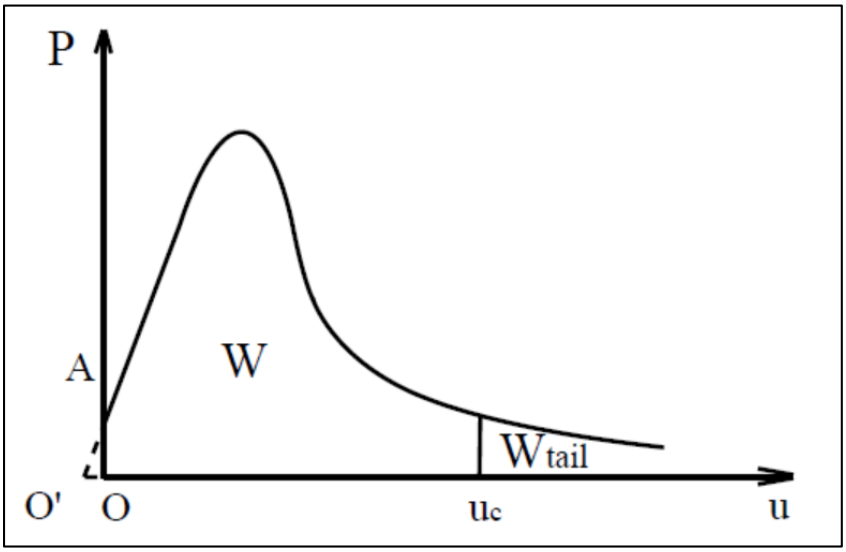

Figure 2.11. Load versus displacement (P-u) curve (AASHTO TP 105-13)

W_f is calculated as follows (AASHTO TP 105-13):

$$G_f = \frac{W_f}{A_{lig}} \quad \textbf{2.4.1}$$

$$W_f = \int P\, du \quad \textbf{2.4.2}$$

$$A_{lig} = (r-a)*t \quad \textbf{2.4.3}$$

Where:

G_f = fracture energy (kJ/m2),

W_f = work of fracture (kJ),

P = applied load (kN),

u = load line displacement (m),

A_{lig} = ligament area (m^2),

r = sample radius (m),

a = notch length (m), and

t = sample thickness (m).

Quadrangle rule is used to calculate the area under the curve obtained from the test (W) using Equation 2.4.4 (AASHTO TP 105-13):

$$W=\sum_{i=1}^{n}(u_{i+1}-u_i)*(P_i)+\frac{1}{2}*(u_{i+1}-u_i)*(P_{i+1}-P_i) \quad \textbf{2.4.4}$$

Where:

P_i = applied load (KN) at the i load step application,

P_{i+1} = applied load (KN) at the i+1 load step application,

u_i = load line displacement (m) at the i step, and

u_{i+1} = load line displacement (m) at the i+1 step.

Power function with a coefficient of -2 is used to fit the post-peak part of the P-u curve starting from the point at which P value is lower than the 60% of the peak load. After fitting the curve, coefficient c is obtained using Equation 2.4.5 (AASHTO TP 105-13). Then the area under the extrapolated tail part (W_{tail}) is estimated using Equation 2.4.6 (AASHTO TP 105-13).

$$P=\frac{c}{u^2} \quad \textbf{2.4.5}$$

$$W_{tail}=\int_{u_c}^{\infty} P\,du=\int_{u_c}^{\infty}\frac{c}{u^2}\,du=\frac{c}{u_c} \quad \textbf{2.4.6}$$

Where:

u = integration variable equal to load line displacement (m), and

u_c = load line displacement value at which the test is stopped (m).

Consequently, total area under the curve (W_f) is obtained as follows (AASHTO TP 105-13):

$$W_f=W+W_{tail} \quad \textbf{2.4.7}$$

- **Fracture Toughness (K_{IC})**

Fracture toughness (K_{IC}) is the stress intensity factor at peak load. It shows how much energy is required for crack formation. Higher K_{IC} indicates higher brittleness of mixtures. The following equation is used to compute K_{IC} (AASHTO TP 105-13):

$$\frac{K_{IC}}{\sigma_0\sqrt{\pi a}}=Y_{I(0.8)} \quad \textbf{2.4.8}$$

$$\sigma_0=\frac{P_{peak}}{2rt} \quad \textbf{2.4.9}$$

$$Y_{I(0.8)}=4.782+1.219\left(\frac{a}{r}\right)+0.063*\exp\left(7.045\left(\frac{a}{r}\right)\right) \quad \textbf{2.4.10}$$

Where:

P_{peak} = peak load (MN),

r = sample radius (m),

t = sample thickness (m),

a = notch length (m), and

$Y_{I(0.8)}$ = the normalized stress intensity factor (dimensionless).

- **Secant Stiffness (S)**

Secant stiffness (S) is the ratio of the peak load to the vertical deformation required to reach the peak deformation. Higher values for S indicate higher resistance to crack initiation and higher brittleness (Harvey et al. 2015).

$$S\ (KN/mm)=\frac{\Delta y}{\Delta x}=\frac{\text{peak load}}{\text{vertical deformation at peak load}} \quad \textbf{2.4.11}$$

- **Flexibility Index (FI)**

Flexibility index (FI) is the ratio of the fracture energy (G_f) to the slope of the line at the post-peak inflection point of the load-displacement curve (Figure 2.12). FI correlates with brittleness, and it was developed for asphalt materials by Ozer et al. (2016). Lower FI values show that the asphalt mixtures are more brittle with higher crack growth rate (Ozer et al. 2016).

$$FI=A*\frac{G_f}{abs(m)} \quad \textbf{2.4.12}$$

Where:

G_f = fracture energy (KJ/m^2),

abs(m) = absolute value of the slope at inflection point of post-peak load-displacement curve, and

A = unit conversion factor and scaling coefficient.

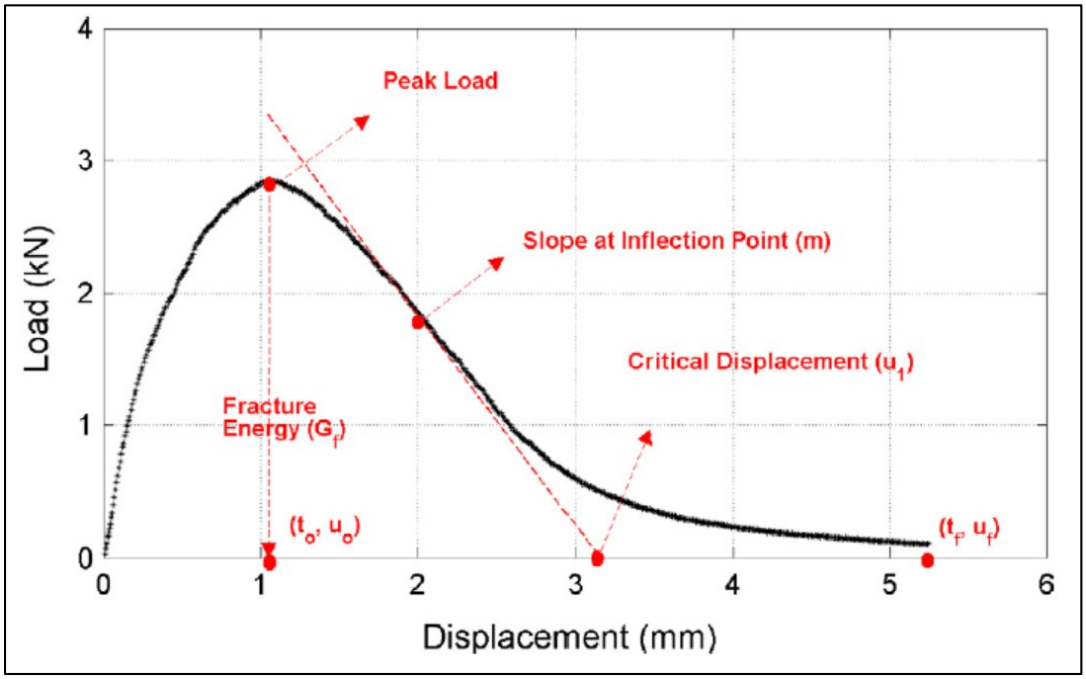

Figure 2.12. Illustration of load-displacement curve and slope at inflection point (m) (Ozer et al. 2016)

2.4.1.4 Comparison of fracture energy (G_f) to flexibility index (FI)

Brittle mixtures require higher energy for crack initiation, but once the crack starts, it propagates rapidly. Conversely, ductile mixtures need less energy for crack initiation, but crack grows slower. Load-displacement curves of ductile and brittle mixtures are shown in Figure 2.13. The area under the load-displacement curve is higher for the brittle mixture compared to the ductile mixture. Thus, the brittle mixture seems to have higher G_f value. On the contrary, since the slope at the inflection point is also higher for the brittle mixture, FI value decreases. The ductile mixture has a smaller area under the curve and smaller slope at the inflection point and it has higher FI than the brittle mixture. It can be concluded that FI is a better performance indicator than G_f since it properly describes crack initiation and propagation stages of the load-displacement curve (Ozer et al. 2016). Results of this study also show that FI is able to identify the effects of binder content, PG grade, and RAP content on cracking resistance (See Section 2.5.1).

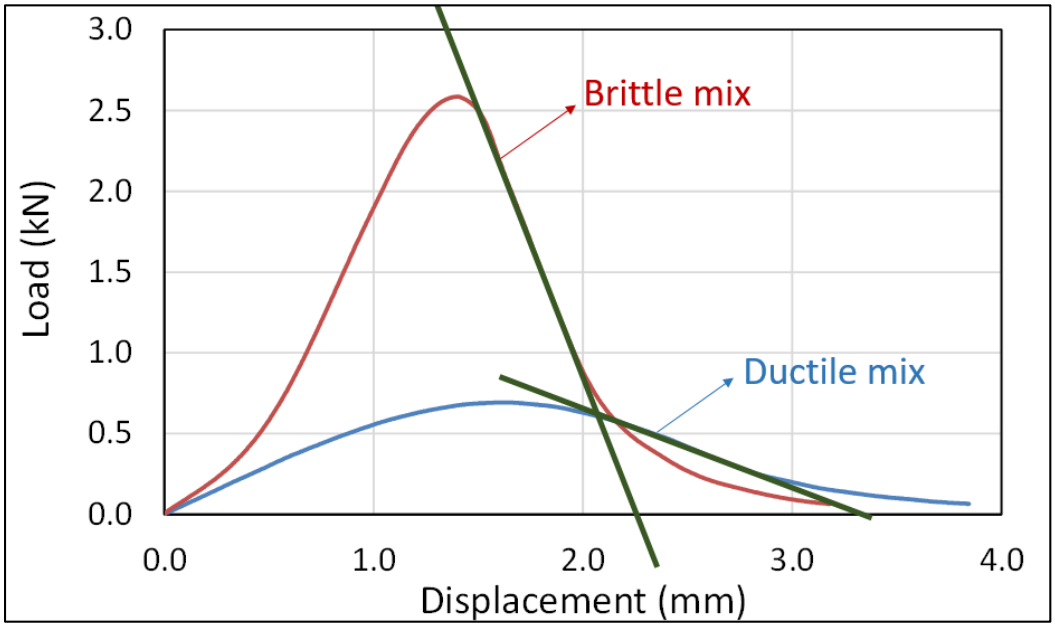

Figure 2.13. Illustration of load-displacement curve of ductile and brittle mixtures

2.4.2 Dynamic modulus test

Asphalt concrete mixtures are viscoelastic materials that show both viscous and elastic behavior. At lower temperatures and higher loading frequencies, elastic behavior becomes more dominant while viscous components are more apparent at higher temperatures and lower loading frequencies. DM tests are conducted to characterize the elastic modulus of asphalt concrete mixtures at different loading frequencies and temperatures. DM tests are performed at low strain levels (about 100με) to determine the elastic modulus in the linear viscoelastic range. The effects of loading time and temperature on elastic modulus is modeled and presented in the form of master curves (Norouzi et al. 2015).

DM test can be used to evaluate rutting and cracking performance of asphalt pavements (Zhou et al. 2015) if the asphalt mixtures do not have special additives such as fibers, polymers or rubber. In this study, DM tests were conducted on prepared samples with different RAP contents (30% and 40%), binder contents (6%, 6.4%, and 6.8%), and binder grades (PG 58-34, PG 64-22, and PG 76-22) (See Table 2.2). The procedure described in AASHTO TP 79-13 for unconfined testing is followed in this study. DM test samples were required to be 150 ± 2.5 mm tall and 100 ± 2.5 mm in diameter. Temperatures of 4 ºC, 20 ºC, and 40 ºC, and frequencies of 0.1 Hz, 0.5 Hz, 1 Hz, 5

Hz, and 10 Hz were used for this study. The frequency of 0.01 Hz was also used for only tests conducted at 40°C. These loading frequencies simulate different traffic speeds. Higher frequencies represent higher vehicle speeds.

DM test is a strong indicator of asphalt mixture performance. Dynamic modulus and phase angle are two performance variables obtained from DM tests. Dynamic modulus shows how stiff an asphalt mixture is. Higher dynamic modulus values represent higher stiffness. The time delay between the time point at which peak stress applied and the time point at which peak strain observed is used to calculate phase angle. Phase angle represents viscoelastic characteristics of asphalt mixtures. Higher phase angle indicates that the samples are more viscous, more susceptible to rutting, and more resistant to cracking (Darnell and Bell 2015).

In this study, 170 mm tall samples were prepared by using gyratory compaction according to AASHTO PP 60-14. Then, samples were cored in 100 mm diameter and their edges were cut off to get 150 mm tall samples. Samples were kept in the chamber for conditioning at the testing temperatures the day before being tested.

After conducting the tests, master curves were developed for dynamic modulus and phase angle following AASHTO PP 61-13 procedure. Master curves display phase angle and dynamic modulus with respect to loading frequencies. Master curves are presented in Section 2.5.3.1. Appendix F shows one example of the data generated by the test equipment for DM test, along with the procedure of developing the master curves.

2.4.3 Flow number test

Flow number (FN) test is a performance test for evaluating rutting performance of asphalt concrete mixtures (Bonaquist et al. 2003). In this test, while constant deviator stress is applied at each load cycle on the test sample, permanent strain at each cycle is measured (Figure 2.14). Permanent deformation of asphalt pavements has three stages: 1) primary or the initial consolidation, 2) secondary, and 3) tertiary or shear deformation (Biligiri et al. 2007). Figure 2.14 shows three stages of permanent deformation. FN is the loading cycle at which the tertiary stage starts after the secondary stage.

In this study, testing conditions and criteria for FN testing described in AASHTO TP 79-13 for unconfined tests were followed. The recommended test temperature, determined by LTPPBind Version 3.1 software, is the average design high pavement temperature at 50% reliability for cities in Oregon with high populations and at a depth of 20 mm (0.79 in) for surface courses (Rodezno et al. 2015). Tests were conducted at the temperature of 54.7ºC with average deviator stress of 600 kPa and minimum (contact) axial stress of 30 kPa. For conditioning, samples were kept in the chamber at the testing temperature a day prior to being tested. To calculate FN, Francken model was used in this study. This model is discussed in Section 2.4.3.1.

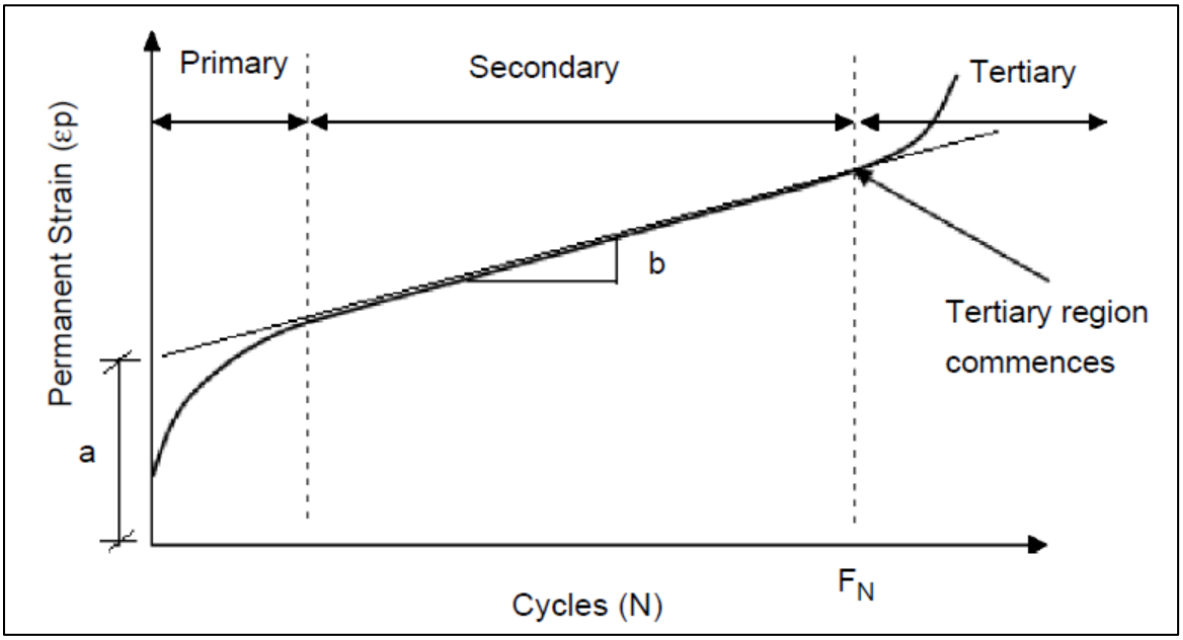

Figure 2.14. Relationship between permanent strain and load cycles in FN test (Biligiri et al. 2007)

Minimum FN values (calculated by using the Francken model) for different traffic levels recommended by AASHTO TP 79-13 are given in Table 2.5 (Rodezno et al. 2015). All high RAP mixes recommended in this study had FN values higher than the 740 limit.

Table 2.5. Minimum average FN requirement for different traffic levels (AASHTO TP 79-13)

Traffic (million ESALs)	Minimum Average FN Requirement
<3	NA
3 to <10	50
10 to <30	190
≥30	740

Note: NA= not applicable.

2.4.3.1 Francken Model

Francken Model was developed for triaxial and uniaxial repeated-load tests for different temperatures and stress levels (Francken 1977). A study carried out by Biligiri et al. (2007) showed that this model calculates FN more accurately compared to other mathematical models. This model can also represent all three stages of deformation (1.primary or the initial consolidation of the mix, 2. secondary, and 3. tertiary or shear deformation) more properly. Moreover, Dongre et al. (2009) confirmed the robustness of Francken model by fitting FN data obtained from field projects. The model is given as follows:

$$\epsilon_p(N)=AN^B+C(e^{DN}-1) \quad \textbf{2.4.13}$$

Where:
$\epsilon_p(N)$ = permanent deformation or permanent strain from F_n test,
N = number of loading cycles, and
A, B, C, D = regression constants.

The rate of change of the slope of the permanent strain is obtained by taking the second derivative of the Francken model (2.4.14). The inflection point, at which the sign of the rate of change of slope changes, is considered as FN and indicates when the tertiary stage begins. FN is the number of cycles at which the second derivative of the Francken model is zero. The second derivative of the model is as follows (Dongre et al. 2009):

$$\frac{\partial^2\epsilon_p}{\partial N^2}=A*B*(B-1)*N^{B-2}+(C*D*e^{D*N}) \quad \textbf{2.4.14}$$

The model shown in Equation 2.4.13 is fitted to the permanent strain versus the number of cycles for each sample. After estimating the regression constants (A, B, C, and D), to find the number of load cycles at the inflection point, FN is computed at which the 2.4.14 (second derivative of Francken model) is equal to zero. In this study, a code was developed using MATLAB (2016) to analyze the data and calculate regression constants (A, B, C, and D) of the Francken model to find the FN for each test.

2.5 RESULTS AND DISCUSSION

This section presents the results of SCB tests to evaluate cracking performance of high RAP asphalt mixtures of this study. FN tests were used to quantify the rutting performance of asphalt mixtures. DM test results were used to quantify the viscous and elastic behavior of all mixes. Regression equations were developed and Monte Carlo simulations were performed using the developed equations to determine the required binder content, binder grade, and RAP content of asphalt mixtures to meet rutting and cracking resistance requirements.

2.5.1 Semi-circular bend test

SCB tests were conducted at 25 ºC in this study to evaluate cracking performance of asphalt mixtures. A full factorial experimental plan with two RAP contents (30% and 40%), three different binder contents (6%, 6.4%, and 6.8%), and three binder grades (PG 58-34, PG 64-22, and PG 76-22) is followed in this study (See Table 2.2). Four replicates were tested for each combination. In total, 72 tests were conducted. Applied peak load (P_{peak}), fracture energy (G_f), fracture toughness (K_{IC}), secant stiffness (S), and flexibility index (FI) are the testing parameters obtained from the test results. The results of SCB tests are presented in Figure 2.15 to Figure 2.18. Appendix E shows the SCB parameters calculated for every sample.

As it is shown in Figure 2.15, FI increases as the binder content increases for mixtures with the same RAP contents. Asphalt mixtures with lower binder contents are more brittle and more susceptible to cracking. Results of this study show that asphalt mixtures with 30% RAP have higher FI than the asphalt mixtures with 40% RAP. Higher RAP contents result in more brittle mixes and less crack resistance. Moreover, using softer binders increases FI. As it is expected, the mixture with the softest binder grade (PG 58-34), the highest binder content (6.8%), and the lowest RAP content has the greatest FI. Conversely, the mixture with PG 76-22 binder grade, 6% binder content, and 40% RAP content shows the lowest FI value. Al-Qadi et al. (Al-Qadi et al. 2015) defined a threshold for FI representing the cracking performance of asphalt mixtures. Mixtures with FI higher than 10 were considered to have high cracking performance (Al-qadi and Ozer 2015). Also, some samples of production mixes were collected from the plant and compacted in the laboratory in ODOT SPR785 project (Coleri 2017). Average FI for the non-polymer mix used

for construction on a major highway in Oregon was around 9, and the mix with the best cracking resistance had FI of 14. Therefore, this study suggests 9 to 14 as a possible range of FI values of mixtures with acceptable cracking performance. In this study six mixtures met the threshold: 1) BC 6%, RAP 30%, PG 58-34, 2) BC[6] 6.8%, RAP 30%, PG 58-34, 3) BC 6.8%, RAP 30%, PG 64-22, 4) BC 6.8%, RAP 40%, PG 58-34, 5) BC 6.8%, RAP 40%, PG 64-22, and 6) BC 6.4%, RAP 30%, PG 58-34. It can be concluded that the FI is a good performance indicator since it can differentiate the cracking performance of asphalt mixtures with different RAP contents, binder contents, and binder grades.

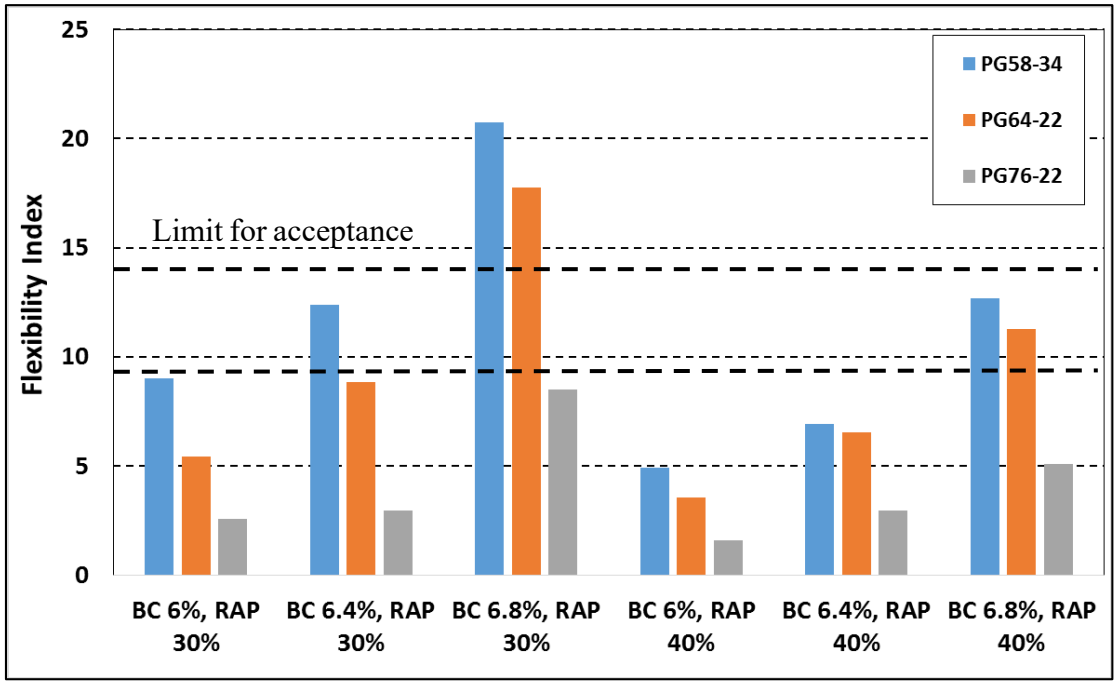

Figure 2.15. Flexibility index for mixtures with different RAP contents (30% and 40%), binder grades (PG 58-34, PG 64-22, and PG 76-22), and binder contents (6%, 6.4%, and 6.8%)

As fracture energy (G_f) increases, the work required for crack formation and propagation increases. Therefore, asphalt mixtures with higher G_f values are expected to show higher resistance to

[6] Binder content

cracking (Ozer et al. 2016). Results of this study show that there is not a strong correlation between the properties of asphalt mixtures and G_f. This is evident especially for mixtures with PG 64-22 binder. As binder content increases, increase in G_f cannot be observed (Figure 2.16). Moreover, G_f has slightly changed for the mixtures with PG 58-34 and PG 76-22 for different binder contents. Also, G_f could not differentiate the cracking performance of the mixtures with different RAP contents. These results suggest that G_f, the most common parameter that has been used to characterize cracking resistance of asphalt mixtures in several research studies, is not an effective parameter to use for cracking performance evaluation.

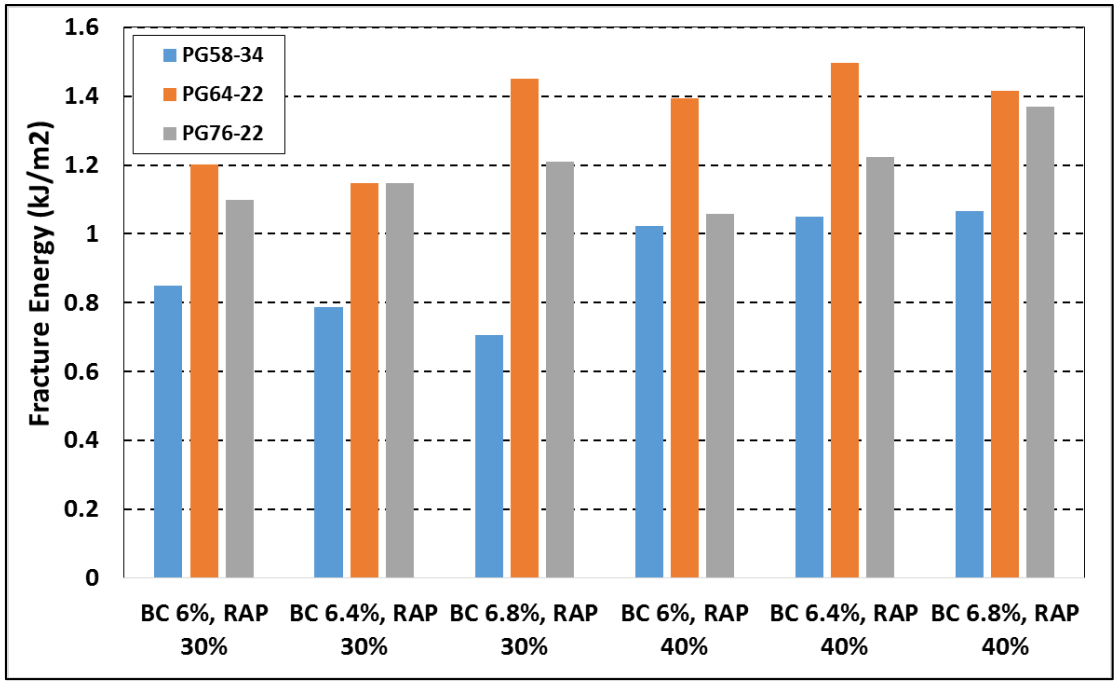

Figure 2.16. Fracture energy for mixtures with different RAP contents (30% and 40%), binder grades (PG 58-34, PG 64-22, and PG 76-22), and binder contents (6%, 6.4%, and 6.8%)

K_{IC} and S correlate well with cracking resistance and brittleness. Higher values for these two variables indicate higher resistance to crack formation and higher brittleness. Figure 2.17 and Figure 2.18 show that mixtures with BC 6.8%, RAP 30%, PG 58-34 and BC 6%, RAP 40%, PG 76-22 have the lowest and the highest S and K_{IC}, respectively. Asphalt mixtures with lower K_{IC} and S values and higher FI require less energy for crack initiation, but since they are more ductile,

they have higher crack propagation resistance. In this study, although the mixture with 40% RAP, 6% binder content, and PG 76-22 has the highest K_{IC} and S values, it has the lowest FI value. It means that it requires higher energy for crack initiation, but once the crack starts, it propagates rapidly. All possible combinations of RAP content, binder content, and binder grade to achieve acceptable cracking and rutting performance are determined using regression equations and provided in Section 2.5.4.

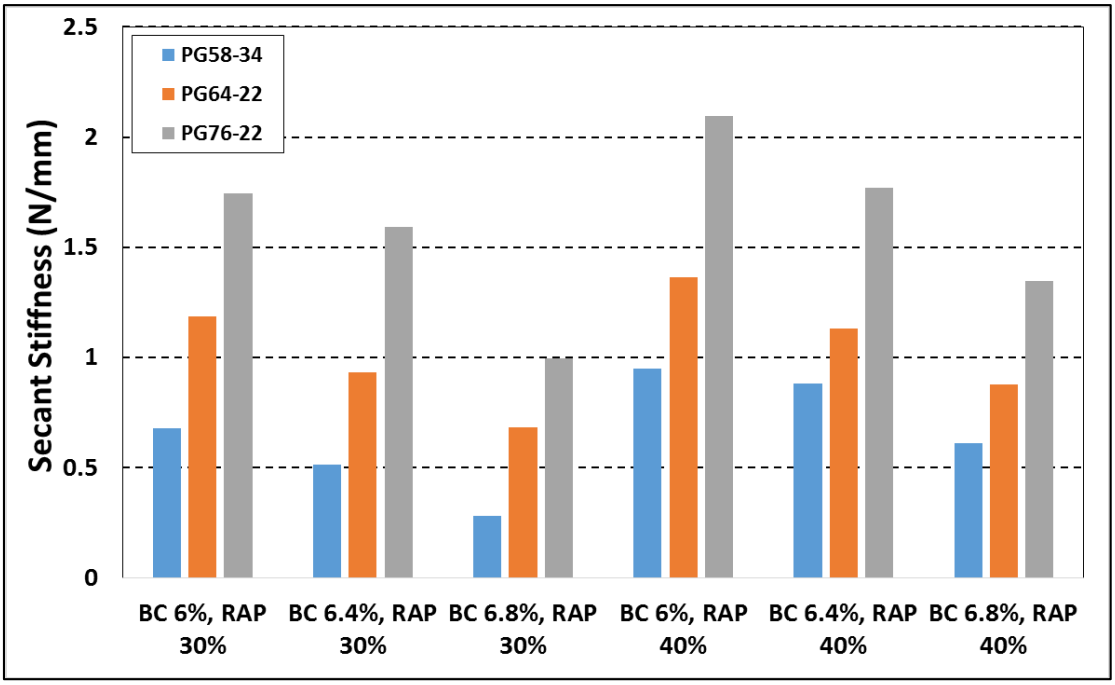

Figure 2.17. Secant stiffness for mixtures with different RAP contents (30% and 40%), binder grades (PG 58-34, PG 64-22, and PG 76-22), and binder contents (6%, 6.4%, and 6.8%)

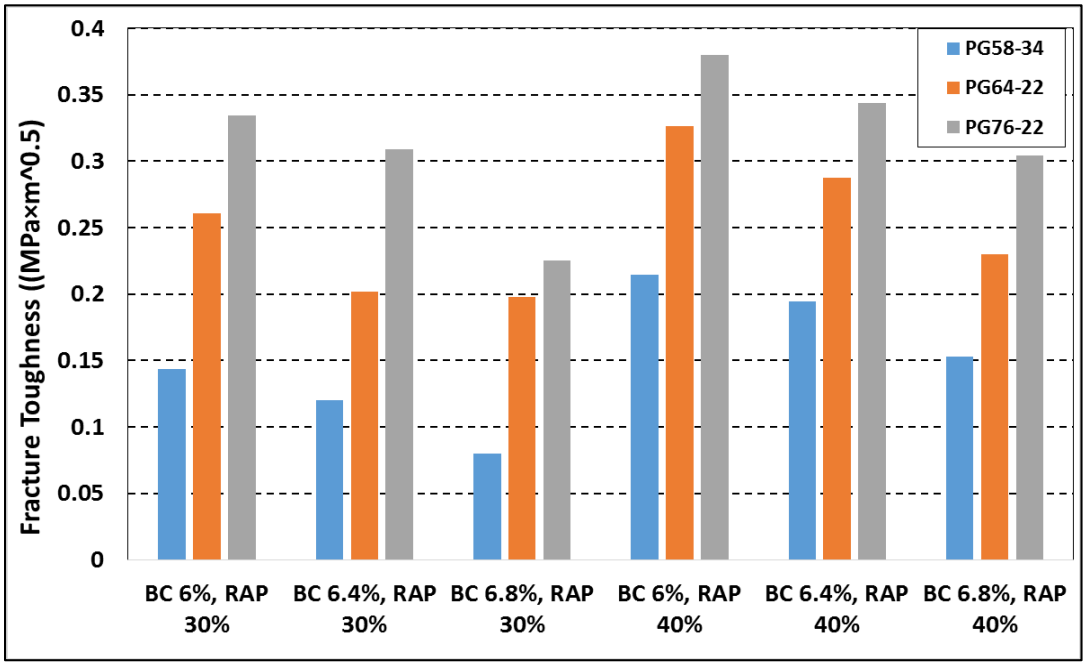

Figure 2.18. Fracture toughness for mixtures with different RAP contents (30% and 40%), binder grades (PG 58-34, PG 64-22, and PG 76-22), and binder contents (6%, 6.4%, and 6.8%)

2.5.2 Flow number test

Flow number (FN) test is a simple performance test for evaluating rutting performance of asphalt concrete mixtures (Bonaquist et al. 2003). High FN values indicate that asphalt mixtures have high rutting resistance. FNs for all experiments are given in Appendix G. Figure 2.19 to Figure 2.21 summarize the FN values for all tested asphalt mixtures.

Minimum required FNs suggested by AASHTO TP 79-13 for different traffic levels are presented in Table 2.5. Suggested FN for the traffic level of 10 million to 30 million ESALs is specified as 190 while the FN limit for roadways with ESALs more than 30 million were specified as 740. In Figure 2.19 to Figure 2.21 dashed red line and solid red line show the recommended FN for the traffic level of 10 to <30 and ≥30 million ESALs, respectively. FN values for all the asphalt mixtures were greater than 50, which is the recommended FN for the traffic level of 3 million to 10 million ESALs. All the asphalt mixtures with PG 64-22 and PG 76-22 binders had FN values higher than 740, except for the mixture with BC 6.8%, RAP 30%, and PG 64-22. Mixtures with

PG 58-34 had acceptable rutting resistance for the traffic level of 10 to <30 million ESALs (with FN greater than 190) except for the mixture with BC 6.8%, RAP 30%, and PG 58-34 (FN=171). Only two mixtures (BC 6%-RAP 40%-PG 58-34 and BC 6.4%-RAP 40%-PG 58-34) had FN greater than 740, meaning that they show acceptable rutting performance for a traffic level of ≥30 million ESALs. FN values for all tested asphalt mixtures are presented in Figure 2.22.

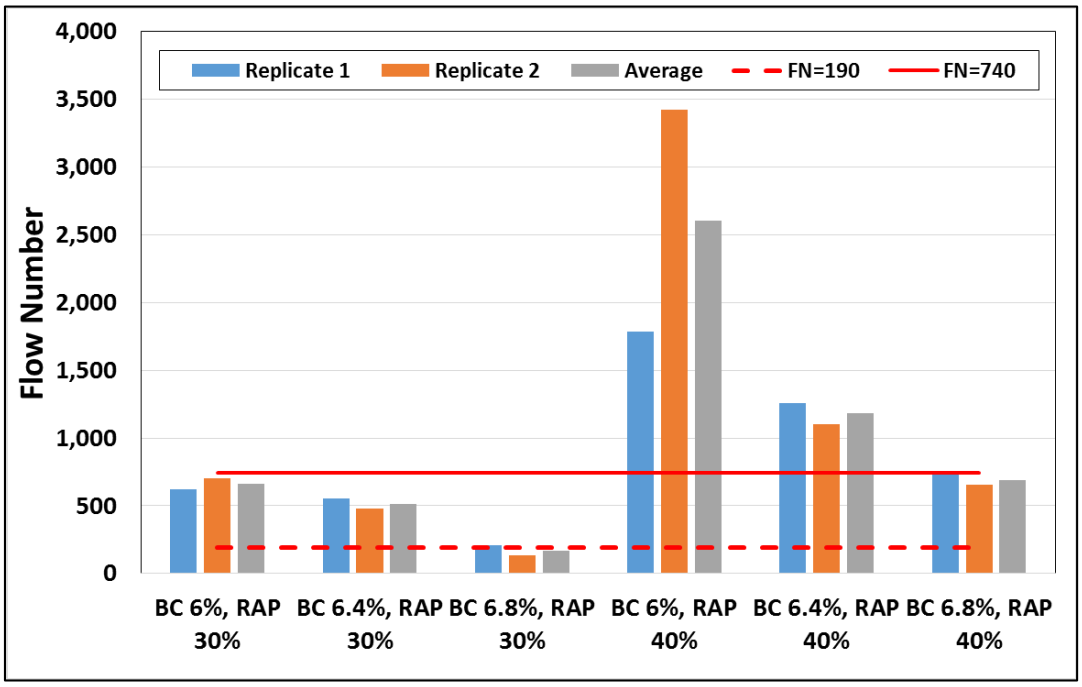

Figure 2.19. Flow number of the mixtures with different RAP contents (30% and 40%), binder grade of PG 58-34, and different binder contents (6%, 6.4%, and 6.8%)

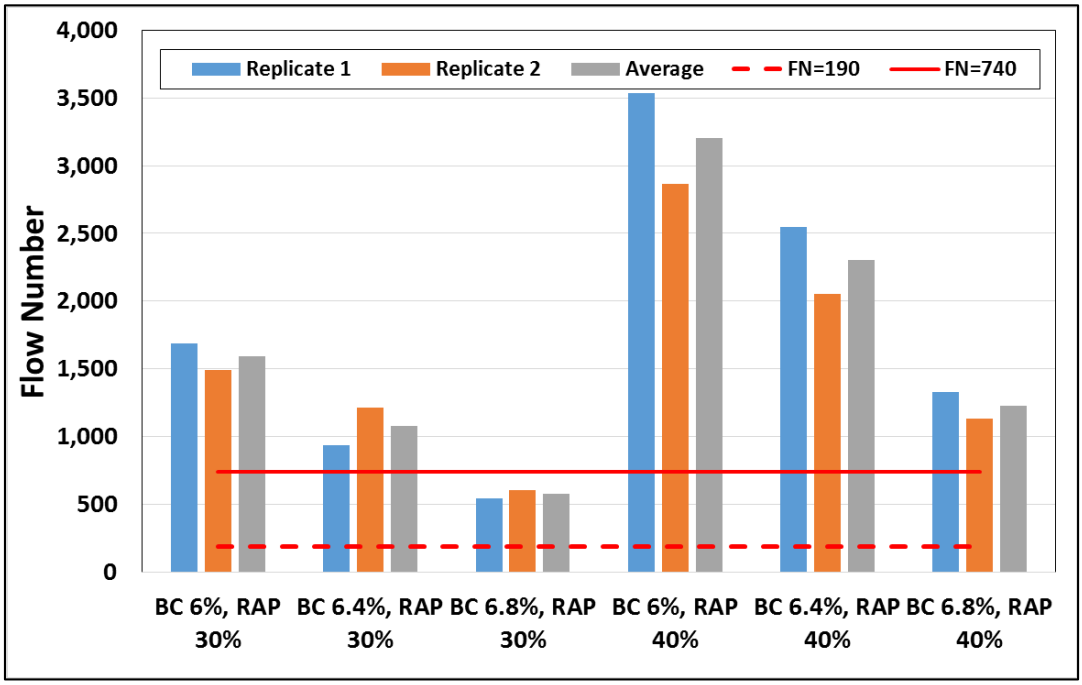

Figure 2.20. Flow number of the mixtures with different RAP contents (30% and 40%), binder grade of PG 64-22, and different binder contents (6%, 6.4%, and 6.8%)

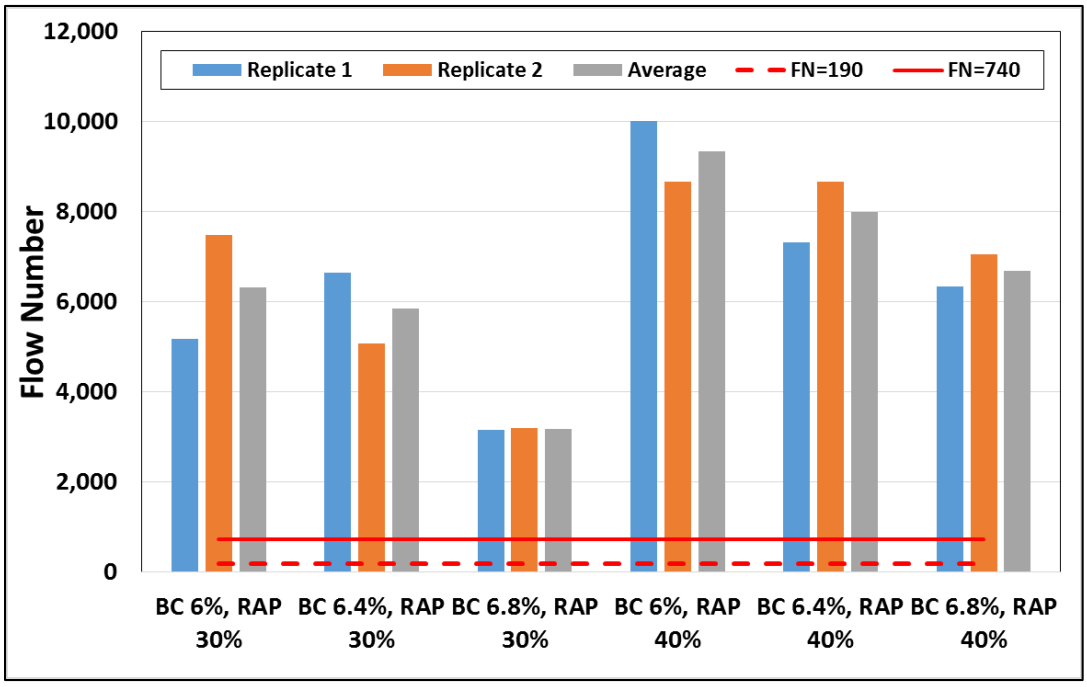

Figure 2.21. Flow number of the mixtures with different RAP contents (30% and 40%), binder grade of PG 76-22, and different binder contents (6%, 6.4%, and 6.8%)

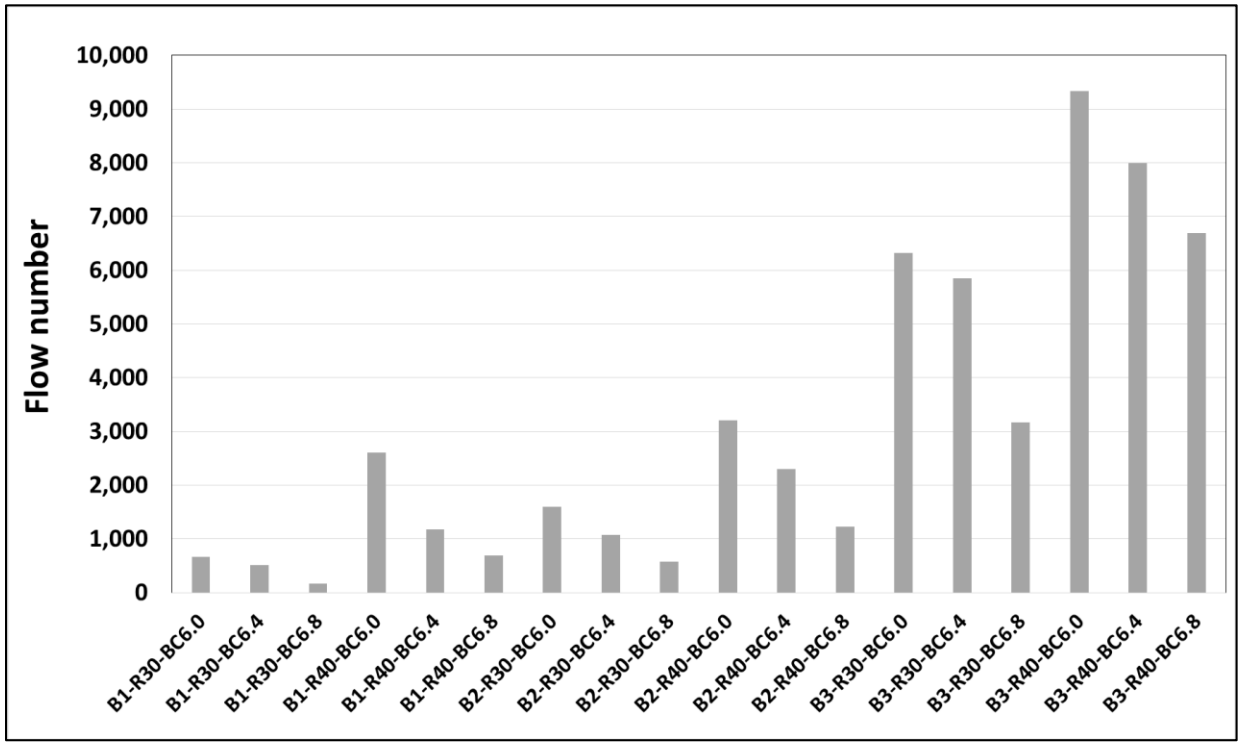

Figure 2.22. Average flow number of the mixtures for all the combinations of RAP contents, binder contents, and binder grades

Note: B1= PG 58-34, B2= PG 64-22, and B3 = PG 76-22.
R30 = 30% RAP, and R40 = 40% RAP.
BC6= 6% binder content, BC6.4 =6.4 % binder content, and BC6.8 = 6.8% binder content.

2.5.3 Dynamic modulus test

In this study, DM tests were conducted on prepared asphalt mixtures with different RAP contents (30% and 40%), binder contents (6%, 6.4%, and 6.8%), and binder grades (PG 58-34, PG 64-22, and PG 76-22). Two replicate experiments were conducted for each combination of the variable of interests. Therefore, 36 mixtures were totally tested at the testing frequencies and temperatures given in Section 2.4.2. The testing procedure was followed as the procedure described in AASHTO TP 79-13 for unconfined mixtures. Dynamic modulus and phase angle master curves are presented and discussed in the following sections.

2.5.3.1 Master curves for dynamic modulus

This section represents the dynamic modulus master curves for asphalt mixtures. Average of test results for two replicate mixtures were used to develop each master curve as recommended by AASHTO TP 79-13.

Master curves of dynamic modulus for the mixtures with different RAP contents (30% and 40%), different binder contents (6%, 6.4%, and 6.8%), and different binder grades (PG 58-34, PG 64-22, and PG 76-22) are presented in Figure 2.23 to Figure 2.25. Reference temperature for all the master curves is 20°C. In general, higher RAP content and lower binder content resulted in higher dynamic modulus. RAP content plays a significant role in cracking resistance of the mixtures. For the same binder grade, the mixtures with 40% RAP had higher dynamic modulus than the mixtures with 30% RAP for all the binder contents.

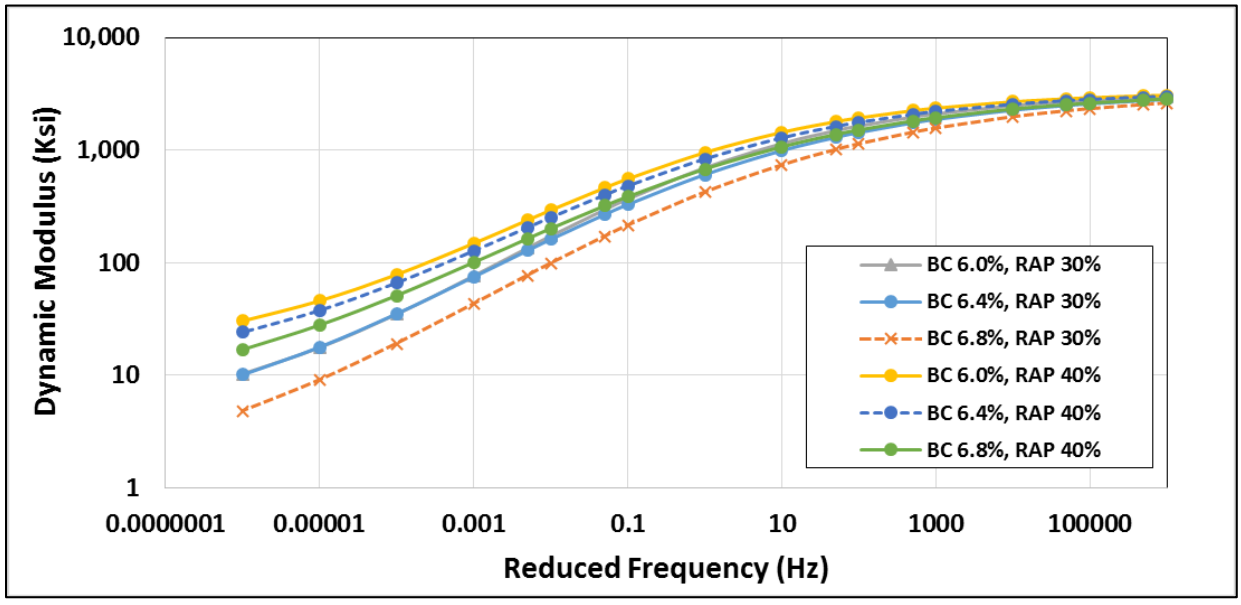

Figure 2.23. Master curves of dynamic modulus for the mixtures with different RAP contents (30% and 40%), binder grade of PG 58-34, and different binder contents (6%, 6.4%, and 6.8%)

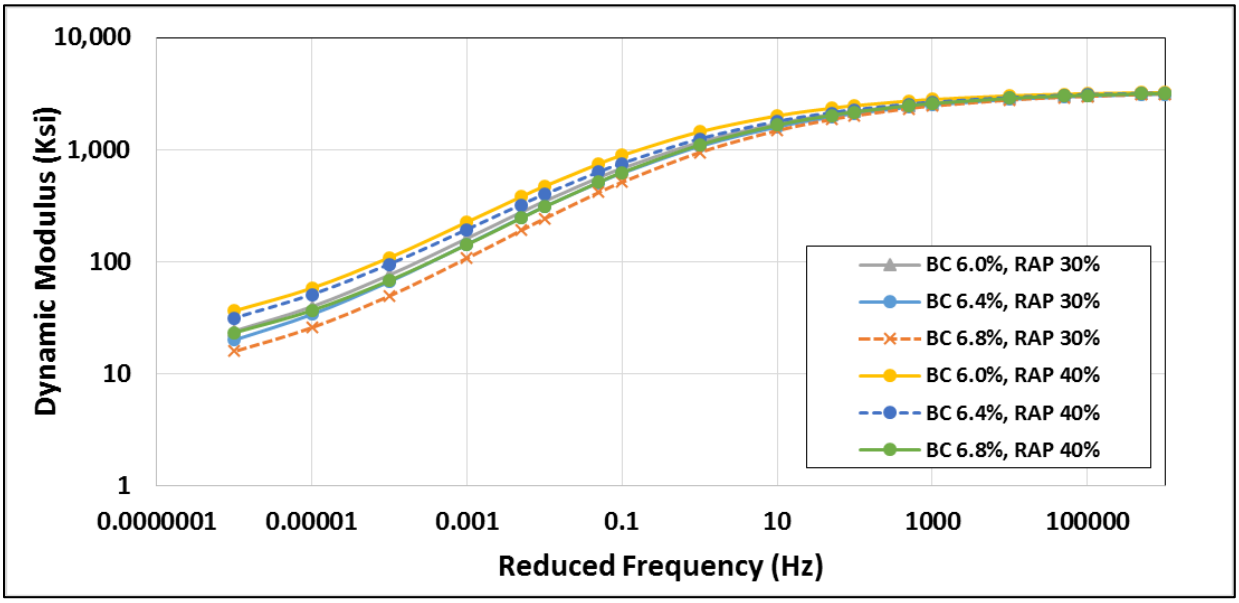

Figure 2.24. Master curves of dynamic modulus for the mixtures with different RAP contents (30% and 40%), binder grade of PG 64-22, and different binder contents (6%, 6.4%, and 6.8%)

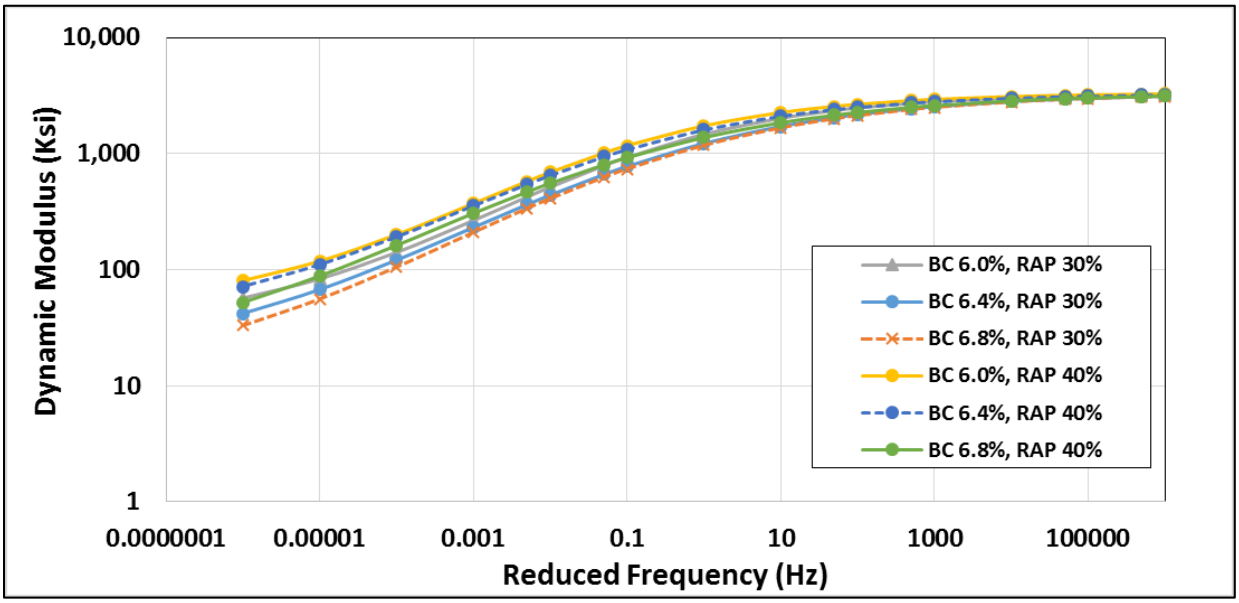

Figure 2.25. Master curves of dynamic modulus for the mixtures with different RAP contents (30% and 40%), binder grade of PG 76-22, and different binder contents (6%, 6.4%, and 6.8%)

To see the effect of binder grade on dynamic modulus, Figure 2.26 to Figure 2.28 were created. It can be seen that binder grade had a significant effect on the stiffness of the mixtures. The mixtures with softer binder had lower dynamic modulus compared to the mixtures with stiffer binder regardless of their RAP contents. Moreover, dynamic modulus decreased with a higher slope with respect to the load frequency for the softer binder, especially at low frequency levels. Moreover, the mixture with BC 6%, RAP 30%, and PG 64-22 had almost the same dynamic modulus as the mixture with BC 6%, RAP 40%, and PG 58-34 for all the frequencies. These two mixtures also had close FI in SCB tests. This result proves that FI in SCB test can describe mixture properties properly. The mixture with BC 6%, RAP 40%, and PG 64-22 seems to have almost the same master curve as the mixture with BC 6%, RAP 30%, and PG 76-22 at higher frequencies (higher vehicle speed condition). However, the mixture with BC 6%, RAP 40%, and PG 64-22 has lower dynamic modulus at lower frequency levels (lower vehicle speed condition), meaning that it has higher rutting resistance.

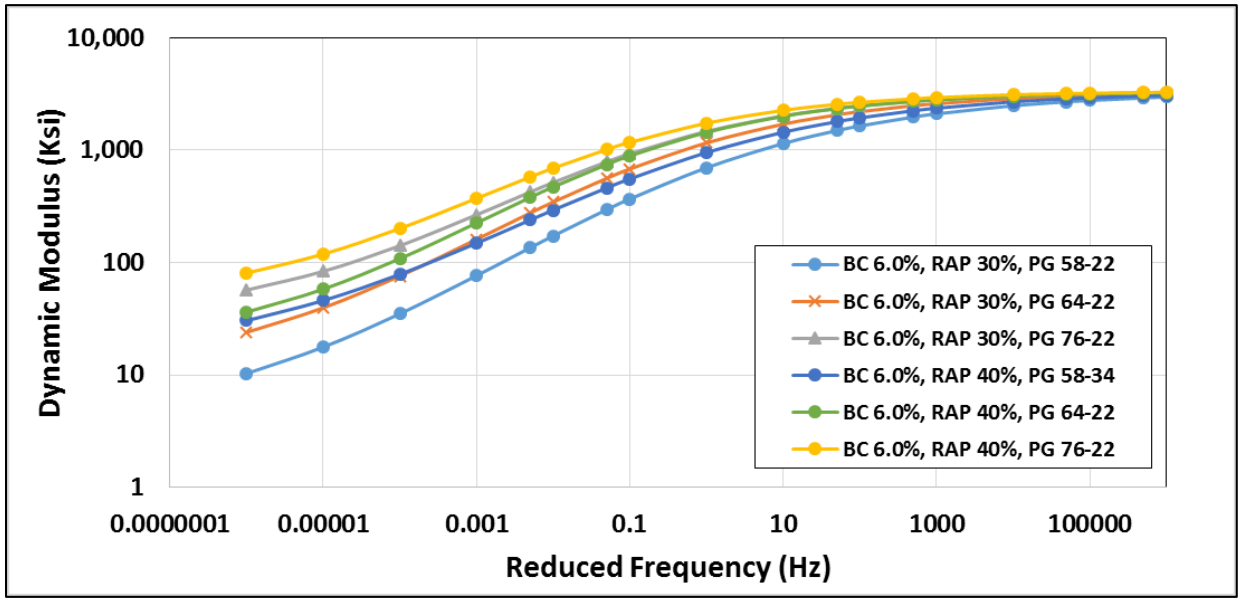

Figure 2.26. Master curves of dynamic modulus for the mixtures with different RAP contents (30% and 40%), different binder grades (PG 58-34, PG 64-22, and PG 76-22), and 6% binder content

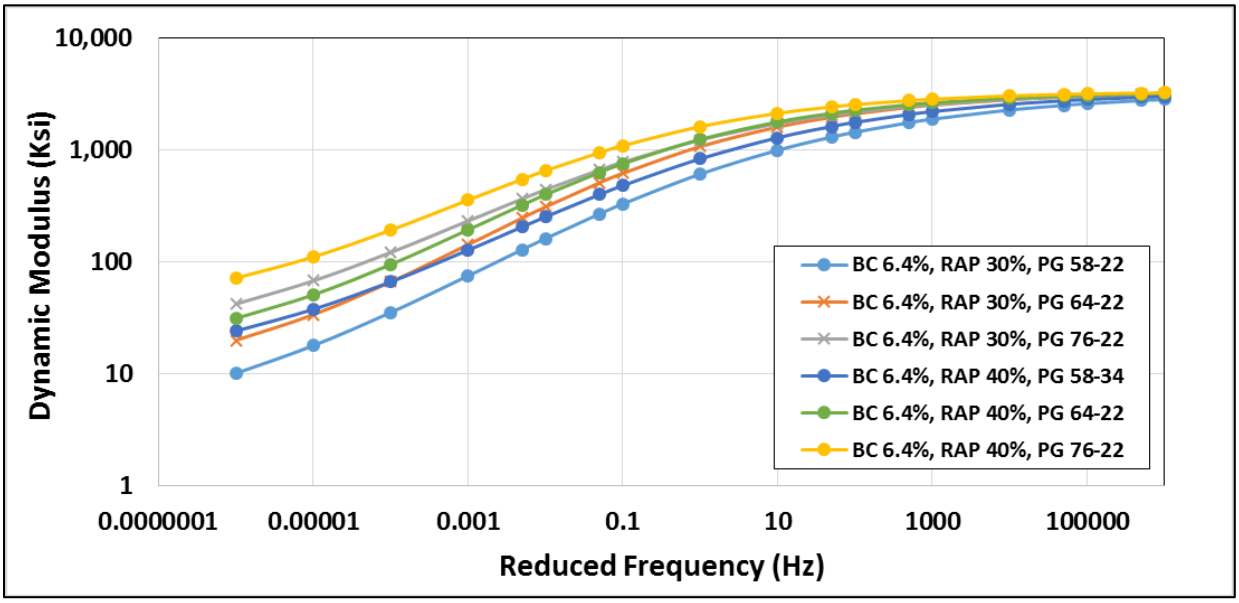

Figure 2.27. Master curves of dynamic modulus for the mixtures with different RAP contents (30% and 40%), different binder grades (PG 58-34, PG 64-22, and PG 76-22), and 6.4% binder content

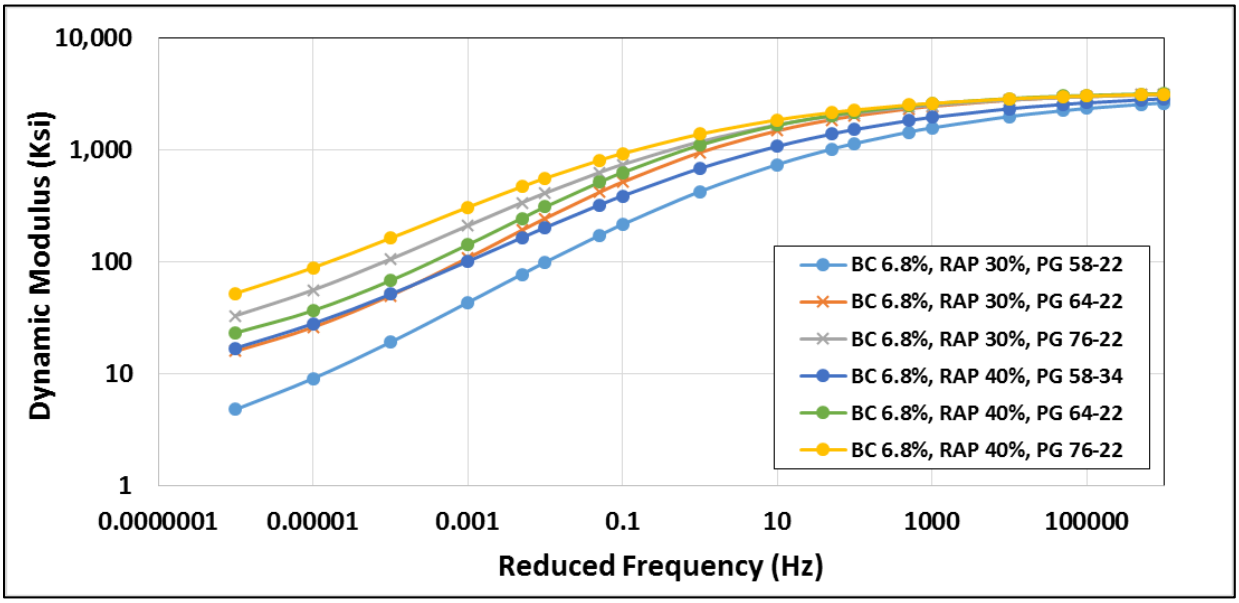

Figure 2.28. Master curves of dynamic modulus for the mixtures with different RAP contents (30% and 40%), different binder grades (PG 58-34, PG 64-22, and PG 76-22), and 6.8% binder content

Based on AASHTO TP 79-13, the coefficient of variation (CV) of the dynamic modulus of each pair of tested samples should not be greater than 9.2%. Figure 2.29 to Figure 2.34 show the dynamic modulus of the mixtures at the frequencies of 10 Hz and 0.1 Hz, temperatures of 4 ºC, 20 ºC, and 40 ºC, all the combinations of RAP contents, binder contents, and binder grades. In these figures, B1 is PG 58-34, B2 is PG 64-22, and B3 is PG 76-22. Also, R30 is RAP 30%, R40 is RAP 40%, and BC refers to binder content. For all the mixtures shown, CV of the paired tested mixtures were less than 9.2% at 4 ºC, and 20 ºC (except for the mixtures with 30% RAP, 6.8% binder content, and PG 58-34 at 20 ºC and 0.1 Hz). However, some of the paired mixtures had higher CV at 40- ºC. Bonaquist (2011) reported in NCHRP Report 702 that the CV could be more than 10% for mixtures with low dynamic modulus. Therefore, observing higher CV dynamic modulus at the test temperature of 40 °C is not unexpected. Moreover, it can be seen that the dynamic modulus decreases as the binder content increases for all the frequency levels and temperatures. It has an opposite trend as the RAP content increases.

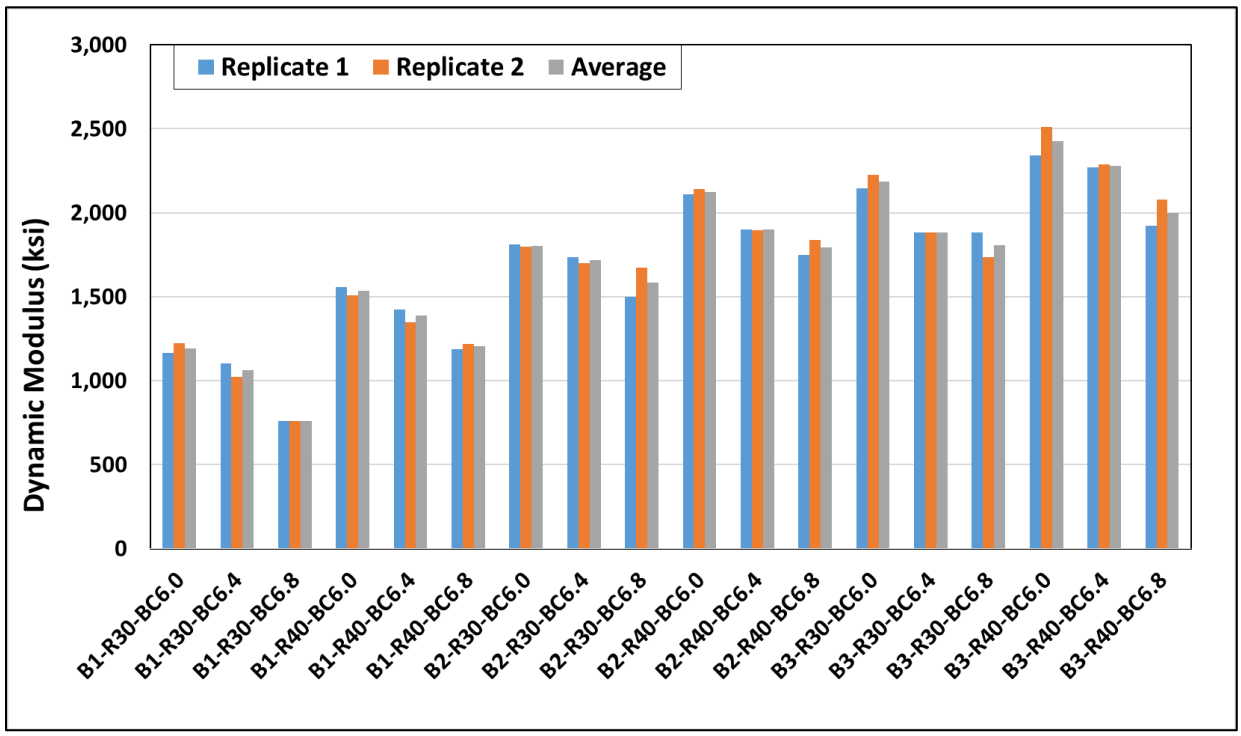

Figure 2.29. Dynamic modulus of the mixtures at 4 ºC and 0.1 Hz and all the combinations of RAP contents, binder contents, and binder grades

Note: B1= PG 58-34, B2= PG 64-22, and B3 = PG 76-22.
R30 = 30% RAP, and R40 = 40% RAP.
BC6= 6% binder content, BC6.4 =6.4 % binder content, and BC6.8 = 6.8% binder content.

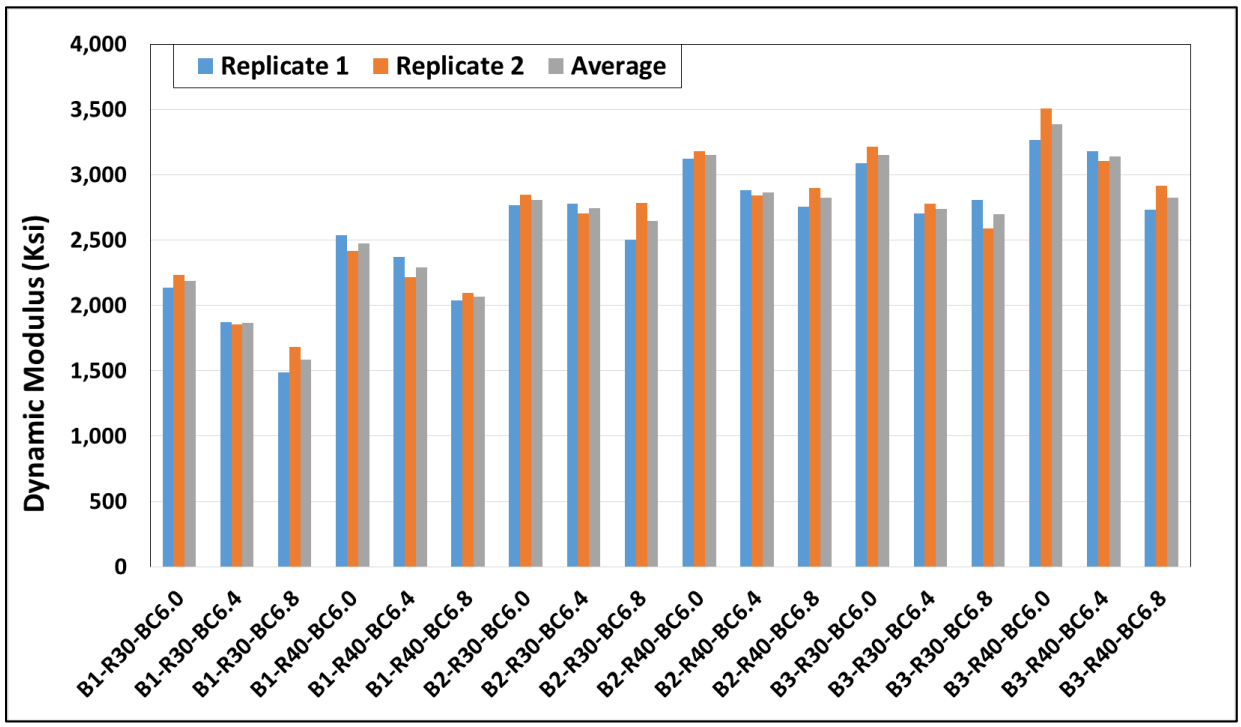

Figure 2.30. Dynamic modulus of the mixtures at 4 °C and 10 Hz and all the combinations of RAP contents, binder contents, and binder grades

Note: B1= PG 58-34, B2= PG 64-22, and B3 = PG 76-22.
R30 = 30% RAP, and R40 = 40% RAP.
BC6= 6% binder content, BC6.4 =6.4 % binder content, and BC6.8 = 6.8% binder content.

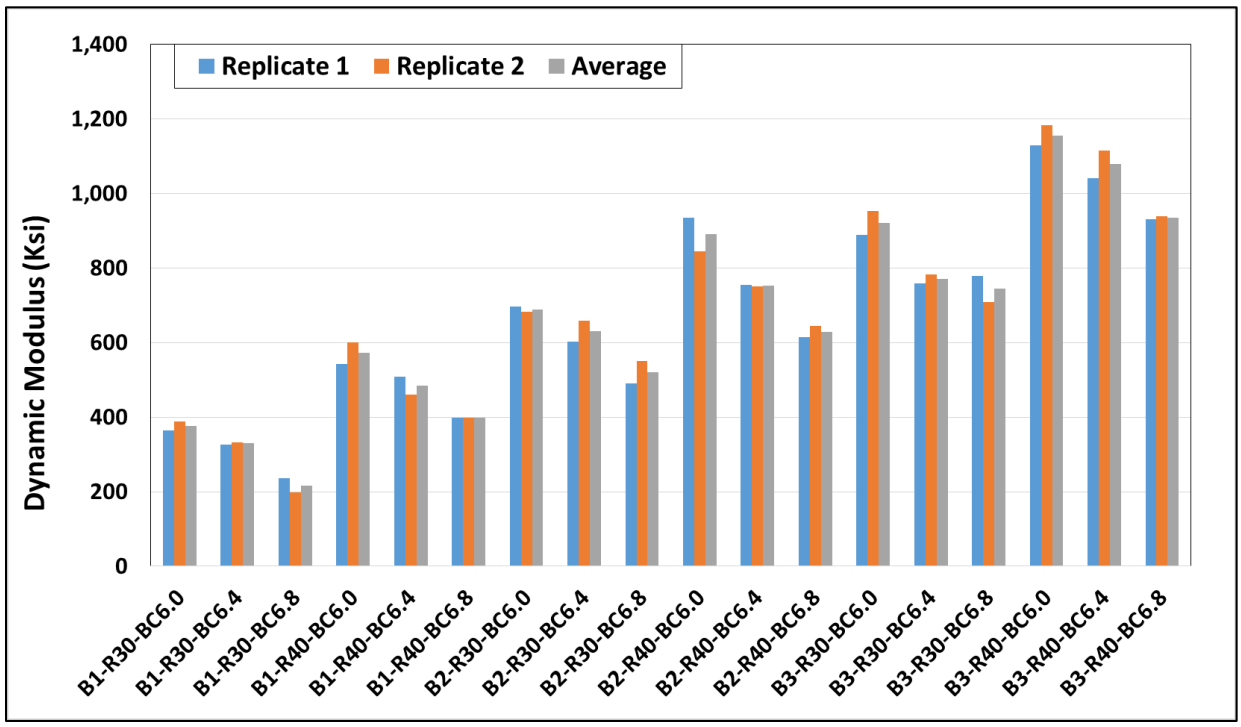

Figure 2.31. Dynamic modulus of the mixtures at 20 ºC and 0.1 Hz and all the combinations of RAP contents, binder contents, and binder grades

Note: B1= PG 58-34, B2= PG 64-22, and B3 = PG 76-22.
R30 = 30% RAP, and R40 = 40% RAP.
BC6= 6% binder content, BC6.4 =6.4 % binder content, and BC6.8 = 6.8% binder content.

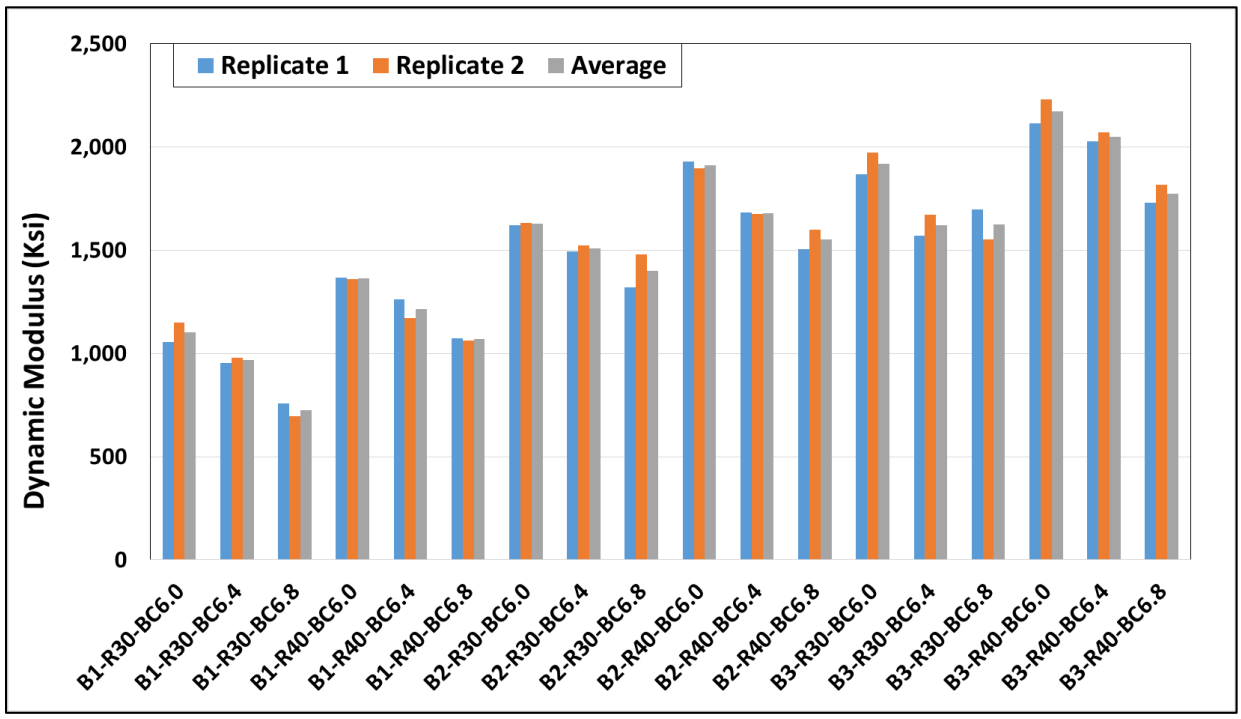

Figure 2.32. Dynamic modulus of the mixtures at 20 ºC and 10 Hz and all the combinations of RAP contents, binder contents, and binder grades

Note: B1= PG 58-34, B2= PG 64-22, and B3 = PG 76-22.
R30 = 30% RAP, and R40 = 40% RAP.
BC6= 6% binder content, BC6.4 =6.4 % binder content, and BC6.8 = 6.8% binder content.

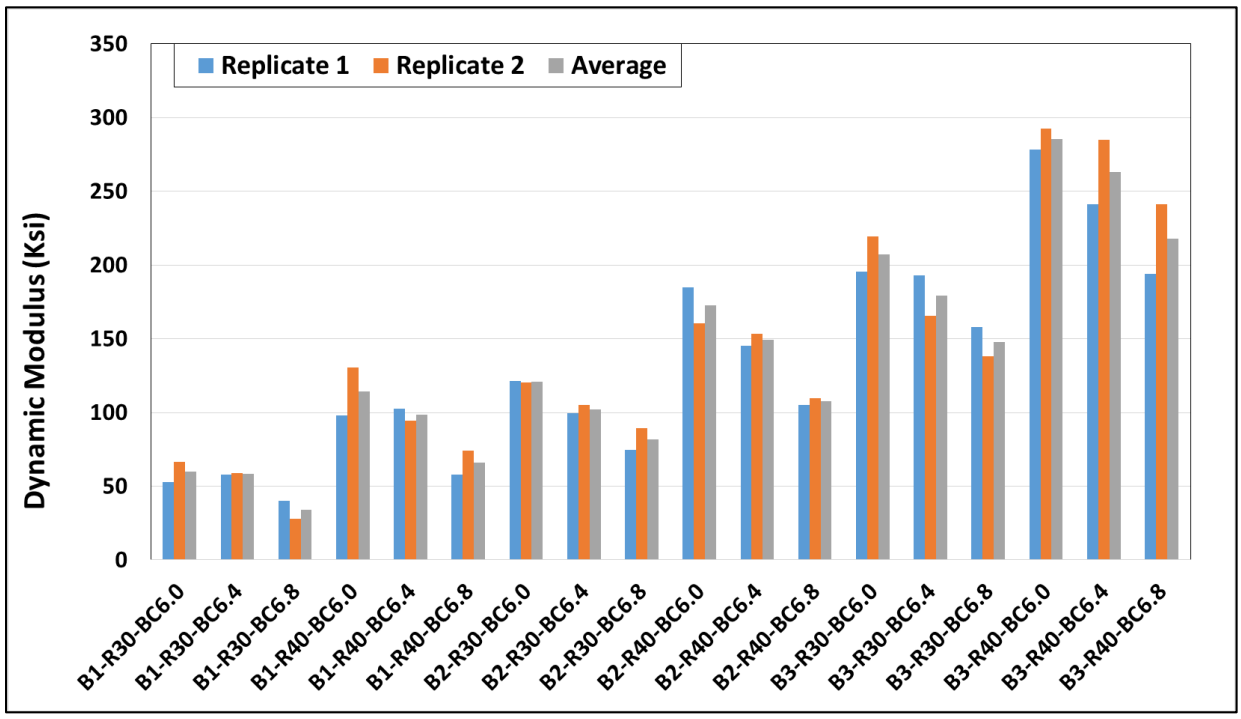

Figure 2.33. Dynamic modulus of the mixtures at 40 ºC and 0.1 Hz and all the combinations of RAP contents, binder contents, and binder grades

Note: B1= PG 58-34, B2= PG 64-22, and B3 = PG 76-22.
R30 = 30% RAP, and R40 = 40% RAP.
BC6= 6% binder content, BC6.4 =6.4 % binder content, and BC6.8 = 6.8% binder content.

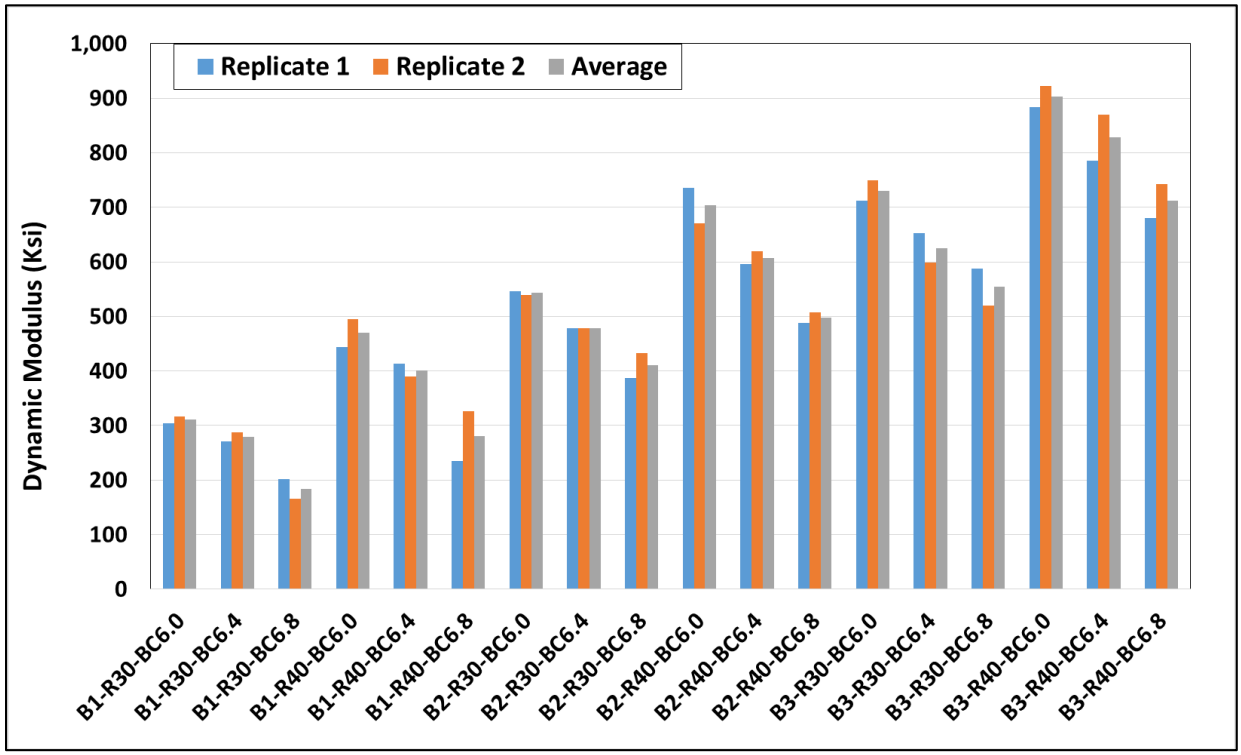

Figure 2.34. Dynamic modulus of the mixtures at 40 ºC and 10 Hz and all the combinations of RAP contents, binder contents, and binder grades

Note: B1= PG 58-34, B2= PG 64-22, and B3 = PG 76-22.
R30 = 30% RAP, and R40 = 40% RAP.
BC6= 6% binder content, BC6.4 =6.4 % binder content, and BC6.8 = 6.8% binder content.

2.5.3.2 Master curves for phase angle

The time delay between the time point at which peak stress applied and the time point at which peak strain observed is used to calculate phase angle. Phase angle shows energy absorption capacity of an asphalt mixture and represents viscoelastic characteristics of asphalt mixtures. Higher phase angle indicates that the asphalt mixture is more viscous, more susceptible to rutting, and more resistant to cracking (Darnell Jr. and Bell 2015). Dynamic modulus and phase angle are inversely related to each other. A mixture with a comparatively high dynamic modulus (high stiffness) at a frequency level has a low phase angle at the same frequency (Darnell Jr. and Bell 2015).

Phase angle master curves for all test results are plotted in Figure 2.35 to Figure 2.40. The same shift factor values, which were calculated and used for developing the master curves for DM tests,

are used to develop the master curves for phase angles. Therefore, these master curves are not as smooth as the master curves of the dynamic modulus. Reference temperature for all master curves is 20 ºC.

Figure 2.37 shows that stiff mixtures with binder grade of PG 76-22 had lower phase angles at lower binder contents and higher RAP contents. For the same binder grade, asphalt mixtures with 40% RAP had smaller phase angles than the asphalt mixtures with 30% RAP for all the binder contents. Mixtures with softer binders (PG 64-22 and PG 58-34 [Figure 2.35 and Figure 2.36]) showed similar trends for the all the frequency levels, except for the lowest frequencies (low-speed condition). For 40% RAP-PG76-22, binder content effect on phase angle is minimal since high RAP content and stiff binder (PG 76-22) create a stiff mixture with low flexibility.

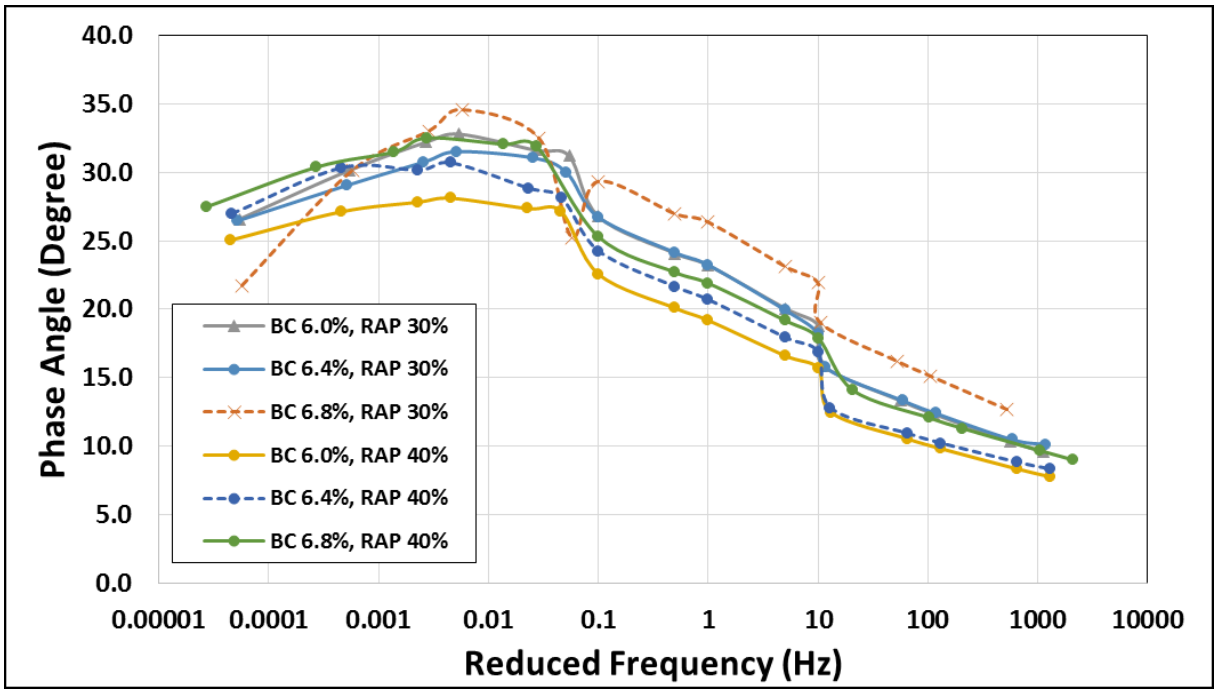

Figure 2.35. Master curves of phase angles for the mixtures with different RAP contents (30% and 40%), binder grade of PG 58-34, and different binder contents (6%, 6.4%, and 6.8%)

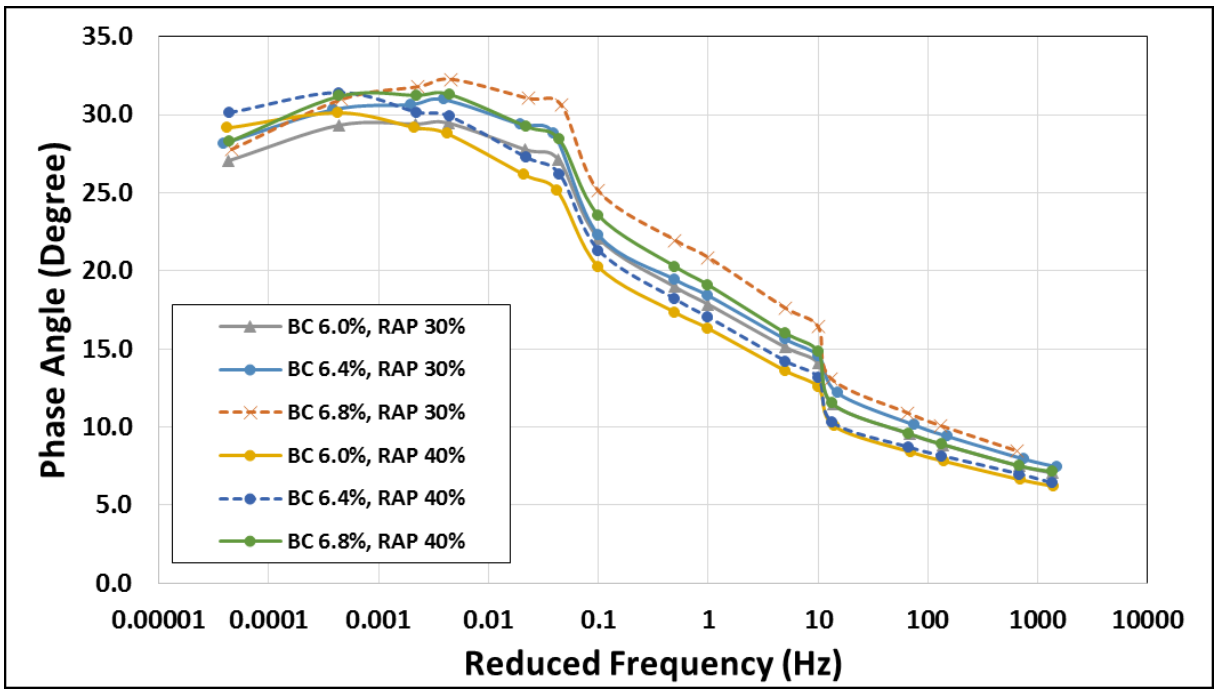

Figure 2.36. Master curves of phase angles for the mixtures with different RAP contents (30% and 40%), binder grade of PG 64-22, and different binder contents (6%, 6.4%, and 6.8%)

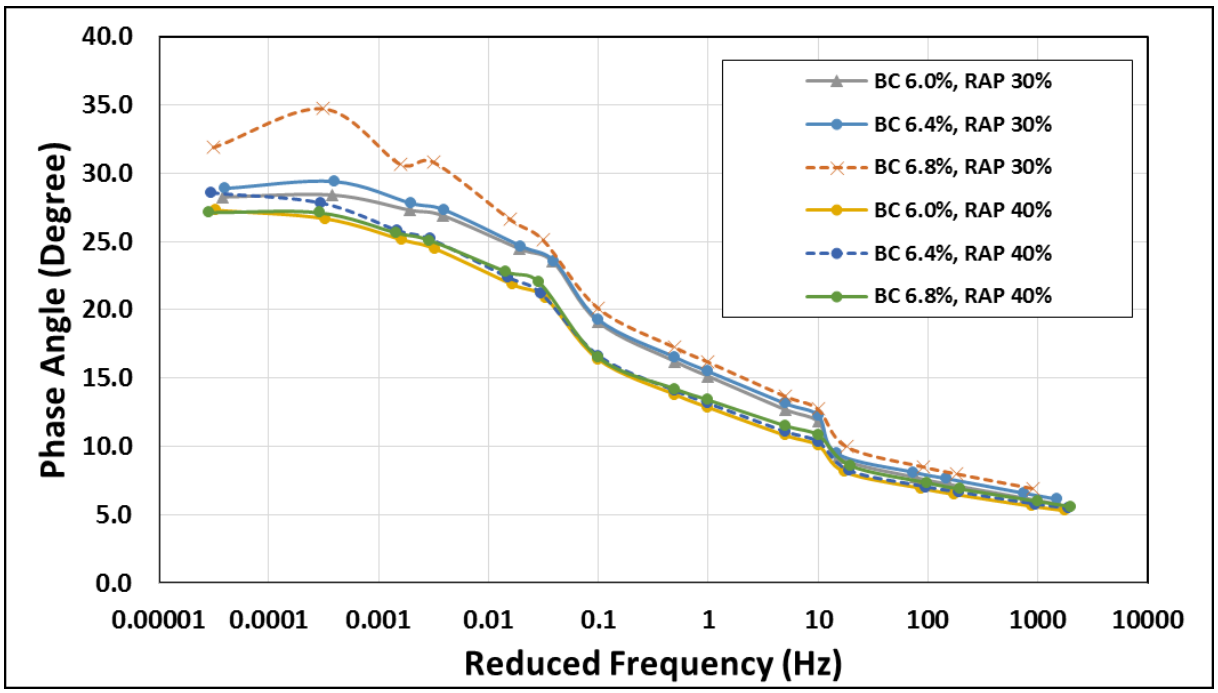

Figure 2.37. Master curves of phase angles for the mixtures with different RAP contents (30% and 40%), binder grade of PG 76-22, and different binder contents (6%, 6.4%, and 6.8%)

To compare the effect of binder grade on phase angle, Figure 2.38 to Figure 2.40 were developed. In general, mixtures with stiffer binder had less phase angles with respect to frequency. Also, it can be seen that the effect of RAP content was significant for the mixtures with PG 64-22 and PG 76-22; Mixtures with 40% RAP had less phase angles than the mixtures with 30% RAP, regardless of their PG grades. On the contrary, mixtures with PG 58-34 had higher phase angles than the mixtures with PG 64-22 and PG 76-22 for the same binder content, regardless of their RAP contents. It can be concluded that RAP content has more significant effect on the phase angle than binder grades for the mixtures with PG 64-22 and PG 76-22 binders. However, the effect of binder grade on phase angle is more significant than RAP content for the mixtures with the softer binder (PG 58-34).

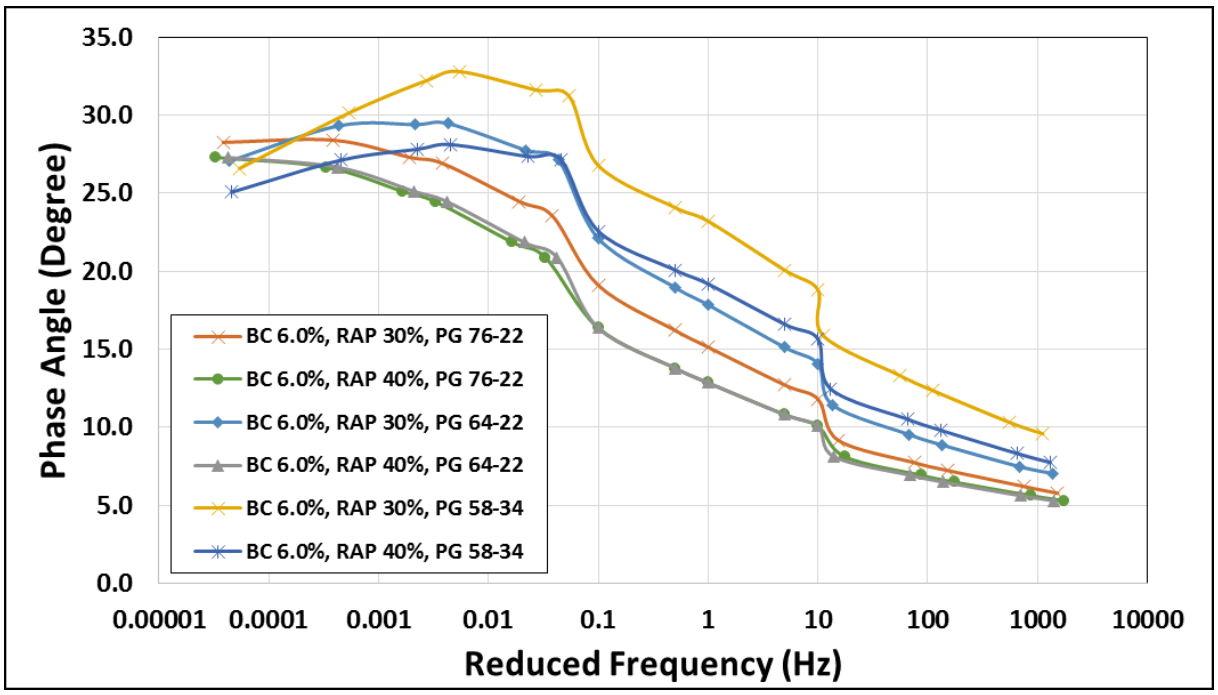

Figure 2.38. Master curves of phase angles for the mixtures with different RAP contents (30% and 40%), different binder grades of (PG 58-34, PG 64-22, and PG 76-22), and 6% binder content

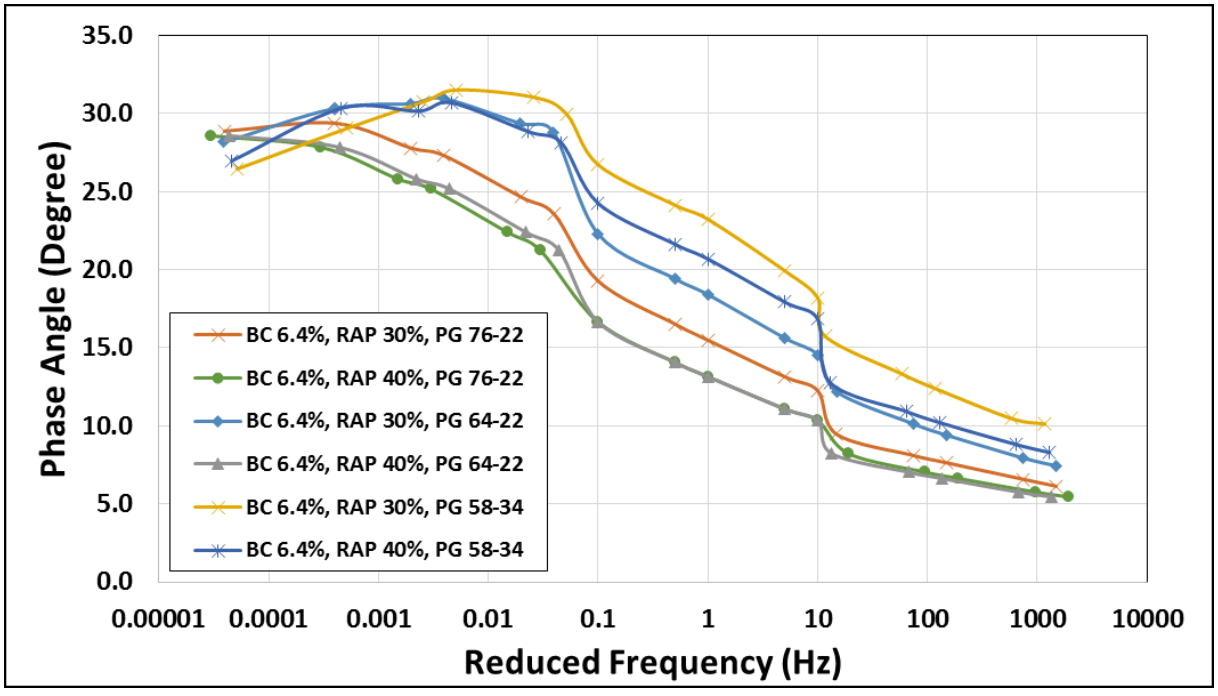

Figure 2.39. Master curves of phase angles for the mixtures with different RAP contents (30% and 40%), different binder grades of (PG 58-34, PG 64-22, and PG 76-22), and 6.4% binder content

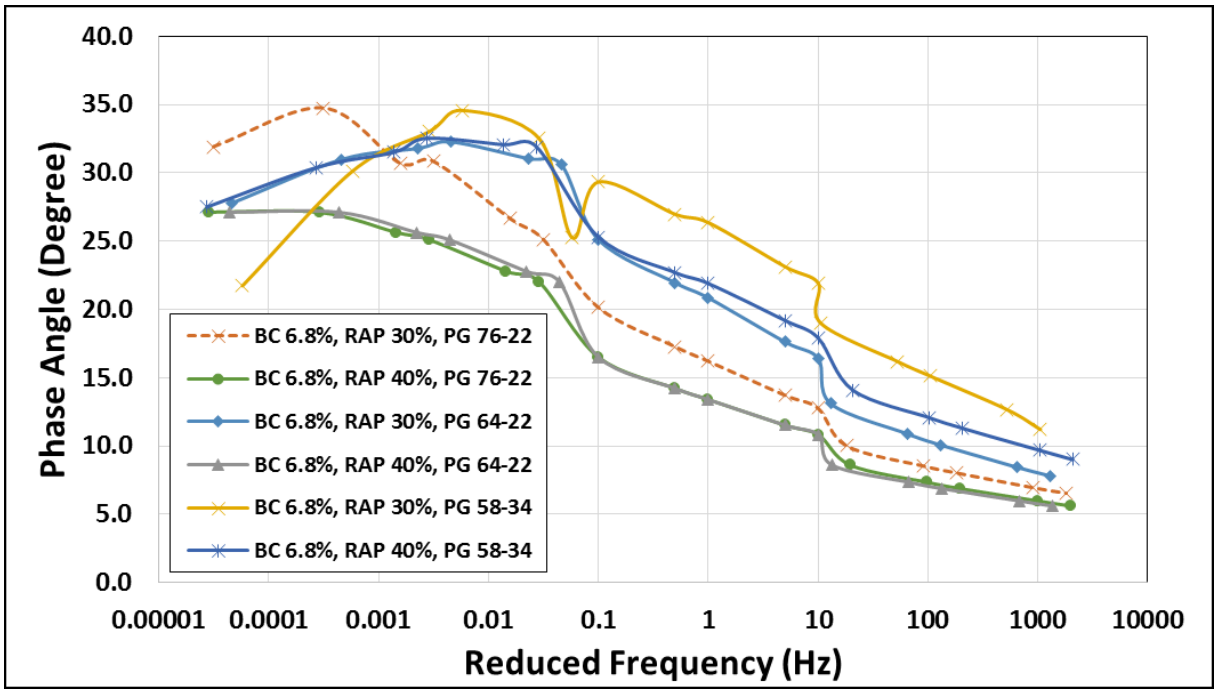

Figure 2.40. Master curves of phase angles for the mixtures with different RAP contents (30% and 40%), different binder grades of (PG 58-34, PG 64-22, and PG 76-22), and 6.8% binder content

2.5.4 Summary of test results

Results of SCB, DM, and FN tests were presented in Sections 2.5.1 to 2.5.3 to evaluate the cracking and rutting performance high RAP asphalt mixtures of this study. This section summarizes the general results of all conducted tests.

Although some of the asphalt mixtures show high cracking resistance (high FI), their rutting performance can be low due to high binder content and softer binders. Figure 2.41 shows the average FI (average of four replicate SCB tests) of the asphalt mixtures with all combinations of RAP contents, binder contents, and binder grades. Average FN of the asphalt mixtures (average of two replicate FN tests) is also illustrated on top of each bar. Asphalt mixture with BC 6.8%, RAP 40%, and PG 64-22 showed a high rutting and cracking performance. It has a FN of 1230, which is higher than the recommended FN (FN=740) for high traffic level (≥30 million ESALs). Also, its FI is within the acceptable range of cracking performance (FI=9-14) based on ODOT SPR785

project (Coleri 2017). Although some mixtures including 1) BC 6.8%, RAP 30%, PG 58-34, 2) BC 6.8%, RAP 30%, PG 64-22, 3) BC 6.8%, RAP 40%, PG 58-34, and 4) BC 6.4%, RAP 30%, PG 58-34 met the threshold for cracking performance, they did not meet the FN criteria required for the high traffic levels (≥30 million ESALs). However, they still can be used for the traffic level of 10 to <30 million ESALs since their FNs are greater than 190. Since the mixtures with BC 6.8%, RAP 40%, and PG 76-22 showed high rutting performance but low cracking performance, asphalt mixtures with 40% RAP, higher binder content (higher than 6.8%) and PG 76-22 may have acceptable cracking and rutting performance. Moreover, mixtures with higher RAP content (higher than 40%), 6.8% binder content, and PG 58-34 may show high resistance to rutting and cracking. In the following section (Section 2.5.5), regression equations were developed and Monte Carlo simulations were performed using the developed equations to determine the required binder content, binder grade, and RAP content of asphalt mixtures to meet rutting (FN>740) and cracking resistance (FI>10) requirements.

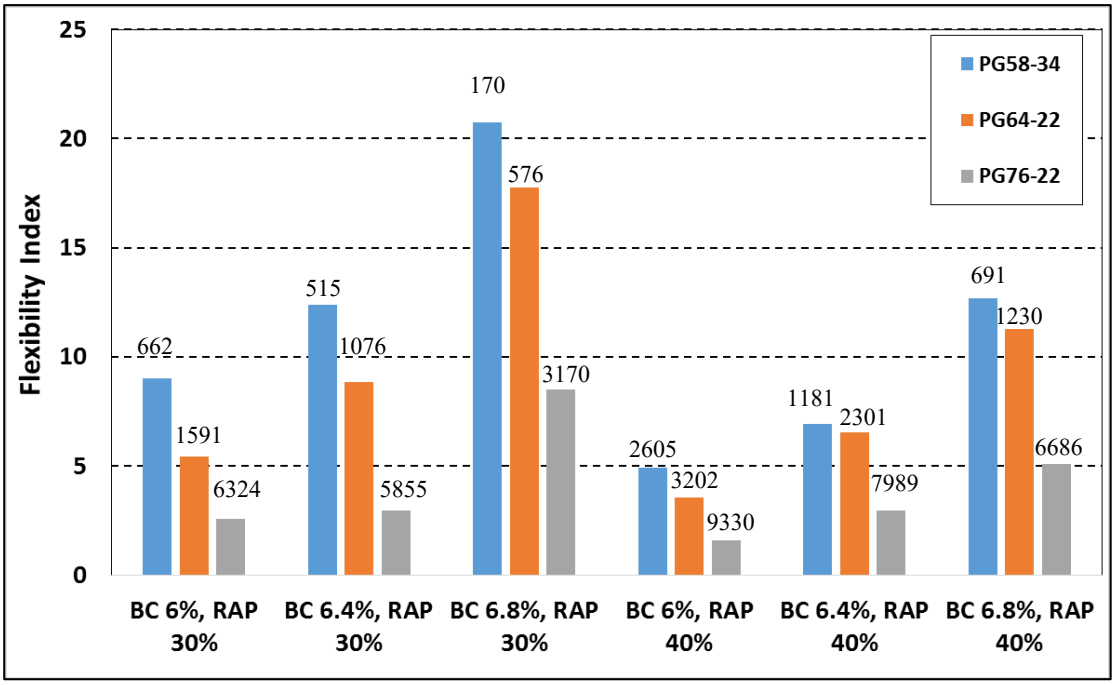

Figure 2.41. Flexibility index and flow number (numbers on each bar) of the mixtures with different RAP contents (30% and 40%), binder grades (PG 58-34, PG 64-22, and PG 76-22), and binder contents (6.0%, 6.4%, and 6.8%)

To evaluate possible correlations of dynamic modulus of mixtures at different temperatures and frequencies with FI and FN, Figure 2.42 to Figure 2.53 were created. It can be seen that dynamic modulus at 40 ºC and 0.1 Hz has the highest correlation with FN. Therefore, dynamic modulus results at 40 ºC and 0.1 Hz can be used to predict FN (rutting resistance of the asphalt mixtures). In general, there is not a strong correlation between dynamic modulus and FI, especially for PG 76-22. However, dynamic modulus has a strong correlation with FI at 20 ºC and 4 ºC for mixtures with PG 58-34 and can be used to predict FI. As the binder becomes stiffer, the correlations between FI and dynamic modulus become weaker.

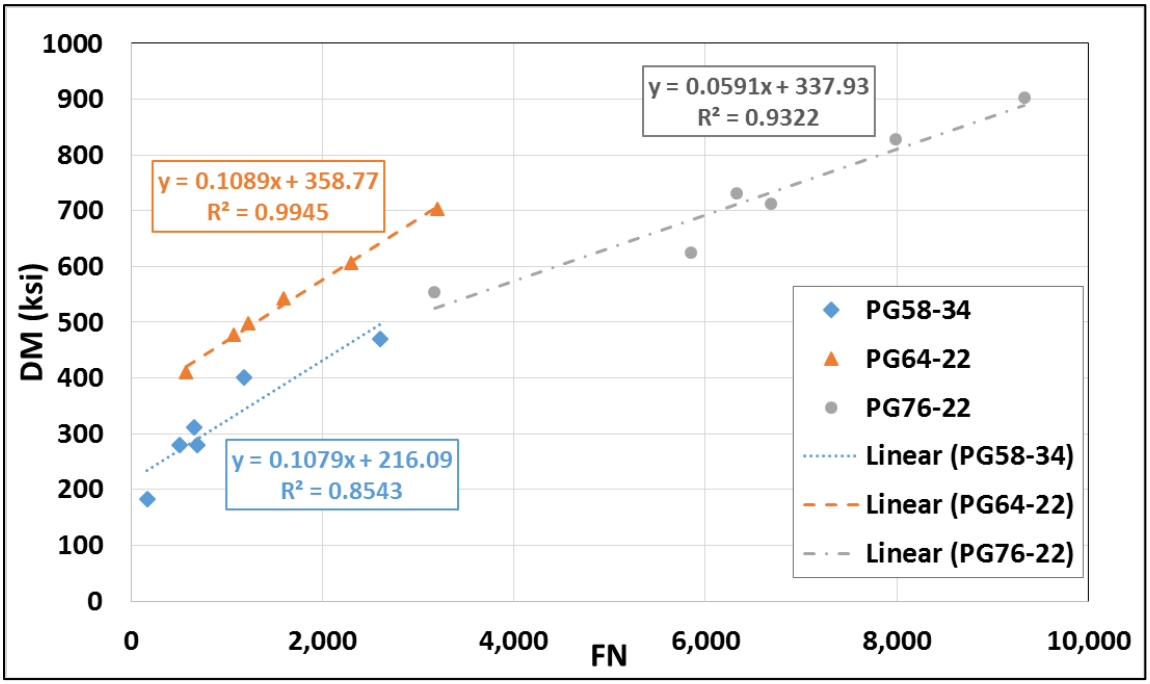

Figure 2.42. Dynamic modulus of mixtures at 40 ºC and 10 Hz versus flow number for all the combinations of RAP content, binder content, and binder grades

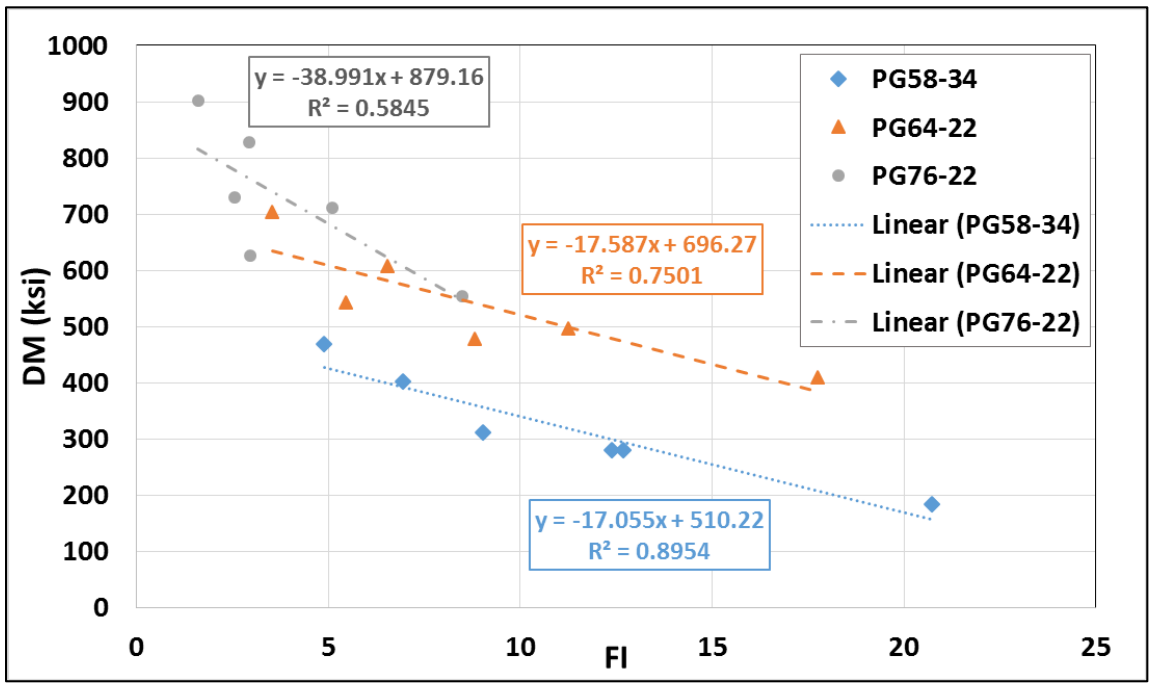

Figure 2.43. Dynamic modulus of mixtures at 40 °C and 10 Hz versus flexibility index for all the combinations of RAP content, binder content, and binder grades

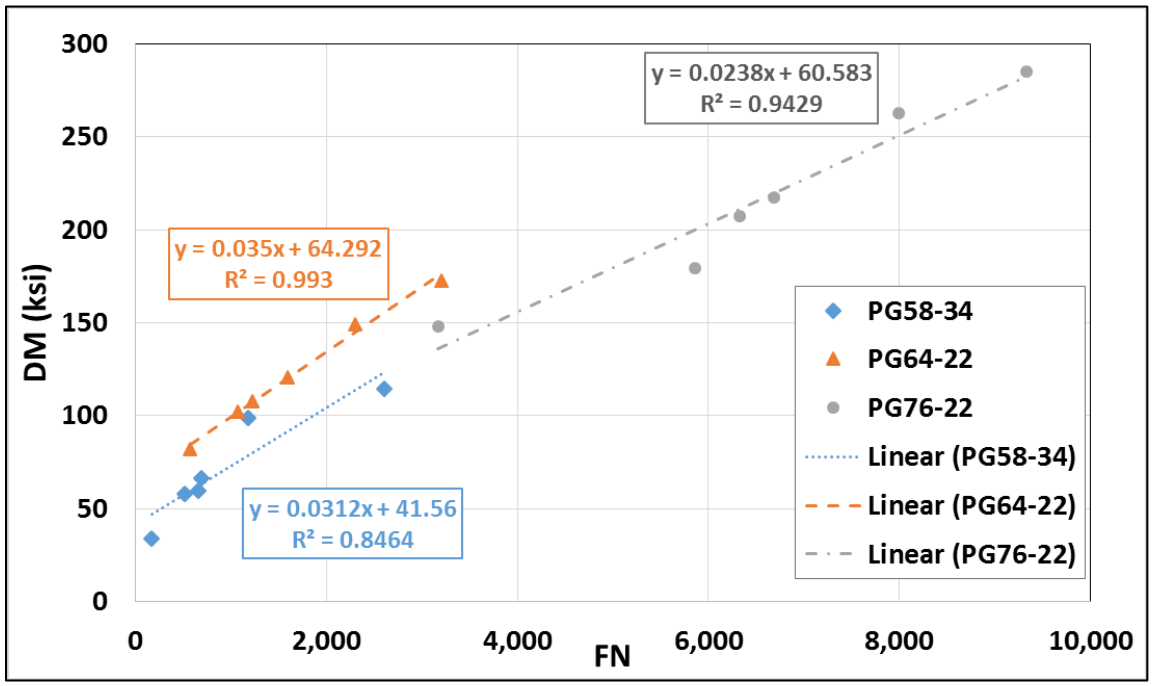

Figure 2.44. Dynamic modulus of mixtures at 40 °C and 0.1 Hz versus flow number for all the combinations of RAP content, binder content, and binder grades

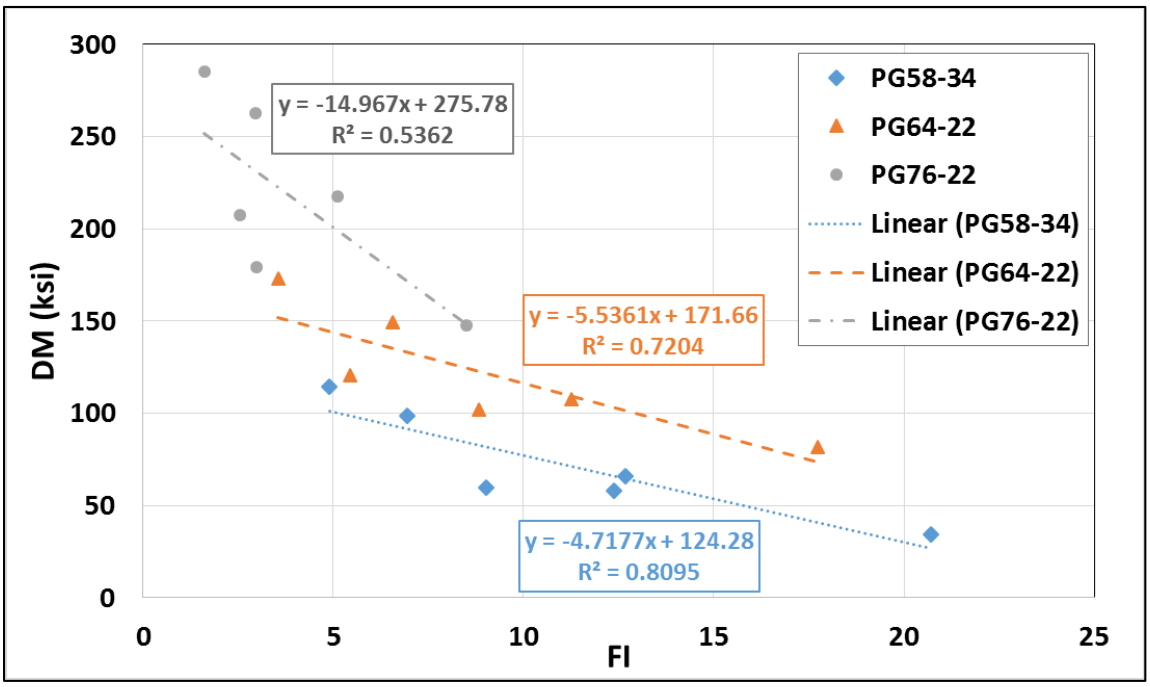

Figure 2.45. Dynamic modulus of mixtures at 40 ºC and 0.1 Hz versus flexibility index for all the combinations of RAP content, binder content, and binder grades

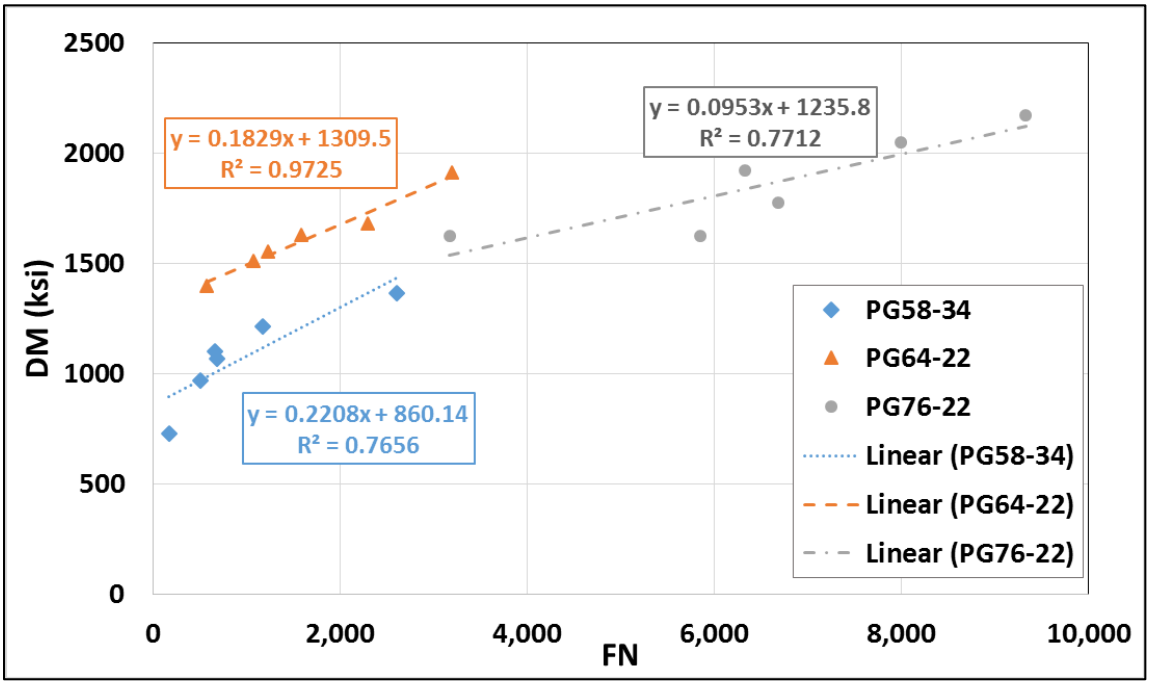

Figure 2.46. Dynamic modulus of mixtures at 20 ºC and 10 Hz versus flow number for all the combinations of RAP content, binder content, and binder grades

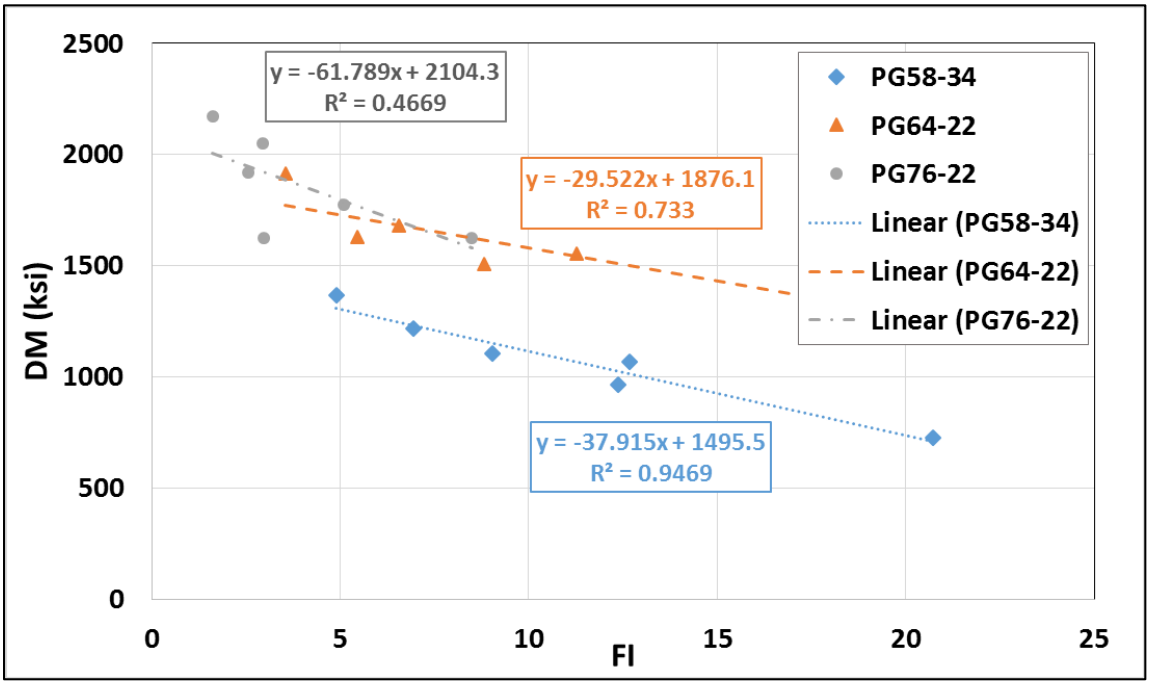

Figure 2.47. Dynamic modulus of mixtures at 20 ºC and 10 Hz versus flexibility index for all the combinations of RAP content, binder content, and binder grades

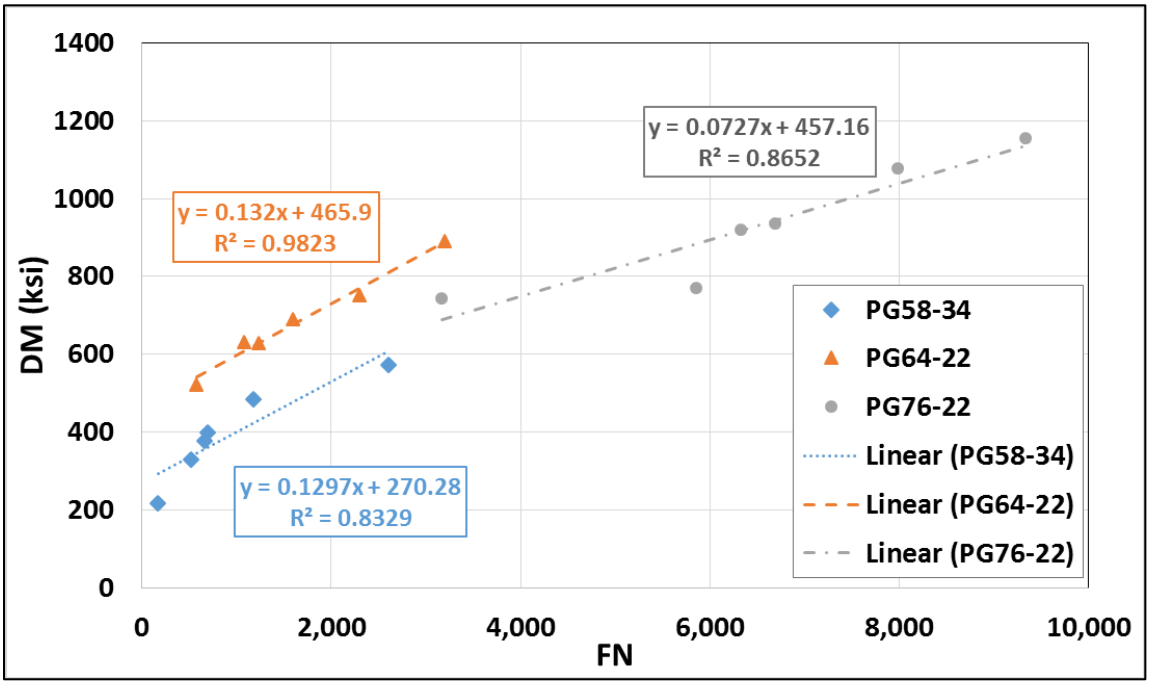

Figure 2.48. Dynamic modulus of mixtures at 20 ºC and 0.1 Hz versus flow number for all the combinations of RAP content, binder content, and binder grades

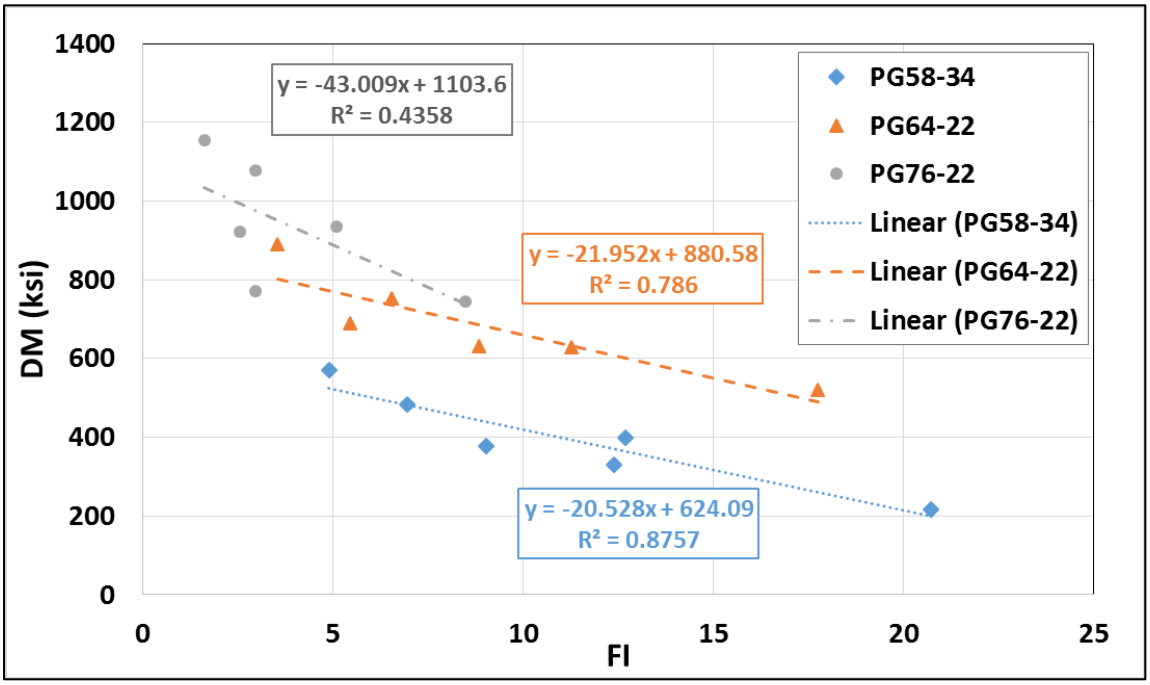

Figure 2.49. Dynamic modulus of mixtures at 20 ºC and 0.1 Hz versus flexibility index for all the combinations of RAP content, binder content, and binder grades

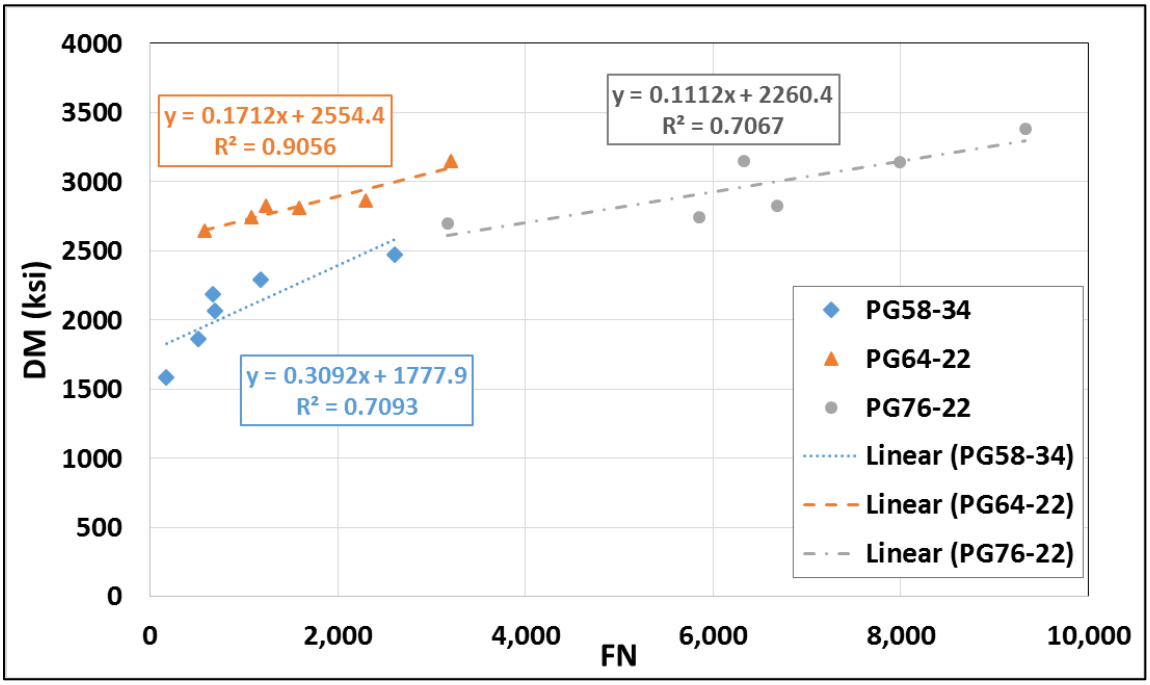

Figure 2.50. Dynamic modulus of mixtures at 4 ºC and 10 Hz versus flow number for all the combinations of RAP content, binder content, and binder grades

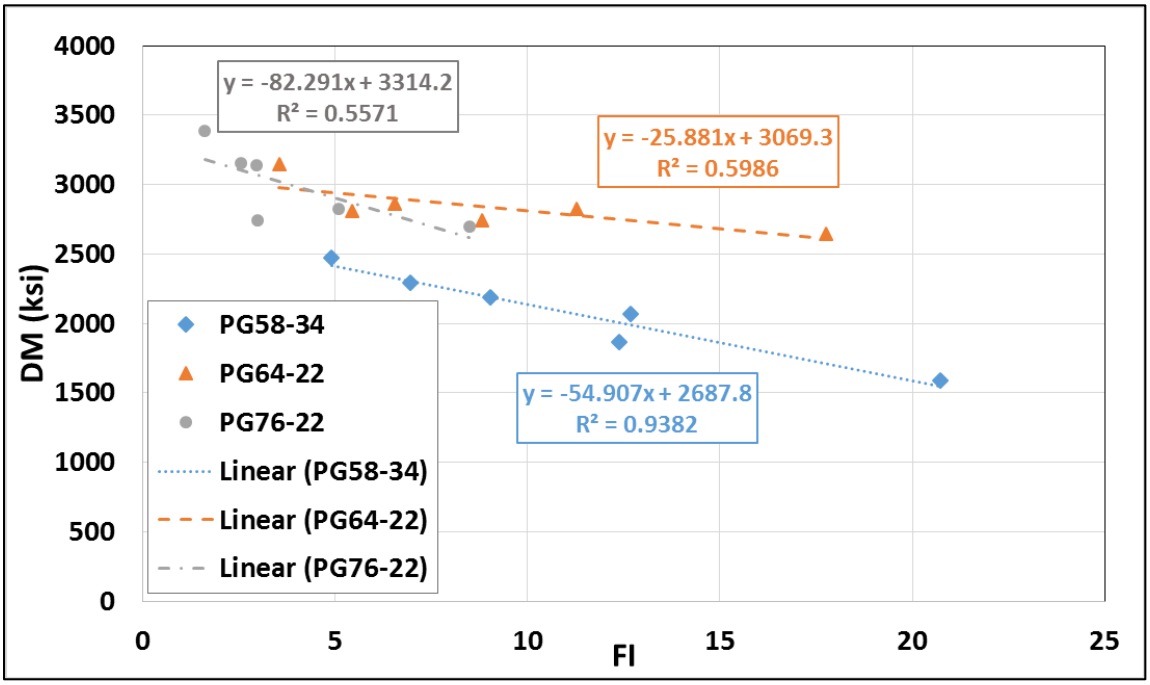

Figure 2.51. Dynamic modulus of mixtures at 4 ºC and 10 Hz versus flexibility index for all the combinations of RAP content, binder content, and binder grades

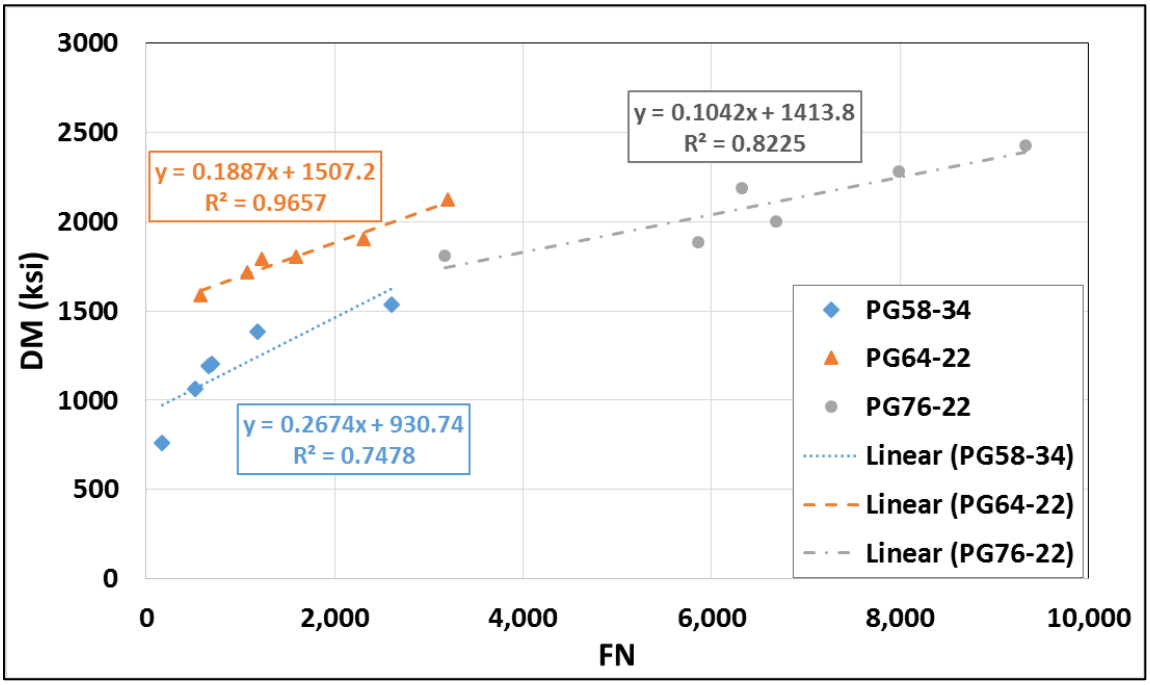

Figure 2.52. Dynamic modulus of mixtures at 4 °C and 0.1 Hz versus flow number for all the combinations of RAP content, binder content, and binder grades

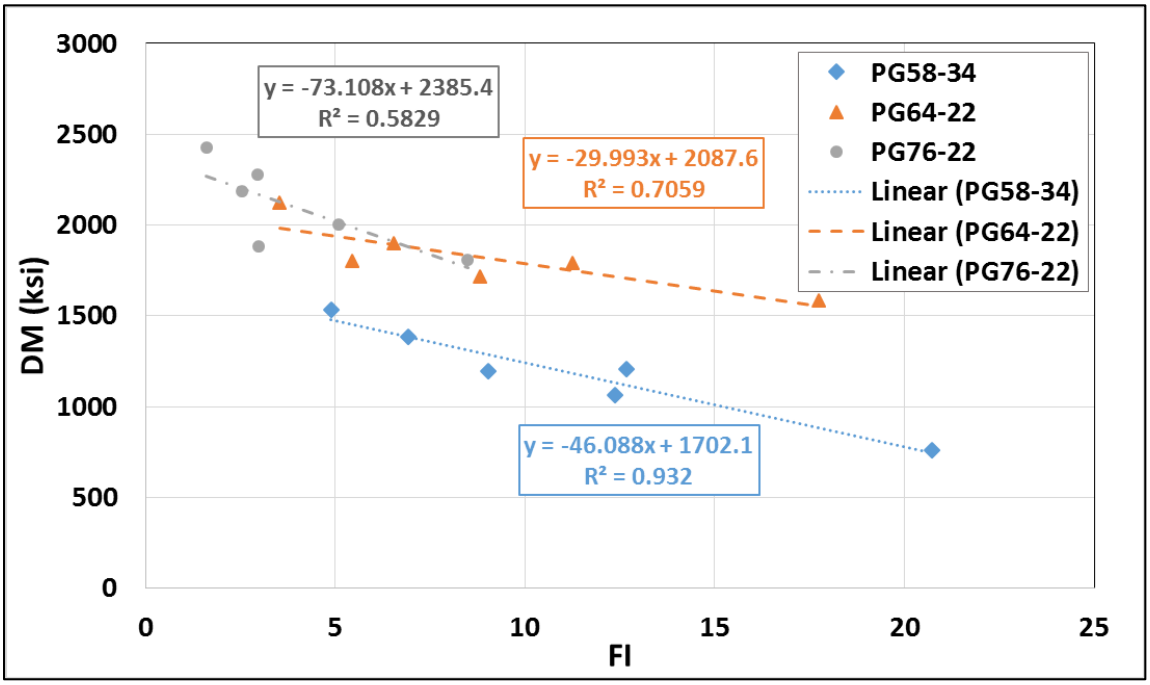

Figure 2.53. Dynamic modulus of mixtures at 4 °C and 0.1 Hz versus flexibility index for all the combinations of RAP content, binder content, and binder grades

Figure 2.54 shows the correlation between FI and FN results for all test results. Although there is a non-linear correlation between FN and FI, correlation is not strong enough to be able to predict FI results using the FN results and vice versa. For this reason, both experiments need to be conducted to evaluate rutting and cracking resistance of asphalt mixtures.

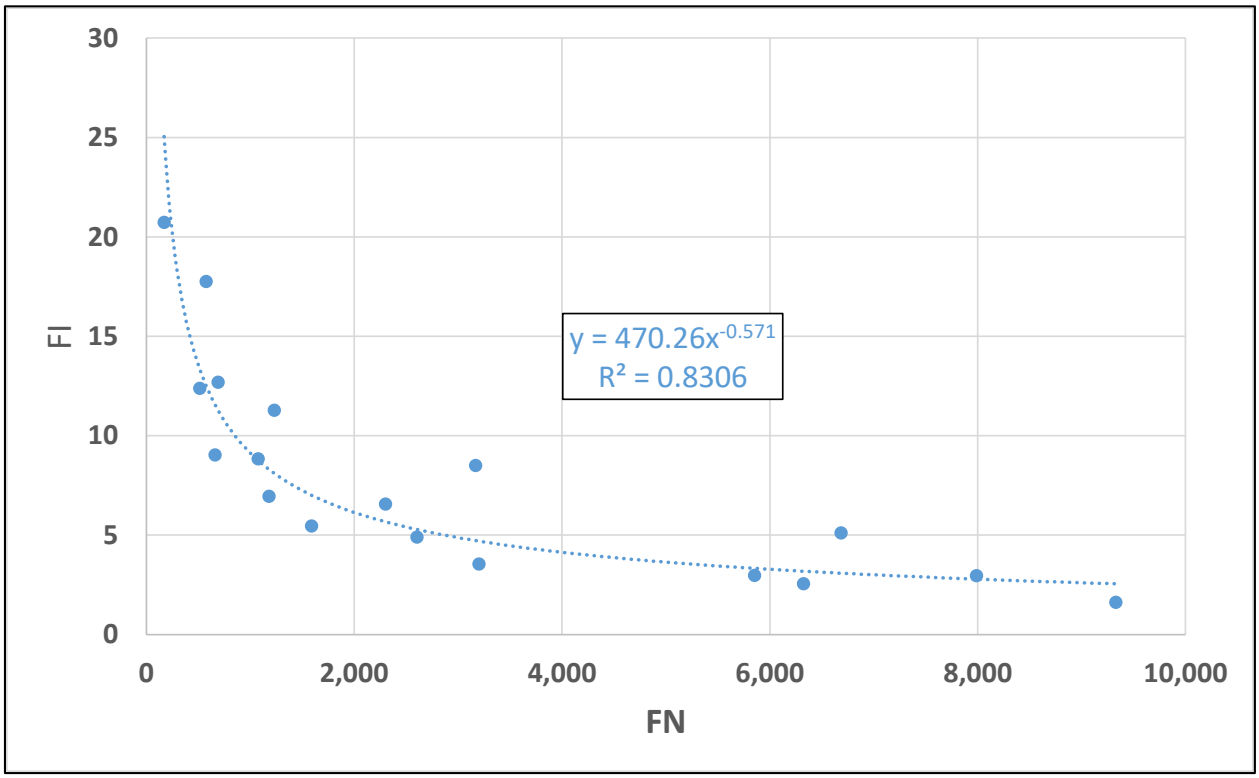

Figure 2.54. Correlation between FI and FN

2.5.5 Regression modeling and Monte Carlo simulations to determine asphalt mixtures with high rutting and cracking performance

Regression analysis is a statistical procedure describing the relationship between a dependent variable (response variable) and independent variables (predictors). In this section, regression analysis was performed to create linear models correlating FN and FI with RAP content, binder content, and binder grade. Results of the FN and SCB tests (Sections 2.5.1 and 2.5.3) were used for FN and FI values, as dependent variables, in the regression model. Firstly, analysis of variance was performed to which independent variables (RAP content, binder content, and binder grade) were important. Then, regression models were developed. Finally, to find possible asphalt

mixtures with acceptable cracking and rutting performance, FI and FN of asphalt mixture with different RAP contents (25% to 45%), binder contents (5% to 8%), and binder grades (PG 58-34, PG 64-22, and PG 76-22) were predicted using the developed regression models (Monte Carlo simulations). All dependent and independent variables used for model development are shown in Table 2.6.

Table 2.6. Independent and dependent variables used for regression models

Variable Type	Symbol	Description	Range
Dependent	FI	Flexibility Index	1.19 to 32.57
	FN	Flow Number	135 to 10000
Independent	RAP	RAP Content	30 and 40
	BC	Binder Content	6, 6.4, and 6.8
Category Independent	PG	Binder Grade	PG 58-34, PG 64-22, and PG 76-22

2.5.5.1 ANOVA table

Analysis of Variance (ANOVA) was performed to estimate the effects of RAP content, binder content, and binder grade on the dependent variables FI and FN. F value in ANOVA analyses shows the statistical significance of each independent variable (Seber 1977). FN and FI were transformed logarithmically and linearly correlated with the dependent variables. As shown in Table 2.7, although all independent variables are important, binder content has the most effect on FI since it has the highest F value. Binder type and RAP content are the second and third significant variables, respectively. Table 2.8 shows that all the independent variables have a significant effect on FN, with binder type being the first, RAP content being the second, and binder content being the third significant variables. The effects of RAP content, binder content, and binder grade on FI and FN were significant based on ANOVA analysis. Therefore, all the independent variables were used for regression model development.

Table 2.7. ANOVA table for the regression model correlating FI test results with RAP content, binder grade, and binder content

	Degrees of Freedom	Sum of Squares	Mean Square	F Value	Pr(F) Value
RAP	1	2.45	2.45	31.58	0.0000
BC	1	13.32	13.32	171.71	0.0000
Binder type	2	14.90	7.45	96.01	0.0000
Residuals	66	5.12	0.08		

Table 2.8. ANOVA table for the regression model correlating FN test results with RAP content, binder grade, and binder content

	Degrees of Freedom	Sum of Squares	Mean Square	F value	Pr(F) Value
RAP	1	5.84	5.84	72.72	0.0000
BC	1	5.28	5.28	65.73	0.0000
Binder type	2	29.78	14.89	185.31	0.0000
Residuals	31	2.49	0.08		

2.5.5.2 Linear regression model for FI

FI values obtained from SBC tests were logarithmically transformed in order to allow the model to be estimated by linear regression. Figure 2.55 shows ln(FI) for each combination of RAP content, binder content, and binder grade. The model correlating ln(FI) with the independent variables was estimated as follows:

$$\underset{}{\ln(FI) = -4.831715} \underset{(0.0000)}{- 0.037713*RAP} \underset{(0.0000)}{+ 1.317014*BC} \underset{(0.0000)}{- 0.239761*(PG64-22)} \underset{(0.0044)}{} \quad \textbf{2.5.1}$$

$$\underset{(0.0000)}{-1.063465*(PG76-22)} \qquad (R^2 = 0.85)$$

In Equation 2.5.1, P-value of the estimated regression coefficients are presented in parenthesis below each coefficient. The coefficient of determination (R^2) for the developed model is 0.85, indicating that 85 percent of the variance in the response would be explained by the explanatory variables.

The residual plots for the regression model are shown in Figure 2.56. Figure 2.56a shows that the assumption of the constant variance in linear regression is met since the residuals are randomly scattered around the zero line. Figure 2.56b represents the observed data versus fitted values.

Figure 2.56c shows that residuals follow a normal distribution. Finally, Figure 2.56d is developed to find the possible outliers (points with standardized residual values greater than 2 or less than -2). Most of the points fall between -2 and 2, so there are no outliers in the data.

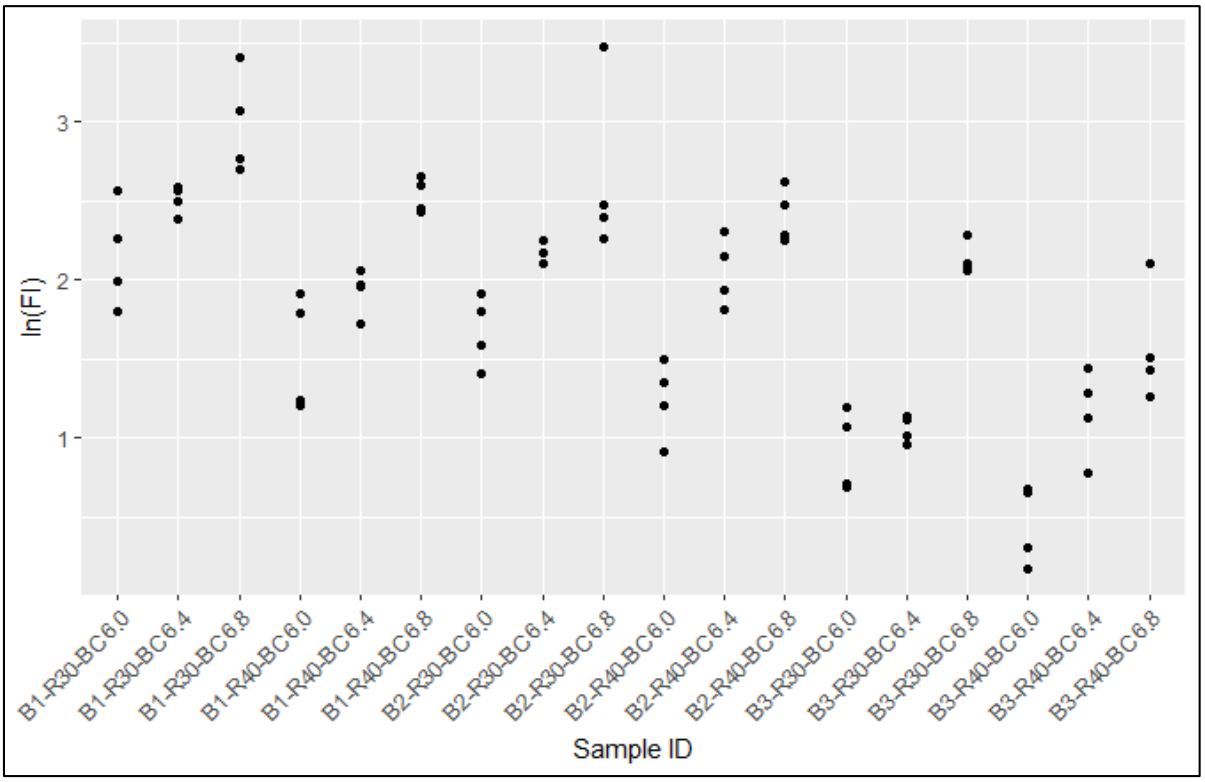

Figure 2.55. ln(FI) for each combination of RAP content, binder content, and binder grade
Note: B1= PG 58-34, B2= PG 64-22, and B3 = PG 76-22.
R30 = 30% RAP, and R40 = 40% RAP.
BC6= 6% binder content, BC6.4 =6.4 % binder content, and BC6.8 = 6.8% binder content.

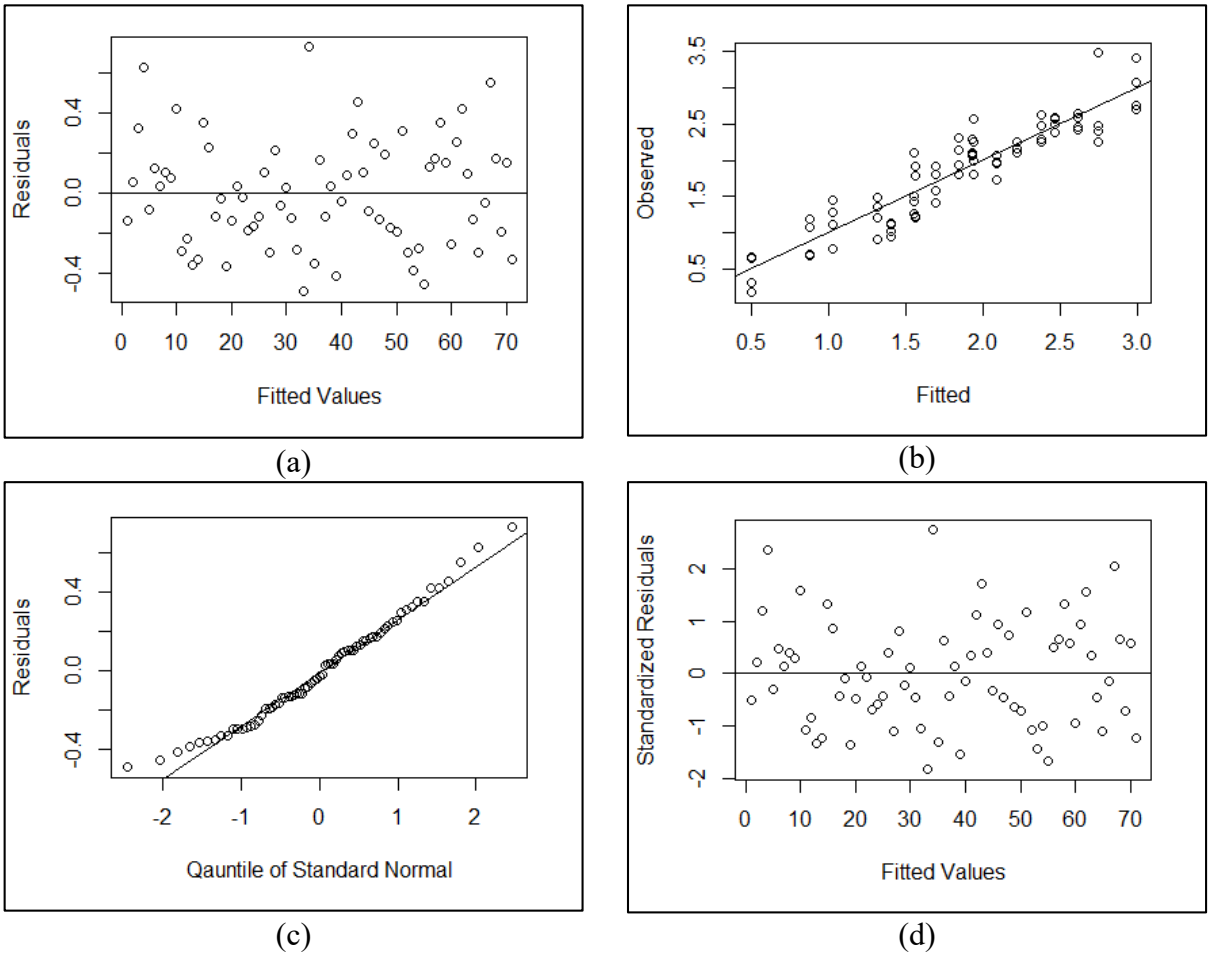

Figure 2.56. Residual plots for the regression model correlating ln(FI) with RAP content, binder content, and binder grade

2.5.5.3 Linear regression model for FN

The FN values obtained from FN tests were logarithmically transformed in order to allow the model to be estimated by linear regression. ln(FN) for all the tested mixtures in Section 2.5.2 are presented in Figure 2.57. Following equation shows the estimated model correlating ln(FN) with RAP content, binder content, and binder grade. P-value of each estimated coefficient is shown in parenthesis. Adjusted R^2 is 0.94, meaning that 94 percent of the variance in response can be explained by the explanatory variables.

$$\ln(FN) = \underset{(0.0000)}{11.230864} + \underset{(0.0000)}{0.080577}*RAP - \underset{(0.0000)}{1.172814}*BC + \underset{(0.0000)}{0.723180}*(PG64-22) + \underset{(0.0000)}{2.186587}*(PG76-22) \quad (R^2 = 0.94) \qquad \textbf{2.5.2}$$

Residual plots of the developed regression model are presented in Figure 2.58. The residuals are scattered randomly around zero in Figure 2.58a, meaning that the assumption of the constant variance in the regression model is met. Figure 2.58b shows observed values versus predicted values. Figure 2.58c shows that the assumption of normality in linear regression is met as well. Finally, the outliers can be identified in Figure 2.58d, with the absolute value of standardized residuals greater than 2. One of the points seems to be an outlier since its standardized residual is around -3. To further investigate the effect of outliers, Figure 2.58e was developed. It can be seen that none of the observations had Cook's distance greater than 0.5. Therefore, the outlier is not expected to create any bias in the developed linear regression model.

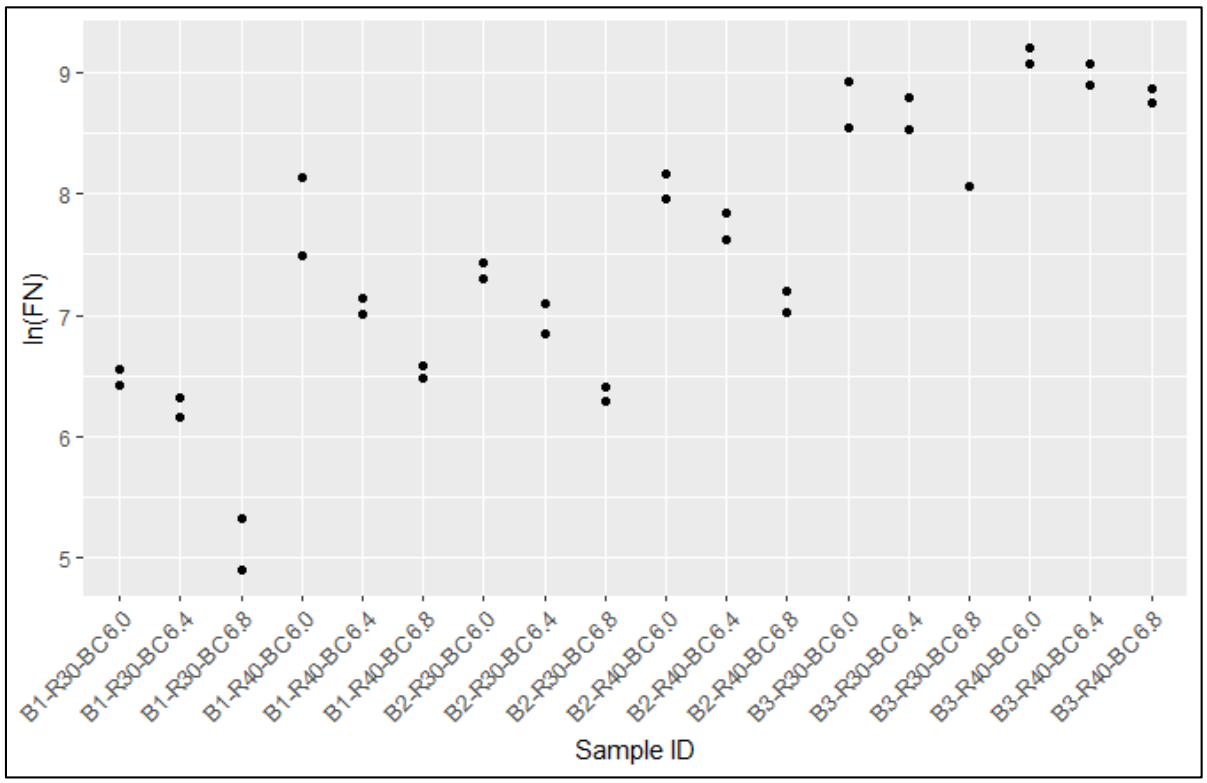

Figure 2.57. ln(FN) for each combination of RAP content, binder content, and binder grade
Note: B1= PG 58-34, B2= PG 64-22, and B3 = PG 76-22.
R30 = 30% RAP, and R40 = 40% RAP.
BC6= 6% binder content, BC6.4 =6.4 % binder content, and BC6.8 = 6.8% binder content.

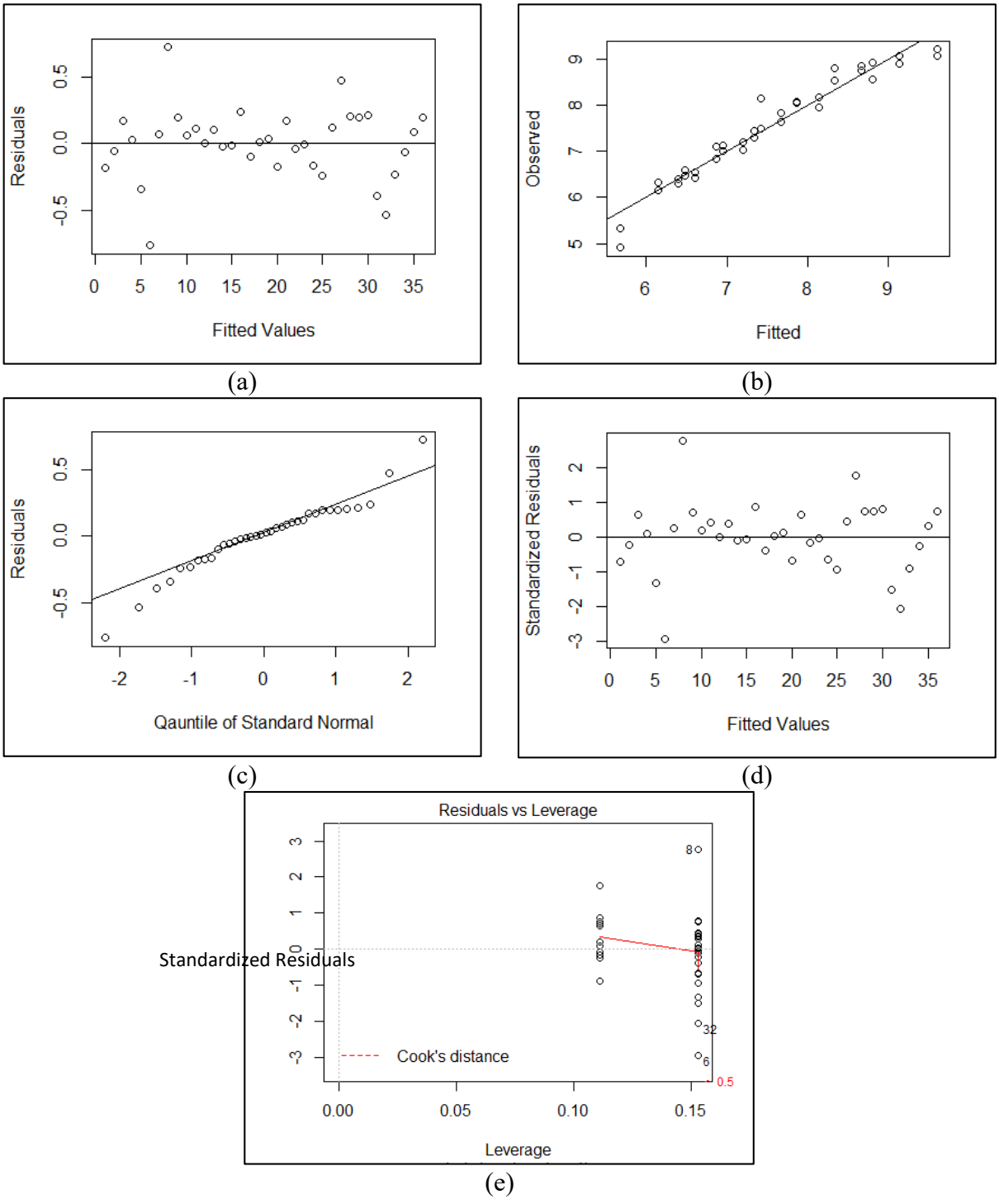

Figure 2.58. Residual plots for the regression model correlating ln(FN) with RAP content, binder content, and binder grade

2.5.5.4 Determination of asphalt mixtures with high cracking and rutting performance – Suggested strategies

To determine asphalt mixtures with high cracking and rutting performance, FI and FN of asphalt mixtures with different RAP contents (25% to 45%), binder contents (5% to 8%), and binder grades (PG 58-34, PG 64-22, and PG 76-22) were predicted using the regression models developed in Sections 2.5.5.2 and 2.5.5.3. All independent variables and their numerical ranges used for FI and FN predictions are presented in Table 2.9.

Predicted FI and FN for different RAP contents, binder contents, and binder grades, along with the region of acceptance for cracking and rutting performance, are presented in Figure 2.59. Then, mixtures falling within the region of acceptance [FI greater than 10 and FN greater than 740 (AASHTO TP 79-13)] were found and presented in Table 2.10 as suggested mixtures. It is worthwhile to note that asphalt mixtures with RAP 40%, BC 6.6%, and PG 58-34 showed acceptable predicted cracking (FI=10.51) and rutting performance (FN=823). Also, asphalt mixtures with RAP 45%, BC 6.8%, and PG 58-34 fell within the region of acceptance although the same mixture with 40% RAP fails in rutting. Asphalt mixtures with 45% RAP and PG 64-22 required higher binder contents (6.9% to 7.6%) than mixtures with PG 58-34 to be resistant to cracking and rutting. For mixtures with RAP 40%, 35% and 30% and PG 64-22, binder content should be between 6.8%-7.3%, 6.7%-6.9%, and 6.5%-6.6%, respectively. For the lowest RAP content (25%), only mixtures with PG 76-22 and BC 7%-7.5% had acceptable predicted FI and FN. For mixtures with RAP 45%, 40%, 35%, and 30% and PG 76-22, mixtures with binder contents of 7.6%-8%, 7.4%-8%, 7.3%-8%, and 7.1%-8.5%, respectively, fell within the region of acceptance.

Table 2.9. Independent variables and their ranges for FI and FN predictions

Variable Type	Symbol	Description	Range
Independent	RAP	RAP Content	25 to 45 with 5 increments
	BC	Binder Content	5 to 8 with 0.1 increments
Category Independent	PG	Binder Grade	PG 58-34, PG 64-22, and PG 76-22

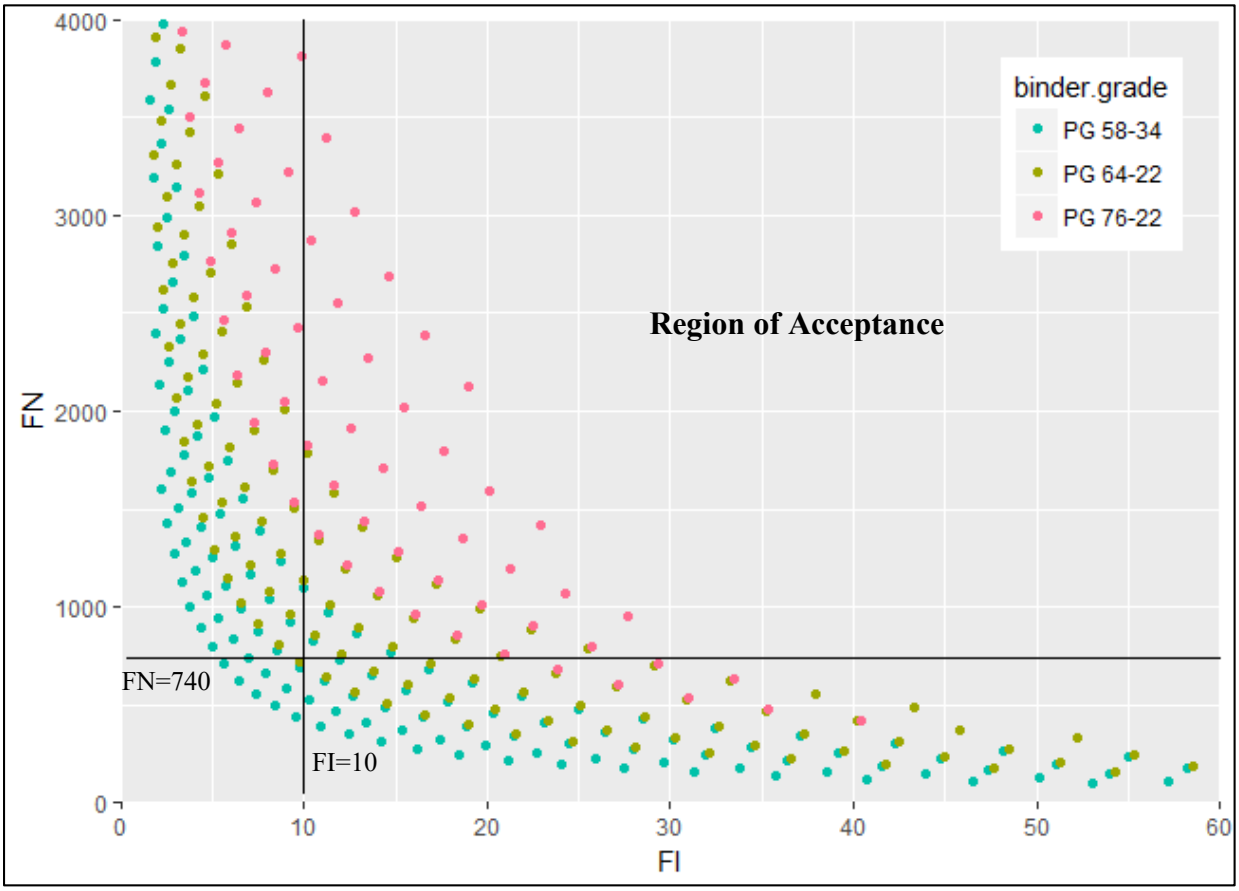

Figure 2.59. Predicted FI and FN for different RAP contents, binder contents, and binder grades

Table 2.10. Suggested strategies - Mixtures with FN greater than 740 and FI greater than 10

#Sample	RAP Content	Binder Content	Binder Grade	FN	FI
1	45	6.8	PG 58-34	974	11.3
2	45	6.9	PG 58-34	866	12.9
3	45	7	PG 58-34	771	14.7
4	45	6.9	PG 64-22	1786	10.2
5	45	7	PG 64-22	1588	11.6
6	45	7.1	PG 64-22	1412	13.2
7	45	7.2	PG 64-22	1256	15.1
8	45	7.3	PG 64-22	1117	17.2
9	45	7.4	PG 64-22	993	19.6
10	45	7.5	PG 64-22	883	22.4
11	45	7.6	PG 64-22	786	25.6
12	45	7.6	PG 76-22	3395	11.2
13	45	7.7	PG 76-22	3019	12.8
14	45	7.8	PG 76-22	2685	14.6
15	45	7.9	PG 76-22	2388	16.7
16	45	8	PG 76-22	2124	19.0
17	40	6.6	PG 58-34	823	10.5
18	40	6.8	PG 64-22	1342	10.8
19	40	6.9	PG 64-22	1194	12.3
20	40	7	PG 64-22	1061	14.0
21	40	7.1	PG 64-22	944	16.0
22	40	7.2	PG 64-22	840	18.2
23	40	7.3	PG 64-22	747	20.8
24	40	7.4	PG 76-22	2869	10.4
25	40	7.5	PG 76-22	2551	11.9
26	40	7.6	PG 76-22	2269	13.5
27	40	7.7	PG 76-22	2018	15.5
28	40	7.8	PG 76-22	1795	17.6
29	40	7.9	PG 76-22	1596	20.1
30	40	8	PG 76-22	1419	22.9
31	35	6.7	PG 64-22	1009	11.4
32	35	6.8	PG 64-22	897	13.0
33	35	6.9	PG 64-22	798	14.8
34	35	7.3	PG 76-22	2156	11.0
35	35	7.4	PG 76-22	1918	12.6
36	35	7.5	PG 76-22	1705	14.3

Table 2.10. Suggested strategies - Mixtures with FN greater than 740 and FI greater than 10 (Continued)

#Sample	RAP Content	Binder Content	Binder Grade	FN	FI
37	35	7.6	PG 76-22	1517	16.4
38	35	7.7	PG 76-22	1349	18.7
39	35	7.8	PG 76-22	1200	21.3
40	35	7.9	PG 76-22	1067	24.3
41	35	8	PG 76-22	949	27.7
42	30	6.5	PG 64-22	852	10.6
43	30	6.6	PG 64-22	758	12.1
44	30	7.1	PG 76-22	1822	10.2
45	30	7.2	PG 76-22	1620	11.7
46	30	7.3	PG 76-22	1441	13.3
47	30	7.4	PG 76-22	1282	15.2
48	30	7.5	PG 76-22	1140	17.3
49	30	7.6	PG 76-22	1014	19.7
50	30	7.7	PG 76-22	902	22.5
51	30	7.8	PG 76-22	802	25.7
52	25	7	PG 76-22	1369	10.8
53	25	7.1	PG 76-22	1218	12.3
54	25	7.2	PG 76-22	1083	14.1
55	25	7.3	PG 76-22	963	16.1
56	25	7.4	PG 76-22	857	18.3
57	25	7.5	PG 76-22	762	20.9

2.6 SUMMARY AND CONCLUSIONS

Recycling highway construction materials and minimizing the use of virgin materials can reduce the pavement life cycle costs, improve highway network condition, conserve natural resources, and protect the environment. Although recycling of asphalt pavements is beneficial in most cases by reducing the need for virgin materials and construction costs, asphalt pavements with high RAP contents should be carefully designed to avoid premature cracking. This study evaluates the effects of binder-grade bumping and high virgin binder content on cracking performance of asphalt mixtures. These two strategies were determined to be effective in improving cracking performance. SCB, DM, and FN tests were conducted on lab prepared samples with two RAP contents (30% and 40%), three binder contents (6%, 6.4%, and 6.8%), and three binder grades (PG 58-34, PG 64-22, and PG 76-22) to assess their cracking and rutting performance. Linear regression models correlating FI and FN (dependent variables) with RAP content, binder content, and binder grade (independent variables) were also developed. Then, possible combinations of these three independent variables to produce asphalt mixtures with acceptable cracking and rutting performance were predicted by using the developed regression models. The following conclusions can be drawn based on the results of this study:

- As RAP content increases, asphalt mixtures get more susceptible to cracking and more resistant to rutting. Increasing the binder content and using softer binder increases cracking resistance, but make mixtures more susceptible to rutting. Hence, rutting and cracking tests should be conducted for asphalt mixture design to produce high-performance mixtures.

- The mixture with 40% RAP, 6.8% binder content, and PG 64-22 showed high rutting (FN greater than 740) and cracking performance (FI greater than 9).

- Although mixtures with binder grade of PG 76-22 showed high rutting resistance, none of them had FI greater than 9, meaning that they are susceptible to cracking. Higher binder content (higher than 6.8%) could enhance their cracking performance. On the contrary, mixtures with binder grade of PG 58-34 had higher cracking resistance, but none of them can be used in highways with the traffic level greater than 30 million ESALs.

- Developed regression models showed that mixture with RAP 40%, BC 6.6%, and PG 58-34 has acceptable predicted cracking (FI=10.5) and rutting performance (FN=823). Also, to increase RAP content up to 40% for mixtures with PG 76-22, binder content should be higher than 7.4%.

- FI is a good performance indicator since it can differentiate the cracking performance of mixtures with different RAP contents, binder contents, and binder grades. Therefore, this study suggests conducting the SCB tests to evaluate cracking performance of asphalt mixtures since it is more practical and easier to perform.

- Although there is a non-linear correlation between FN and FI, correlation is not strong enough to be able to predict FI results using the FN results and vice versa. For this reason, both experiments need to be conducted to evaluate rutting and cracking resistance of asphalt mixtures.

- Dynamic modulus results at 40 ºC and 0.1 Hz can be used to predict FN (rutting resistance of the asphalt mixtures). In general, there is not a strong correlation between dynamic modulus and FI, especially for PG 76-22. However, dynamic modulus has a strong correlation with FI at 20 ºC and 4 ºC for mixtures with PG 58-34 and can be used to predict FI. As the binder becomes stiffer, the correlations between FI and dynamic modulus become weaker.

2.7 FUTURE STUDY

Based on the conclusions from this research, the following recommendations are suggested:

- Effect of rejuvenators on rutting and cracking resistance of asphalt mixtures should be evaluated.

- This study considers a complete blending of RAP binder and virgin binder. Further investigation is required to assess how much RAP binder is blended with virgin binder after mixing virgin aggregates, virgin binders, and RAP materials.

- To estimate the service life and field performance of asphalt mixtures with RAP, Mechanistic-Empirical Pavement Design Guide (MEPDG) modeling should be conducted using the DM test results and AASHTOWare Pavement ME Design (2008) software.

- Suggested mixtures should be used to construct pilot sections in Oregon to determine the in-situ rutting and cracking performances. This field investigation will validate the results of this research study and open up the way for implementation.

- Cost analysis should be performed to find the most cost-effective combinations of RAP content, binder content, and binder grade.

2.8 ACKNOWLEDGMENTS

The authors would like to express their acknowledgment to the Oregon Department of Transportation (ODOT) for funding this research project. The views and opinions expressed in this article are the authors' own and do not necessarily reflect the view and official policies of the Oregon Department of Transportation or the Federal Highway Administration. The authors would like to thank Yuqi Zhang, Tim Flowerday, Nicholas Kolstad, John Paul Morton, Andrew Johnson, Natasha Anisimova, Matthew Haynes, Jawad Qassem, and Sunny Lewis for their collaborations in sieving, batching, and measuring theoretical maximum specific gravity of prepared samples, as well as James Batti for his help in the laboratory. Also, a special thank you to the members of the ODOT Project Technical Advisory Committee for their advice and assistance, to Terri Zahler from McCall Oil for providing asphalt binders, and to Mike Miller from Oldcastle Materials for providing aggregates and RAP materials used in this study.

2.9 REFERENCES

AASHTO PP 60-14. *Standard Practice for Preparation of Cylindrical Performance Test Specimens Using the Superpave Gyratory Compactor.* Washington, DC: American Association of State and Highway Transportation Officials, 2014.

AASHTO PP 61-13. *Standard Practice for Developing Dynamic Modulus Master Curves for Hot Mix Asphalt (HMA) Using the Asphalt Mixture Performance Tester (AMPT).* Washington, DC: American Association of State and Highway Transportation Officials, 2013.

AASHTO R 30-10. *Standard Practice for Mixture Conditioning of Hot Mix Asphalt (HMA).* Washington, DC: American Association of State and Highway Transportation Officials, 2010.

AASHTO R 43-07. *Standard Practice for Quantifying Roughness of Pavements*. Washington, DC: American Association of State and Highway Transportation Officials, 2013.

AASHTO T 166-12. *Bulk Specific Gravity (Gmb) of Compacted Hot Mix Asphalt (HMA) using Saturated Surface-Dry Specimens.* Washington, DC: American Association of State Highway and Transportation Officials, 2012.

AASHTO T 209-12. *Theoretical Maximum Specific Gravity (Gmm) and Density of Hot Mix Asphalt.* Washington, DC: American Association of State Highway and Transportation Officials, 2012.

AASHTO T 27-11. *Standard Method of Test for Sieve Analysis of Fine and Coarse Aggregates.* Washington, DC: American Association of State Highway and Transportation Officials, 2011.

AASHTO T 30-10. *Standard Method of Test for Mechanical Analysis of Extracted Aggregate.* Washington, DC: American Association of State Highway and Transportation Officials, 2010.

AASHTO T 308-10. *Determining the Asphalt Binder Content of Hot Mix Asphalt (HMA) by the Ignition Method.* Washington, DC: American Association of State and Highway Transportation Officials, 2010.

AASHTO T 312-12. *Preparing and Determining the Density of Hot Mix Asphalt (HMA) Specimens by Means of the Superpave Gyratory Compactor.* Washington, DC: American Association of State Highway and Transportation Officials, 2012.

AASHTO T 316-11. *Viscosity Determination of Asphalt Binder Using Rotational Viscometer.* Washington, DC: American Association of State and Highway Transportation Officials, 2011.

AASHTO T 321–07. *Standard Method of Test for Determining the Fatigue Life of Compacted Hot-Mix Asphalt (HMA) Subjected to Repeated Flexural Bending*. Washington, DC: American Association of State and Highway Transportation Officials, 2007.

AASHTO TP 105-13. *Standard Method for Determining the Fracture Energy of Asphalt Mixtures Using the Semi Circular Bend Geometry (SCB)*. Washington, DC: American Association of State Highway and Transportation Officials, 2013.

AASHTO TP 79-13. *Standard Method for Determining the Dynamic Modulus and Flow Number for Hot Mix Asphalt (HMA) Using the Asphalt Mixture Performance Tester (AMPT).* Washington, DC: American Association of State and Highway Transportation Officials*,* 2013.

AASHTOWare-Pavement ME Design 1.0™. American Association of State Highway and Transportation Officials (AASHTO), 2008.

Aguiar-Moya, J., F. Hong, J. Prozzi. RAP: Save Today, Pay Later? Proceedings 90th Annual Meeting of the Transportation Research Board, Washington D.C, 2011.

Al-Qadi, I. L., and Ozer, H. Impact of RAS and RAP on Asphalt Mixtures' Fracture: The Need for a Cracking Potential Index. Illinois Center for Transportation University of Illinois at Urbana-Champaign, 2015.

Al-Qadi, I.L., Ozer, H., Lambros, J., El Khatib, A., Singhvi, P., Khan, T., Rivera-Perez, J. and Doll, B. *Testing Protocols to Ensure Performance of High Asphalt Binder Replacement Mixes Using RAP and RAS*. Publication FHWA-ICT-15-017. Illinois Center for Transportation/Illinois Department of Transportation, 2015.

Andreen, B., H. Rocheville, K. Ksaibati. A Method of Cost-Benefit Analysis of RAP in Various Highway Applications. Proceedings 91st Annual Meeting of the Transportation Research Board, Washington D.C., 2012.

Asphalt Institute Technical Advisory Committee Version 1.1. *Determining Laboratory Mixing and Compaction Temperatures*, 2014.

Aurangzeb, Q., I. Al-Qadi, I. Abuawad, W. Pine, and J. Trepanier. Achieving Desired Volumetrics and Performance for Mixtures with High Percentage of Reclaimed Asphalt Pavement. *Transportation Research Record: Journal of the Transportation Research Board*, No. 2294, 2012, pp.34-42.

Aurangzeb, Q., I. L. Al-Qadi, H. Ozer, R. Yang. Hybrid Life Cycle Assessment for Asphalt Mixtures with High RAP Content. *Journal of Resources, Conservation and Recycling*, 2013.

Bennert, T., J. Daniel, and W. Mogawer. Strategies for Incorporating Higher Recycled Asphalt Pavement Percentages: Review of Implementation Trials in Northeast States. *Transportation Research Record: Journal of the Transportation Research Board*, No. 2445, 2014, pp. 83-93.

Biligiri, K., Kaloush, K., Mamlouk, M. and Witczak, M. Rational Modeling of Tertiary Flow for Asphalt Mixtures. *Transportation Research Record: Journal of the Transportation Research Board* 2001, 2007, pp.63-72.

Bonaquist, R.F. *Precision of the Dynamic Modulus and Flow Number Tests Conducted with the Asphalt Mixture Performance Tester*. NCHRP Report, No. 702, National Cooperative Highway Research Program, Washington D.C., 2011.

Bonaquist, R.F., Christensen, D.W. and Stump, W. *Simple Performance Tester for Superpave Mix Design: First-Article Development and Evaluation.* Transportation Research Board, 2003, Vol. 513.

Carpenter, S.H. and J. R. Wolosick. Modifier Influence in the Characterization of Hot-Mix Recycled Material. *Transportation Research Record: Journal of the Transportation Research Board*, 1980, No. 777, pp.15-22.

Carvalho, R., H. Shirazi, M. Ayres Jr, and O. Selezneva. Performance of Recycled Hot-Mix Asphalt Overlays in Rehabilitation of Flexible Pavements. *Transportation Research Record: Journal of the Transportation Research Board*, 2010, No. 2155, pp.55-62.

Copeland, A. *Reclaimed Asphalt Pavement in Asphalt Mixtures: State of the Practice*. Federal Highway Administration, No. FHWA-HRT-11-021, 2011.

Darnell Jr, J. and Bell, C.A. *Performance Based Selection of RAP/RAS in Asphalt Mixtures*. Federal Highway Administration, No. FHWA-OR-RD-16-08, 2015.

Dongré, R., D'Angelo, J. and Copeland, A. Refinement of Flow Number as Determined by Asphalt Mixture Performance Tester: Use in Routine Quality Control—Quality Assurance Practice. *Transportation Research Record: Journal of the Transportation Research Board,* (2127), 2009, pp.127-136.

Coleri, E. Adjusting Asphalt Mixes for Increased Durability and Implementation of a Performance Tester to Evaluate Fatigue Cracking of Asphalt Concrete. ODOT Research Project Progress Presentation. 04/17/2017, Salem Oregon.

Francken, L. Pavement Deformation Law of Bituminous Road Mixes in Repeated Load Triaxial Compression. Presented at Fourth International Conference on the Structural Design of Asphalt Pavements, University of Michigan, Ann Arbor, 1977.

Hajj, E.Y., P. E. Sebaaly, and R. Shrestha. Laboratory Evaluation of Mixes Containing Recycled Asphalt Pavement (RAP). *Road Materials and Pavement Design*, 2009, 10(3), 495-517.

Hansen, K. R. and A. Copeland. Asphalt Pavement Industry Survey on Recycled Materials and Warm Mix Asphalt Usage (5th ed). Lanham, MD: *National Asphalt Pavement Association (NAPA)*, 2014.

Harvey, J., Liu, A., Zhou, J., Signore, M., Coleri, E. and HE, Y. *Superpave Implementation Phase II: Comparison of Performance-Related Test Results.* UCPRC Research Report No: UCPRC-RR-2015-01, 2014.

Lee, N., C. Chou, K. Chen. Benefits in Energy Savings and CO2 Reduction by Using RAP. Proceedings 91st Annual Meeting of the Transportation Research Board, Washington D.C., 2012.

Li, X., M. O. Marasteanu, R. C. Williams, and T. R. Clyne. Effect of Reclaimed Asphalt Pavement (Proportion and Type) and Binder Grade on Asphalt Mixtures. *Transportation Research Record: Journal of the Transportation Research Board*, 2008, No.2051, pp.90–97.

Mallick, R. B., P. S. Kandhal, and R. L. Bradbury. Using Warm-Mix Asphalt Technology to Incorporate High Percentage of Reclaimed Asphalt Pavement Material in Asphalt Mixtures. *Transportation Research Record: Journal of the Transportation Research Board*, 2008, No. 2051, pp.71–79.

MATLAB R2016b: MATLAB and Statistics Toolbox. The MathWorks, Inc., Natick, Massachusetts, United States, 2016.

McDaniel, R., and R. M. Anderson. NCHRP Web Document 30: Recommended Use of Reclaimed Asphalt Pavement in the Superpave Mix Design Method–Project 9-12. *Final Report*, 2001.

Mohammad, L. N., B. Samuel, Cooper Jr, and A. E. Mostafa. Characterization of HMA Mixtures Containing High Reclaimed Asphalt Pavement Content with Crumb Rubber Additives. *Journal of Materials in Civil Engineering* 23, No. 11, 2011, pp.1560-1568.

Newcomb, D. E., E. R. Brown, and J. A. Epps. *Designing HMA Mixtures with High RAP Content: A Practical Guide.* National Asphalt Pavement Association (NAPA), 2007.

Newcomb, D. *Thin Asphalt Overlays for Pavement Preservation.* National Asphalt Pavement Association (NAPA). Information Series 135, 2009.

Norouzi, A., Kim, D. and Kim, Y.R. Numerical Evaluation of Pavement Design Parameters for the Fatigue Cracking and Rutting Performance of Asphalt Pavements. *Materials and Structures*, 49(9), 2016, pp.3619-3634.

Nsengiyumva, G. Development of Semi-Circular Bending (SCB) Fracture Test for Bituminous Mixtures, 2015.

ODOT TM 319. *Preparation and Characterization of Recycled Asphalt Materials for Mix Design*, Oregon Department of Transportation, undated.

Oliveira, J. R., H. M. Silva, C. M. Jesus, L. P. Abreu, and S. R. Fernandes. Pushing the Asphalt Recycling Technology to the Limit. *International Journal of Pavement Research and Technology*, 6(2), 2013, pp.109.

Ozer, H., Al-Qadi, I. L., Lambros, J., El-Khatib, A., Singhvi, P., & Doll, B. Development of the Fracture-Based Flexibility Index tor Asphalt Concrete Cracking Potential Using Modified Semi-Circle Bending Test Parameters. *Construction and Building Materials*, 115, 2016, 390–401

Paul, H. R. Evaluation of Recycled Projects for Performance. *Asphalt Paving Technology*, 1996, No. 65, pp.231-254.

Pavement Interactive. *Bulk Specific Gravity.* Retrieved from: http://www.pavementinteractive.org/bulk-specific-gravity. Accessed May 14, 2017.

Petersen, J. C. Chemical Composition of Asphalt as Related to Asphalt Durability: State of the Art. *Transportation Research Record: Journal of the Transportation Research Board*, 1984, No.999.

Roberts, F. L., P. S. Kandhal, E. R. Brown, D. Y. Lee, and T. W. Kennedy. Hot Mix Asphalt Materials, Mixture Design and Construction. *National Asphalt Pavement Association Research and Education Foundation*, Lanham, MD., 1996.

Rodezno, M.C., West, R. and Taylor, A. Flow Number Test and Assessment of AASHTO TP 79-13 Rutting Criteria: Comparison of Rutting Performance of Hot-Mix and Warm-Mix Asphalt Mixtures. *Transportation Research Record: Journal of the Transportation Research Board,* (2507), 2015, pp.100-107.

Seber, G.A.F. *Linear Regression Analysis*, John Wiley & Sons, 1977.

Shen, J., S. Amirkhanian, and J. Aune Miller, J. Effects of Rejuvenating Agents on Superpave Mixtures Containing Reclaimed Asphalt Pavement. *Journal of Materials in Civil Engineering*, 19(5), 2007, pp.376–384.

Tao, M., and R. Mallick. Effects of Warm-Mix Asphalt Additives on Workability and Mechanical Properties of Reclaimed Asphalt Pavement Material. *Transportation Research Record: Journal of the Transportation Research Board*, No. 2126, 2009, pp.151-160.

Terrel, R. L., and J. A. Epps. *Using Additives and Modifiers in Hot Mix Asphalt.* National Asphalt Pavement Association (NAPA), Section A No. QIP-114A. 1989.

Tran, N., A. Taylor, and R. Willis. *Effect of Rejuvenator on Performance Properties of HMA Mixtures with High RAP and RAS Contents.* National Center for Asphalt Technology, NCAT Report 12–05, June 2012.

University of California (UC). International Symposium on Pavement LCA 2014, 2014. Retrieved from Summary Review Session (Day 3): http://www.ucprc.ucdavis.edu/p-lca2014/ProgramBreakouts.aspx

West, R., A. Kvasnak, N. Tran, B. Powell, and P. Turner. Testing of Moderate and High Reclaimed Asphalt Pavement Content Mixes: Laboratory and Accelerated Field Performance Testing at the National Center for Asphalt Technology Test Track. *Transportation Research Record: Journal of the Transportation Research Board*, No. 2126, 2009, 100-108.

West, R., J. Michael, R. Turochy, and S. Maghsoodloo. Use of Data from Specific Pavement Studies Experiment 5 in the Long-Term Pavement Performance Program to Compare Virgin and Recycled Asphalt Pavements. *Transportation Research Record: Journal of the Transportation Research Board*, No. 2208, 2011, pp.82-89.

West, R., Timm, D., Willis, R., Powell, B., Tran, N., Watson, D., Sakhaeifar, M., Brown, R., Robbins, M., Nordcbeck, A.V. and Villacorta, F.L. *Phase IV NCAT Pavement Test Track Findings.* Auburn, AL: National Center for Asphalt Technology, Report Number NCAT 12-10, 2012.

Williams, R. S., and R. Shaidur. *Premature Asphalt Concrete Pavement Cracking.* SPR 734, Final Report for Oregon Department of Transportation, Salem, Oregon, 2015.

Willis, J. R. Effect of Recycled Materials on Pavement Life-cycle Assessment: A Case Study. Proceedings 94th Annual Meeting of the Transportation Research Board, Washington D.C, 2015.

Willis, J. R., P. Turner, G. Julian, A. J. Taylor, N. Tran, and F. Padula. *Effects of Changing Virgin Binder Grade and Content on RAP Mixture Properties*. National Center for Asphalt Technology Report, (12-03), 2012.

World Highways. *Recycling Asphalt Provides Green Result*. 2013. Retrieved from http://www.worldhighways.com/categories/materials-production-supply/features/recycling-asphalt-provides-green-result. Accessed October 15, 2015.

Wu, Z., Mohammad, L.N., Wang, L.B. and Mull, M.A. Fracture Resistance Characterization of Superpave Mixtures Using the Semi-Circular Bending Test. *Journal of ASTM International,* 2(3), 2005, pp.1-15.

Xiao, F., S. Amirkhanian, and C. H. Juang. Rutting Resistance of Rubberized Asphalt Concrete Pavements Containing Reclaimed Asphalt Pavement Mixtures. *Journal of Materials in Civil Engineering*, 19(6), 2007, pp.475–483.

Xiao, F., S. N. Amirkhanian, J. Shen, and B. Putman. Influences of Crumb Rubber Size and Type on Reclaimed Asphalt Pavement (RAP) Mixtures. *Construction and Building Materials*, *23*(2), 2009, pp.1028-1034.

Zaumanis, M., R. Mallick, and R. Frank. Evaluation of Rejuvenator's Effectiveness with Conventional Mix Testing for 100 % Reclaimed Asphalt Pavement Mixtures. *Transportation Research Record: Journal of the Transportation Research Board*, No. 2370, 2013, pp.17–25.

Zhao, S., B. Huang, X. Shu, X. Jia, and M. Woods. Laboratory Performance Evaluation of Warm-Mix Asphalt Containing High Percentages of Reclaimed Asphalt Pavement. *Transportation Research Record: Journal of the Transportation Research Board*, No. 2294, 2012, pp.98-105.

Zhou, F., S. Im, D. Morton, R. Lee, S. Hu, and T. Scullion. Rejuvenator Characterization, Blend Characteristics, and Proposed Mix Design Method. *Association of Asphalt Paving Technologists,* 2015.

3. CHAPTER 3 - A NETWORK-LEVEL DECISION-MAKING TOOL FOR PAVEMENT MAINTENANCE AND USER SAFETY

Sogol Sadat Haddadi[7] , Erdem Coleri[8] , and Blaine Wruck[9]

Abstract: Although inflation has raised the cost of paving, pavement program funding levels are about 30% lower than a decade ago. Resurfacing treatments typically last 10 to 20 years but current pavement funding only allows for resurfacing every 30 years or longer. Thus, higher user costs (mostly related to vehicle maintenance and fuel consumption) are expected to be observed due to the increased pavement roughness. The goal of this study is to develop a network-level decision-making tool (software) suggesting the most efficient maintenance and rehabilitation strategies by minimizing user and agency costs and maximizing their benefits. This study also investigated the use of a maximum roughness level of 5 m/km to increase user safety. Effects of different trigger roughness levels (trigger IRIs) and different treatment methods (1. Considering one value for trigger IRI for all the sections regardless of the traffic levels, and 2. Considering different trigger IRIs for sections based on their traffic levels) on user benefits and agency costs were evaluated. This study found the first method more optimal. In addition, results showed that optimal trigger IRI depends on the available budget level. Considering a lower value for trigger IRI requires a higher budget level and increases user benefits.

Keywords: Pavement roughness, user safety, user benefits, agency costs, trigger IRI, pavement maintenance, decision-making tools.

---

[7] Graduate Research Assistant, School of Civil and Construction Engineering, Oregon State University, 101 Kearney Hall, Corvallis, OR, USA, 97331, Email: haddadis@oregonstate.edu.

[8] Assistant Professor, School of Civil and Construction Engineering, Oregon State University, 101 Kearney Hall, Corvallis, OR, USA, 97331, Tel: (541) 737-0944, Email: erdem.coleri@oregonstate.edu.

[9] Graduate Research Assistant, School of Civil and Construction Engineering, Oregon State University, 101 Kearney Hall, Corvallis, OR, USA, 97331, Email: wruckb@oregonstate.edu.

3.1 INTRODUCTION

The 2012 Pavement Condition Report released by ODOT (2013) indicated that pavement program funding levels are about 30% less than they were a decade ago, while inflation has simultaneously raised the cost of paving. Resurfacing treatments typically last 10 to 20 years but current pavement rehabilitation funding only allows for resurfacing every 30 years at minimum. Thus, higher user costs (mostly related to vehicle maintenance and fuel consumption) are expected to be observed due to increased pavement roughness. Although performance-based pavement design procedures have been implemented by all state DOTs, pavement roughness and vehicle operating costs are not directly considered in the decision-making process. Recent research by Chatti and Zaabar (2012) and European Asphalt Pavement Association (EAPA) (2004) showed that consideration of vehicle maintenance and fuel consumption costs in pavement design can change the current maintenance and rehabilitation strategies. International Roughness Index (IRI) is used for quantifying the longitudinal profile of the traveled wheel track and it is computed as the cumulative suspension displacement per unit of distance traveled and expressed as m/km or inches/mile. Trigger IRI, a value for IRI indicating failure of the pavement, values for different climate regions and traffic levels in the Pacific Northwest need to be determined by considering agency-user costs and safety. When the IRI reaches the trigger point, maintenance and rehabilitation are required.

A National Transportation Research Group (TRIP) (2015) reported that more than 28 percent of urban roads including interstates, freeways and arterial routes are in substandard conditions with IRIs above 170 inches/mile (2.68 m/km), providing poor ride quality and increased fuel/maintenance costs for road users. TRIP (2015) goes on to say that 41 percent of urban roads are in mediocre and fair condition with IRIs between 95 and 170 inches/mile and acceptable driving quality and 31 percent are in good condition with IRI ratings below 95 inches/mile. TRIP (2015) also manifested that road users in urban areas with population exceeding 500,000 pay an additional $516 annually by driving on poor condition pavements because of increased fuel consumption, vehicle maintenance/repair costs and accelerated vehicle deterioration. Substandard road conditions cost drivers on a national level about $109.3 billion annually in terms of Vehicle Operating Costs (VOC).

The impact of road roughness and surface texture on user safety is also an important issue in the decision-making process. Although reducing road roughness and surface texture decreases road user costs, it can also reduce skid resistance which can increase accident rates, especially during rain events. On the other hand, although skid resistance increases over time due to increased roughness and texture of roads, accumulation of severe cracks, rutting, and potholes on roads can also create safety issues. For this reason, the impact of pavement distresses and changes in roughness and texture (during the use phase and after construction) on road user safety should be considered in the pavement maintenance and rehabilitation decision-making process. Upper and lower roughness, texture and distress limits (trigger values) should be set to assure user safety. This study considers maximum IRI of 5 m/km for pavement maintenance and rehabilitation to increase safety and to reduce accident rates (Tighe et al. 2000).

3.1.1 Key objectives of this study

The objectives of this study are given as follows:

- Develop a network-level decision-making tool to select the most efficient pavement maintenance and rehabilitation strategies to minimize agency and user costs and maximize their benefits;
- Find the optimal trigger IRI for different budget levels to maximize user benefits by considering user safety;
- Compare different treatment methods (1. Considering one value for trigger IRI for all the sections regardless of the traffic levels, and 2. Considering different trigger IRIs for sections based on their traffic levels); and
- Integration of the developed decision-making tool with Geographic Information Systems (GIS).

3.1.2 Organization of the chapter

This introduction section is followed by the literature review in Chapter 3.2. Research methodology and procedure for developing the decision-making tool are discussed in Chapter 3.3. Chapter 3.4 shows the results of simulations conducted with the developed decision-making tool. In addition, different treatment methods (1. Considering one value for trigger IRI for all the

sections regardless of the traffic levels, and 2. Considering different trigger IRIs for sections based on their traffic levels) are compared, and optimal trigger IRIs for different budget levels are suggested in Chapter 3.4. Chapter 3.5 summarizes the process followed for the integration of the developed decision-making tool with Geographic Information Systems (GIS). Summary and conclusions are presented in Chapter 3.6 while future recommendations are discussed in Chapter 3.7.

3.2 LITERATURE REVIEW

3.2.1 Pavement roughness

Roughness refers to the irregularity of the pavement surface resulting in poor ride quality for road users. Roughness can be measured by the Present Serviceability Rating (PSR). PSR is the mean roughness on the 0 to 5 scale given by a panel of passengers in a vehicle (Al-Omari and Darter 1994). PSR is a subjective/judgmental observation about the serviceability of the pavement and it reflects the ride quality based on passenger interpretations. Therefore, it can be considered to be a measurement of roughness since roughness and ride quality are correlated (Pavement Interactive 2017). Figure 3.1 shows the chart used for rating pavement serviceability. Roughness can be also measured by International Roughness Index (IRI). IRI is the most common index used for quantifying road roughness (Pavement Interactive 2017). IRI is computed as the cumulative vertical suspension displacement per unit of distance traveled and expressed as m/km or inches/mile. It is used for quantifying the longitudinal roughness of the traveled wheel track. Figure 3.2 represents the IRI scale for different pavement types and conditions (Pavement Interactive 2017). To measure IRI, vehicles equipped with inertial profilers are driven at highway speeds to measure surface profiles. Quarter-car model, a mathematical model representing a single wheel moving on a pavement texture, is used to convert the surface profile to vertical vehicle suspension movement and roughness (Sayers 1989).

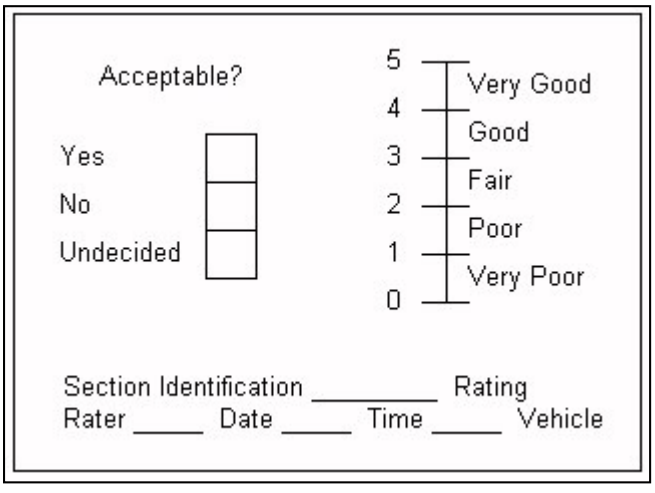

Figure 3.1. PSR rating (Pavement Interactive 2017)

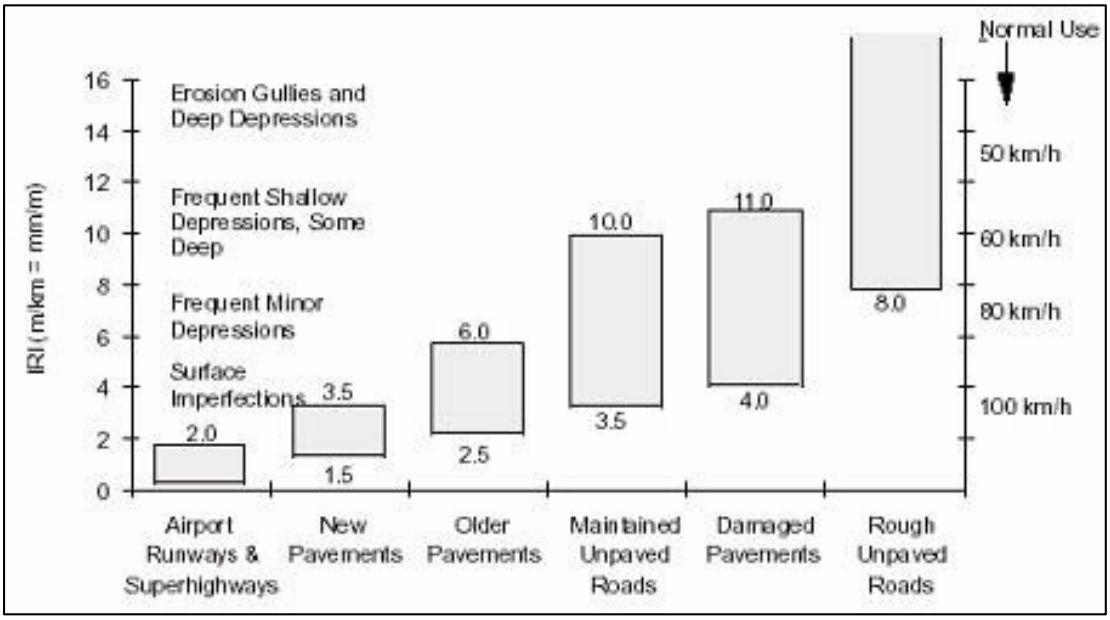

Figure 3.2. IRI roughness scale (Pavement Interactive 2017)

3.2.2 Effects of roughness on vehicle operating costs

Costs related to operating a vehicle, such as fuel consumption, oil and lubrication, tire wear, repair and maintenance, depreciation, license and insurance are referred to as vehicle operating costs (VOC). VOC models attempt to model fuel and oil consumption, repair and maintenance, depreciation, and tire wear separately and estimate total vehicle operating costs by summing them all together (Chatti and Zaabar 2012). Since the IRI directly affects VOCs and ride quality (user comfort), it is used to describe the condition of the roadways (Sayers et al. 1986).

The Highway Development and Management model (HDM) is developed by the World Bank in 1977. It is a computer model used for cost estimation of construction, maintenance, and roadway use. Since roadway user cost is a major part of transportation costs, it is the most important part to be precisely evaluated. In the HDM-4 model, fuel consumption, oil and lubricant consumption, labor hours, parts usage, depreciation, interest and overhead are included in the total VOCs. These costs can be affected by pavement condition, roadway geometry, operating speed and other factors related to vehicle type and technology (Bennett and Greenwood 2003). Although HDM-4 is expected to be an effective tool for VOC calculations, HDM-4 models were developed based on the data from developing countries and needed to be calibrated using the data for the USA.

Chatti and Zabaar (2012) calibrated HDM-4 models by considering United States' vehicle types, load levels, and pavement conditions. Fuel consumption, tire wear, and repair and maintenance costs, which are the factors most heavily affected by pavement conditions, were measured and evaluated. To accomplish this objective, surveys were conducted to collect data on pavement condition and field tests were performed in order to collect fuel consumption and tire wear data. Then, the collected data were used to validate and calibrate the HDM-4 fuel consumption and tire wear models. Additionally, mechanistic-empirical repair and maintenance models were developed for a full range of vehicle types and were designed to be compatible with the pavement conditions of the United States. Results showed that for the speed of 55 mph (88 km/h) at 30ºC with a mean profile depth (MPD) of 1 mm and a surface grade of 0%, increasing the IRI from 63.4 inches/mile to 190.2 inches/mile (1 m/km to 3 m/km) increased the fuel consumption around 1.8% and 2.9% for light trucks and articulated trucks, respectively. An IRI increase of 63.4 inches/mile (1 m/km) resulted in a fuel consumption increase of around 2% for passenger cars regardless of their speed. This study also manifested that, for a 17ºC temperature, a 1 mm (0.04 inches) MPD and a 0% grade, a 63.4 inches/mile (1 m/km) reduction in IRI reduced the tire wear costs by around 1%. This reduction had a tendency to increase with vehicle speeds for passenger cars. Moreover, it was concluded that there is no significant effect of IRI on vehicle maintenance and repair costs when IRI values are lower than 190.08 inches/mile (3 m/km). After this threshold, an increase in IRI of about 1 m/km increased the repair and maintenance costs around 10% for passenger cars and heavy trucks. Increases in IRI up to 316.8 inches/mile (5 m/km) resulted in maintenance cost increases of 40% for passenger cars and 50% for heavy trucks.

The WesTrack research study (Mitchell 2000) was conducted in Nevada for estimating the effect of pavement smoothness on fuel and maintenance costs of trucks. Four trucks applied about 4.9 million 80-kN Equivalent Single Axle Loads[10] (ESALs) in this project before and after rehabilitation of a specific pavement section. The section was milled around 100 mm and

[10]ESAL is a concept to compare the pavement damage caused by wheel loads with different magnitudes and repetitions. For this reason, different axle types with various carried loads are converted to a reference axle load. The reference axle load is an 18000-lb single-axle with dual tires (Pavement Interactive 2017).

resurfaced to improve the IRI of the pavement by at least 10 percent. The average fuel consumption of four trucks over the eight-week period prior to rehabilitation was estimated to be 4.2mi/gal (1.79 km/l) and about 4.4 mi/gal (10.35 km/l) over the seven-week period after rehabilitation. The improvement in fuel economy due to the reduction of IRI was about 4.5 percent. Moreover, this project stated that as the roughness of the pavement increased, the frequency of the failure of truck components increased as well. The four trucks' trailers tested in this study had a total of 40 springs. Eight trailer springs failed 8 weeks prior to the resurfacing during the application of 265,000 ESALs. However, only one trailer spring failed in the 7-week period after rehabilitation during the application of 350,000 ESALs. Figure 3.3 shows the number of spring failures per million ESALs.

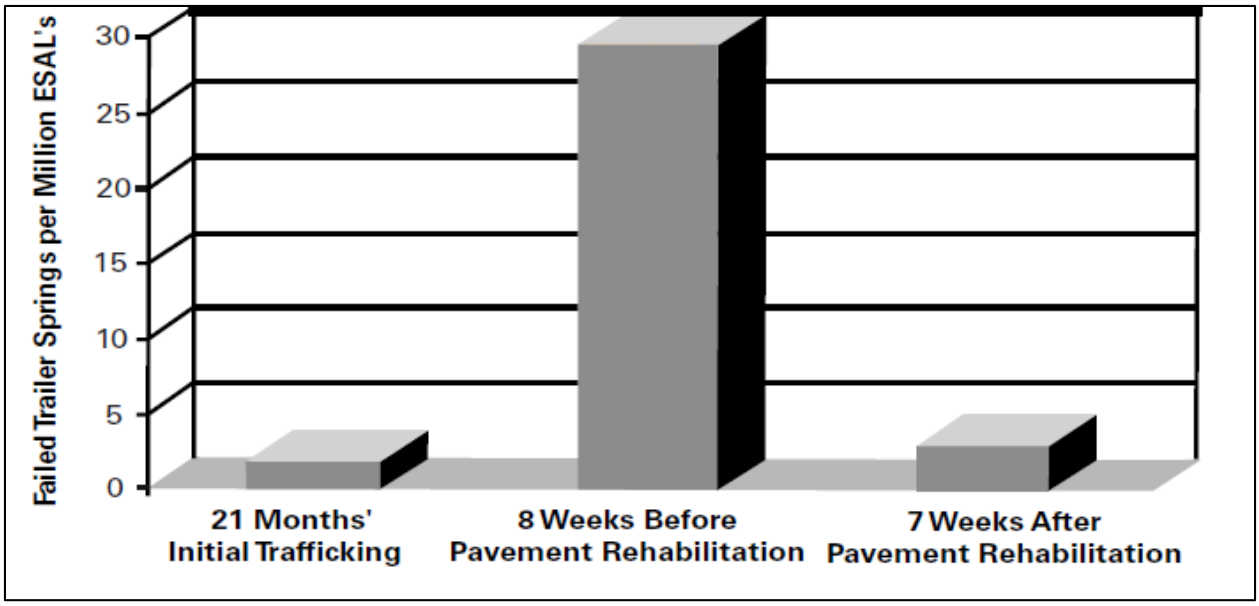

Figure 3.3. Effect of pavement condition on truck health (Mitchell 2000)

Barnes and Langworthy (2004) estimated per mile costs of operating automobiles and trucks by applying adjustment factors to costs derived from previous studies. Fuel consumption, maintenance and repair, tire replacement and depreciation were estimated as marginal VOCs. A smooth pavement condition (PSI=3.5, IRI=80 inches/mile) was considered as the baseline pavement condition. Marginal VOCs were measured for automobiles, pickups (including other large personal vehicles such as vans and SUVs), as well as commercial trucks. Results showed that fuel consumption was the primary cost component followed by maintenance/repair costs and

tire wear/replacement costs. Comparing the baseline condition with a city driving condition (frequent stops and starts), total marginal costs increased about 3.8 cents per mile for automobiles and about 9.5 cents per mile for trucks. Rough pavements (PSI=2, IRI=170 inches/mile) increased the total marginal baseline costs about 2.7 cents per mile for personal vehicles and 5.5 cents per mile for trucks. Barnes and Langworthy (2004) did not include the effect of roughness on fuel consumption. Detailed representations of the influence of pavement roughness and city driving conditions on VOCs are shown in Table 3.1 to Table 3.3. It was reported that city driving condition, with frequent stops and starts, could increase fuel consumption from 5.0 to 7.0 cents per mile for automobiles, 7.8 to 10.1 cents per mile for pickups/vans/SUVs, and 21.4 to 28.0 cents per mile for commercial trucks. Since the effect of roughness on fuel consumption was not considered, rough roadways with poor ride quality did not increase the fuel consumption in Barnes and Langworthy (2004) report (Table 3.3). Rough pavements with PSI=2 increased the maintenance and repair costs around 0.8, 0.9 and 2.6 cents per mile for automobiles, pickups/vans/SUVs and commercial trucks, respectively. Likewise, tire wear/replacement costs on extremely rough pavements were estimated to be 17.9, 22.0 and 48.9 cents per mile for automobiles, pickups/vans/SUVs and commercial trucks, respectively.

Table 3.1. Baseline costs (cents per mile) (Barnes and Langworthy 2004)

Cost Category	Automobiles	Pickup/Van/SUV	Commercial Trucks
Total Marginal Costs	15.3	19.2	43.4
Fuel	5.1	7.8	21.4
Maintenance/Repair	3.1	3.7	10.5
Tires	0.9	1.0	3.5
Depreciation	6.2	6.7	0.8

Table 3.2. Costs with city driving conditions (cents per mile) (Barnes and Langworthy 2004)

Cost Category	Automobiles	Pickup/Van/SUV	Commercial Trucks
Total Marginal Costs	19.1	23.1	52.9
Fuel	7.0	10.1	28.0
Maintenance/Repair	3.7	4.2	12.1
Tires	0.9	1.0	3.5
Depreciation	7.5	7.7	9.2

Table 3.3. Costs for poor pavement quality (cents per mile) (Barnes and Langworthy 2004)

Cost Category	Automobiles	Pickup/Van/SUV	Commercial Trucks
Total Marginal Costs	17.9	22.0	48.9
Fuel	5.1	7.8	21.4
Maintenance/Repair	3.9	4.6	13.1
Tires	1.1	1.2	4.4
Depreciation	7.8	8.4	10.0

Islam and Buttlar (2012) derived equations relating the IRI factor to fuel consumption, tire-wear costs, rehabilitation and maintenance costs, and depreciation costs based on the results of previous studies. This study also estimated the impact of different maintenance and rehabilitation scenarios on VOCs. They used the Mechanical-Empirical Pavement Design Guide (MEPDG) for predicting the roughness of the pavement in terms of IRI at different traffic levels, initial IRIs, and weather conditions. The increase in VOCs with increasing IRI is illustrated in Table 3.4. They also suggested new maintenance and rehabilitation strategies, such as resurfacing every seven years instead of every 10 years and concluded that it is possible to save $5.1 million to $5.7 million (37% to 52%) in user costs over a 35-year life cycle period with an additional $108,000 investment from agencies.

Table 3.4. Increase in user costs for passenger cars and pickup trucks due to pavement roughness (Islam and Buttlar 2012)

IRI (in./mi)	Increase in Fuel Cost ($/mi)	Increase in R&M costs ($/mi)	Increase in depreciation costs ($/mi)	Increase in tire costs ($/mi)	Total increase in user costs ($/mi)	Total cost per year for 10,000 vehicles ($)	Total costs per year per vehicle ($)
63.00	0.00000	0	0	0	0.00000	----------	----------
76.3	0.00031	0	0.00008	0	0.00039	46,428	5
80.1	0.00040	0	0.00024	0	0.00063	75,841	8
83	0.00046	0	0.00035	0	0.00082	98,113	10
86.6	0.00055	0.000742	0.00050	0	0.00179	214,581	21
89.6	0.00062	0.001575	0.00061	0.00016	0.00297	356,126	36
93.5	0.00071	0.002648	0.00077	0.00036	0.00449	538,386	54
98.5	0.00083	0.004009	0.00096	0.00061	0.00641	769,284	77
101.4	0.00090	0.00479	0.00106	0.00076	0.00751	901,780	90
104.3	0.00097	0.005565	0.00117	0.00090	0.00861	1,033,230	103
1083	0.00106	0.006625	0.00132	0.00110	0.01011	1,212,824	121
100[a]	0.00087	0.004413	0.00101	0.00069	0.00698	837,947	84
110[b]	0.00111	0.007072	0.00138	0.00118	0.01074	1,288,548	129
125[c]	0.00146	0.010931	0.00190	0.00188	0.01618	1,941,125	194
175[d]	0.00265	0.022673	0.00340	0.00390	0.03262	3,914,234	391
200[e]	0.00324	0.027896	0.00401	0.00472	0.03987	4,784,164	478

Note: — = not applicable.

a) IRI level for adequate smooth pavement of Interstate highways.

b) IRI level for adequate smooth pavement of primary roads.

c) IRI level for adequate smooth pavement of secondary roads.

d) IRI level for inadequate smooth pavement of Interstate highways.

e) IRI level for inadequate smooth pavement of primary roads.

3.2.3 Effect of roughness on user safety

Pavement roughness has a direct correlation to road user safety. It alters vehicle handling characteristics and user driving habits. Skidding, reduced steering control, and vehicle bouncing are notable safety hazards attributable to rough pavement surfaces. Below are summaries of two research studies that focused on the relationship between road accident rate and road roughness.

The effect of road features (roughness, skid resistance, and terrain) on user safety is important in roadway design and maintenance. Road roughness and human error can result in accidents. Bester (2003) evaluated the effect of riding quality and road roughness on accident rates in South Africa. Different factors associated with accident rates and severity were considered including terrain type, riding quality and different types of accidents. According to Bester (2003), continuous vehicle vibration due to road roughness causes fatigue. Moreover, the suspension movement induced by roughness could be magnified when the road roughness is out of phase with the vehicle suspension frequency, which could lead to cornering problems and inconsistent braking characteristics. Bester (2002) also claimed that potholes alter the user's driving habits, causing them to swerve to avoid potholes and potentially lose control of the vehicle. Therefore, it was concluded that road roughness is influential of vehicle steering capabilities, vehicle braking, and road accidents. This study suggested that the most typical accidents associated with road roughness are loss of control, running off the road and hitting fixed or moving objects. To evaluate the impact of road roughness on user safety, data related to daily traffic volume, the terrain description, riding quality (PSI), and number of accidents and their severity over a three-year period were collected. It was found that road roughness, shoulder width, and topography affect the accident rates simultaneously. Rough roads increase accident rates only in rolling terrains.

A study conducted by Anastasopoulos et al. (2008) quantified the impact of IRI on accident rates on interstate highways using a Tobit regression analysis technique. This study focused on accident data collected from a highway in Indiana over a 5-year period. Anastasopoulos et al. (2008) found that a 27.1% decrease in number of accidents per 100M vehicle miles traveled (VMT) can be realized if the pavement IRI is kept below 75 inches/mile (1.1 m/km), based on a Tobit regression analysis of the Indiana highway data.

Most of the above studies advocate for a decrease in pavement roughness. Tighe et al. (2000) looked at pavement roughness from another perspective. It was reported that 97 percent of all reported fatal and personal-injury accidents are on roadways that are in good conditions with low roughness levels, whereas only 1.8 percent of reported fatal accidents and 1.5 percent of reported personal-injury accidents were on roadways with poor-conditions. It was concluded that the tendency of drivers to exercise more caution and travel at lower speeds on poor-condition roadways would decrease the number of single-vehicle accidents with high severity on two-way roadways. On the contrary, multiple-vehicle accident rates increase with an increase in roughness level. It was proposed that due to road defects, including potholes and improper patching, drivers change their speeds and paths abruptly. Such changes in driving behavior could be the reason for an increase in multiple-vehicles accidents on two-way primary roads. Figure 3.4 shows the relationship between road accident rate and road roughness. Tighe et al. (2000) suggested that to increase safety and to reduce accident rates IRI should be below 316.8 inches/mile (5 m/km).

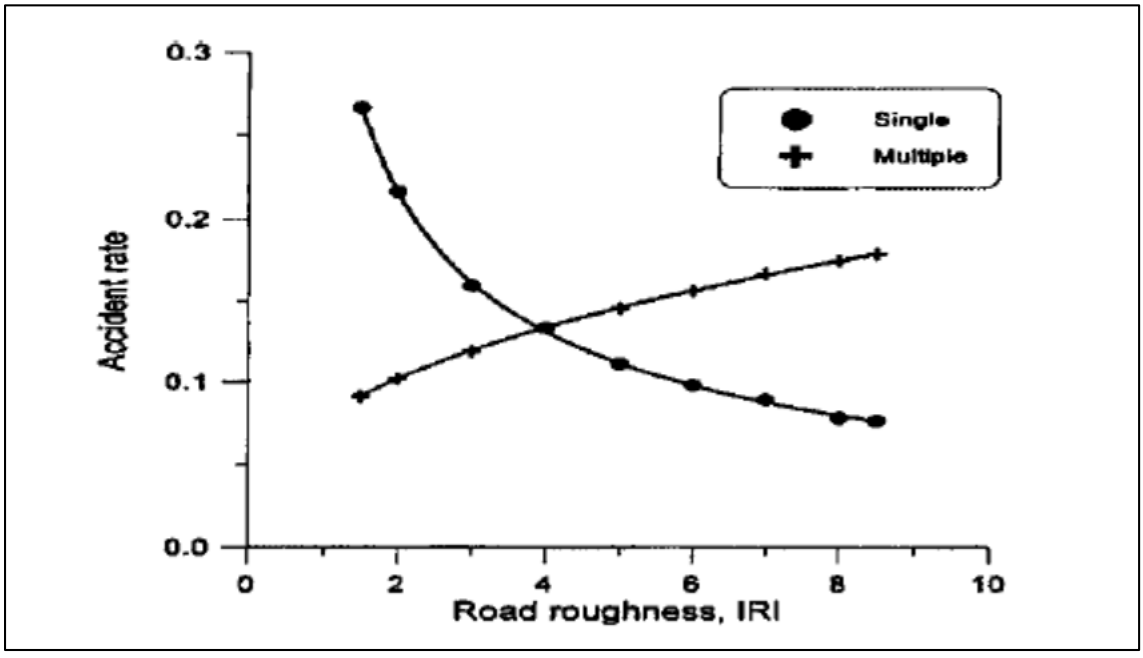

Figure 3.4. Relation between road accident rate and road roughness (Tighe et al. 2000)

In general, pavement surface roughness creates a safety hazard for the whole of road users. Although roughness may discourage unsafe driving on a per user basis, the uncommon maneuvers

that drivers perform give rise to higher probability of multiple vehicle accidents. Roughness is also hazardous in the sense that it decreases the effectiveness of vehicle handling characteristics that are necessary for safe driving, such as braking and turning forces. A combination of these road user behavioral and vehicular handling factors indicates that roughness is a serious problem for roads in the USA. Therefore, pavement roughness level and user safety should be considered in pavement management along with other important factors including user and agency costs.

3.2.4 Pavement life cycle assessment

Annually, around $160 billion and $320 million metric tons of raw materials are used for activities related to highway construction, maintenance, and rehabilitation in the USA. This significant use of materials requires excessive energy consumption, which results in production of a vast amount of emissions including greenhouse gases (GHGs), other air pollutants and water pollutants, among other environmental impacts (Harvey et al. 2010). By applying Life-Cycle Assessment (LCA), the environmental impacts of pavements are characterized and quantified. LCA is an approach that assesses environmental impacts, energy consumption, material used and other factors contributing to a product system throughout its life cycle, and quantifies these factors from cradle-to-grave stages. Due to data intensity, LCA should be framed in a systematic and standardized way, so that it can be used as a comprehensive and accurate pavement analysis technique. As shown in Figure 3.5, pavement LCA includes five phases: 1) material production; 2) construction; 3) use; 4) maintenance (recycled pavement materials are used in this phase); and 5) end-of life (Santero et al. 2011). Using LCA combined with Life-Cycle Cost Analysis (LCCA) leads to selection of the best pavement type and maintenance/rehabilitation method in single or multiple projects and road networks.

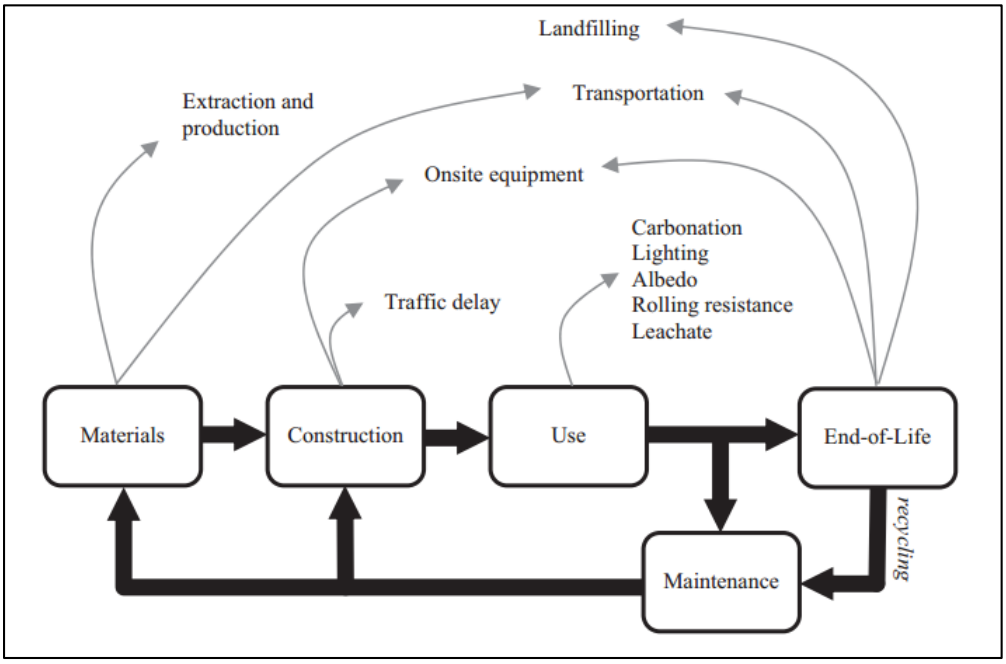

Figure 3.5. Phases and components of the pavement life-cycle (Santero et al. 2011)

There are two methods to perform LCA: 1) a process-based method, and 2) an economic input-output-based method. The process-based method divides each system into individual process and measures the environmental impacts of each process separately. In this method, boundaries are defined for the LCA system and emissions for each activity are calculated within those boundaries. Materials used and environmental impacts of each material are evaluated in detail. While creating boundaries makes the model more practical and easier to use, sometimes the choice of boundaries is not clear, leading to the elimination of some life cycle impacts of a product or process. On the other hand, the economic-input-output-based method contributes to economic transactions and resource interactions between a set of economic sectors using the 480*480 input-output matrix of United States economy to recognize the entire chain of suppliers (Hendrickson et al. 2006). In this method, the entire US economy is broken into 480 sectors including transportation, metal production, and etc., and inputs and outputs (transactions) from different sectors are measured in dollars.

Most state highway agencies use a single standard rehabilitation method for all pavements in life-cycle assessment based on their historical performance. However, historical data are not representative of the performance of the new design since they are based on old pavement design

features (Mack et al. 2014). There are various rehabilitation scenarios that could be applied to pavements, which may be different from the method used in standard LCA, leading to environmental LCA results that do not represent the actual rehabilitation implemented on pavements. Mack et al. (2014) suggested using a decision-making tree analysis to evaluate different rehabilitation methods in LCA. Accordingly, decision trees of different rehabilitation scenarios were developed for Portland Cement Concrete (PCC) and Asphalt Concrete (AC) pavements. The probability of occurrence of each activity was assigned based on the Ohio Department of Transportation's (ODOT) suggestions. The expected value of each scenario was then calculated by multiplying the probability of each activity by the global warming potential (GWP) of that activity. By comparing the GWP of standard rehabilitation schedules with different rehabilitation scenarios obtained from decision tree, it was concluded that decision-making tree analysis could give a range of potential GWP instead of a single LCA output. As a result, the associated risk profile of each alternative could be included in the analysis. Consequently, more robust LCAs could be developed.

Incorporating LCA along with LCCA to pavement design and rehabilitation provides more realistic solutions. LCA is important to assess environmental impacts, energy consumption, material used, and other factors contributing to a pavement life-cycle from cradle-to-grave. Material production, construction, and use phases of LCA are discussed in the next sections.

3.2.4.1 Material production and construction phases

Asphalt is a byproduct of petroleum refining, which was estimated to produce 268 million metric tons of energy-related carbon dioxide emissions in 2013 (EIA 2015). Asphalt production consists of six phases: 1) extraction; 2) transportation and storage; 3) heating; 4) distillation; 5) cooling; and 6) final processing (Zapata and Gambatese 2005). Around 40% of energy consumption in the refining process is attributed to bitumen and the rest is used for lighter products (Stripple 2001). For asphalt concrete mixture production, asphalt is heated to keep its fluidity and mixed with aggregates. Prior to mixing, aggregates are dried by heating them to a temperature between 150 ^{o}C to 170^{o}C. The final mix is transported to the roadway section for construction.

EIA (2015) reported that cement and lime production released around 30 million metric tons of energy-related carbon dioxide emissions in 2013. Energy consumption in phases of PCC production, including mixing and transportation, are insignificant compared to the energy consumption in production of Portland cement (Zapata and Gambatese 2005). Aggregates do not need to be preheated prior to mixing with cement. Therefore, the major proportion of energy consumption in PCC pavements is related to raw material production for PCC. Even energy consumed in the transportation of raw materials is negligible compared to the energy used in the production of the cement (Zapata and Gambatese 2005).

Zapata and Gambatese (2005) provided a Life-Cycle Inventory Assessment (LCI)[11] on Continuously Reinforced Concrete Pavement (CRCP) and asphalt pavement in terms of energy consumption in the construction of roadways. A one-kilometer road section of a two-lane highway (each lane was 3.6 m wide) with a high traffic volume (10 million 80 kN single-axle loads) was selected for this study. The CRCP had a 220 mm thickness with longitudinal and transverse steel reinforcement spaced 100mm and 1.3m on center, respectively. The PCC was designed to have 12% cement, 43% coarse aggregate, 28% fine aggregate and 17% water by weight. The asphalt concrete had 300 mm thickness with 5% asphalt binder content and 95% aggregate content by weight. Information about energy consumption attributed to materials was gathered through literature reviews of previous works and interviews with two national heavy-civil construction contractors. Then, the average values of energy consumption were reported for three phases of pavement life-cycle: 1) raw material extraction and initial material transformation; 2) manufacturing of asphalt, PCC and rebar; and 3) placing the materials on the construction site. Results showed that energy consumed for CRCP and asphalt pavement were around $4.58 * 10^6$ MJ and $3.78 * 10^6$ MJ per kilometer, respectively, showing that CRCP required 21% more energy than asphalt pavement over the three phases of the pavement life-cycle. However, PCC has a higher average design life than asphalt pavement. Life Cycle Cost Analysis (LCCA) needs to be conducted in order to be able to compare the energy consumption of PCC and asphalt pavements. Extraction of raw materials and concrete placement, cement production, steel production and the

[11] LCI quantifies and gathers inputs and outputs in life cycle assessment. An LCI can also be conducted as a separate part from LCA (ISO 14040, 2006).

concrete mixing process constituted 6%, 65%, 34%, and 1% of total energy consumptions for CRCP, respectively. For asphalt pavements, extraction of raw materials and asphalt pavement placement, asphalt mixing and drying of aggregates, production of bitumen and storage accounted for 8.46%, 53%, 43%, and 4% of total energy consumed, respectively. These results suggested that energy consumption for the extraction of aggregates and placing of pavement materials were insignificant compared to other activities in the procurement of asphalt and PCC concrete surfacings. It should be noted that Zapata and Gambatese (2005) only focused on material production and construction (placing the materials on the construction site) stages while the contribution of use phase to the total energy use was not investigated. Moreover, the benefits of using RAP was not considered for asphalt pavements.

3.2.4.2 Use phase

The pavement use phase consists of VOCs (additional fuel consumption, tire wear costs and vehicle maintenance costs due to pavement roughness), the heat island effect[12], the non-GHG climate change effect[13], electricity used in roadway lighting, carbonation[14] and water pollution from leachate and runoff (Harvey et al. 2010). It is crucial to assess costs contributing to different pavement preservation methods in the life-cycle period of pavements. Below are summaries of previous studies focused on energy use, GHG emissions and associated costs for the use phase.

Chehovits and Galehouse (2010) evaluated energy usage and GHG emissions of different pavement preservation methods for asphalt concrete pavements. Pavement preservation treatments were compared based on annualized energy usage and GHG emissions within the extended pavement life-time due to applied treatments. Results of this study showed that HMA overlays,

---

[12] Due to albedo, a portion of incoming solar radiation reflects back to the surrounding area. Therefore, temperature of metropolitan areas usually become warmer than their surrounding rural areas. Additionally, since pavements trap subsurface water and do not allow it to evaporate, temperature rises even more (Harvey et al. 2010).

[13] High albedo could result in global cooling since only a portion of incoming radiation reflects back to space. This negative radiative forcing can be converted to CO_2 equivalents (Harvey et al. 2010).

[14] "Carbonation occurs when the components of cement, such as $Ca(OH)_2$, react with CO_2, and sequester it in the pavement" (Harvey et al. 2010).

hot in-place recycling, new construction and major rehabilitation had the highest annualized energy use (around 4.9-15.4 MJ/m^2-yr) and the highest GHG emissions (around 0.4-1.3 kg/m^2-yr). Chip seals, micro-surfacing and crack fill exhibited 1.0-3.3 MJ/yd^2-yr energy use and 0.13 to 0.07-0.20 kg/m2-yr GHG emissions per year of extended pavement life. Fog sealing and crack sealing had the lowest annualized energy use, ranging from 0.4 to 1.1 MJ/m^2-yr, and GHG emissions ranging from 0.02 to 0.08 kg/m2-yr. It was concluded that pavement preservation treatments could reduce energy use and emissions substantially compared with conventional rehabilitation and reconstruction methods.

A study carried out by Wang et al. (2013) developed a LCA approach to evaluate the impact of network-level pavement maintenance and rehabilitation methods on GHG emissions and energy use within the California highway network. This study included finding the optimal trigger roughness values (IRI) at which life-cycle energy consumption and GHG emissions are minimized. Cost-effectiveness of implementing the trigger values are considered as well. Three treatment methods were considered: 1) a medium-thickness asphalt overlay on asphalt-surfaced pavement; 2) diamond grinding and concrete slab replacement on concrete-surfaced pavement; and 3) concrete lane replacement. A ten-year analysis period was used. Due to heterogeneity, the network was divided into groups based on traffic levels in order to develop different IRI trigger values for each group. Different IRI trigger values were considered to estimate the optimal trigger value for each group, in which the GHG emission reduction is at a maximum. Results showed that congestion and road gradient had an insignificant effect on changes in fuel economy. Compared to a “do nothing” scenario (keeping the IRI at or below 279 inches/mile (4.4 m/km) with minimal maintenance of the pavement) and the current California Department of Transportation (Caltrans) IRI trigger value (170 inches/mile [2.68 m/km] on all pavements), implementing optimal trigger IRI values resulted in GHG reduction of 1.38 MMT and 0.57 MMT, respectively. Moreover, smoothness achieved after treatment had a significant effect on GHG reduction.

3.2.5 Decision-making tools

Due to limited budget of agencies, finding an optimized solution to allocate road maintenance and repair resources is critical. Not only do pavement management approaches influence costs to agencies and users (Li and Madanat 2002; Ouyang and Madanat 2006), but they also have significant environmental impacts (Wang et al. 2013). Below are summaries of previous models and tools developed to find optimal pavement management strategies.

Li and Madanat (2002) suggested a steady-state approach for optimizing the frequency and intensity (thickness) of pavement resurfacing based on the minimum serviceability index (maximum allowable roughness). This approach was created for continuous time and continuous state cases with deterministic pavement deterioration. In Li and Madanat (2002) study, the pavement condition state represented in an infinite time period. The first resurfacing occurred at the trigger point, where the minimum serviceability, or trigger IRI value, was reached. The treatment strategy was considered to be the same for the remaining life of the pavement. This approach did not depend on the initial condition of the pavement, provided that the initial condition had a higher serviceability index than the condition after resurfacing. The purpose of this study was to minimize present value of costs to users and agencies associated with pavement conditions, using the following expressions:

$$\min J=\sum_{n=1}^{\infty}\left\{\int_{t_{n-1}}^{t_n} C\big(s(t)\big)e^{-rt}dt+M(w_n)e^{-rt_n}\right\} \qquad \textbf{3.2.1}$$

$$\text{s.t.} \quad \frac{ds(t)}{dt}=F\big(s(t)\big),$$

$$s_{2n}-s_{1n}=G(w_n,s_{2n}),$$

$$s(0)=s_0$$

Where:

J = present value of agency and user cost,

t_n = the time of n_{th} resurfacing,

s(t) = the pavement roughness as a function of time,

C(s(t)) = the user cost rate as a function of pavement roughness,

w_n = the intensity (thickness) of n_{th} resurfacing,

$M(w_n)$ = the agency cost as a function of resurfacing intensity,

r = the discount rate,

F(s(t)) = the deterioration as a function of pavement roughness, and

$G(w_n, s_{2n})$ = improvement in pavement condition as a function of resurfacing intensity and pavement roughness immediately before resurfacing.

Pavement deterioration and increase in roughness (s) were assumed to follow a saw-tooth trajectory (Tsunokawa and Schofer 1994) for every cycle time (τ), as shown in Figure 3.6, with a fixed maximum roughness before resurfacing (S_2) and after resurfacing (S_1). This study manifested that the discounted life-time cost was not very sensitive to the cycle time (τ), but rather the roughness levels were more influential.

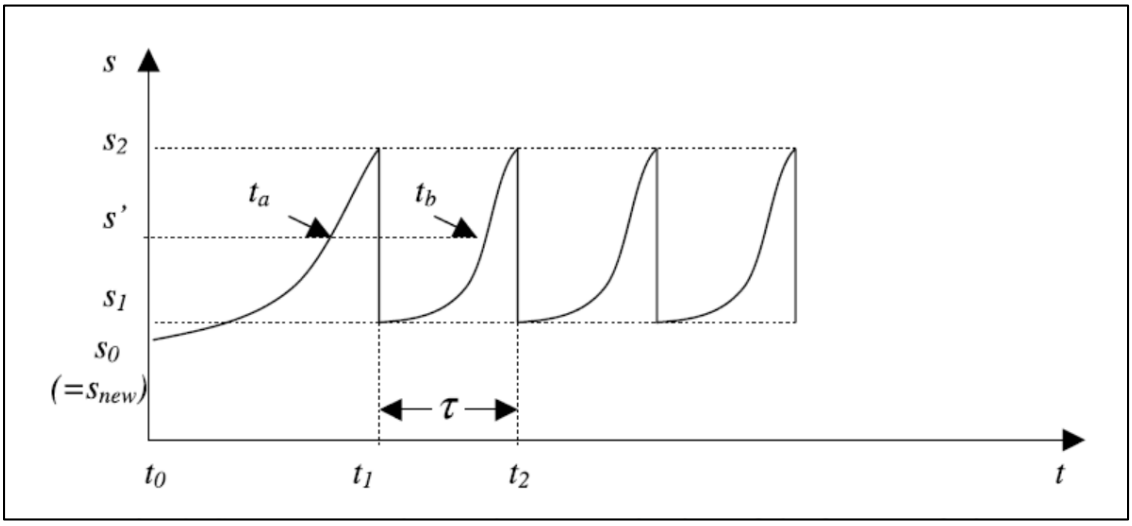

Figure 3.6. System enters the steady state at the time of the first resurfacing(Li and Madanat, 2002)

Sathaye and Madanat (2011) developed an optimized approach for determining the frequency and intensity of resurfacing for multiple highway facilities. This study used deterministic, continuous-state formulation to address performance predictions and maintenance/repair decision-making. Bottom-up pavement management formulation, which considered the heterogeneous facilities, was used. Methodology for solving the problem was formulated as follows:

$$\min \sum_{j=1}^{J} V_j = \sum_{j=1}^{J} \frac{M_j + U_j}{1 - e^{-r\tau_j}} \qquad \textbf{3.2.2}$$

$$\text{s.t.} \sum_{j=1}^{J} \frac{M_j}{\tau_j} \leq B$$

Where:

V_j = Total infinite horizon costs,

M_j = The maintenance cost for a single resurfacing activity,

U_j = User cost incurred between resurfacing activities,

$r < 1$ = The discount rate,

τ_j = The time between overlays, and

B = Agency budget per time for resurfacing activities.

Results for a three-facility network was developed based on the above methodology. The effect of yearly budget (B) on trigger roughness values (s_j^-) and network-level optimal costs ($\sum_{j=1}^{J} V_j$) are shown in Figure 3.7 and Figure 3.8, respectively. When the yearly budget is low, an increase in budget resulted in a significant decrease in the total costs, and likewise, the trigger roughness values. However, as yearly budget increased, the incremental decrease in total cost and trigger roughness values waned.

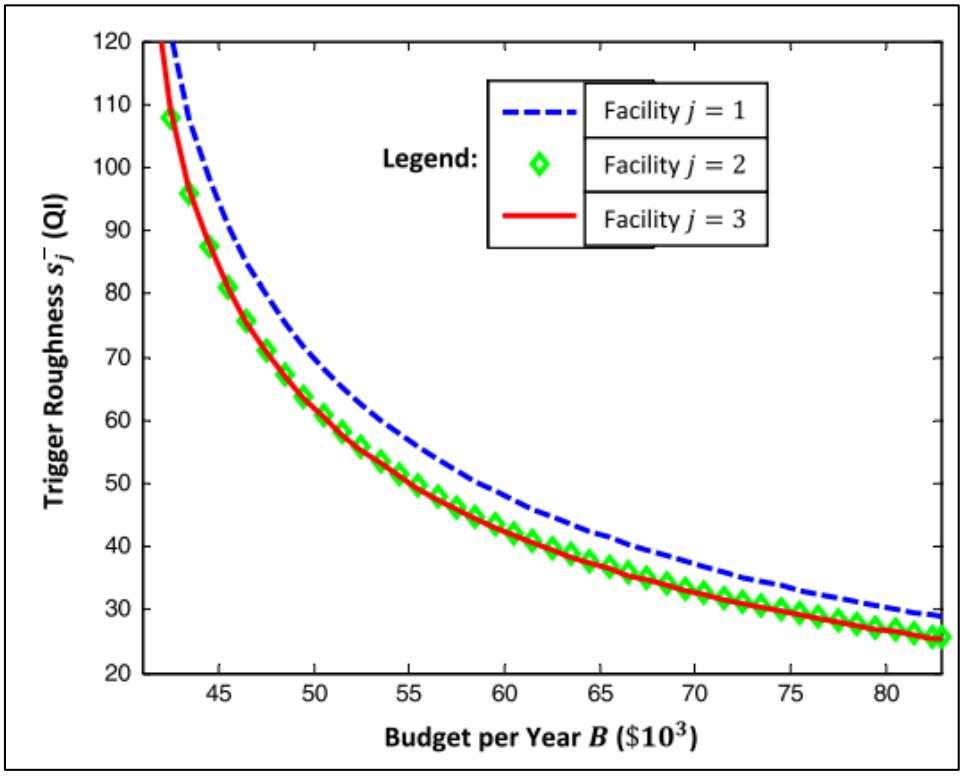

Figure 3.7. Effect of budget on trigger roughness values (Sathaye and Madanat 2011)

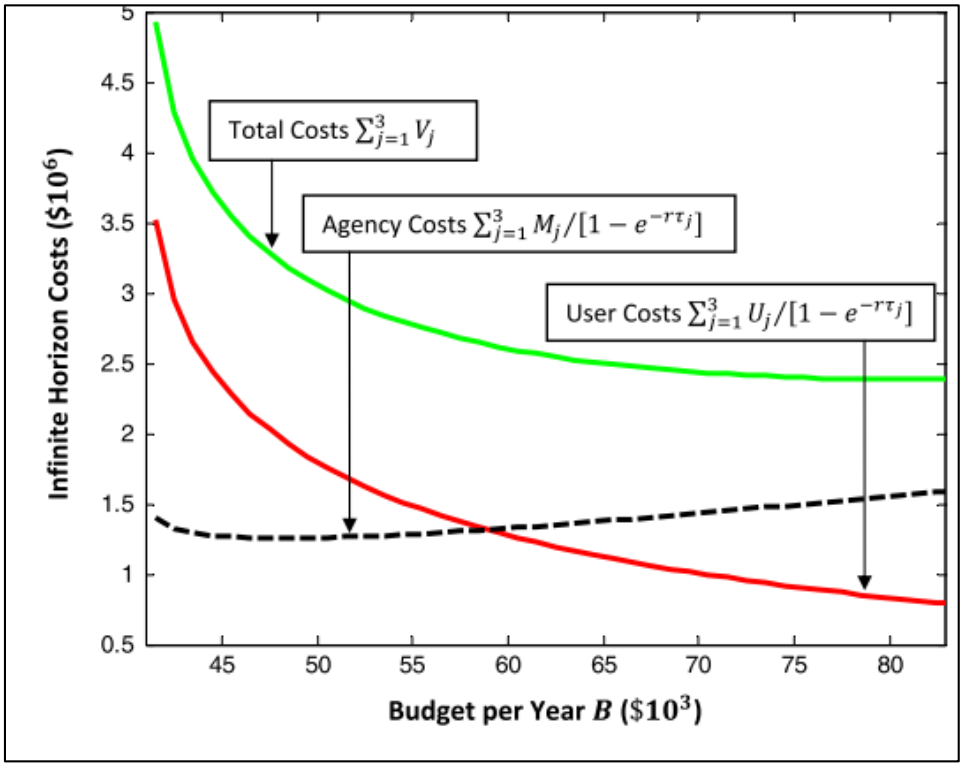

Figure 3.8. Effect of budget on network-level optimal costs (Sathaye and Madanat 2011)

Zhang et al. (2010) developed a LCA-LCCA model, a pavement overlay deterioration model, and a Life-Cycle Optimization (LCO) model to find the optimal overlay preservation method. The LCA model was divided into costs and environmental impacts related to material production, construction, distribution, traffic congestion, usage and end of life stages (Zhang et al. 2009). Results of the LCA model were used in the LCCA model to estimate agency and user life-cycle costs. In pavement overlay deterioration model, distress index (DI) was used to predict the pavement performance rather than IRI. DI is a measurement of pavement condition including pavement roughness and deterioration. The LCO model estimated the optimized method for evaluating the energy consumption, environmental impacts, and costs associated with all stages of products and life-cycle. Traffic congestion, traffic growth, overlay deterioration and pavement roughness impacts were considered in this model as well. Three overlay systems were used including: 1) a concrete overlay with 175 mm thickness; 2) an engineered cementitious composite (ECC) with 100 mm thickness; and 3) a HMA overlay with 190 mm thickness. The objective of this model was to minimize life-cycle burdens (energy consumption, environmental impacts (GHG

emissions) and costs to users and agencies). The constraint was to keep the system within a defined performance standard (DI<50) within the 40 year analysis period, using the following expression:

$$B_b[i,j,DI(i)] = \begin{cases} material\ [i,j,DI(i)]w_b^{material} + construction[i,j,DI(i)]w_b^{construction} \\ + distribution[i,j,DI(i)]w_b^{distribution} + congestion[i,j,DI(i)]w_b^{congestion} \\ +usage[i,j,DI(i)]w_b^{usage} + EOL[i,j,DI(i)]w_b^{EOL} & ,if\ i > 0 \\ 0 & ,if\ i = 0 \end{cases} \quad \textbf{3.2.3}$$

Where:

b	= life cycle energy consumption, GHG emissions, or costs,
i	= index of year,
j	= maintenance alternative decisions (0, 1 and 2 mean no action, minor maintenance, and major maintenance, respectively),
DI(i)	= distress index value at year I,
w_b	= life cycle energy consumption, GHG emissions or costs associated with one unit of raw material, utility or process,
$B_b[i,j,DI(i)]$	= burden life-cycle energy consumption, GHG emissions or costs at year i with decision j for one DI value,
$material[i,j,DI(i)]$	= material consumption costs at year i with decision j for one DI value,
$construction[i,j,DI(i)]$	= construction equipment usage at year i with decision j for one DI value,
$distribution[i,j,DI(i)]$	= transportation of materials and equipment at year i with decision j for one DI value,
$congestion[i,j,DI(i)]$	= construction-related traffic congestion at year i with decision j for one DI value,
$usage[i,j,DI(i)]$	= pavement surface roughness impact at year i with decision j for one DI value, and
$EOL[i,j,DI(i)]$	= end of life management of pavement system at year i with decision j for one DI value.

Results showed that, by implementing the optimal strategy, which is shown in Figure 3.9, reductions in life-cycle energy consumption of around 5-30%, GHG emission around 4-40% and cost by 0.4-12% could be realized for the three overlay systems compared to conventional MDOT[15] preservation strategies. Moreover, by evaluating impacts of traffic growth, it was concluded that this model could create more benefits than the MDOT conventional method. Additionally, it was stated that the ECC overlay system had a greater influence on the reduction of energy consumption, GHG emissions and costs compared to concrete and HMA overlays.

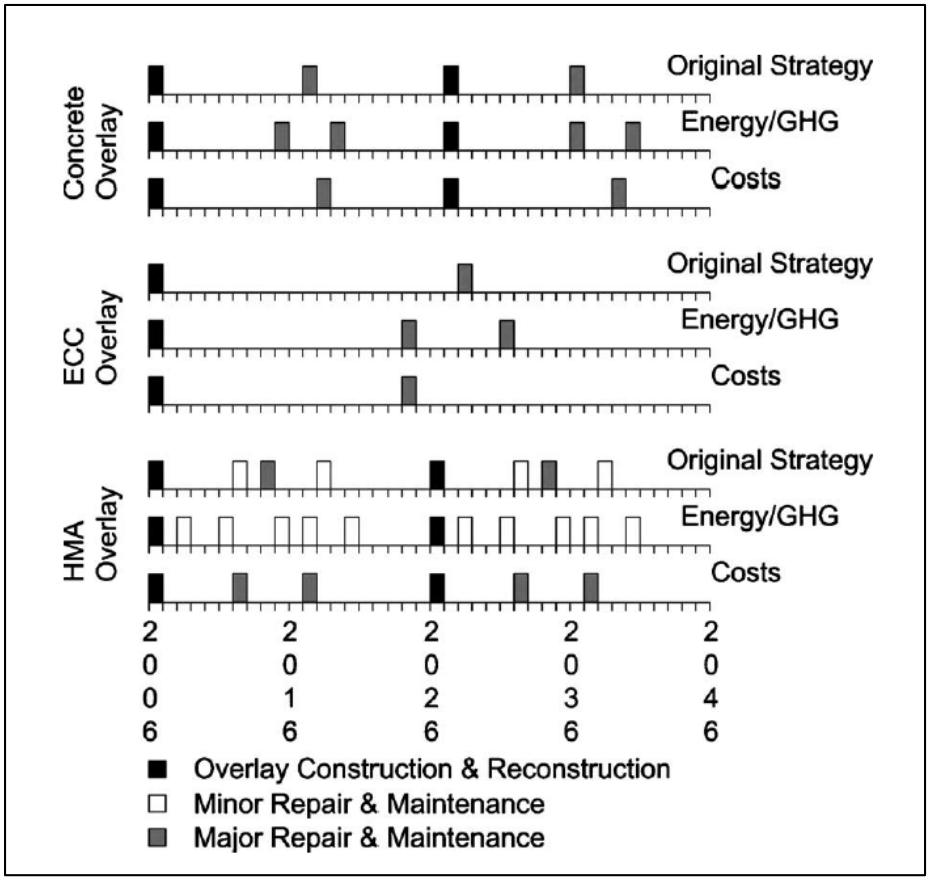

Figure 3.9. Optimal preservation strategies for three overlay systems without considering the traffic growth (Zhang et al. 2010)

[15] Michigan Department of Transportation

3.3 RESEARCH METHODOLOGY

3.3.1 Analysis of framework – code development

In this study, a prototype network-level decision-making tool was developed to select the most efficient pavement maintenance and rehabilitation strategies to minimize agency and user costs and maximize their benefits. Field data from 91 roadway sections in Oregon, Idaho, Washington, and California were used to develop and test the developed tool. Field data associated with maintenance history, location, pavement structure, profile, and traffic were obtained from Federal Highway Administration (FHWA) website (LTPP InfoPave 2016) for all the sections. Dataset included previous treatment types, previous treatment thicknesses, annual average daily traffic (AADT), annual average daily truck traffic (AADTT) and annually collected IRI of the last treatments. Treatment types used in this study were dense graded asphalt concrete (DGAC) overlay, chip seal on dense graded asphalt concrete (DGAC-CS), slurry seal on dense graded asphalt concrete (DGAC-SS), chip seal with modified binder (DGAC-CSMB), asphalt concrete pavement on concrete pavement (CP), asphalt concrete pavement with recycled asphalt pavement (RAP) on concrete pavement (CPR), central plant mixed and cold-laid[16] RAP (RAPCL), central plant mixed and hot-laid[17] RAP (RAPHL) and open-graded asphalt concrete pavement (OGAC). Pavement history and structures for each section are presented in Appendix H in detail.

In this study, pavement conditions were evaluated over a 40-year analysis period. Traffic data in terms of AADTT and AADT for the past years were used to develop linear models to predict the traffic for each section over the analysis period. Having annually collected IRI data for the past years and treatments, nonlinear models were developed to predict the pavement performance in terms of IRI for each section. To find the optimal budget allocation for pavement maintenance and rehabilitation, a code was developed using MATLAB 2016. The general framework for the decision-making tool development is given in Figure 3.10. Data corresponding to traffic, treatment types and thicknesses, annual IRI, and material and construction costs were used as inputs to the software. For each section, IRI and Net Present Value (NPV) of user benefits were estimated for

[16] Placement temperatures below 175 °F

[17] Placement temperatures above 175 °F

each year. If the estimated IRI reached the trigger IRI, a treatment was applied and NPV of agency cost was estimated. If the predicted IRI was less than the trigger IRI, a “do nothing” scenario was chosen and the IRI for the next year was predicted for the existing treatment type. This procedure was continued until the 40-year analysis period was reached. Having agency costs and user benefits based on the treatment types and the frequency of resurfacing of each section, sections were ranked according to benefit-to-cost (B/C) ratios over the analysis period. Subsequently, the available budget was allocated to the sections with higher priority for treatment (sections with higher B/C ratios). This process was continued until the budget was expended.

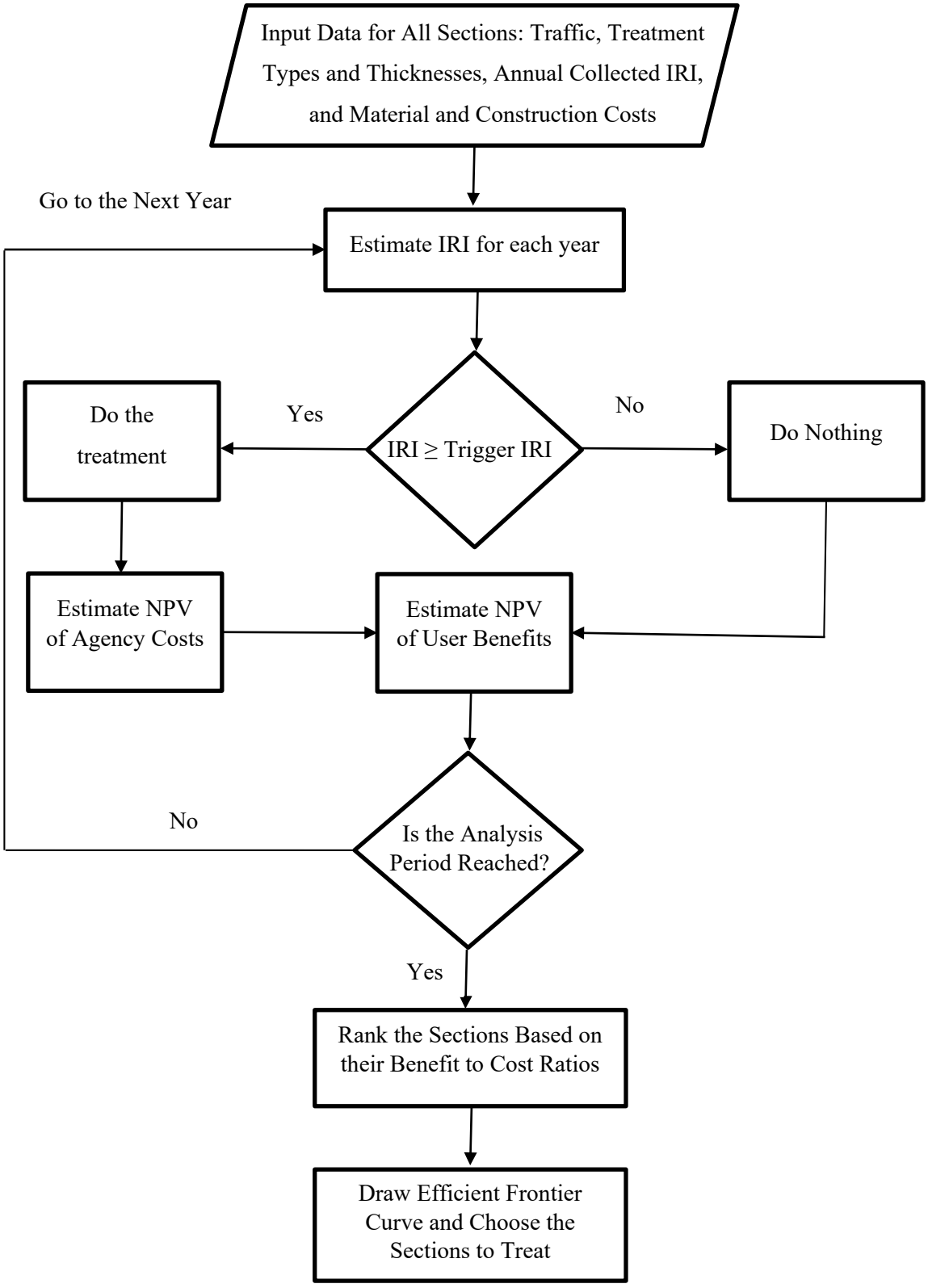

Figure 3.10. Flowchart of procedure to develop the decision-making tool (MATLAB code)

The steps followed for model development are as follows. Each step is discussed in detail in Section 3.3.2.

1. Traffic data in terms of AADTT and AADT for the approximate 40 years (from 1970s to 2010s) were used to develop linear models to predict traffic for each section over the 40-year analysis period.
2. Annually collected IRI data for the last applied treatment were used to develop nonlinear models to predict pavement performance in terms of IRI for each section over the 40-year analysis period.
3. Data corresponding to traffic, treatment types and thicknesses, annual IRI, and material and construction costs were used as inputs to the software.
4. Pavement performance in terms of IRI was predicted for each section based on the nonlinear IRI models developed in Step 2 after new treatment.
5. Failure points, at which the treatments were applied, were determined over the analysis period for each section.
6. Initial IRIs after each treatment were estimated.
7. NPV of agency costs (traffic handling, materials, lane closure, and labor and equipment costs) were estimated for each section according to their treatment types and layer thicknesses.
8. Having failure points for each section, the NPV of user benefits was calculated over the analysis period.
9. Sections were ranked and selected for treatment based on their B/C ratios, and an efficient frontier curve was developed. The priority for treatment was given to the sections with higher B/C ratios. This process was continued until the budget was expended.

3.3.2 Steps followed for model development

Field data from 91 roadway sections in Oregon, Idaho, Washington, and California were used to develop and test the decision-making tool. Field data associated with history, pavement structure, profile, and traffic were obtained from Federal Highway Administration (FHWA) website (LTPP

InfoPave 2016) for all the sections. Below is the description of each step followed for model development.

3.3.2.1 Step 1 – LTPP traffic data

Traffic levels, as dependent variables, were categorized into two groups (AADTT and AADT) and were linearly correlated with year, the independent variable. The traffic equation is shown below:

$$Traffic=a+b*Year \quad \textbf{3.3.1}$$

In the equation above, Traffic is traffic level in terms of AADTT or AADT, Year is number of years since the last treatment is applied, a is the initial AADTT or AADT, and b is a coefficient indicating the rate of change of traffic over each year. Coefficients a and b are estimated over the analysis period for all the sections by conducting a linear regression in software RStudio 2015.

Figure 3.11 shows an example of AADTT versus year for a section in Washington where chip seal was the last treatment. The AADTT data was annually gathered from 1973 to 2009. As illustrated, the linear model was fitted to the data as follows:

$$AADTT=54.72+7.697*Year \quad \textbf{3.3.2}$$

The last treatment (chip seal) was applied in the year of 1990. To predict the AADTT over the 40-year analysis period, the base year was considered as 1990. Therefore, the coefficient a was shifted to 185.57 from 54.72.

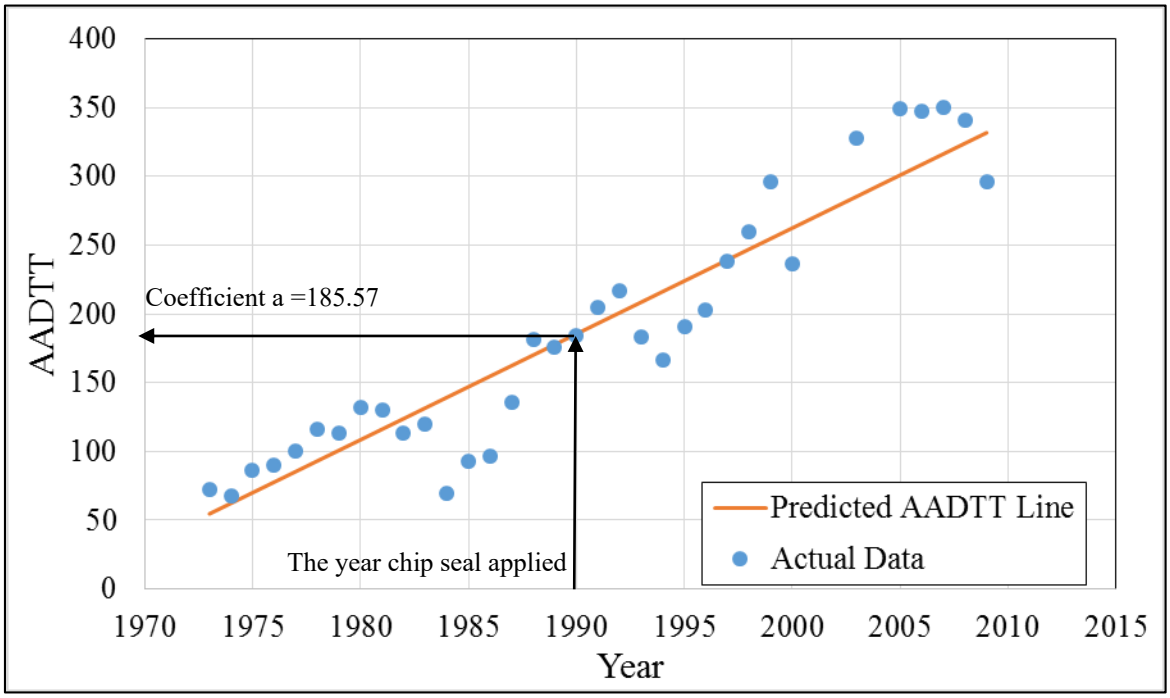

Figure 3.11. Example of AADTT versus year for a section in Washington where chip seal is the last treatment (WA-C350-DGAC-CS)

3.3.2.1 Step 2 – LTPP IRI data

In this study, IRI was considered as the only pavement performance variable indicating pavement life and failure point. Having annually collected IRI data of the last treatments, performance equations for IRI were developed, with the value of IRI for that section in each future year being the dependent variable and number of years being the independent variable. Figure 3.12 shows the annually collected IRI versus year for all the sections in Oregon.

The performance equation for average IRI was formulated as follows:

$$IRI\left(\frac{m}{km}\right)=a+b*Age^{c} \quad \textbf{3.3.3}$$

In this equation, IRI is the average IRI in each year of the analysis period, a is the initial IRI, Age is the number of years since the last treatment, and b and c are the coefficients indicating the rate of change of IRI in each year. To predict the annual average IRI for each section since the last treatment was applied, coefficients a, b, and c were estimated by performing non-linear regressions using RStudio 2015. The initial IRI depends on the quality of the construction. It was possible to

have very rough pavements after construction in the past, but the new requirements force contractors to have roughness levels of 0.95-1.1 m/km (60-70 inches/mile) after construction. In order to make the initial IRIs more consistent and comparable, averages of initial IRIs for chip seals and slurry seals were taken and their performance equations were shifted to the average value. Similarly, performance equations for overlays were shifted to their average initial IRI. Thus, value a in Equation 3.3.3 for chip seal and slurry seal was 1.2814 m/km (81.19 inches/mile) and for overlays was 0.9727 m/km (61.63 inches/mile).

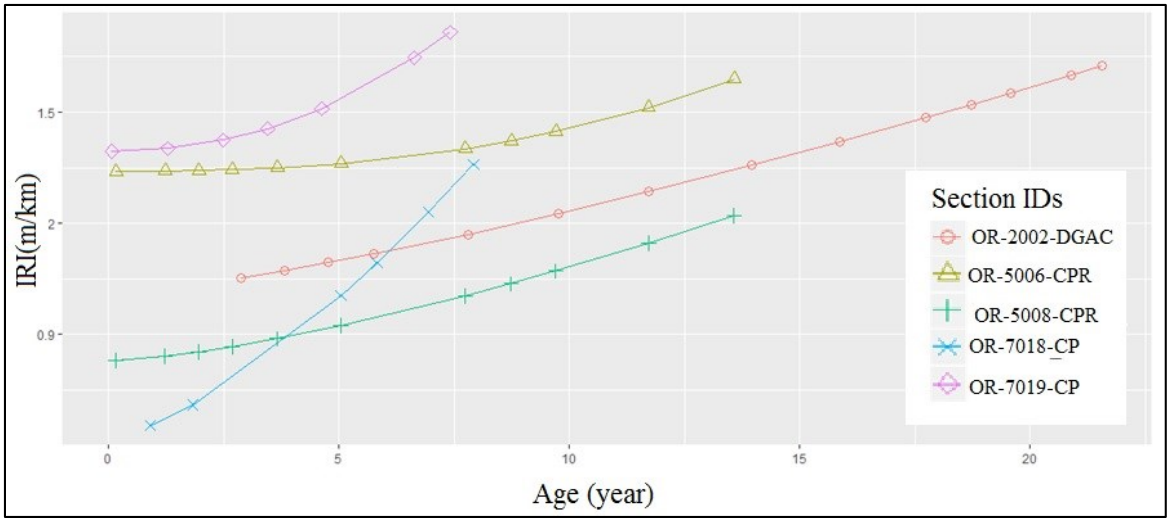

Note:
DGAC: dense graded asphalt concrete.
CP: composite pavement.
CPR: composite pavement having RAP.

Figure 3.12. Annually collected IRI of the last treatment versus year of the last treatment for all the sections in Oregon

3.3.2.2 Step 3 – Input data

Data corresponding to treatment types, treatment thicknesses, and material and construction costs were used as inputs to the software. All the data was obtained from Federal Highway Administration (FHWA) website (LTPP InfoPave 2016). Moreover, coefficients of traffic and IRI equations for each section were inputted to the software to predict their traffic levels and pavement performance over the analysis period.

3.3.2.3 Step 4 - Prediction of pavement performance (IRI) after new treatment

To estimate user benefits for each section, the IRI was predicted for new treatments using performance equations developed in Step 2. Figure 3.13 shows the predicted IRI versus age for the section in Washington where chip seal was the last treatment. It can be seen that the initial IRI immediately after construction is 0.911 m/km (57.72 inches/mile). The IRI has an increasing trend over time (age). The IRI performance equation of this section is as follows:

$$\text{IRI}\left(\frac{\text{m}}{\text{km}}\right) = 0.911 + 0.0042 * \text{Age}^{2.5349} \quad \textbf{3.3.4}$$

After predicting the performance curves, initial IRIs were shifted to the specified values mentioned in Step 2. For this section, the initial IRI was shifted to 1.2814 m/km (81.19 inches/mile) since chip seal was the applied treatment. Shifted predicted pavement performance curve is also illustrated in Figure 3.13.

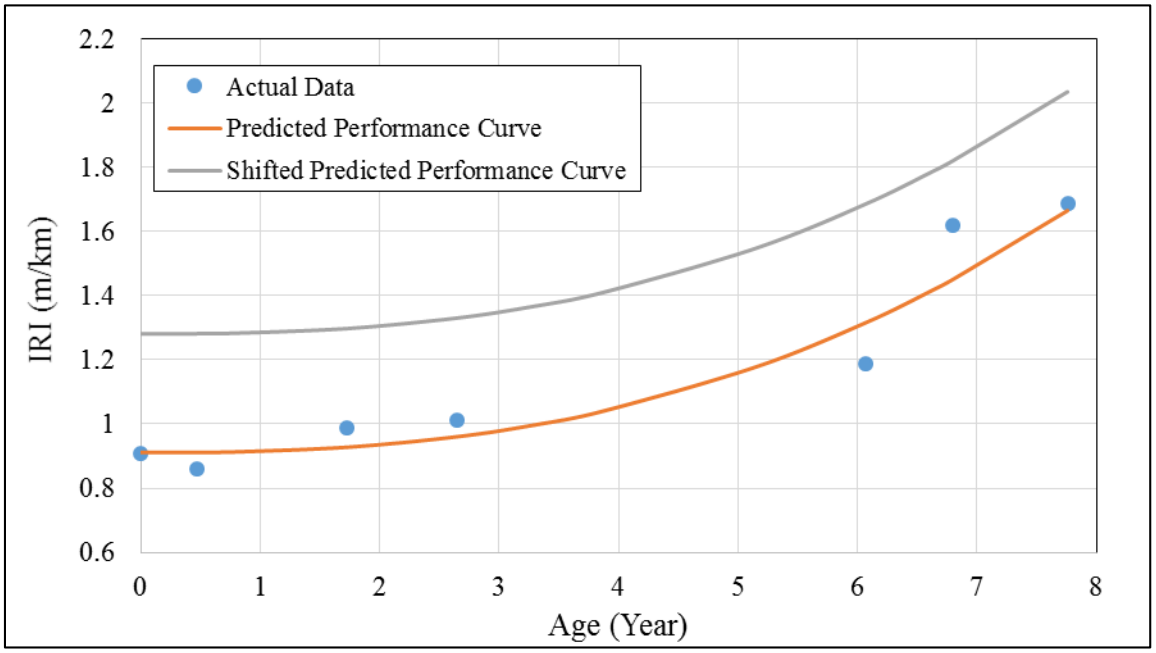

Figure 3.13. Example of performance equation of IRI versus year for a section in Washington where chip seal is the last treatment (WA-C350-DGAC-CS)

3.3.2.4 Step 5 - Indicating the failure points

The IRI was considered as the only pavement performance variable used to calculate pavement life and failure point. The Failure Point was defined as the year at which the pavement reached the

trigger IRI and the treatment was applied. For a 40-year analysis period, it was assumed that similar treatment types with the same IRI performance were repeated over the analysis period for each section. For instance, if the last treatment was chip seal, when pavement reaches its failure point, a chip seal treatment is applied again, and the application of chip seal is subsequently repeated over the remaining years in the analysis period to maintain the same pavement performance. Each treatment is applied to reduce IRI to a specified level and this process is repeated over the 40 year-period. Figure 3.14 shows the methodology of this study for finding the frequency of resurfacing and treating a section in California (CA-0504-DGAC) with a dense graded asphalt concrete (DGAC) overlay. As it is presented in Figure 3.14, the first failure point was in the year 19 and the second treatment occurred in year 38. The trigger IRI was 1.66 m/km (105 inches/mile) for this section. It can be seen that at the year where the trigger IRI is reached, a treatment was applied. The initial IRI right after construction was 0.9727 inches/mile (61.63 inches/mile). The IRI performance equations determined in Step 2 were used to estimate the annual IRI in this step.

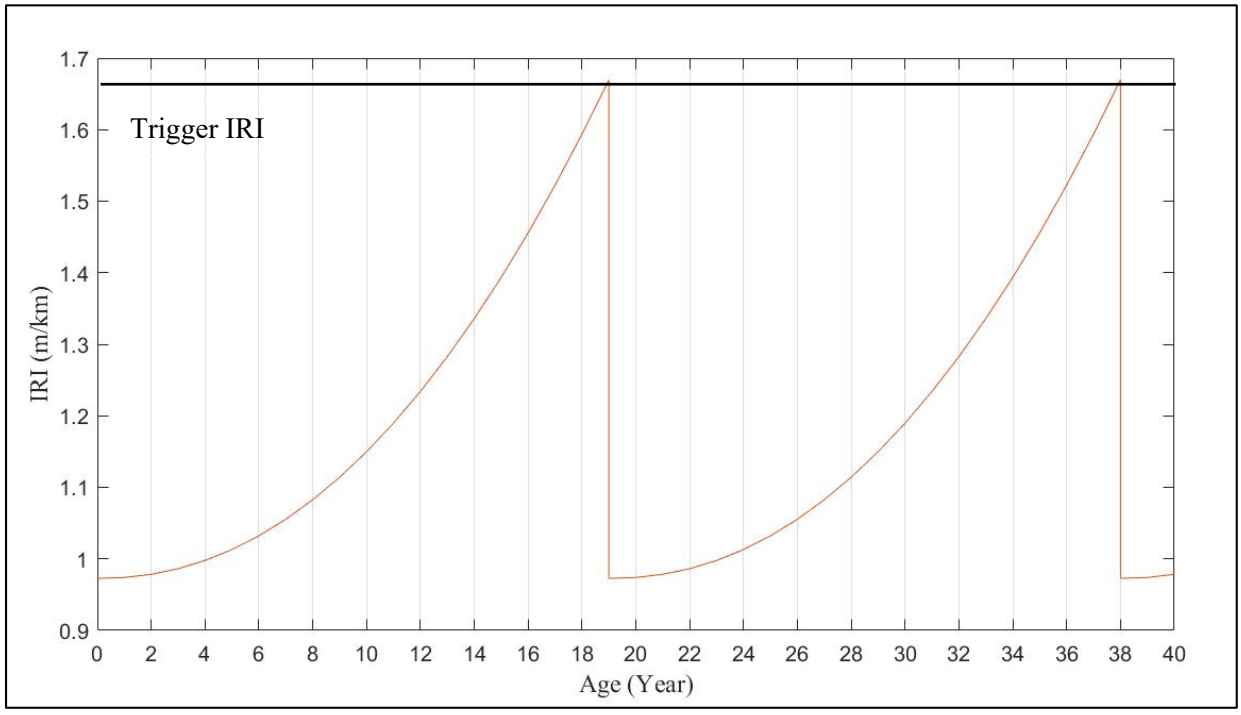

Figure 3.14. Example of the approach for obtaining the frequency of resurfacing and treating for the CA-0504-DGAC section

3.3.2.5 Step 6 - Finding IRI after each treatment

Average decrease in pavement IRI after application of chip seal and slurry seal is around 20 inches/mile, thin overlay (<0.1 ft) is 0.71 m/km (45 inches/mile), medium overlay (≥0.1 ft and ≤ 0.25 ft) is 0.95 m/km (60 inches/mile), and thick overlay (>0.25 ft) is 1.58 m/km (100 inches/mile) (Harvey et al. 2010) After each treatment, the maximum of actual IRI and decreased IRI was taken as the initial IRI. For instance, if the trigger IRI is 177 inches/mile, application of thin overlay reduces the IRI to 177-45=132 inches/mile. LTPP IRI data shows the average initial IRI (actual IRI) for overlays as 61.63 inches/mile (0.973 m/km). Thus, the maximum of these two numbers (132 inches/mile) is taken as the initial IRI for this treatment.

3.3.2.6 Step 7 - Calculating Net Present Value (NPV) of agency costs

Agency costs were comprised of material, equipment, total labor, traffic handling and lane closure costs, which are described as follows:

- **Material costs**

In this study, each section was assumed to be a single-lane having a width of 3.7 m and a length of 1 km, and material costs were calculated for all the sections based on their treatment types and thicknesses.

Unit costs of the materials for slurry seal, dense-graded asphalt concrete, and open-graded asphalt concrete were obtained from State of California Business, Transportation and Housing Agency Department of Transportation contract cost data (2015). The average price per unit (tonne) of the materials were estimated based on their quantity per project. Figure 3.15 shows the average price per unit (tonne) versus quantity per project for OGAC. The dashed line represents the fitted power curve to the data. The fitted curve is shown in Equation 3.3.5. Coefficients a and b are estimated to be 640.12 and -0.239, respectively, for OGAC.

$$\text{Average price per unit (tonne)} = a * \text{quantity per project}^{b} \quad \textbf{3.3.5}$$

Then, total material costs were estimated for each section based on the quantity of materials used for treatment. For instance, the total quantity of OGAC was calculated, and Equation 3.3.5 was used to predict the average price per unit (tonne) of OGAC. Total OGAC costs were estimated by multiplying the average price per unit (tonne) by the total OGAC used for treatment. The volume of the materials used for treating and resurfacing each section was estimated based on the treatment thicknesses and section assumptions described above. To calculate the quantity of materials in tonnes, densities of 2.4 kg/m^3, 2.2 kg/m^3, and 1.2 kg/m^3 were considered for DGAC, OGAC and slurry seal, respectively.

Using RAP materials varying between 20% and 50% could result in cost savings ranging from 14% to 34% compared with using HMA (Hossain et al. 2012). To estimate material costs for sections with RAP, it was assumed that using RAP reduced material costs around 20%. Average costs of chip seal application is reported to be $2.50 to $5.00 per square yard (Stroup-Gardiner et al. 2009). In this study, costs associated with chip seal and chip seal with modified binder were considered as 3 dollars and 5 dollars per square yard, respectively.

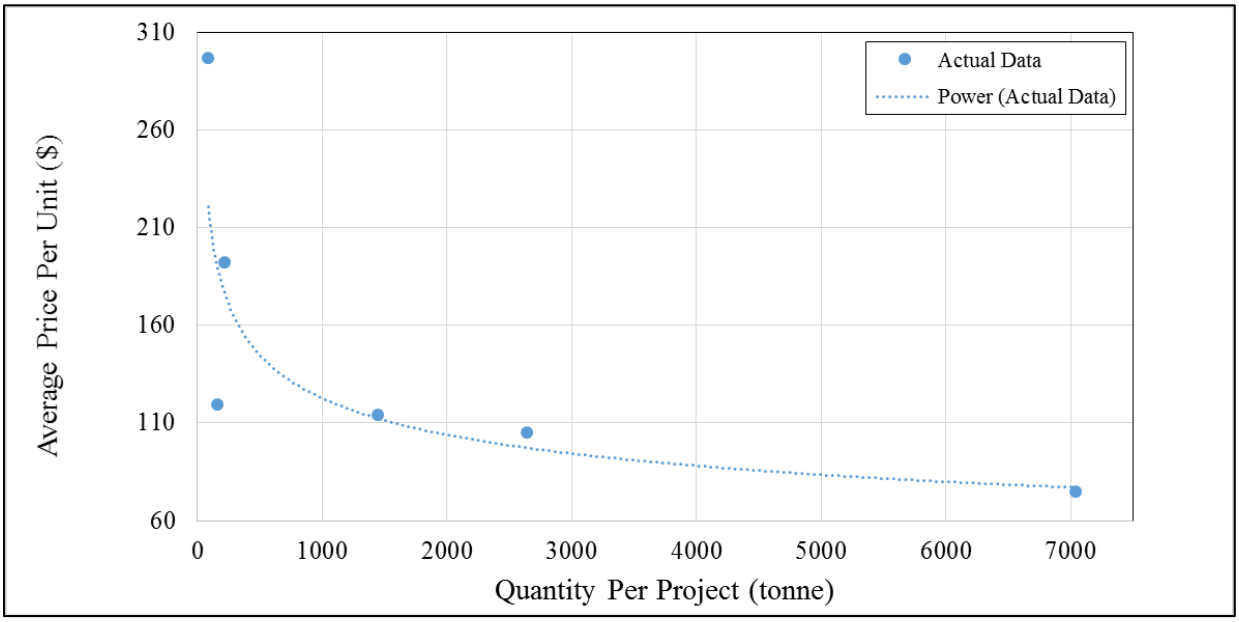

Figure 3.15. Average price per unit tonne of DGAC versus quantity per project

- **Traffic handling, lane closure, labor, and equipment costs**

Costs corresponding to lane closure and traffic handling were considered to be 4000 dollars per day (Caltrans 2013). North Carolina Department of Transportation (NCDOT) (2014) has reported the rate of application of asphalt pavement to be around 200 to 500 tons/day. In order to estimate operation days, lane closure, and traffic handling costs, a rate of application of 500 tons/day was assumed for overlays. The Chip Seal process is generally accomplished in one day for a one-kilometer section. Thus, a one-day closure lane was estimated for chip seal applications.

Based on the data obtained from Berkeley Lab (Berkeley Lab 2017), equipment and total labor costs for different treatments are estimated using the following relationships:

1) Slurry seal: 0.38 *(total construction costs including material costs);
2) Chip seal: 0.39*(total construction costs including material costs);
3) Overlay: 0.19*(total construction costs including material costs).

Total agency costs were calculated by summing up the equipment, total labor, material, traffic handling and lane closure costs. After finding the failure points, agency costs were estimated for

each year at which the treatment was applied. NPV of agency costs were determined afterwards using 4 percent interest rate by Equation 3.3.6. At the end of the analysis period, NPV of the salvage value of the pavements were computed as the agency benefits and added up to NPV of agency costs.

$$NPV = \sum_{t=0}^{T} \frac{C_t}{(1+r)^t} \qquad \textbf{3.3.6}$$

Where:

C_t = estimated user benefit or agency costs at year t,

r = interest rate, and

T = number of time periods.

3.3.2.7 Step 8 - Calculating Net Present Value (NPV) of user benefits

Road-user costs are calculated from the total user-cost equations developed in the World Bank's HDM4 models (Bennett and Greenwood 2003). These equations give higher priority for road maintenance and rehabilitation to roads with greater percentages of trucks. 3-axle trucks and passenger cars are two vehicle classes considered in this study. Four percent interest rate was considered to estimate the NPV of user benefits. NPV was calculated using the Equation 3.3.6.

User benefit was estimated as the difference in road user costs between IRI after treatment and maximum IRI (IRI_{max}). User benefit was weighted for traffic volume by multiplying user costs by the number of vehicles (trucks and passenger cars) using the lane. In this study, IRI_{max} was considered to be 5.05 m/km (320 inches/mile) since the suggested maximum trigger IRI for all the sections is 5 m/km (316.8 inches/mile) (an IRI limit for user safety) (Tighe et al. 2000). IRI_{max} should be greater than all the suggested trigger IRI values, which is 5 m/km (320 inches/mile) in this study. Because this study aims to compare user benefits for different sections with different traffic levels and treatment types, **predicted user benefits are non-monetary**. This approach, however, could appropriately compare user benefits for different strategies. Moreover, the cost equations from HDM4 models are not adjusted for inflation and they are not the actual costs. Figure 3.16 shows how the user benefit was calculated. The difference in user costs between IRI_{max}

and IRI after treatment was estimated for each year (presented as vectors in Figure 3.16). Then, weighted user benefits at each year were converted to NPV and summed up to find the total benefits of applying the treatment.

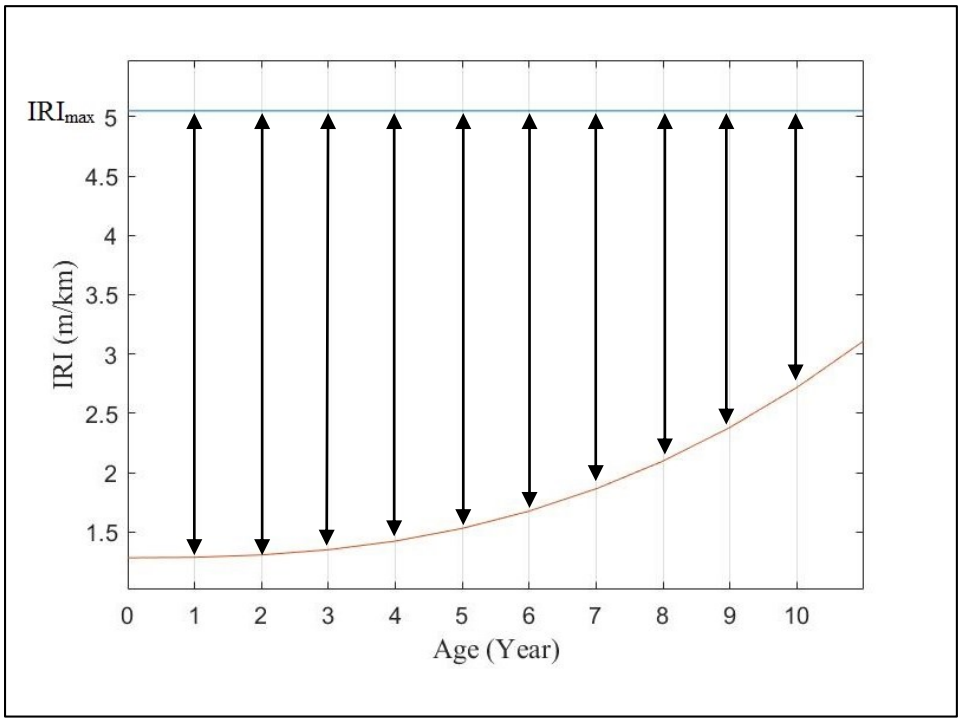

Figure 3.16. Illustration of user benefits for a section in Washington where chip seal is the last treatment (WA-C350-DGAC-CS)

3.3.2.8 Step 9 - Efficient frontier curve

Developing efficient frontier curve can be depicted by the plot of cumulative benefit versus cumulative cost for all the sections. The arrow showing benefits and costs of the section with the highest B/C ratio comes first on the plot. The arrows of benefits and costs of other sections are connected end-to-end in order of decreasing B/C ratio. This plot is called "Efficient frontier curve" (Merton 1972; Mbwana 2001), and it is presented in Figure 3.17. After plotting the efficient frontier curve, sections having the highest benefit to cost ratios can be selected for maintenance and rehabilitation with the currently available budget. For the example given in Figure 3.17, if the available budget is $\$2.8 * 10^5$, sections CA-2051-DGAC, CA-8150-DGAC, WA-6048-RAPHL, and CA-0567-OGAC should be selected for maintenance. Additionally, required budget to achieve a specific benefit level can be estimated using the developed efficient frontier curve. User benefits

and required budgets associated with treating the sections are presented in Table 3.5 in tabular form.

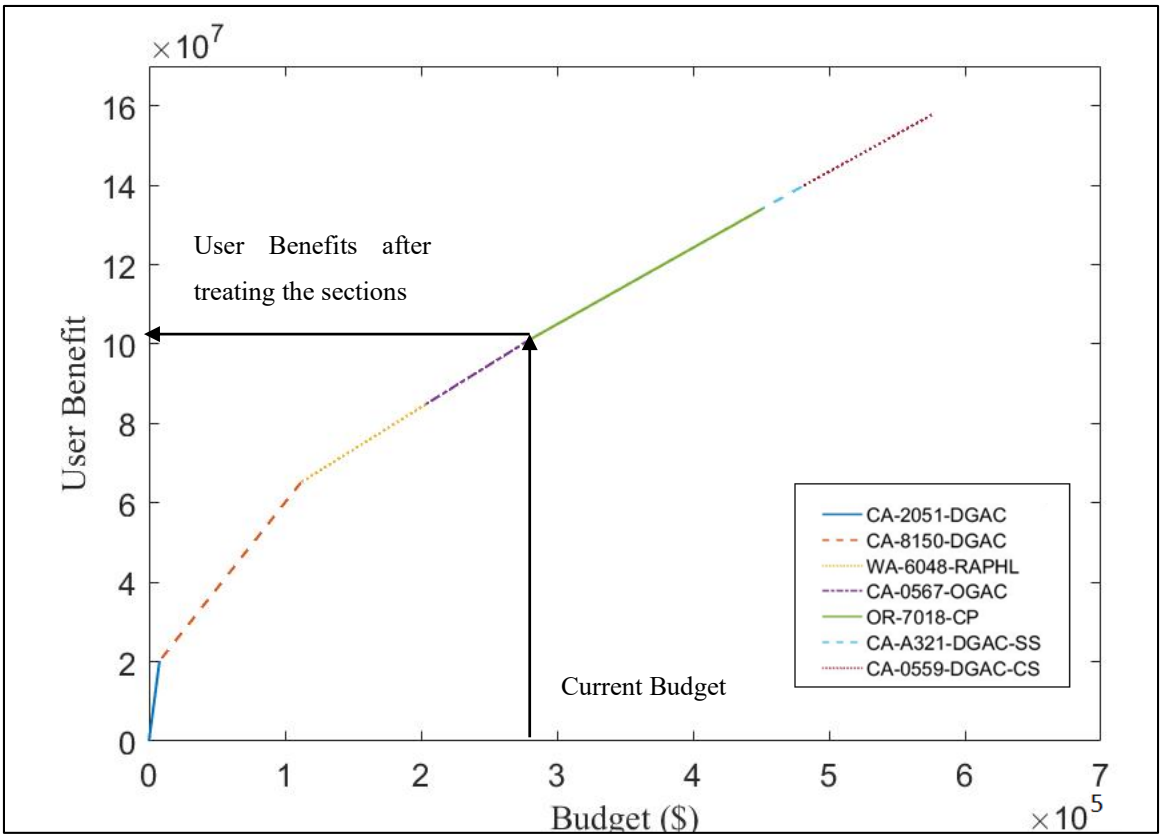

Figure 3.17. Illustration of efficient frontier curve for 7 sections of this study

Table 3.5. User benefits, available budget, and B/C ratios of 7 sections

Section IDs	User Benefits	Budget ($)	B/C
CA-2051-DGAC	20,180,862	7,750	2,604
CA-8150-DGAC	45,008,923	104,072	432
WA-6048-RAPHL	19,685,652	91,873	214
CA-0567-OGAC	16,382,191	77,000	213
OR-7018-CP	32,873,537	170,644	193
CA-A321-DGAC-SS	5,514,009	28,700	192

3.3.3 Methodology of finding the trigger IRI by considering user safety, user cost benefits, and agency costs

This study follows two methods to find the trigger IRI and apply the treatments: 1) Considering one value for the trigger IRI for all the sections regardless of the traffic levels, and 2) Considering different trigger IRIs for sections based on their traffic levels (Madanat 2014).

The first approach considers one value for trigger IRI for all the sections regardless of the traffic levels. As the IRI reaches that trigger IRI, a treatment is applied and the IRI is reduced to a certain value. For example, if the trigger IRI is assumed to be 177 inches/mile, the failure point for all the sections is when the IRI reaches 177 inches/mile over the analysis period.

The second approach follows Madanat (2014) method. Sathaye and Madanat suggested to use different trigger IRI values for different traffic levels (Figure 3.18). Suggested trigger IRIs for different traffic levels are:

Trigger IRI = 1.6 m/km (101 inches/mile) for 30% of roadway network with highest traffic (top 30% traffic volume)

Trigger IRI = 2 to 2.8 m/km (127 to 177 inches/mile) for 25% to 70% of roadway network traffic (medium traffic level)

Trigger IRI = 5 m/km (316.8 inches/mile) for 25% of roadway network with lowest traffic (lowest 25% traffic volume)

Tighe et al. (2000) suggested that to increase safety and to reduce accident rates, IRI should be below 5 m/km (316.8 inches/mile). Therefore, this study considers a trigger IRI of 5 m/km (316.8 inches/mile) for lower 25% percentile network traffic level. Following the procedure developed by Madanat (2014), sections were ranked based on their traffic levels, and trigger IRIs were assigned to sections according to their traffic levels in the network.

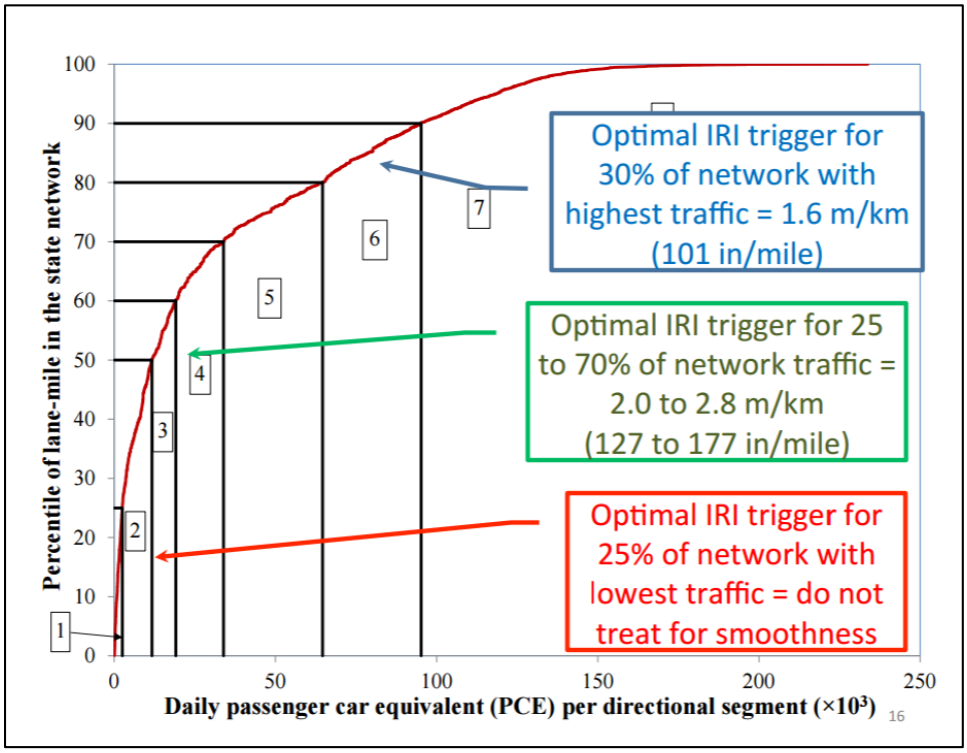

Figure 3.18. Optimal trigger IRI for different traffic levels (Madanat 2014)

3.4 RESULTS AND DISCUSSION

The decision-making tool was developed for two trigger IRI methods discussed in the previous section. Results are given as follows:

3.4.1 One value for trigger IRI

In this section, efficient frontier curves were developed for different trigger IRI values, ranging from 1.42 to 5.05 m/km (90 to 320 inches/mile). As shown in Figure 3.19, reducing trigger IRI values increases user benefits but requires higher budgets for paving. As the trigger IRI increased, user benefits and required budget for treating and resurfacing the sections both decreased. Figure 3.19 shows that budget levels control the optimal selected IRI levels. For instance, if the available budget is greater than $\$9.5 * 10^6$, a trigger IRI of 1.58 m/km (100 inches/mile) over the analysis period creates higher user benefits. On the other hand, if the available budget is less than $\$9.5 * 10^6$, a trigger IRI of 1.74 m/km (110 inches/mile) results in higher user benefits.

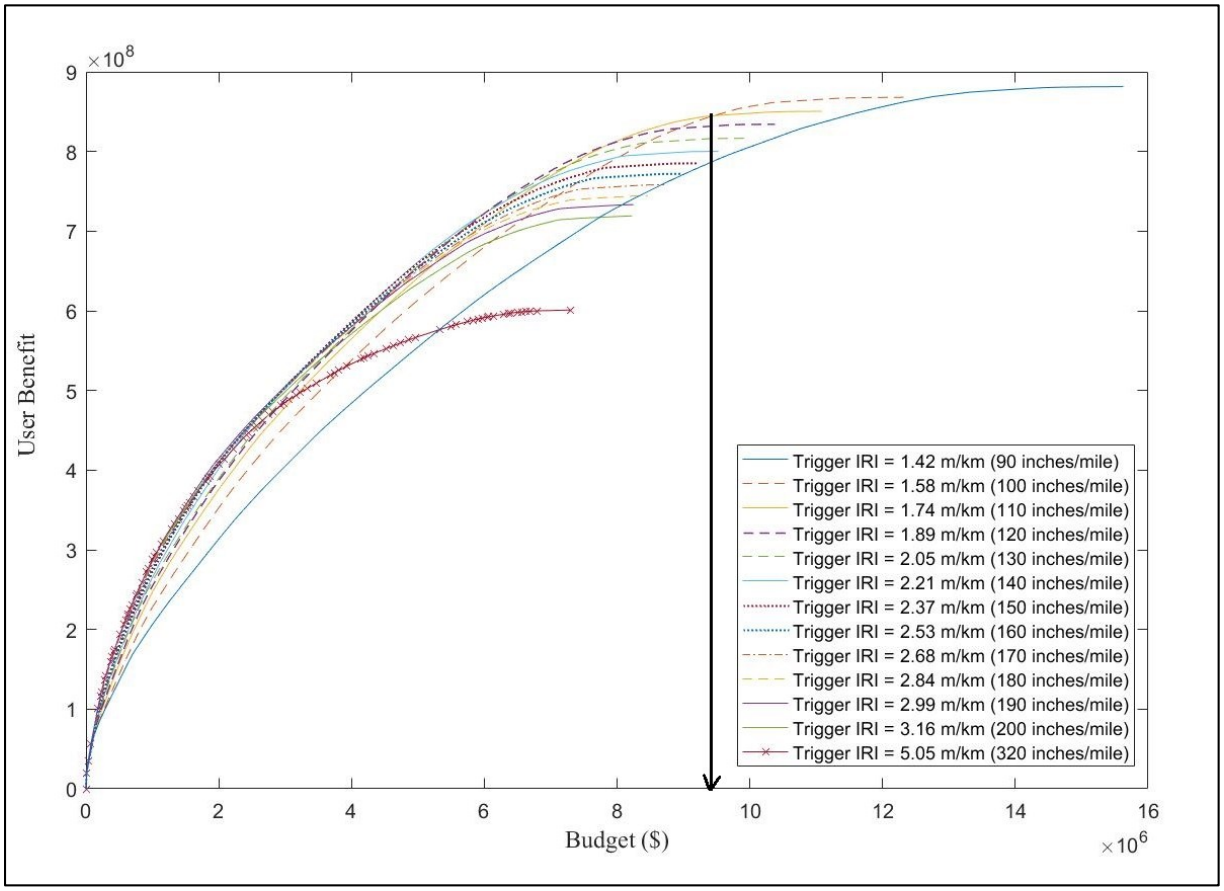

Figure 3.19. Efficient frontier curve for different values of trigger IRI regardless of traffic levels

3.4.2 Different trigger IRI values based on traffic levels

In this section, traffic levels are considered in developing the efficient frontier curve (Sathaye and Madanat 2012). Since different values for the trigger IRI are considered for 25% to 70% of network traffic, ranging from 2 to 2.8 m/km (127 to 177 inches/mile), the efficient frontier curve was developed for different trigger IRIs for this middle range of traffic. According to Sathaye and Madanat (2012), sections should be ranked based on the daily passenger car equivalent. To estimate the passenger car equivalents of the 3-axle trucks, AADTTs were multiplied by the coefficient of 1.2175 and ranked based on their traffic levels in each year of the analysis period (Ahmed, 2010). Optimal trigger IRIs were annually assigned to the sections after each year. Figure 3.20 shows the efficient frontier curve for trigger IRI values of 2 m/km, 2.5 m/km and 2.8 m/km (127 inches/mile, 157 inches/mile, and 177 inches/mile). As is shown in the figure, a lower

trigger IRI for 25% to 70% of network traffic (medium traffic level) could increase the required budget and user benefits slightly, but not significantly.

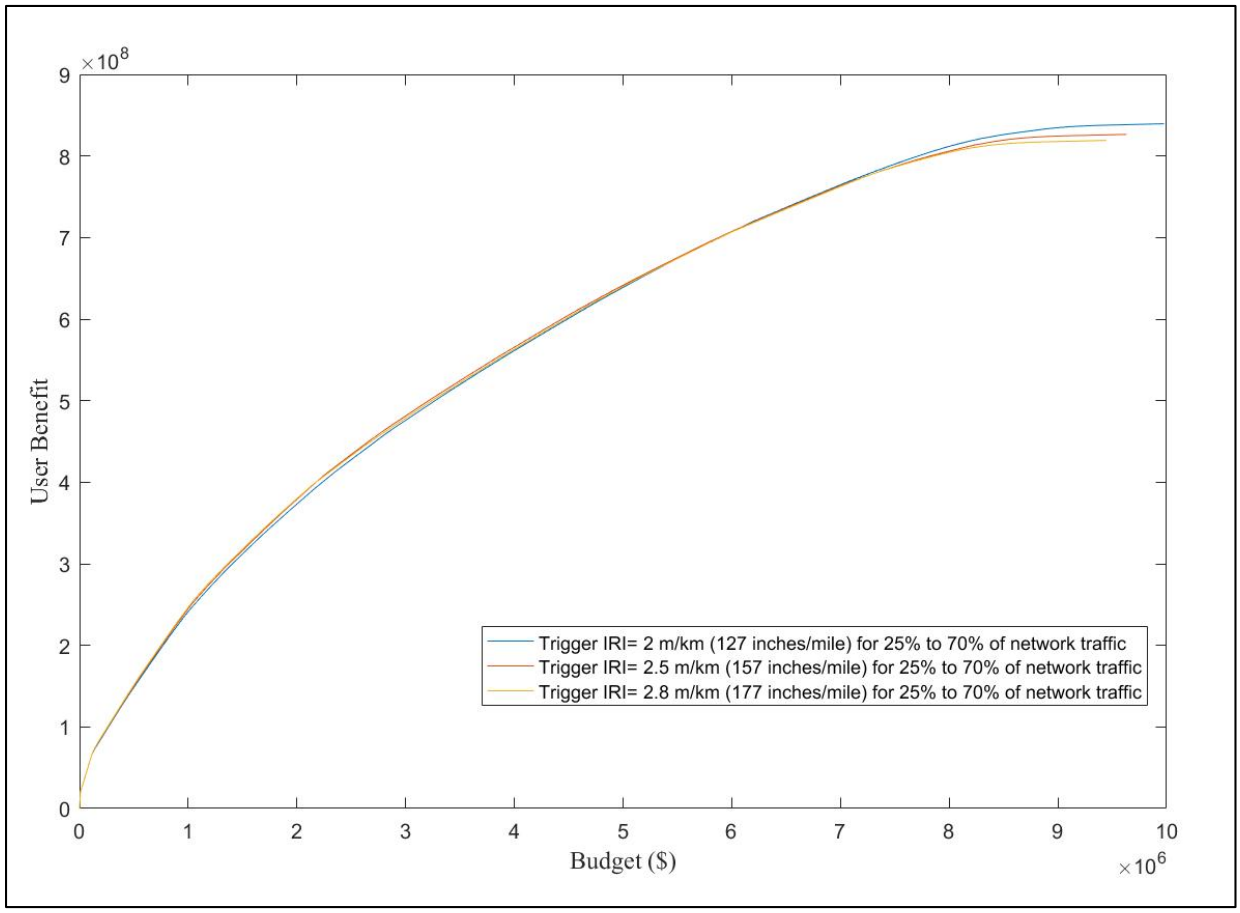

Figure 3.20. Efficient frontier curve for different values of trigger IRI by considering traffic levels

3.4.3 Optimal trigger IRI according to the available budget

In this section, efficient frontier curves for different values of trigger IRI and different methods are compared. The first method is using one value for the trigger IRI for all sections regardless of traffic levels (Section 3.4.1) and the second is using different trigger IRI values for different traffic levels (section 3.4.2). Figure 3.21 shows the efficient frontier curves for different scenarios. The "line of maximum benefit for different trigger IRI values" was found in order to find the optimal trigger IRI for different budget levels at which the user benefit was at a maximum. To find the "line of maximum benefit for different trigger IRI values", the budget level was divided into small

intervals, and in each interval maximum user benefit and the corresponding trigger IRI value were determined. Subsequently, the optimal trigger IRI versus budget was plotted as is presented in Figure 3.23. It can be seen that as the budget increased, the trigger IRI at which the user benefit was maximum decreased. Figure 3.22 shows that considering one trigger IRI for all the sections regardless of their traffic level will give higher benefits than following the Madanat (2014) method. Suggested trigger IRI for different budget levels is also shown in Table 3.6.

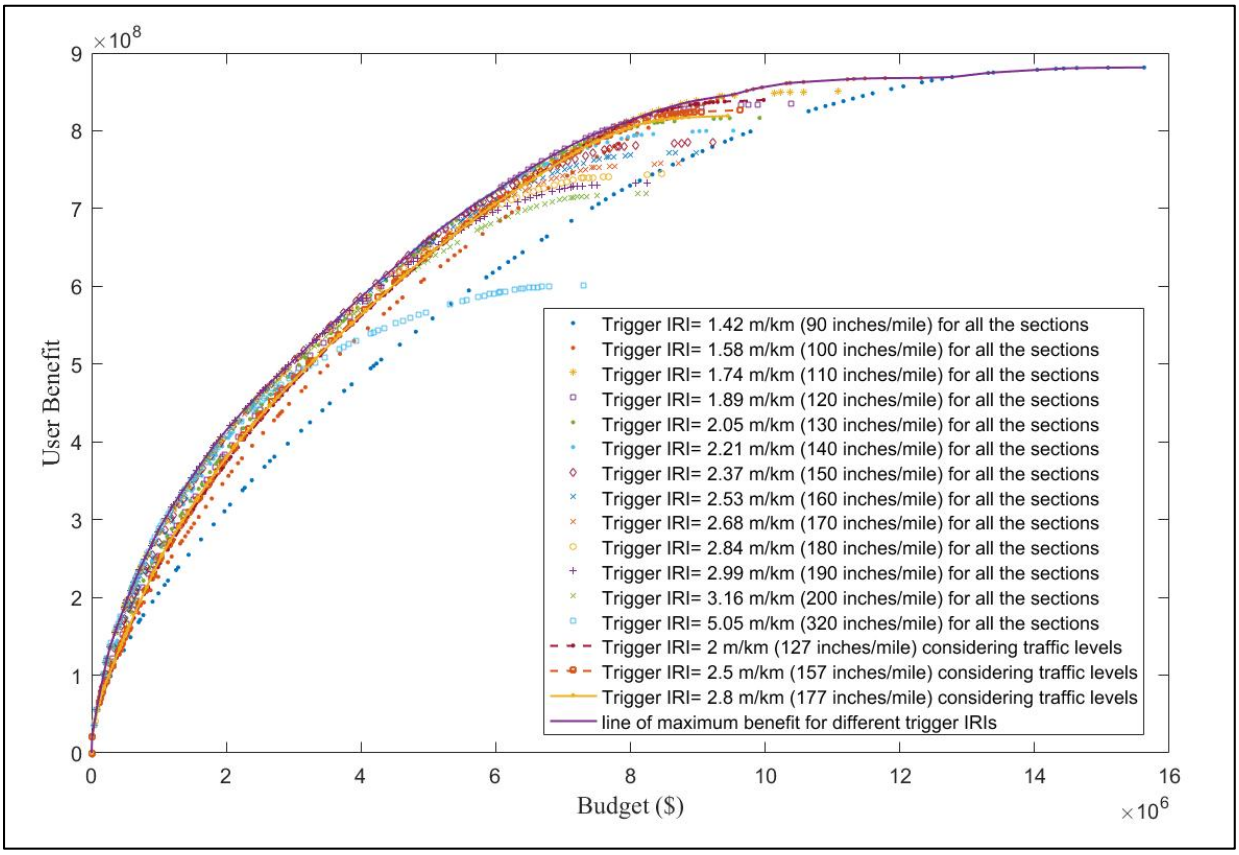

Figure 3.21. Illustration of finding optimal IRI for different budget levels

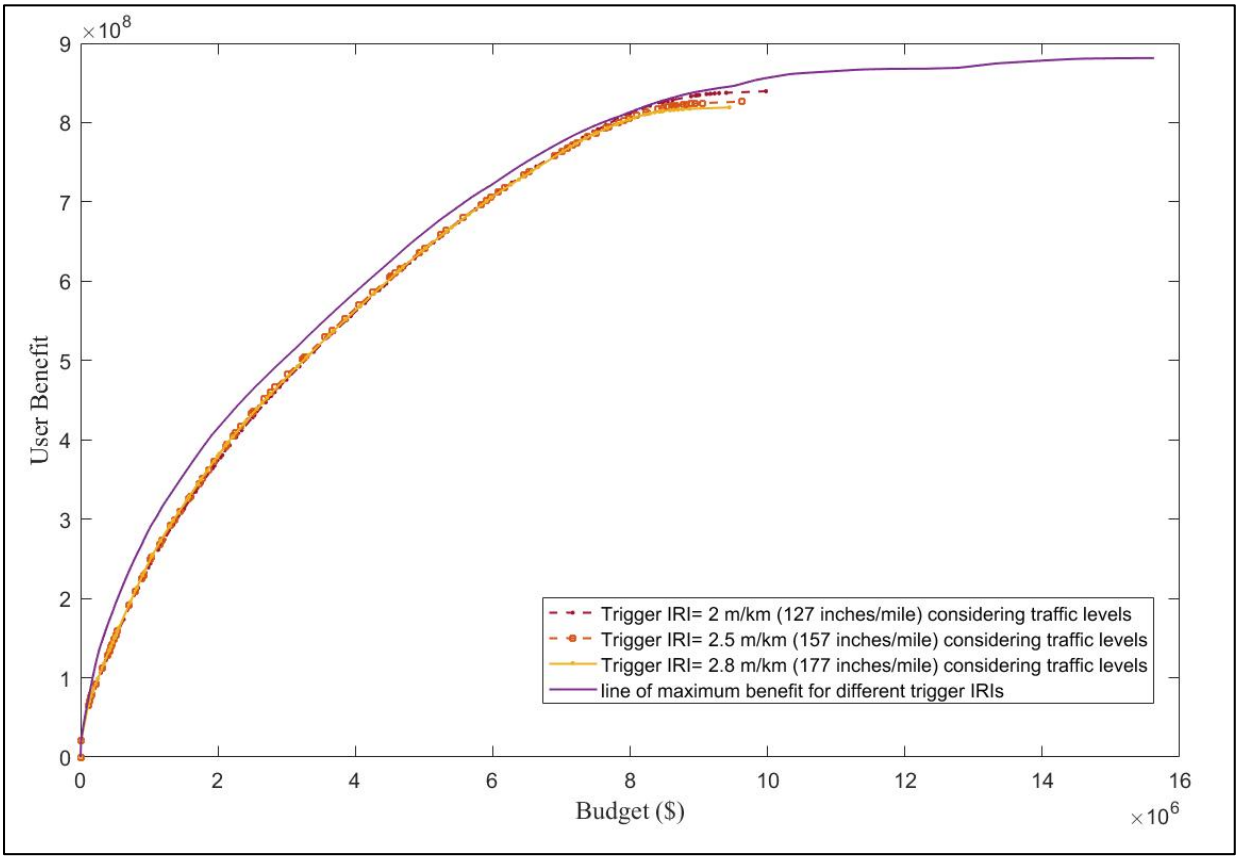

Figure 3.22. Illustration of optimal IRI for different budget levels and efficient frontier curve for different values of trigger IRI by considering traffic levels

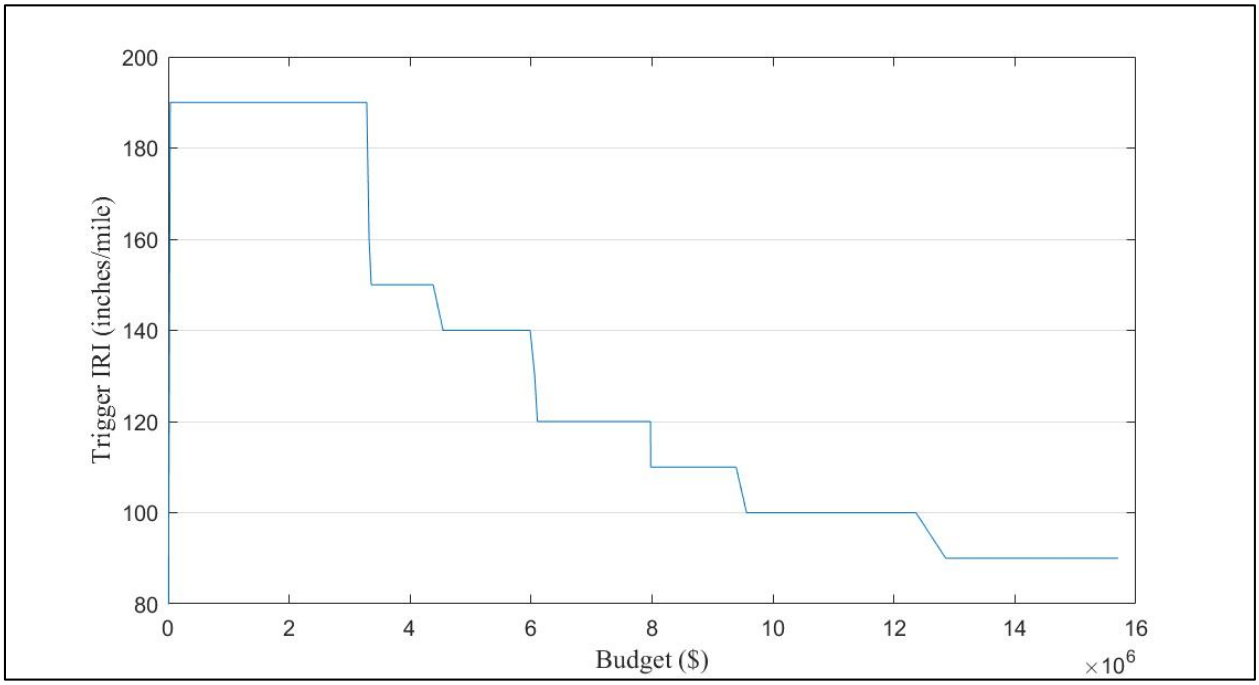

Figure 3.23. Optimal trigger IRI versus agency costs (budget)

Table 3.6. Suggested optimal trigger IRI for different budget levels

Trigger IRI (inches/mile)	Budget ($)	
	from	to
Value of trigger IRI does not matter	0	7.75E+03
190	7.75E+03	3.28E+06
160	3.28E+06	3.32E+06
150	3.32E+06	4.38E+06
140	4.38E+06	5.90E+06
140	5.90E+06	5.98E+06
130	5.98E+06	6.06E+06
120	6.06E+06	7.97E+06
110	7.97E+06	9.39E+06
100	9.39E+06	1.24E+07
90	1.24E+07	1.57E+07

3.5 INTEGRATION OF THE DEVELOPED DECISION-MAKING TOOL WITH GEOGRAPHIC INFORMATION SYSTEMS (GIS)

The network-level decision-making tool is immensely useful for analyzing which roadway sections within the network will provide the most efficient allocation of agency maintenance budgets and yield the most benefit to road users. This tool could be even more useful if the roadway sections were spatially cataloged such that users of the tool could visually analyze which sections are more critical to maintain or rehabilitate. An extension of this tool is the integration of MATLAB code results with a Geospatial Information Systems (GIS) map. Although this was an auxiliary focus of this study, the potential benefits of pursuing a GIS map are discussed below.

GIS is a powerful tool that is used to spatially catalog information. It is incredibly useful for asset management, decision-making and client outreach in a variety of fields, including transportation engineering. GIS is comprised of one or more databases that store information about objects of interest which are spatially referenced in a map. This information is stored in data layers, or feature classes, that have attribute tables detailing pertinent information about an object of interest. Information can be stored as point, line or polygon features within the GIS map. A common software used in GIS operations is ArcGIS. This software provides an environment that allows a user to examine, process and prepare spatial data efficiently for a variety of purposes. A GIS user can query and expand upon information stored in a database readily and easily using built-in tools within the ArcGIS environment. Also, a GIS developer has the ability to create custom tools that can suit any data processing need. GIS data is easily shareable, meaning that it can be viewed by anyone with GIS software installed on their computer. What is even more powerful is the use of online maps, which involves publishing a GIS database to an online web server; an inherent function of ArcGIS software. This way, any interested party can view GIS data easily from within a web browser, eliminating the necessity of having a GIS software license.

The utility of GIS in the framework of pavement management is to allow for accurate and expedient record keeping of past maintenance strategies and easy access to data by multiple stakeholders. Many state DOTs, including Oregon and Utah, have successfully implemented web-based GIS portals that allow interested parties to view and query information about the state's transportation infrastructure (Oregon Department of Transportation 2017; Esri 2015). These maps

have valuable information, but for the purposes of this study, they are currently limited by their ability to provide a means of decision-making in terms of choosing maintenance strategies for road sections.

To extend the utility of the network-level decision-making tool developed in this study, a prototype GIS map was created using ArcGIS in order to investigate the feasibility of integrating results of the decision-making tool with the spatial referencing power of GIS. The goal of the GIS map was to create the ability for users to import LTPP road section data and the tool's MATLAB results into the GIS environment, spatially catalog this information and finally rank, highlight, and export selected roadway sections that present the highest benefit-to-cost ratios, or highest maintenance priority. This output illustrates which sections should receive maintenance and rehabilitation first for a given budget and trigger IRI value and shows where they are located geographically. It is essentially a spatial representation of the Efficient Frontier Curve for a given trigger IRI and state's roadway network.

To prove the methodology of the GIS process, 20 sections in the LTPP database, namely five sections in Oregon and 15 sections in Idaho, were selected to spatially catalog. MATLAB outputs for single trigger IRI of 170 inches/mile were selected as arbitrary trial subjects. A custom geodatabase was created and base data for the Oregon and Idaho highway networks was obtained from online geospatial data clearinghouses for each respective state. A custom feature class, or data layer, containing point features was created for each state in order to import LTPP road section data from Excel spreadsheet files into the respective data layer's attribute table. These feature classes utilized the State Plane coordinate systems of each respective state. The MATLAB code outputs were also imported to these custom feature classes. A custom ArcGIS tool was created using Python scripting that allowed the user to calculate the benefit-to-cost ratios for each road section. Another custom tool was created that ranked each section sequentially based on which benefit-to-cost ratios were greatest.

Figure 3.24 shows the LTPP sections for Oregon spatially cataloged within the GIS map.

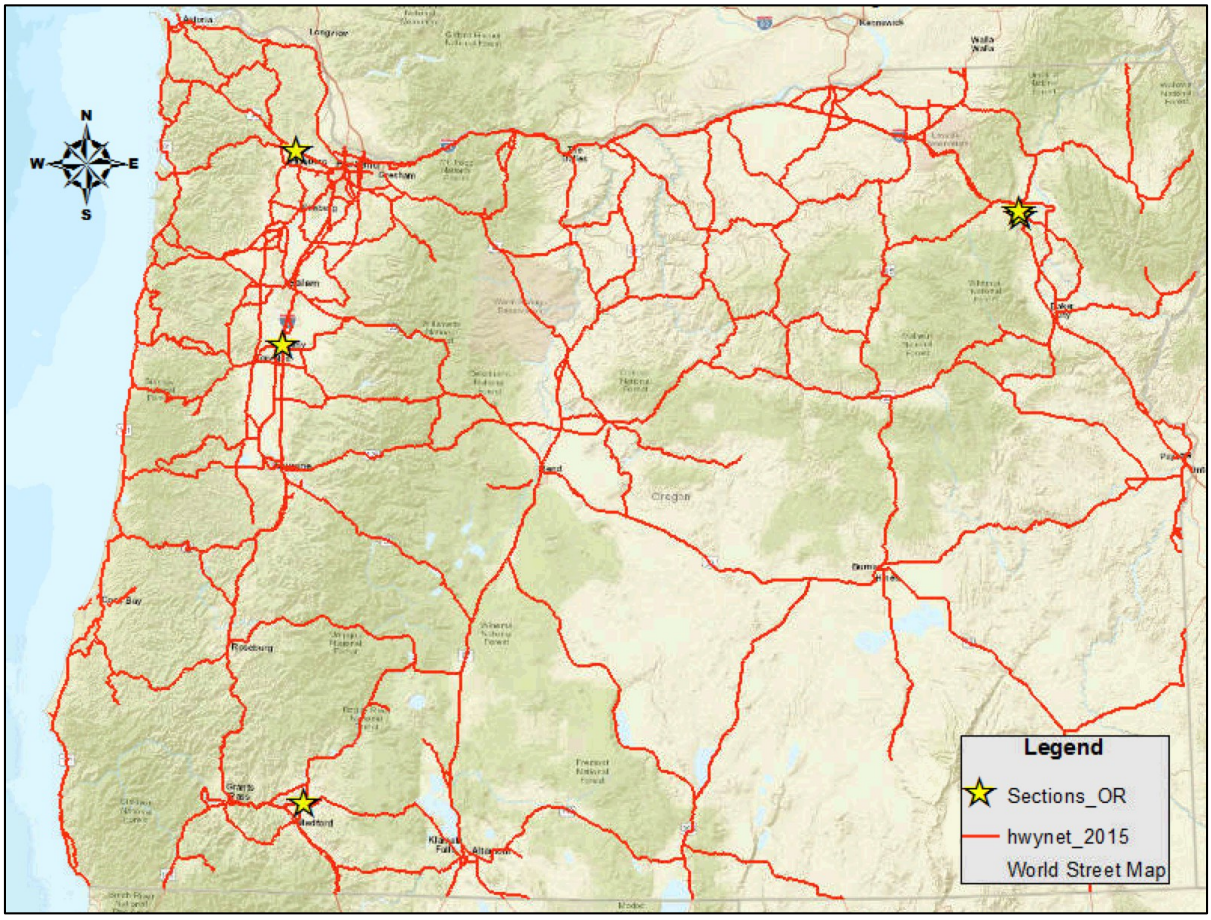

Figure 3.24. Map of Oregon highway network with LTPP sections shown

Table 3.7 shows the attribute table for Oregon LTPP sections, including imported MATLAB output data as well as GIS-derived benefit-to-cost ratios and ranking.

Table 3.7. Attribute table for Oregon LTPP sections with MATLAB outputs, benefit-to-cost ratios and ranking

sectiontreatment	AVGTRUCKTRAFFIC	AVGCARTRAFFIC	USERBENEFIT_TRUCK	USERBENEFIT_CAR	USERBENEFIT_TOTAL	COSTS_MATERIAL	B_C_RATIO	RANK
OR-2002-DGAC	264977	3337035	4187850	11862451	9973219	76733	130	2
OR-5006-CPR	684245	759758	10297796	2714393	8085420	79755	101	3
OR-5008-CPR	645642	698773	9536201	2447826	7446548	78174	95	4
OR-7018-CP	1964753	5266160	26704050	16670134	26951535	109228	247	1
OR-7019-CP	263840	2083715	4019025	6697919	6659216	146267	46	5

Once data processing was complete, the attributes of the point feature classes for Oregon and Idaho were migrated to the highway line features for each state. This was done by using built-in ArcGIS Buffer, Clip and Join functions, which allow the user to select a portion of a dataset based on

proximity and copy attribute information to the newly selected features. The resulting data layer was a line feature class comprised of 1km test sections for each LTPP pavement section of interest and containing all MATLAB and Efficient Frontier Curve information previously obtained in the above steps.

Figure 3.25 shows a zoomed-in view of one of the LTPP sections in Oregon, with highway network line data clipped to a 1km test section.

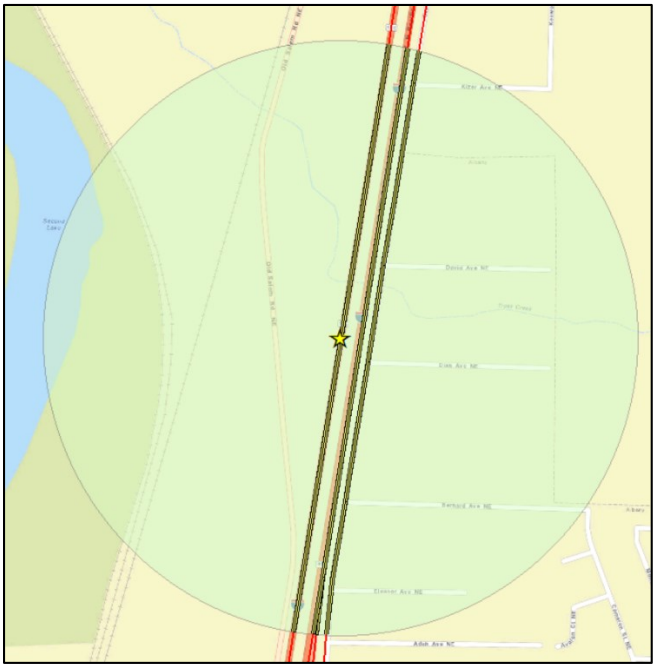

Figure 3.25. Close-up view of Oregon LTPP section with clipped line data

To further integrate the GIS map with the decision-making tool results, all sections that should be maintained based on a given budget were selected in the ArcGIS attribute table based on their benefit-to-cost ratio rankings. This relates to the Efficient Frontier Curve, essentially allowing the user to select all road sections that have the highest priority for maintenance for a given budget (i.e. all the sections to the left of the budget amount) based on their benefit-to-cost ratios. Then, these sections were exported to a new feature class/data layer using built-in ArcGIS functionality. This way, the data can be shared with other stakeholders who can easily load the data layer in a GIS environment to see the spatial location of the road sections and all accompanying attribute data in the attribute table.

For instance, consider an example for select LTPP road sections in Oregon and Idaho for a trigger IRI of 170 inches/mile where the available budget is $500,000 for each state. A plot of the efficient frontier curve for both states for this situation is shown below in Figure 3.26 and Figure 3.27.

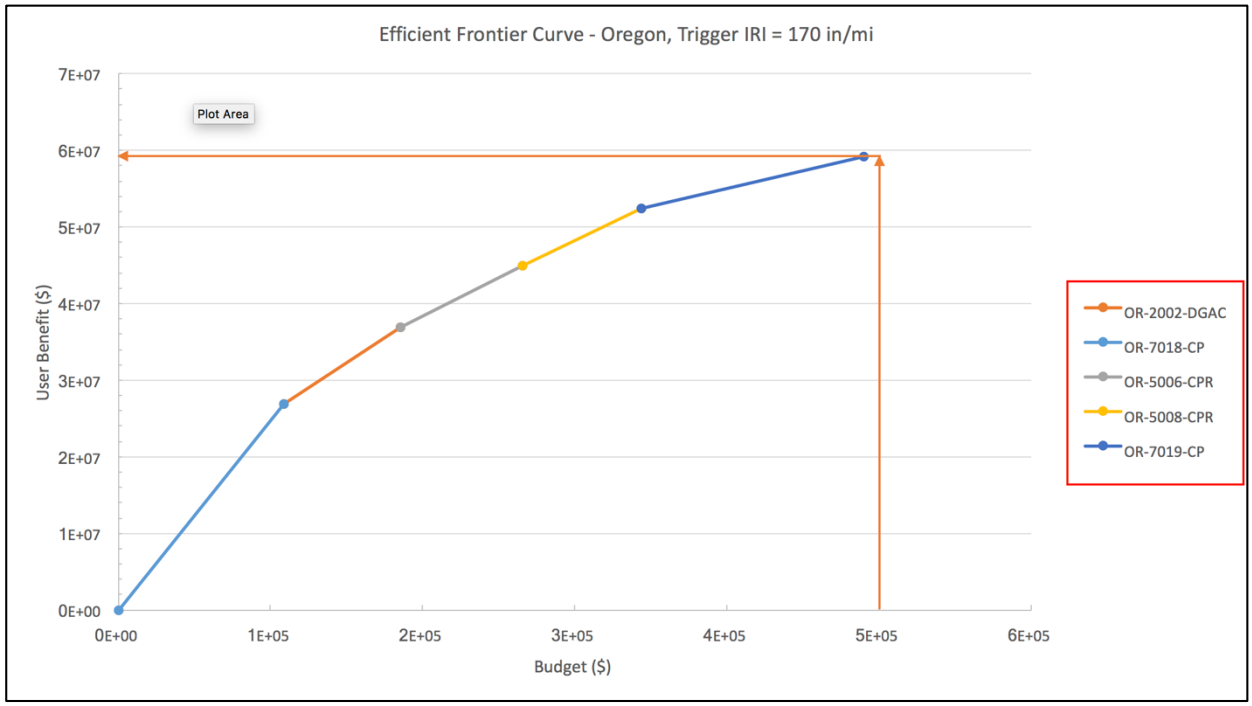

Figure 3.26. Efficient Frontier Curve for Oregon at an IRI value of 170 inches/mile

As is shown in Figure 3.26, the sections in Oregon that can be treated for this budget are OR-2002-DGAC, OR-7018-CP, OR 5006-CPR, OR-5008-CPR and OR-7019-CP. Therefore, for the budget level of $500,000, Oregon can treat all of these LTPP road sections.

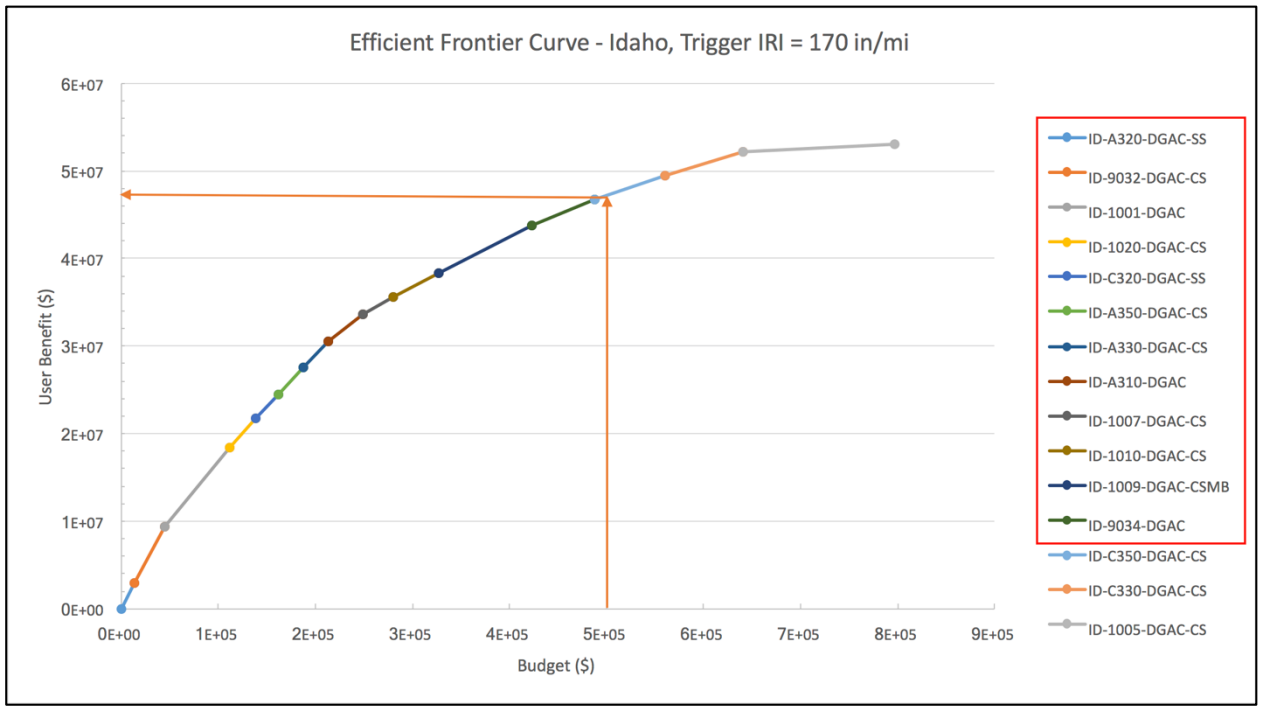

Figure 3.27. Efficient Frontier Curve for Idaho at an IRI value of 170 inches/mile

As is shown in Figure 3.27, the sections in Idaho that can be treated for this budget are ID-A320-DGAC-SS, ID-9032-DGAC-CS, ID-1001-DGAC, ID-1020-DGAC-CS, ID-C320-DGAC-SS, ID-A350-DGAC-CS, ID-A330-DGAC-CS, ID-A310-DGAC, ID-1007-DGAC-CS, ID-1010-DGAC-CS, ID-1009-DGAC-CSMB and ID-9034-DGAC. Therefore, for a budget of $500,000, Idaho can treat these select LTPP road sections.

After obtaining these results from the Efficient Frontier Curve, a user of the GIS tool can then select these particular sections on the GIS map from within the attribute table for each state and export the selection to a new data layer. This data layer representing the highest priority sections to be maintained for a given budget based on benefit-to-cost ratios could be easily shared with other stakeholders and interested parties.

Figure 3.28 shows a methodology flowchart for GIS operations.

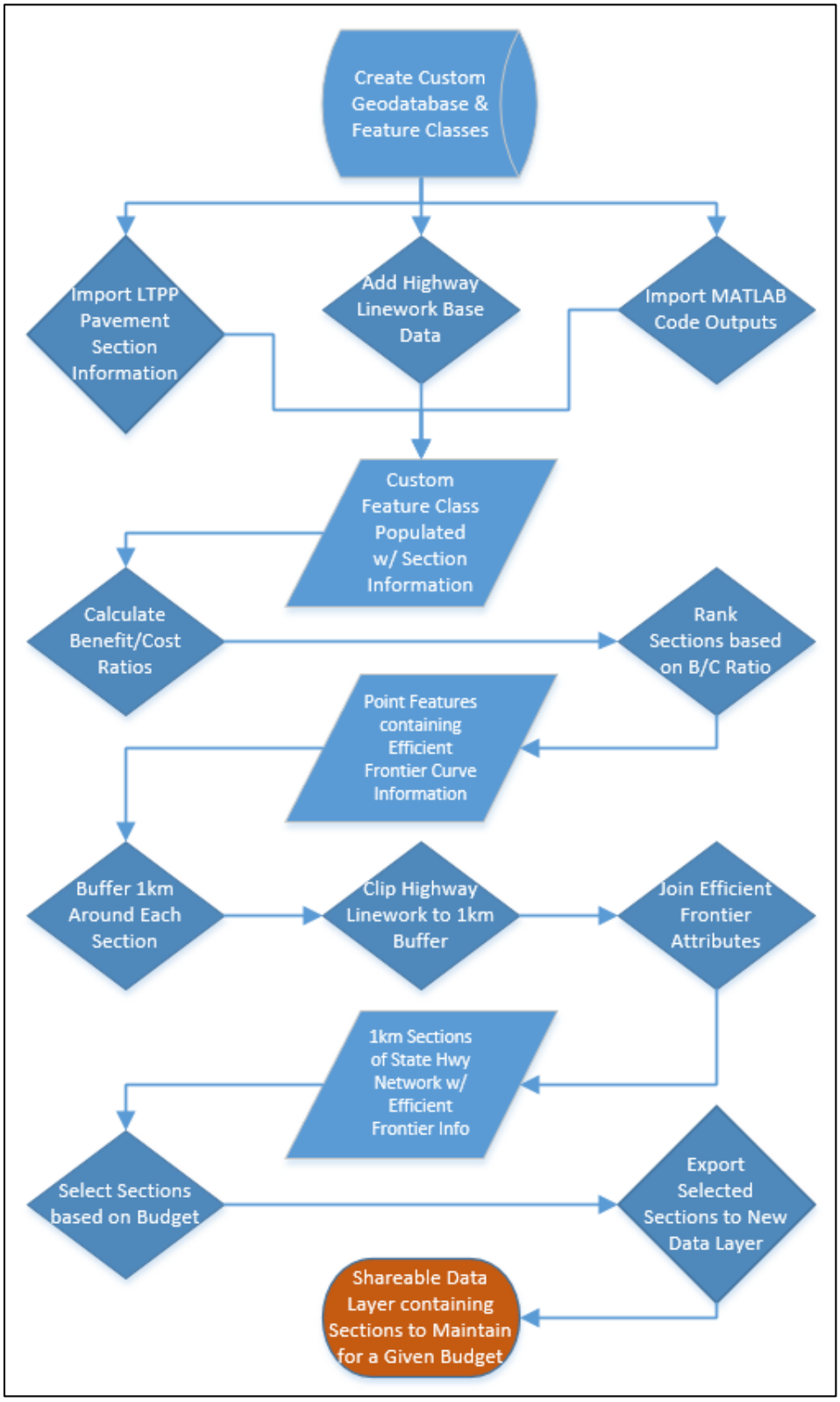

Figure 3.28. Flowchart for GIS Methodology

This section illustrates a brief overview of how GIS can be applied as an extension to the decision-making tool. It adds an element of spatial visualization to the decision-making tool results, making it easier for stakeholders to pinpoint where particular sections are and why they should be maintained. The creation of a shareable data layer with a small file size including the sections to be maintained for a given budget allows for easy communication of road maintenance needs. Since state DOTs are beginning to increase use of GIS for asset management, their organizations will be able to access the contents of this data layer easily. Furthermore, this data layer could be published to an online web map so that stakeholders can easily view it from a web browser, regardless if they have access to GIS software.

This GIS tool can also be applied to multiple trigger IRI scenarios. Using the custom tools created within the ArcGIS environment, a user can easily import MATLAB results for other trigger IRI values in order to produce a robust array of data layers encompassing multiple maintenance scenarios.

3.6 SUMMARY AND CONCLUSIONS

The goal of this study is to develop a network-level decision-making tool for efficient budget allocation for road maintenance and rehabilitation. Data associated with pavement structure, profile and traffic were obtained for 91 sections in Oregon, Idaho, Washington, and California. The IRI was considered as the only pavement performance variable indicating pavement life and failure point. Two methods were used to estimate the failure points over 40 year-period for each section: 1) Considering one value for trigger IRI for all the sections regardless of the traffic levels, and 2) Considering different trigger IRIs for sections based on their traffic levels (Madanat 2014). After estimating the user benefits and agency costs, efficient frontier curves were developed for different trigger IRI values. Efficient frontier curves were compared with each other and the optimal trigger IRI for different budget levels, at which the user benefit was maximum, were obtained.

The results of this study show that as the budget increases, the trigger IRI at which the user benefit is maximum decreases. It was also concluded that the method of considering one value for trigger IRI regardless of the traffic levels is more optimal for maximizing benefits than the Madanat (2014) method. It was also concluded that budget level controls the most optimal trigger IRI. By allocating a higher budget level to road maintenance (considering a lower value for trigger IRI), higher user benefits can be obtained.

Finally, to extend the utility of the network-level decision-making tool developed in this study, a prototype GIS map was created using ArcGIS. The goal was to create the ability for users to import LTPP road section data and the tool's MATLAB results into the GIS environment, spatially catalog this information and finally rank, highlight, and export selected roadway sections that present the highest benefit-to-cost ratios, or highest maintenance priority. To prove the methodology of the GIS process, 20 sections (5 sections in Oregon and 15 sections in Idaho) in the LTPP database were selected to spatially catalog. MATLAB outputs for single trigger IRI of 170 inches/mile were selected as arbitrary trial subjects. Then, sections with higher priority to receive maintenance and rehabilitation first for a given budget and trigger IRI value were located geographically. Spatial visualization of the decision-making tool results facilitates stakeholders to pinpoint where particular sections are and which sections should be maintained.

3.7 FUTURE STUDY

Based on the conclusions from this research, the following recommendations are suggested:

- In this study, only IRI is used as a performance indicator. Structural number, wheel path cracking and other performance variables from pavement management systems should be considered for characterizing pavement performance.

- Decision trees should be developed to choose the best treatment type at the end of the pavement life rather than repeating the same treatment type over the analysis period.

- Reduction in energy consumption and GHG emissions should also be included in user benefits.

- The developed decision-making tool should be used to analyze the entire network for a state (all sections) using the automated pavement condition survey data.

- Currently, section coordinates are manually imported to GIS. A complete integration of MATLAB code with the GIS map system is needed so that section will be selected by MATLAB. Then, sections' information should be sent to GIS to be automatically highlighted.

3.8 SUGGESTED IMPLEMENTATION STRATEGY

After following the recommendations suggested in section 1.7, finalized decision-making tool can be implemented. Two possible implementation strategies are given as follows:

1. State DOTs can allocate budget to districts based on pavement condition ratings. Each district will use the developed tool to identify the sections (or road segments) that will provide the highest level of user and agency benefits by considering user safety. The network for the analysis will be each district, not the whole state.

2. The tool can perform the budget allocation for the entire state DOTs highway network. DOTs can also incorporate their priorities (safety, structural integrity, minimum allowed pavement ratings, critical commercial areas, and etc.) into the software to change-modify the tools recommendations. The tool will estimate required budget for each district, and those amounts will be directed to every district. Then, each district will make their own prioritization to maintain the sections. Districts can consider tool's recommendation in their decision process to maximize user benefits and safety.

Maps and tables showing the IRI trigger levels for different climate regions and traffic levels should also be developed. These maps and tables can be used by DOTs pavement engineers and managers during the maintenance and rehabilitation decision-making process. Using the developed software, case studies should be developed to evaluate software decisions. A report and a presentation file will be prepared to document research findings and recommendations. It is expected that state DOTs Maintenance Departments will implement the research findings to more effectively and efficiently manage roadway maintenance and rehabilitation.

3.9 ACKNOWLEDGMENTS

The authors would like to express their acknowledgment to the Pacific Northwest Transportation Consortium (PacTrans) for funding this research. The views and opinions expressed in this article are the authors' own and do not necessarily reflect the view and official policies of the Federal Highway Administration or the Pacific Northwest Transportation Consortium. A special thank you to John Paul Morton and Andrew Johnson for their constructive suggestions throughout this study.

3.10 REFERENCES

Ahmed, U. *Passenger Car Equivalent Factors for Level Freeway Segments Operating Under Moderate and Congested Conditions.* Dissertations, Theses, and Professional Projects*,* 2010.

Al-Omari, B. and Darter, M.I. Relationships between International Roughness Index and Present Serviceability Rating. *Transportation Research Record: Journal of the Transportation Research Board*, 1435(2), 1994.

Anastasopoulos, P.C., Tarko, A.P. and Mannering, F.L. Tobit Analysis of Vehicle Accident Rates on Interstate Highways. *Accident Analysis & Prevention*, 40(2), 2008, pp.768-775.

Barnes, G. and Langworthy, P. Per Mile Costs of Operating Automobiles and Trucks. *Transportation Research Record: Journal of the Transportation Research Board*, (1864), 2004, pp.71-77.

Bennett, C.R. and Greenwood, I.D. Volume 5: HDM-4 Calibration Reference Manual. *ISOHDM World Road Association (PIARC),* 2003, pp.174-181.

Berkeley Lab, Energy End-Use Forecasting Group, Retrieved form: http://enduse.lbl.gov/http://enduse.lbl.gov/, enduse.lbl.gov/Info/pavements_LCCA_web.xls. Accessed February 14, 2017.

Bester, C.J. January. The Effect of Road Roughness on Safety. In 82nd Annual Meeting of the Transportation Research Board, Washington, DC, 2003.

Chatti, K., and I. Zaabar. Estimating the Effects of Pavement Condition on Vehicle Operating Costs. *Publication NCHRP Report 720. National Cooperative Highway Research Program, Transportation Research Board,* 2012.

Chehovits, J. and Galehouse, L. Energy Usage and Greenhouse Gas Emissions of Pavement Preservation Processes for Asphalt Concrete Pavements. In *Compendium of Papers from the First International Conference on Pavement Preservation,* 2010, pp. 27-41.

EAPA. *Environmental Impacts and Fuel Efficiency of Road Pavements*. EAPA & Eurobitume Industry Report, 2004.

Harvey, J., Kendall, A., Lee, I.S., Santero, N., Dam, T.V. and Wang, T. Pavement Life Cycle Assessment Workshop: Discussion Summary and Guidelines. *University of California Pavement Research Center, California,* 2010.

Hendrickson, C.; Lave, L. B.; Matthews, H. S. *Environmental Life Cycle Assessment of Goods and Services - An Input-Output Approach.* Resources for the Future: Washington, DC, 2006.

Hossain, M., Musty, H.Y. and Sabahfer, N. Use of High-Volume Reclaimed Asphalt Pavement (RAP) for Asphalt Pavement Rehabilitation Due to Increased Highway Truck Traffic from Freight Transportation. *Final Reports & Technical Briefs from Mid-America Transportation Center*, 2012.

Islam, S. and Buttlar, W. Effect of Pavement Roughness on User Costs. *Transportation Research Record: Journal of the Transportation Research Board,* (2285), 2012, pp.47-55.

Li, Y. and Madanat, S. A Steady-State Solution for the Optimal Pavement Resurfacing Problem. *Transportation Research Part A: Policy and Practice,* 36(6), 2002, pp.525-535.

LTPP InfoPave. *Long-Term Pavement Performance.* Retrieved from: https://infopave.fhwa.dot.gov. Accessed September 15, 2016.

Mack, J.W., Gregory, J. and Kirchain, R., Developing Robust Rehabilitation Scenario Profiles for Life Cycle Assessment Using Decision Tree Analysis. *Pavement LCA 2014, International Symposium on Pavement Life Cycle Assessment*, 2014.

Madanat, S., Horvath, A. and Reger, D. Integration of LCA into Pavement Management Systems, Presented at University of California Pavement Research Center, 2014.

MATLAB R2016b: MATLAB and Statistics Toolbox. The MathWorks, Inc., Natick, Massachusetts, United States, 2016.

Mbwana, J.R. A Framework for Developing Stochastic Multi-Objective Pavement Management Systems. In *First Road Transportation Technology Transfer Conference in Africa 2001,* 2001, pp. 350-363.

Merton, R. E. An Analytic Derivation of the Efficient Portfolio Frontier. *Journal of Financial and Quantitative Analysis 7*, 1972, 1851-72.

Mitchell, T. *Westrack Track Roughness, Fuel Consumption and Maintenance Cost*. Federal Highway Administration, FHWA-RD-00-052. U.S. Department of Transportation, 2000.

North Carolina Department of Transportation (2014). *Guidance for Determining Contract Times*, 2014.

Oregon Department of Transportation, *2012 Pavement Condition Report.* Pavement Services Unit, 2013.

Ouyang, Y. and Madanat, S. An Analytical Solution for the Finite-Horizon Pavement Resurfacing Planning Problem. *Transportation Research Part B: Methodological,* 40(9), 2006, pp.767-778.

Pavement Interactive. *Roughness.* Retrieved from: http://www.pavementinteractive.org/roughness. Accessed April 15, 2017.

Pavement Interactive. *Equivalent Single Axle Load.* Retrieved from: http://www.pavementinteractive.org/equivalent-single-axle-load. Accessed May 14, 2017.

RStudio: Integrated Development for R. RStudio, Inc., RStudio Team, Boston, 2015.

Sathaye, N. and Madanat, S. A Bottom-Up Optimal Pavement Resurfacing Solution Approach for Large-Scale Networks. *Transportation Research Part B: Methodological*, 46(4), 2012, pp.520-528.

Sathaye, N. and Madanat, S. A Bottom-Up Solution for the Multi-Facility Optimal Pavement Resurfacing Problem. *Transportation Research Part B: Methodological*, 45(7), 2011, pp.1004-1017

Sayers, M.W. Two quarter-car models for defining road roughness: IRI and HRI. *Transportation Research Record*, (1215), 1989.

Sayers, M.W., Gillespie, T.D. and Paterson, W.D. *Guidelines for Conducting and Calibrating Road Roughness Measurements.* The World Bank, Washington, D.C., No., 1986.

State of California Business, Transportation and Housing Agency Department of Transportation. *2015 Contract Cost Data.* A Summary of Cost by Items for Highway Construction Projects, 2015.

State of California Department of Transportation Division of Maintenance Pavement Program (Calstrans). *Life-Cycle Cost Analysis Procedures Manual*, 2013.

Stripple, H. Life Cycle Assessment of Road. *A Pilot Study for Inventory Analysis. 2nd Revised Edition. Report from the IVL Swedish Environmental Research Institute*, *96*, 2001.

Stroup-Gardiner, M. and Shatnawi, S. January. *The Economics of Flexible Pavement Preservation.* In CD-ROM, 88th Annual Meeting of the Transportation Board, Washington, DC, 2009.

Tighe, S., Li, N., Falls, L. and Haas, R. Incorporating Road Safety Into Pavement Management. *Transportation Research Record: Journal of the Transportation Research Board*, (1699), 2000, pp.1-10.

TRIP. *Hold the Wheel Steady : Bumpy Roads Ahead: America's Roughest Rides and Strategies to Make our Roads Smoother*. A National Transportation Research Group. Washington, DC, 2015.

Tsunokawa, K. and Schofer, J.L. Trend Curve Optimal Control Model for Highway Pavement Maintenance: Case Study and Evaluation. *Transportation Research Part A: Policy and Practice,* 28(2), 1994, pp.151-166.

U.S. Energy Information Administration (EIA). *Annual Energy Outlook 2015 with Projections to 2040.* Report DOE/EIA-0383(2015), 2015.

Wang, T., Harvey, J., Kendall, A. and University of California (System). Network-Level Life-Cycle Energy Consumption and Greenhouse Gas from CAPM Treatments. *Pavement Research Center*, 2013, No. CA16-2376A.

Zapata, P. and Gambatese, J.A. Energy Consumption of Asphalt and Reinforced Concrete Pavement Materials and Construction. *Journal of Infrastructure Systems*, 11(1), 2005, pp.9-20.

Zhang, H., Keoleian, G.A., Lepech, M.D. and Kendall, A. Life-Cycle Optimization of Pavement Overlay Systems. *Journal of infrastructure systems*, 16(4), 2010, pp.310-322.

Zhang, H., Lepech, M.D., Keoleian, G.A., Qian, S. and Li, V.C. Dynamic Life-Cycle Modeling of Pavement Overlay Systems: Capturing the Impacts of Users, Construction, and Roadway Deterioration. *Journal of Infrastructure Systems*, 16(4), 2009, pp.299-309.

4. CHAPTER 4 – CONCLUSION

Due to a general reduction in pavement program funding levels over the past decade, optimal pavement maintenance and rehabilitation strategies should be developed for the available budget levels. Using RAP in asphalt pavements can reduce pavement life cycle costs and save more resources for roadway treatments. However, careful considerations are required in RAP mixture design since mixtures with high RAP contents are susceptible to cracking.

In this thesis, Chapter 2 investigated the effects of binder-grade bumping and high virgin binder contents on rutting and cracking performance of asphalt mixtures with high amounts of RAP. To evaluate rutting and cracking performance of asphalt mixtures with two RAP contents (30% and 40%), three binder contents (6%, 6.4%, and 6.8%), and three virgin binder grades (PG 58-34, PG 64-22, and PG 76-22), SCB, DM, and FN tests were conducted. Only the asphalt mixture with 40% RAP content, 6.8% binder content, and PG 64-22 showed high cracking and rutting performance. This study found that flexibility index (FI) is a promising indicator of asphalt mixtures' cracking performance. Therefore, SCB test is suggested to evaluate the cracking performance of asphalt mixtures. Also, regression models correlating FI and FN (dependent variables) with RAP content, binder content, and binder grade were developed (independent variables), and possible combinations of the independent variables to produce asphalt mixtures with high cracking and rutting performance were suggested.

Chapter 3 evaluated the impacts of developing a network-level decision-making tool and selecting the most efficient pavement maintenance and rehabilitation strategies on agency costs and user benefits. Different treatment methods (1. Considering one value for trigger IRI for all the sections regardless of the traffic levels, and 2. Considering different trigger IRIs for sections based on their traffic levels) were compared, and optimal trigger IRI were determined for different budget levels. Finally, developed decision-making tool was integrated with GIS to provide the ability for agencies to import LTPP road section data and the tool's MATLAB results into the GIS environment and visually illustrate roadway sections with highest maintenance priority.

Implementation of the developed decision-making tool, along with the use of high-performance asphalt pavements with high RAP contents, are expected to reduce agency costs, increase user benefits, and enhance drivers' safety. Integration of the decision-making tool to GIS will facilitate stakeholders to visually pinpoint where particular sections are and which sections should be maintained.

5. BIBLIOGRAPHY

AASHTO PP 60-14. *Standard Practice for Preparation of Cylindrical Performance Test Specimens Using the Superpave Gyratory Compactor.* Washington, DC: American Association of State and Highway Transportation Officials, 2014.

AASHTO PP 61-13. *Standard Practice for Developing Dynamic Modulus Master Curves for Hot Mix Asphalt (HMA) Using the Asphalt Mixture Performance Tester (AMPT).* Washington, DC: American Association of State and Highway Transportation Officials, 2013.

AASHTO R 30-10. *Standard Practice for Mixture Conditioning of Hot Mix Asphalt (HMA).* Washington, DC: American Association of State and Highway Transportation Officials, 2010.

AASHTO R 43-07. *Standard Practice for Quantifying Roughness of Pavements*. Washington, DC: American Association of State and Highway Transportation Officials, 2013.

AASHTO T 166-12. *Bulk Specific Gravity (Gmb) of Compacted Hot Mix Asphalt (HMA) using Saturated Surface-Dry Specimens.* Washington, DC: American Association of State Highway and Transportation Officials, 2012.

AASHTO T 209-12. *Theoretical Maximum Specific Gravity (Gmm) and Density of Hot Mix Asphalt.* Washington, DC: American Association of State Highway and Transportation Officials, 2012.

AASHTO T 27-11. *Standard Method of Test for Sieve Analysis of Fine and Coarse Aggregates.* Washington, DC: American Association of State Highway and Transportation Officials, 2011.

AASHTO T 30-10. *Standard Method of Test for Mechanical Analysis of Extracted Aggregate.* Washington, DC: American Association of State Highway and Transportation Officials, 2010.

AASHTO T 308-10. *Determining the Asphalt Binder Content of Hot Mix Asphalt (HMA) by the Ignition Method.* Washington, DC: American Association of State and Highway Transportation Officials, 2010.

AASHTO T 312-12. *Preparing and Determining the Density of Hot Mix Asphalt (HMA) Specimens by Means of the Superpave Gyratory Compactor.* Washington, DC: American Association of State Highway and Transportation Officials, 2012.

AASHTO T 316-11. *Viscosity Determination of Asphalt Binder Using Rotational Viscometer.* Washington, DC: American Association of State and Highway Transportation Officials, 2011.

AASHTO T 321–07. *Standard Method of Test for Determining the Fatigue Life of Compacted Hot-Mix Asphalt (HMA) Subjected to Repeated Flexural Bending*. Washington, DC: American Association of State and Highway Transportation Officials, 2007.

AASHTO TP 105-13. *Standard Method for Determining the Fracture Energy of Asphalt Mixtures Using the Semi Circular Bend Geometry (SCB)*. Washington, DC: American Association of State Highway and Transportation Officials, 2013.

AASHTO TP 79-13. *Standard Method for Determining the Dynamic Modulus and Flow Number for Hot Mix Asphalt (HMA) Using the Asphalt Mixture Performance Tester (AMPT).* Washington, DC: American Association of State and Highway Transportation Officials*,* 2013.

AASHTOWare-Pavement ME Design 1.0™. American Association of State Highway and Transportation Officials (AASHTO), 2008.

Aguiar-Moya, J., F. Hong, J. Prozzi. RAP: Save Today, Pay Later? Proceedings 90th Annual Meeting of the Transportation Research Board, Washington D.C, 2011.

Ahmed, U. *Passenger Car Equivalent Factors for Level Freeway Segments Operating Under Moderate and Congested Conditions.* Dissertations, Theses, and Professional Projects*,* 2010.

Al-Omari, B. and Darter, M.I. Relationships between International Roughness Index and Present Serviceability Rating. *Transportation Research Record: Journal of the Transportation Research Board*, 1435(2), 1994.

Al-Qadi, I. L., and Ozer, H. Impact of RAS and RAP on Asphalt Mixtures' Fracture: The Need for a Cracking Potential Index. Illinois Center for Transportation University of Illinois at Urbana-Champaign, 2015.

Al-Qadi, I. L., Ozer, H., Lambros, J., El Khatib, A., Singhvi, P., Khan, T., Rivera-Perez, J. and Doll, B. *Testing Protocols to Ensure Performance of High Asphalt Binder Replacement Mixes Using RAP and RAS*. Publication FHWA-ICT-15-017. Illinois Center for Transportation/Illinois Department of Transportation, 2015.

Anastasopoulos, P.C., Tarko, A.P. and Mannering, F.L. Tobit Analysis of Vehicle Accident Rates on Interstate Highways. *Accident Analysis & Prevention*, 40(2), 2008, pp.768-775.

Andreen, B., H. Rocheville, K. Ksaibati. A Method of Cost-Benefit Analysis of RAP in Various Highway Applications. Proceedings 91st Annual Meeting of the Transportation Research Board, Washington D.C., 2012.

Asphalt Institute Technical Advisory Committee. *Determining Laboratory Mixing and Compaction Temperatures*, 2016.

Aurangzeb, Q., I. Al-Qadi, I. Abuawad, W. Pine, and J. Trepanier. Achieving Desired Volumetrics and Performance for Mixtures with High Percentage of Reclaimed Asphalt Pavement. *Transportation Research Record: Journal of the Transportation Research Board*, No. 2294, 2012, pp.34-42.

Aurangzeb, Q., I. L. Al-Qadi, H. Ozer, R. Yang. Hybrid Life Cycle Assessment for Asphalt Mixtures with High RAP Content. *Journal of Resources, Conservation and Recycling*, 2013.

Barnes, G. and Langworthy, P. Per Mile Costs of Operating Automobiles and Trucks. *Transportation Research Record: Journal of the Transportation Research Board*, (1864), 2004, pp.71-77.

Bennert, T., J. Daniel, and W. Mogawer. Strategies for Incorporating Higher Recycled Asphalt Pavement Percentages: Review of Implementation Trials in Northeast States. *Transportation Research Record: Journal of the Transportation Research Board*, No. 2445, 2014, pp. 83-93.

Bennett, C.R. and Greenwood, I.D. Volume 5: HDM-4 Calibration Reference Manual. *ISOHDM World Road Association (PIARC),* 2003, pp.174-181.

Berkeley Lab, Energy End-Use Forecasting Group, Retrieved form: http://enduse.lbl.gov/http://enduse.lbl.gov/, enduse.lbl.gov/Info/pavements_LCCA_web.xls. Accessed February 14, 2017.

Bester, C.J. January. The Effect of Road Roughness on Safety. In 82nd Annual Meeting of the Transportation Research Board, Washington, DC, 2003.

Biligiri, K., Kaloush, K., Mamlouk, M. and Witczak, M. Rational Modeling of Tertiary Flow for Asphalt Mixtures. *Transportation Research Record: Journal of the Transportation Research Board* 2001, 2007, pp.63-72.

Bonaquist, R.F. *Precision of the Dynamic Modulus and Flow Number Tests Conducted with the Asphalt Mixture Performance Tester*. NCHRP Report, No. 702, National Cooperative Highway Research Program, Washington D.C., 2011.

Bonaquist, R.F., Christensen, D.W. and Stump, W. *Simple Performance Tester for Superpave Mix Design: First-Article Development and Evaluation.* Transportation Research Board, 2003, Vol. 513.

Carpenter, S.H. and J. R. Wolosick. Modifier Influence in the Characterization of Hot-Mix Recycled Material. *Transportation Research Record: Journal of the Transportation Research Board*, 1980, No. 777, pp.15-22.

Carvalho, R., H. Shirazi, M. Ayres Jr, and O. Selezneva. Performance of Recycled Hot-Mix Asphalt Overlays in Rehabilitation of Flexible Pavements. *Transportation Research Record: Journal of the Transportation Research Board*, 2010, No. 2155, pp.55-62.

Chatti, K., and I. Zaabar. Estimating the Effects of Pavement Condition on Vehicle Operating Costs. *Publication NCHRP Report 720. National Cooperative Highway Research Program, Transportation Research Board,* 2012.

Chehovits, J. and Galehouse, L. Energy Usage and Greenhouse Gas Emissions of Pavement Preservation Processes for Asphalt Concrete Pavements. In *Compendium of Papers from the First International Conference on Pavement Preservation,* 2010, pp. 27-41.

Coleri, E. Adjusting Asphalt Mixes for Increased Durability and Implementation of a Performance Tester to Evaluate Fatigue Cracking of Asphalt Concrete. ODOT Research Project Progress Presentation. 04/17/2017, Salem Oregon.

Copeland, A. *Reclaimed Asphalt Pavement in Asphalt Mixtures: State of the Practice*. Federal Highway Administration, No. FHWA-HRT-11-021, 2011.

Darnell Jr, J. and Bell, C.A. *Performance Based Selection of RAP/RAS in Asphalt Mixtures*. Federal Highway Administration, No. FHWA-OR-RD-16-08, 2015.

Dongré, R., D'Angelo, J. and Copeland, A. Refinement of Flow Number as Determined by Asphalt Mixture Performance Tester: Use in Routine Quality Control—Quality Assurance Practice. *Transportation Research Record: Journal of the Transportation Research Board,* (2127), 2009, pp.127-136.

EAPA. *Environmental Impacts and Fuel Efficiency of Road Pavements*. EAPA & Eurobitume Industry Report, 2004.

Francken, L. Pavement Deformation Law of Bituminous Road Mixes in Repeated Load Triaxial Compression. Presented at Fourth International Conference on the Structural Design of Asphalt Pavements, University of Michigan, Ann Arbor, 1977.

Guo, X.X., Zhou, B.W. and Zhang, C. Analysis of Rutting Index for Pavement Maintenance Based on Driving Safety on Surface Gathered Water Consideration. In CICTP 2014: *Safe, Smart, and Sustainable Multimodal Transportation Systems*, 2014, pp. 909-918.

Hajj, E.Y., P. E. Sebaaly, and R. Shrestha. Laboratory Evaluation of Mixes Containing Recycled Asphalt Pavement (RAP). *Road Materials and Pavement Design*, 2009, 10(3), 495-517.

Hansen, K. R. and A. Copeland. Asphalt Pavement Industry Survey on Recycled Materials and Warm Mix Asphalt Usage (5th ed). Lanham, MD: *National Asphalt Pavement Association (NAPA)*, 2014.

Harvey, J., Kendall, A., Lee, I.S., Santero, N., Dam, T.V. and Wang, T. Pavement Life Cycle Assessment Workshop: Discussion Summary and Guidelines. *University of California Pavement Research Center, California,* 2010.

Harvey, J., Liu, A., Zhou, J., Signore, M., Coleri, E. and HE, Y. *Superpave Implementation Phase II: Comparison of Performance-Related Test Results.* UCPRC Research Report No: UCPRC-RR-2015-01, 2014.

Hendrickson, C.; Lave, L. B.; Matthews, H. S. *Environmental Life Cycle Assessment of Goods and Services - An Input-Output Approach.* Resources for the Future: Washington, DC, 2006.

Hossain, M., Musty, H.Y. and Sabahfer, N. Use of High-Volume Reclaimed Asphalt Pavement (RAP) for Asphalt Pavement Rehabilitation Due to Increased Highway Truck Traffic from Freight Transportation. *Final Reports & Technical Briefs from Mid-America Transportation Center*, 2012.

Islam, S. and Buttlar, W. Effect of Pavement Roughness on User Costs. *Transportation Research Record: Journal of the Transportation Research Board,* (2285), 2012, pp.47-55.

Lee, N., C. Chou, K. Chen. Benefits in Energy Savings and CO2 Reduction by Using RAP. Proceedings 91st Annual Meeting of the Transportation Research Board, Washington D.C., 2012.

Li, X., M. O. Marasteanu, R. C. Williams, and T. R. Clyne. Effect of Reclaimed Asphalt Pavement (Proportion and Type) and Binder Grade on Asphalt Mixtures. *Transportation Research Record: Journal of the Transportation Research Board*, 2008, No.2051, pp.90–97.

Li, Y. and Madanat, S. A Steady-State Solution for the Optimal Pavement Resurfacing Problem. *Transportation Research Part A: Policy and Practice,* 36(6), 2002, pp.525-535.

LTPP InfoPave. *Long-Term Pavement Performance.* Retrieved from: https://infopave.fhwa.dot.gov. Accessed September 15, 2016.

Mack, J.W., Gregory, J. and Kirchain, R., Developing Robust Rehabilitation Scenario Profiles for Life Cycle Assessment Using Decision Tree Analysis. Pavement LCA 2014, International Symposium on Pavement Life Cycle Assessment, 2014.

Madanat, S., Horvath, A. and Reger, D. Integration of LCA into Pavement Management Systems, Presented at University of California Pavement Research Center, 2014.

Mallick, R. B., P. S. Kandhal, and R. L. Bradbury. Using Warm-Mix Asphalt Technology to Incorporate High Percentage of Reclaimed Asphalt Pavement Material in Asphalt Mixtures. *Transportation Research Record: Journal of the Transportation Research Board*, 2008, No. 2051, pp.71–79.

MATLAB R2016b: MATLAB and Statistics Toolbox. The MathWorks, Inc., Natick, Massachusetts, United States, 2016.

Mbwana, J.R. A Framework for Developing Stochastic Multi-Objective Pavement Management Systems. In *First Road Transportation Technology Transfer Conference in Africa 2001,* 2001, pp. 350-363.

McDaniel, R., and R. M. Anderson. NCHRP Web Document 30: Recommended Use of Reclaimed Asphalt Pavement in the Superpave Mix Design Method–Project 9-12. *Final Report*, 2001.

Merton, R. E. An Analytic Derivation of the Efficient Portfolio Frontier. *Journal of Financial and Quantitative Analysis 7*, 1972, 1851-72.

Mitchell, T. *Westrack Track Roughness, Fuel Consumption and Maintenance Cost*. Federal Highway Administration, FHWA-RD-00-052. U.S. Department of Transportation, 2000.

Mohammad, L. N., B. Samuel, Cooper Jr, and A. E. Mostafa. Characterization of HMA Mixtures Containing High Reclaimed Asphalt Pavement Content with Crumb Rubber Additives. *Journal of Materials in Civil Engineering* 23, No. 11, 2011, pp.1560-1568.

Newcomb, D. E., E. R. Brown, and J. A. Epps. *Designing HMA Mixtures with High RAP Content: A Practical Guide.* National Asphalt Pavement Association (NAPA), 2007.

Newcomb, D. *Thin Asphalt Overlays for Pavement Preservation.* National Asphalt Pavement Association (NAPA). Information Series 135, 2009.

Norouzi, A., Kim, D. and Kim, Y.R. Numerical Evaluation of Pavement Design Parameters for the Fatigue Cracking and Rutting Performance of Asphalt Pavements. *Materials and Structures*, 49(9), 2016, pp.3619-3634.

North Carolina Department of Transportation (2014). *Guidance for Determining Contract Times*, 2014.

Nsengiyumva, G. Development of Semi-Circular Bending (SCB) Fracture Test for Bituminous Mixtures, 2015.

ODOT TM 319. *Preparation and Characterization of Recycled Asphalt Materials for Mix Design*, Oregon Department of Transportation, undated.

Oliveira, J. R., H. M. Silva, C. M. Jesus, L. P. Abreu, and S. R. Fernandes. Pushing the Asphalt Recycling Technology to the Limit. *International Journal of Pavement Research and Technology*, 6(2), 2013, pp.109.

Oregon Department of Transportation, *2012 Pavement Condition Report.* Pavement Services Unit, 2013.

Ouyang, Y. and Madanat, S. An Analytical Solution for the Finite-Horizon Pavement Resurfacing Planning Problem. *Transportation Research Part B: Methodological,* 40(9), 2006, pp.767-778.

Ozer, H., Al-Qadi, I. L., Lambros, J., El-Khatib, A., Singhvi, P., & Doll, B. Development of the Fracture-Based Flexibility Index tor Asphalt Concrete Cracking Potential Using Modified Semi-Circle Bending Test Parameters. *Construction and Building Materials*, 115, 2016, 390–401

Paul, H. R. Evaluation of Recycled Projects for Performance. *Asphalt Paving Technology*, 1996, No. 65, pp.231-254.

Pavement Interactive. *Roughness.* Retrieved from: http://www.pavementinteractive.org/roughness. Accessed April 15, 2017.

Pavement Interactive. *Bulk Specific Gravity.* Retrieved from: http://www.pavementinteractive.org/bulk-specific-gravity. Accessed May 14, 2017.

Pavement Interactive. *Equivalent Single Axle Load.* Retrieved from: http://www.pavementinteractive.org/equivalent-single-axle-load. Accessed May 14, 2017.

Petersen, J. C. Chemical Composition of Asphalt as Related to Asphalt Durability: State of the Art. *Transportation Research Record: Journal of the Transportation Research Board*, 1984, No.999.

Roberts, F. L., P. S. Kandhal, E. R. Brown, D. Y. Lee, and T. W. Kennedy. Hot Mix Asphalt Materials, Mixture Design and Construction. *National Asphalt Pavement Association Research and Education Foundation*, Lanham, MD., 1996.

Rodezno, M.C., West, R. and Taylor, A. Flow Number Test and Assessment of AASHTO TP 79-13 Rutting Criteria: Comparison of Rutting Performance of Hot-Mix and Warm-Mix Asphalt Mixtures. *Transportation Research Record: Journal of the Transportation Research Board,* (2507), 2015, pp.100-107.

RStudio: Integrated Development for R. RStudio, Inc., RStudio Team, Boston, 2015.

Santero, N.J., Masanet, E., and Horvath, A. Life-Cycle Assessment of Pavements. Part I: Critical Review. *Resources, Conservation and Recycling,* 55(9), 2011, pp.801-809.

Sathaye, N. and Madanat, S. A Bottom-Up Optimal Pavement Resurfacing Solution Approach for Large-Scale Networks. *Transportation Research Part B: Methodological*, 46(4), 2012, pp.520-528.

Sathaye, N. and Madanat, S. A Bottom-Up Solution for the Multi-Facility Optimal Pavement Resurfacing Problem. *Transportation Research Part B: Methodological*, 45(7), 2011, pp.1004-1017.

Sayers, M.W. Two quarter-car models for defining road roughness: IRI and HRI. *Transportation Research Record*, (1215), 1989.

Sayers, M.W., Gillespie, T.D. and Paterson, W.D. *Guidelines for Conducting and Calibrating Road Roughness Measurements.* The World Bank, Washington, D.C., No., 1986.

Seber, G.A.F. *Linear Regression Analysis*, John Wiley & Sons, 1977.

Sha, Q.L. *Premature damage and its preservative measures of bituminous pavement on expressway.* Beijing: China Communications Press, 2008.

Shen, J., S. Amirkhanian, and J. Aune Miller, J. Effects of Rejuvenating Agents on Superpave Mixtures Containing Reclaimed Asphalt Pavement. *Journal of Materials in Civil Engineering*, 19(5), 2007, pp.376–384.

State of California Business, Transportation and Housing Agency Department of Transportation. *2015 Contract Cost Data.* A Summary of Cost by Items for Highway Construction Projects, 2015.

State of California Department of Transportation Division of Maintenance Pavement Program (Calstrans). *Life-Cycle Cost Analysis Procedures Manual*, 2013.

Stripple, H. Life Cycle Assessment of Road. *A Pilot Study for Inventory Analysis. 2nd Revised Edition. Report from the IVL Swedish Environmental Research Institute*, *96*, 2001.

Stroup-Gardiner, M. and Shatnawi, S. January. *The Economics of Flexible Pavement Preservation.* In CD-ROM, 88th Annual Meeting of the Transportation Board, Washington, DC, 2009.

Tao, M., and R. Mallick. Effects of Warm-Mix Asphalt Additives on Workability and Mechanical Properties of Reclaimed Asphalt Pavement Material. *Transportation Research Record: Journal of the Transportation Research Board*, No. 2126, 2009, pp.151-160.

Terrel, R. L., and J. A. Epps. *Using Additives and Modifiers in Hot Mix Asphalt.* National Asphalt Pavement Association (NAPA), Section A No. QIP-114A. 1989.

Tighe, S., Li, N., Falls, L. and Haas, R. Incorporating Road Safety Into Pavement Management. *Transportation Research Record: Journal of the Transportation Research Board*, (1699), 2000, pp.1-10.

Tran, N., A. Taylor, and R. Willis. *Effect of Rejuvenator on Performance Properties of HMA Mixtures with High RAP and RAS Contents.* National Center for Asphalt Technology, NCAT Report 12–05, June 2012.

TRIP. *Hold the Wheel Steady : Bumpy Roads Ahead: America's Roughest Rides and Strategies to Make our Roads Smoother*. A National Transportation Research Group. Washington, DC, 2015.

Tsunokawa, K. and Schofer, J.L. Trend Curve Optimal Control Model for Highway Pavement Maintenance: Case Study and Evaluation. *Transportation Research Part A: Policy and Practice,* 28(2), 1994, pp.151-166.

U.S. Energy Information Administration (EIA). *Annual Energy Outlook 2015 with Projections to 2040.* Report DOE/EIA-0383(2015), 2015.

University of California (UC). International Symposium on Pavement LCA 2014, 2014. Retrieved from Summary Review Session (Day 3): http://www.ucprc.ucdavis.edu/p-lca2014/ProgramBreakouts.aspx

Wang, T., Harvey, J., Kendall, A. and University of California (System). Network-Level Life-Cycle Energy Consumption and Greenhouse Gas from CAPM Treatments. *Pavement Research Center*, 2013, No. CA16-2376A.

West, R., A. Kvasnak, N. Tran, B. Powell, and P. Turner. Testing of Moderate and High Reclaimed Asphalt Pavement Content Mixes: Laboratory and Accelerated Field Performance Testing at the National Center for Asphalt Technology Test Track. *Transportation Research Record: Journal of the Transportation Research Board*, No. 2126, 2009, 100-108.

West, R., et al. *Phase IV NCAT Pavement Test Track Findings.* Auburn, AL: National Center for Asphalt Technology, Report Number NCAT 12-10, 2012.

West, R., J. Michael, R. Turochy, and S. Maghsoodloo. Use of Data from Specific Pavement Studies Experiment 5 in the Long-Term Pavement Performance Program to Compare Virgin and Recycled Asphalt Pavements. *Transportation Research Record: Journal of the Transportation Research Board*, No. 2208, 2011, pp.82-89.

Williams, R. S., and R. Shaidur. *Premature Asphalt Concrete Pavement Cracking.* SPR 734, Final Report for Oregon Department of Transportation, Salem, Oregon, 2015.

Willis, J. R. Effect of Recycled Materials on Pavement Life-cycle Assessment: A Case Study. Proceedings 94th Annual Meeting of the Transportation Research Board, Washington D.C, 2015.

Willis, J. R., P. Turner, G. Julian, A. J. Taylor, N. Tran, and F. Padula. *Effects of Changing Virgin Binder Grade and Content on RAP Mixture Properties*. National Center for Asphalt Technology Report, (12-03), 2012.

World Highways. *Recycling Asphalt Provides Green Result*. 2013. Retrieved from http://www.worldhighways.com/categories/materials-production-supply/features/recycling-asphalt-provides-green-result. Accessed October 15, 2015.

Wu, Z., Mohammad, L.N., Wang, L.B. and Mull, M.A. Fracture Resistance Characterization of Superpave Mixtures Using the Semi-Circular Bending Test. *Journal of ASTM International,* 2(3), 2005, pp.1-15.

Xiao, F., S. Amirkhanian, and C. H. Juang. Rutting Resistance of Rubberized Asphalt Concrete Pavements Containing Reclaimed Asphalt Pavement Mixtures. *Journal of Materials in Civil Engineering*, 19(6), 2007, pp.475–483.

Xiao, F., S. N. Amirkhanian, J. Shen, and B. Putman. Influences of Crumb Rubber Size and Type on Reclaimed Asphalt Pavement (RAP) Mixtures. *Construction and Building Materials*, *23*(2), 2009, pp.1028-1034.

Zapata, P. and Gambatese, J.A. Energy Consumption of Asphalt and Reinforced Concrete Pavement Materials and Construction. *Journal of Infrastructure Systems*, 11(1), 2005, pp.9-20.

Zaumanis, M., R. Mallick, and R. Frank. Evaluation of Rejuvenator's Effectiveness with Conventional Mix Testing for 100 % Reclaimed Asphalt Pavement Mixtures. *Transportation Research Record: Journal of the Transportation Research Board*, No. 2370, 2013, pp.17–25.

Zhang, H., Keoleian, G.A., Lepech, M.D. and Kendall, A. Life-Cycle Optimization of Pavement Overlay Systems. *Journal of infrastructure systems*, 16(4), 2010, pp.310-322.

Zhang, H., Lepech, M.D., Keoleian, G.A., Qian, S. and Li, V.C. Dynamic Life-Cycle Modeling of Pavement Overlay Systems: Capturing the Impacts of Users, Construction, and Roadway Deterioration. *Journal of Infrastructure Systems*, 16(4), 2009, pp.299-309.

Zhao, S., B. Huang, X. Shu, X. Jia, and M. Woods. Laboratory Performance Evaluation of Warm-Mix Asphalt Containing High Percentages of Reclaimed Asphalt Pavement. *Transportation Research Record: Journal of the Transportation Research Board*, No. 2294, 2012, pp.98-105.

Zhou, F., S. Im, D. Morton, R. Lee, S. Hu, and T. Scullion. Rejuvenator Characterization, Blend Characteristics, and Proposed Mix Design Method. *Association of Asphalt Paving Technologists,* 2015.

APPENDICES

APPENDIX A: GRADATION AND BINDER CONTENT OF RAP

This section represents the gradation, binder content, and theoretical maximum specific gravity (G_{mm}) of RAP materials provided by ODOT. The RAP was provided by Old Castle for this study.

GRADATION OF RAP WORKSHEET

Project Name:
Mix Type:
Seperated Size:

Contract # :
Date : 10/28/15

Sample : 1

Mass Initial Dry: 1633.4
Mass Before Sieve: 1498.9

Sieve	Mass Ret.	% Ret.	%Pass
3/4	0	0	100
1/2	32	2.0	98.0
3/8	158.3	9.7	88.3
1/4	286.6	17.5	70.8
No. 4	155	9.5	61.3
No. 8	281.1	17.2	44.1
No. 16	213.2	13.1	31.1
No. 30	124.3	7.6	23.4
No. 50	104.1	6.4	17.1
No. 100	68.3	4.2	12.9
No. 200	54.5	3.3	9.6
Pan	21.1		
Mass After	1498.5	Sieve Dev.	0.0

Sample : 2

Mass Initial Dry: 1633.5
Mass Before Sieve: 1503.8

Sieve	Mass Ret.	% Ret.	%Pass
3/4	0	0	100
1/2	38.7	2.4	97.6
3/8	165	10.1	87.5
1/4	302.7	18.5	69.0
No. 4	143.7	8.8	60.2
No. 8	288.7	17.7	42.5
No. 16	203.1	12.4	30.1
No. 30	128.3	7.9	22.2
No. 50	93.5	5.7	16.5
No. 100	66.5	4.1	12.4
No. 200	53.2	3.3	9.2
Pan	18.9		
Mass After	1502.3	Sieve Dev.	0.1

Sample : 3

Mass Initial Dry: 1628.5
Mass Before Sieve: 1483.2

Sieve	Mass Ret.	% Ret.	%Pass
3/4	0	0	100
1/2	19.4	1.2	98.8
3/8	180.2	11.1	87.7
1/4	239.4	14.7	73.0
No. 4	149.3	9.2	63.9
No. 8	279.5	17.2	46.7
No. 16	213.5	13.1	33.6
No. 30	129.3	7.9	25.7
No. 50	113.1	6.9	18.7
No. 100	78	4.8	13.9
No. 200	60.6	3.7	10.2
Pan	20.5		
Mass After	1482.8	Sieve Dev.	0.0

Sample : 4

Mass Initial Dry: 1627.5
Mass Before Sieve: 1496.4

Sieve	Mass Ret.	% Ret.	%Pass
3/4	0	0	100
1/2	24.4	1.5	98.5
3/8	125.8	7.7	90.8
1/4	253.7	15.6	75.2
No. 4	156.1	9.6	65.6
No. 8	298.1	18.3	47.3
No. 16	222.8	13.7	33.6
No. 30	144.8	8.9	24.7
No. 50	105.6	6.5	18.2
No. 100	77.2	4.7	13.5
No. 200	62.7	3.9	9.6
Pan	24.8		
Mass After	1496	Sieve Dev.	0.0

Sample : 5

Mass Initial Dry: 1637.8
Mass Before Sieve: 1515.5

Sieve	Mass Ret.	% Ret.	%Pass
3/4	0	0	100
1/2	24.2	1.5	98.5
3/8	186.4	11.4	87.1
1/4	305	18.6	68.5
No. 4	165.8	10.1	58.4
No. 8	300.4	18.3	40.1
No. 16	209	12.8	27.3
No. 30	111	6.8	20.5
No. 50	87	5.3	15.2
No. 100	57.5	3.5	11.7
No. 200	51	3.1	8.6
Pan	17.5		
Mass After	1514.8	Sieve Dev.	0.0

DESIGN AVERAGE

Sieve	Percent Passing
3/4	100
1/2	98.3
3/8	88.3
1/4	71.3
No. 4	61.9
No. 8	44.1
No. 16	31.1
No. 30	23.3
No. 50	17.1
No. 100	12.9
No. 200	8.4

Figure A 1. RAP aggregate gradation

PROJECT	2016 RAP	MIX CLASS	
CONTRACT NO.		LEVEL (2,3,4)	
MIX PRODUCER		PROJECT MANAGER	
CMDT (print)		CMDT JMF MIX ID NO	

RAP WORKSHEET

Separated Size	1/2" - 0	G_b	1.026

AASHTO T-209: Theoretical Maximum Specific Gravity

Sample	1	2	3
Mass of Dry RAP (R_{hot})	1746.8	1794.2	1744.7
Mass of Added Binder ($Binder_{new}$)	52.4	53.8	52.3
$P_{b\text{-}new}$, %	2.912	2.911	2.910
Mass of Coated Sample (C)	1800.5	1849.3	1795.3
Actual Dry Mass Uncoated Sample (A)	1748.1	1795.5	1743.0
Actual Mass of Added Binder (C-A)	52.4	53.8	52.3
Mass @ SSD	1803.8	1853.6	1800.5
Pycnometer + Water	7391.5	7391.5	7391.5
Pycnometer + Water + Mix	8433.2	8462.0	8434.7
RAP G_{mm} SSD	2.459	2.457	2.468

Asphalt Content of RAP

Sample	1	2	3	4	5	
Basket Tare	3044.9	3046.2	3043.7	3045.7	3043.3	
Mass of Coated RAP + Basket	4794.4	4795.8	4793.1	4795.1	4793.7	
Mass of Agg and Basket	4678.3	4679.7	4672.2	4673.2	4681.1	
Mass Initial, M_i	1749.5	1749.6	1749.4	1749.4	1750.4	
Mass Final, M_f	1633.4	1633.5	1628.5	1627.5	1637.8	
$\%I = \{[M_i - M_f]/[M_i]\}x100$	6.64	6.64	6.91	6.97	6.43	Average
Corrected P_b, C_f = 0.50	6.14	6.14	6.41	6.47	5.93	6.22
					RAP Gse	2.713

AASHTO T-85: Specific Gravity and Absorption of Coarse Aggregate

Size	+ #4		Average
Source	Various		
A) Mass of Dry Sample	2013.7	2039.5	
B) Mass of SSD Sample	2055.4	2083.5	
C) Mass of Sample Immersed	1282.3	1295.7	
Bulk Specific Gravity (G_{sb})	2.605	2.589	2.597
Bulk Specific Gravity (SSD)	2.659	2.645	2.652
Apparent Specific Gravity (G_{sa})	2.753	2.742	2.748
Absorption (%)	2.07	2.16	2.11

Combined Specific Gravity
T-84 & T-85

Size	1/2"-0
Split Sieve	#4
Percent Retained Split Sieve	38.1
Burnt Bulk Specific Gravity (G_{sb})	2.611
Burnt Bulk Specific Gravity (SSD)	2.662
Burnt Apparent Specific Gravity	2.753
Absorption (%)	2.0

AASHTO T-84: Specific Gravity and Absorption of Fine Aggregate

Size	- #4		Average
Source	Various		
S) Mass of SSD Sample	500.0	500.0	
B) Mass of Pyc. + Water	658.9	654.2	
C) Mass of Pyc.+H2O+Sample	971.5	966.9	
Mass of Dry Sample + Pan			
Mass of Pan			
A) Mass of Dry Sample	490.8	490.6	
Bulk Specific Gravity (G_{sb})	2.619	2.619	2.619
Bulk Specific Gravity (SSD)	2.668	2.670	2.669
Apparent Specific Gravity (G_{sa})	2.754	2.758	2.756
Absorption (%)	1.87	1.92	1.9

Combined RAP Specific Gravity
ODOT TM-319

RAP G_{sb}	2.636
RAP G_{sa}	2.766

Certified Technician and Card Number:

Figure A 2. Binder content and theoretical maximum specific gravity (G_{mm}) of RAP

APPENDIX B: TEMPERATURE CURVES FOR VIRGIN BINDERS

The data below represents binder temperature curves used for this study. All temperature curves were provided by McCall Oil.

Table B 1. Mixing and compaction temperatures of PG 76-22 binder

Binder	**PG 76-22**
Temp (F)	Viscosity (cp)
275	**768**
329	**250**

Mixing Temperature Range, F	345 - 359
Compaction Temperature Range, F	318 - 329

Specific Gravity@ 60F	**1.0377**

Table B 2. Mixing and compaction temperatures of PG 64-22 binder

Binder	**PG 64-22**
Temp (F)	Viscosity (cp)
275	**363**
329	**113**

Mixing Temperature Range, F	303 - 314
Compaction Temperature Range, F	281 - 291

Specific Gravity@ 60F	**1.0306**

Table B 3. Mixing and compaction temperatures of PG 58-34 binder

Binder	**PG 58-34**
Temp (F)	Viscosity (cp)
275	**250**
329	**113**

Mixing Temperature Range, F	292 - 308
Compaction Temperature Range, F	262 - 275

Specific Gravity@ 60F	**1.0291**

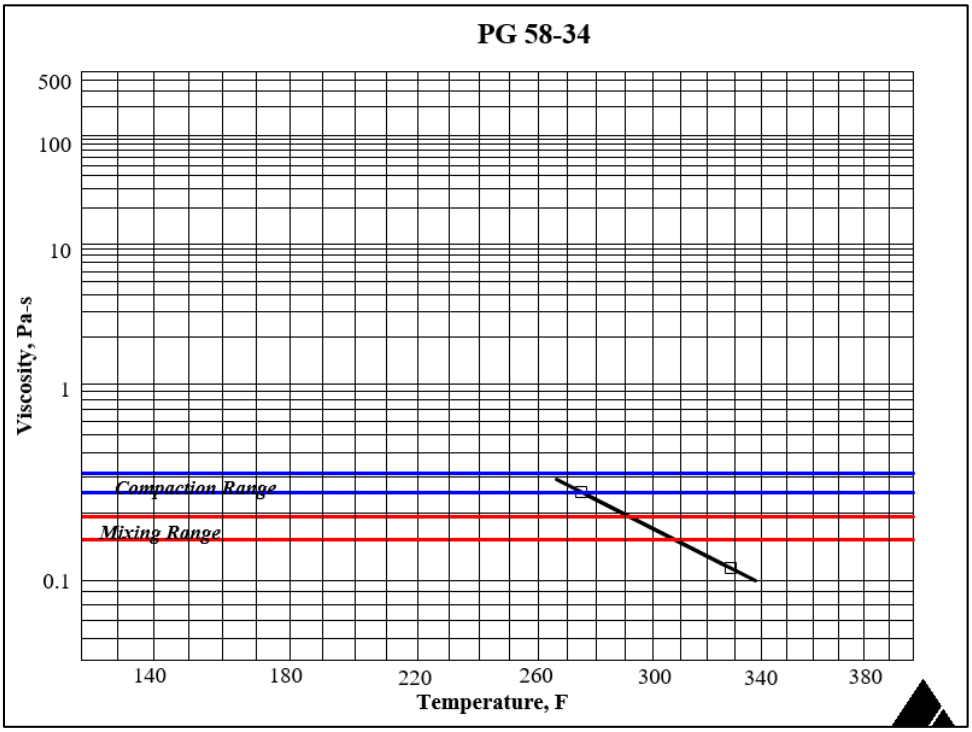

Figure B 1. Temperature curve of PG 58-34 binder

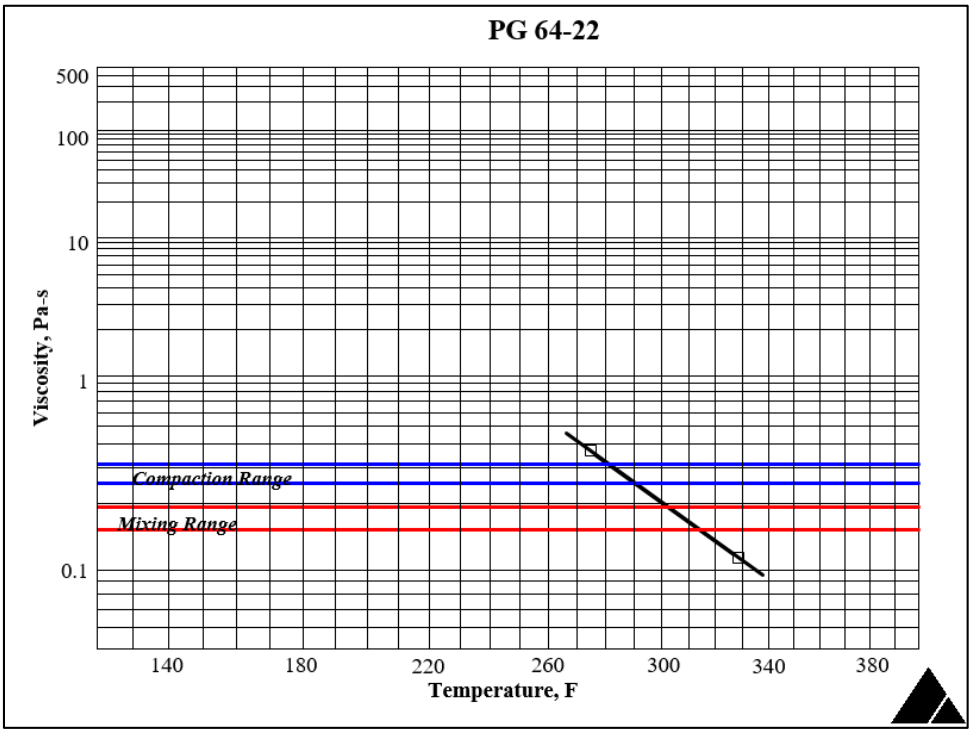

Figure B 2. Temperature curve of PG 64-22 binder

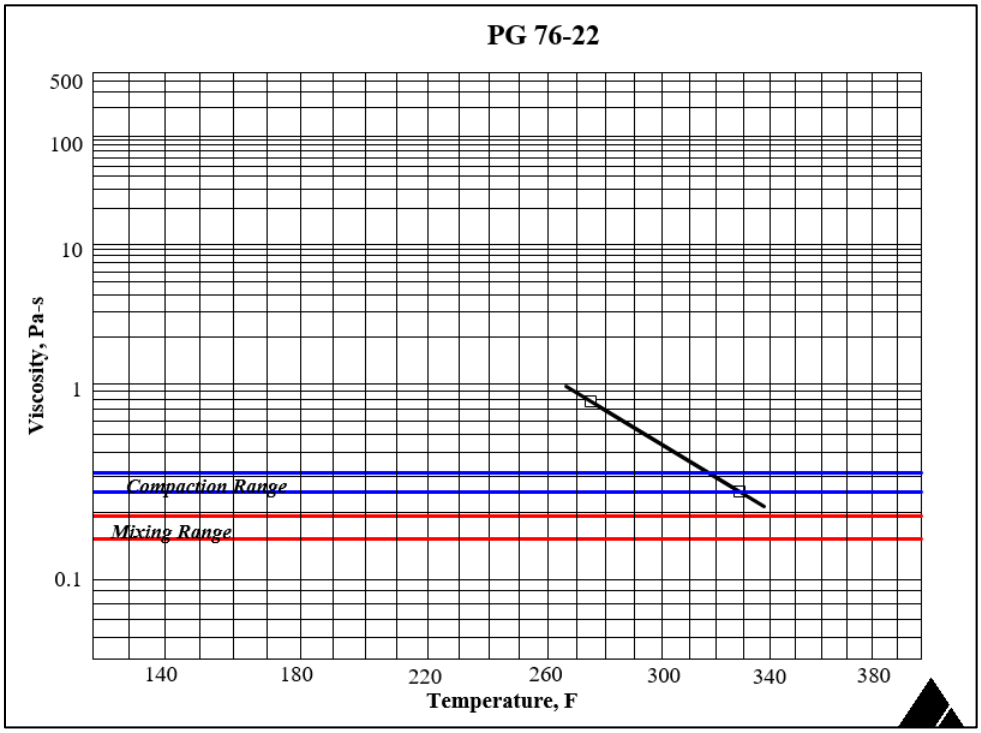

Figure B 3. Temperature curve of PG 76-22 binder

The following figures show the binder properties provided by McCall Oil.

PG 58-34

Certificate of Analysis

		Specification
Original Properties		
Specific Gravity @ 15.6 C (58 F)	1.0219	
Flashpoint, C	330	230+
Dynamic Shear, G*/sin δ, 58 C, kPa	1.38	1.0+
Fail Temp	60.7	
Rotational Viscosity, 135 C, Pas	0.288	3.00-
RTFO Residue Properties		
Loss on Heat, %	-0.514	1.00-
Dynamic Shear, G*/sin δ, 58 C, kPa	3.93	2.20+
Fail Temp	62.8	
PAV Residue Properties		
Dynamic Shear, G*sin δ, 16 C, kPa	3480	5000-
Fail Temp	8.0	
Creep Stiffness, -24 C, Mpa	250	300-
m-value, -24 C	0.303	0.300+
Fail Temp Creep Stiffness	-31.85	
Fail Temp M Value	-24.35	

True Grade PG 60.7-34.35

I certify that the asphaltic material identified above complies with current AASHTO M-320 (formerly MP-1) specifications, ASTM D6373, Washington State Department of Transportation Specifications for Asphalt Materials.

Figure B 4. PG 58-34 binder properties

PG64-22

Certificate of Analysis

Original Properties	Result	Test Method AASHTO	SPEC.
Flashpoint, C	310	T48	230 +
Brookfield Viscosity, Pa sec	0.363	T316	3.000 -
Dynamic Shear @ 64 C, G*/sin delta, kPa	1.23	T315	1.0 +
Rolling Thin Film Oven Residue Properties			
R.T.F.O. Loss on Heat, %	0.040	T240	1.000 -
Dynamic Shear @ 64 C, G*/sin delta, kPa	2.54	T315	2.2 +
Pressure Aging Vessel Residue			
Dynamic Shear @ 25 C, G*sin delta, kPa	1890	T315	5000 -
Bending Beam @ -12 C			
Stiffness, Mpa	156	T313	300 -
m-value	0.330	T313	0.30 +

True Grade PG 64.5 – 26.03

I certify that the asphaltic material identified above complies with current AASHTO M-320 specifications, ASTM D6373, Washington State Department of Transportation, Oregon Department of Transportation, and Idaho Department of Transportation Standard Specifications for Asphalt Materials.

Figure B 5. PG 64-22 binder properties

PG76-22

Certificate of Analysis

		Specification
Original Properties		
Specific Gravity @ 15.6 C (60 F)	1.0408	
Flashpoint, C	250+	230+
Dynamic Shear, G*/sin δ, 76 C, kPa	1.27	1.0+
Rotation Viscosity, 135 C, Pas	0.788	3.00-
RTFO Residue Properties		
Loss on Heat, %	0.313	1.00-
Dynamic Shear, G*/sin δ, 76 C, kPa	4.64	2.20+
PAV Residue Properties		
Dynamic Shear, G*sin δ, 31 C, kPa	2020	5000-
Creep Stiffness, -12 C, Mpa	170	300-
m-value, -12 C	0.315	0.300+

I certify that the asphaltic material identified above complies with current AASHTO M-320 (formerly MP-1) specifications, ASTM D6373, Washington State Department of Transportation and Oregon Department of Transportation, Standard Specifications for Asphalt Materials.

Figure B 6. PG 76-22 binder properties

APPENDIX C: THEORETICAL MAXIMUM SPECIFIC GRAVITIES

Table C 1. Theoretical maximum specific of the mixtures with 30% RAP content, binder contents of 6%, 6.4%, and 6.8%, and binder grades of PG 58-34, PG 64-22, and PG 76-22

Sample	A	B	C	D	E	F	G
	Bag Weight (g)	Sample Weight in Air (g)	Weight of Bags+ Sample in Water	Volume in Water (A+B-C)	Volume of Bag (A/Vc)	Sample Volume (D-E)	Gmm (g/cm3)
PG 58-34, BC6, RAP30%	78.4	1929.4	1129.4	878.4	103.17	775.23	2.49
PG 58-34, BC6, RAP30%	78.0	1984.6	1133.4	929.2	102.89	826.31	2.40
PG 58-34, BC6, RAP30%	77.6	1952.0	1141.8	887.8	102.28	785.52	2.48
PG 58-34, BC6.4, RAP30%	78.6	1953.4	1145.6	886.4	103.50	782.90	2.50
PG 58-34, BC6.4, RAP30%	78.8	1974.4	1153.6	899.6	103.83	795.77	2.48
PG 58-34, BC6.4, RAP30%	78.8	1982.8	1158.0	903.6	103.86	799.74	2.48
PG 58-34, BC6.8,RAP30%	78.2	1922.6	1122.2	878.6	102.90	775.70	2.48
PG 58-34, BC6.8, RAP30%	78.0	1963.4	1143.6	897.8	102.81	794.99	2.47
PG 58-34, BC6.8, RAP30%	77.6	1957.6	1138.8	896.4	102.30	794.10	2.47
PG 64-22, BC6, RAP30%	77.6	1966.4	1157.2	886.8	102.33	784.47	2.51
PG 64-22, BC6, RAP30%	78.0	1957.2	1151.0	884.2	102.79	781.41	2.50
PG 64-22, BC6, RAP30%	77.6	1981.6	1164.2	895.0	102.39	792.61	2.50
PG 64-22, BC6.4, RAP30%	78.0	1964.2	1151.2	891.0	102.81	788.19	2.49
PG 64-22, BC6.4, RAP30%	77.6	1960.4	1148.8	889.2	102.31	786.89	2.49
PG 64-22, BC6.4, RAP30%	77.8	1977.4	1157.2	898.0	102.62	795.38	2.49
PG 64-22, BC6.8, RAP30%	77.8	1917.0	1121.4	873.4	102.39	771.01	2.49
PG 64-22, BC6.8, RAP30%	77.8	1939.0	1134.6	882.2	102.47	779.73	2.49
PG 64-22, BC6.8, RAP30%	78.2	1948.4	1137.6	889.0	103.00	786.00	2.48
PG 76-22, BC6, RAP30%	79.4	1942.6	1142.2	879.8	104.44	775.36	2.51
PG 76-22, BC6, RAP30%	78.0	1936.0	1140.2	873.8	102.70	771.10	2.51
PG 76-22, BC6, RAP30%	78.0	1960.0	1152.2	885.8	102.80	783.00	2.50
PG 76-22, BC6.4,RAP30%	78.4	1960.0	1146.4	892.0	103.29	788.71	2.49
PG 76-22, BC6.4, RAP30%	78.0	1964.8	1147.8	895.0	102.82	792.18	2.48
PG 76-22, BC6.4, RAP30%	78.2	1946.2	1140.0	884.4	102.99	781.41	2.49
PG 76-22, BC6.8,RAP30%	78.0	1941.0	1133.0	886.0	102.72	783.28	2.48
PG 76-22, BC6.8, RAP30%	77.6	1960.8	1142.2	896.2	102.31	793.89	2.47
PG 76-22, BC6.8, RAP30%	77.2	1970.6	1147.6	900.2	101.86	798.34	2.47

Note: BC6= 6% binder content, BC6.4 =6.4 % binder content, and BC6.8 = 6.8% binder content.

Table C 2. Theoretical maximum specific of the mixtures with 40% RAP content, binder contents of 6%, 6.4%, and 6.8%, and binder grades of PG 58-34, PG 64-22, and PG 76-22

Sample	A	B	C	D	E	F	G
	Bag Weight (g)	Sample Weight in Air (g)	Weight of Bags+ Sample in Water	Volume in Water (A+B-C)	Volume of Bag (A/Vc)	Sample Volume (D-E)	Gmm (g/cm3)
PG 58-34, BC6, RAP40%	78.6	1959.8	1158.6	879.8	103.53	776.27	2.52
PG 58-34, BC6, RAP40%	78.6	1959.0	1158.0	879.6	103.53	776.07	2.52
PG 58-34, BC6, RAP40%	78.6	2018.8	1192.2	905.2	103.76	801.44	2.52
PG 58-34, BC6.4, RAP40%	79.0	1941.0	1145.2	874.8	103.94	770.86	2.52
PG 58-34, BC6.4, RAP40%	78.8	1999.2	1177.6	900.4	103.93	796.47	2.51
PG 58-34, BC6.4, RAP40%	78.2	1988.6	1171.8	895.0	103.15	791.85	2.51
PG 58-34, BC6.8, RAP40%	78.2	1933.8	1134.4	877.6	102.94	774.66	2.50
PG 58-34, BC6.8, RAP40%	78.0	1933.4	1134.6	876.8	102.69	774.11	2.50
PG 58-34, BC6.8, RAP40%	77.6	2026.2	1182.8	921.0	102.57	818.43	2.48
PG 64-22, BC6, RAP40%	80.2	1957.9	1151.0	887.1	105.47	781.63	2.50
PG 64-22, BC6, RAP40%	80.3	1956.5	1150.0	886.8	105.59	781.21	2.50
PG 64-22, BC6, RAP40%	80.5	1952.8	1148.6	884.7	105.82	778.88	2.51
PG 64-22, BC6.4, RAP40%	78.2	1967.6	1155.2	890.6	103.07	787.53	2.50
PG 64-22, BC6.4, RAP40%	77.4	1954.4	1149.2	882.6	102.04	780.56	2.50
PG 64-22, BC6.4, RAP40%	80.2	1963.4	1155.6	888.0	105.50	782.50	2.51
PG 64-22, BC6.8, RAP40%	79.8	1947.4	1140.2	887.0	104.94	782.06	2.49
PG 64-22, BC6.8, RAP40%	80.0	1960.4	1150.2	890.2	105.24	784.96	2.50
PG 64-22, BC6.8, RAP40%	77.2	1935.2	1134.2	878.2	101.73	776.47	2.49
PG 76-22, BC6, RAP40%	79.4	1979.4	1163.8	895.0	104.58	790.42	2.50
PG 76-22, BC6, RAP40%	79.2	1969.2	1157.8	890.6	104.30	786.30	2.50
PG 76-22, BC6, RAP40%	79.4	1942.4	1146.0	875.8	104.44	771.36	2.52
PG 76-22, BC6.4, RAP40%	77.6	1962.2	1151.6	888.2	102.32	785.88	2.50
PG 76-22, BC6.4, RAP40%	77.0	1959.4	1150.2	886.2	101.58	784.62	2.50
PG 76-22, BC6.4, RAP40%	76.8	1942.6	1141.4	878.0	101.27	776.73	2.50
PG 76-22, BC6.8, RAP40%	78.2	1942.8	1137.6	883.4	102.97	780.43	2.49
PG 76-22, BC6.8, RAP40%	77.8	1950.8	1138.4	890.2	102.52	787.68	2.48
PG 76-22, BC6.8, RAP40%	77.0	1963.0	1144.8	895.2	101.59	793.61	2.47

Note: BC6= 6% binder content, BC6.4 =6.4 % binder content, and BC6.8 = 6.8% binder content.

APPENDIX D: ONE EXAMPLE OF BATCHING

The following example shows the procedure of calculating the quantity of materials for the mixture with 30% RAP, 6% binder content, and binder grade of PG 58-34.

Table D 1. Quantity of coarse, medium, and fine aggregates and RAP materials for the mixture with 30% RAP, 6% binder content, and binder grade of PG 58-34

stockpile	coarse	medium	fine	RAP	Comparison: Combined vs. Target					
stockpile percentage, Psi	32	18	20	30						
total percentage	100				combined aggregate					
sieve size	percentage passing				%retained	cum. Retained	%passing	target %pass	Diff	Diff^2
3/4"	100.0	100.0	100.0	100.0	0.0	0.0	100.0	100	0.0	0.0
1/2"	95.8	100.0	100.0	98.3	1.9	1.9	98.1	98	-0.1	0.0
3/8"	53.1	98.2	100.0	88.3	16.8	18.7	81.3	83	1.7	2.9
1/4"	21.9	64.9	100.0	71.3	21.0	39.7	60.3	59	-1.3	1.7
#4	13.2	38.0	99.9	61.9	10.5	50.2	49.8	49	-0.8	0.7
#8	2.3	3.3	83.3	44.1	18.5	68.6	31.4	31	-0.4	0.1
#16	1.3	1.3	55.1	31.1	10.3	78.9	21.1	22	0.9	0.8
#30	1.2	1.2	35.8	23.3	6.3	85.2	14.8	16	1.2	1.5
#50	1.1	1.1	23.7	17.1	4.3	89.5	10.5	11	0.5	0.3
#100	1.1	1.1	15.6	12.9	2.9	92.5	7.5	8	0.5	0.2
#200	0.9	1.0	10.7	8.4	2.4	94.8	5.2	6.3	1.1	1.3
pan	0	0	0	0	5.2	100.0	0.0	0	0.0	0.0
binder conent	---	----	----	6.22	root mean square error					9.4

stockpile	coarse	medium	fine	RAP	coarse	medium	fine	RAP (agg)			
stockpile percentage, Psi	32	18	20	30	32	18	20	30			
total percentage	100								Virgin	RAP	RAP + binder
sieve size	percentage retained				batch mass, grams				Agg (g)	(total,g)	%remained
3/4"	0.0	0.0	0.0	0.0	0.0	0.0	0.0	0.0	0.0	0.0	0.0
1/2"	4.2	0.0	0.0	1.7	91.9	0.0	0.0	34.9	91.9	26.5	1.2
3/8"	42.7	1.8	0.0	10.0	923.5	22.8	0.0	205.1	946.2	429.5	19.6
1/4"	31.2	33.3	0.0	17.0	674.9	414.0	0.0	348.7	1088.9	596.6	27.3
#4	8.7	26.9	0.1	9.4	187.4	335.0	0.9	192.8	523.3	251.8	11.5
#8	10.9	34.7	16.6	17.8	236.5	432.1	228.7	365.2	897.3	366.8	16.8
#16	1.0	1.9	28.3	13.0	21.2	24.2	389.5	266.7	434.9	205.5	9.4
#30	0.1	0.1	19.3	7.8	2.9	1.8	266.3	160.0	271.0	125.3	5.7
#50	0.1	0.1	12.1	6.2	1.3	0.6	166.3	127.2	168.2	89.5	4.1
#100	0.1	0.0	8.1	4.2	1.3	0.5	112.1	86.2	114.0	43.0	2.0
#200	0.1	0.1	4.9	4.5	2.4	1.0	67.1	92.3	70.6	25.3	1.2
pan	0.9	1.0	10.7	8.4	20.5	12.6	147.4	172.3	180.5	27.6	1.3
					total weight						
					2163.63	1244.66	1378.40	2051.43	4786.7	2187.49	

Table D 2. Quantity of binder, RAP materials, and total aggregates for the the mixture with 30% RAP, 6% binder content, and binder grade of PG 58-34

target binder content %	6
aggregate mass, g	6838.107495
mixture mass, g	7274.582441

RAP binder (gr)	136.06
RAS binder (gr)	0
virgin binder (gr)	300.4127948

Gmm	2.487
Gmb	2.31291
airvoid content (%)	7
gyratory height	0.17
mass of sample in GC (g)	6928.173754

APPENDIX E: SEMI-CIRCULAR BEND TEST RESULTS

The following tables and figures show output data from UTM device of SCB test of the mixture with 30% RAP content, 6% binder content, and PG 58-34 binder grade.

Specimen Information

Identification: 6.0%AC_30%RAP_PG58
Conditioning time: 30 MIN
Properties/Comments:

Dimensions	Point 1	Point 2	Point 3	Point 4	Point 5	Point 6	Average	Std Dev.
Diameter (mm)	148.75					62.10	148.75	
Thickness (mm)				15.03	15.03			62.100
Notch Depth (mm)		82.50	82.50					

Cross-sectional area (mm²): 1.0

Test Parameters

Target temperature (°C): 25

Pre-Load Conditions	Test Conditions	Termination Conditions
Initial tensile seating load (kN): 0.04	Control Channel: Actuator LVDT	Post peak tensile load level (kN): 0.1
Initial actuator loading rate (mm/s): 0.05	Loading rate (mm/s): 0.5	Trigger point (kN): 0.5
		Actuator deformation limit (mm): xxx.xx

Test Data

Start Date and Time: Wednesday, February 8, 2017, at 10:44:25 AM

	Current	Peak
Time (sec):	490.17	216.97
Load (kN):	0.100	1.348
Actuator displacement (mm):	4.125	1.826
Core temperature (°C):	24.6	24.7
Surface temperature (°C):	24.9	25.0

Fracture Energy (J/m²): 0.000
Post Peak Slope:
Critical Displacement (mm):
Flexibility Index:

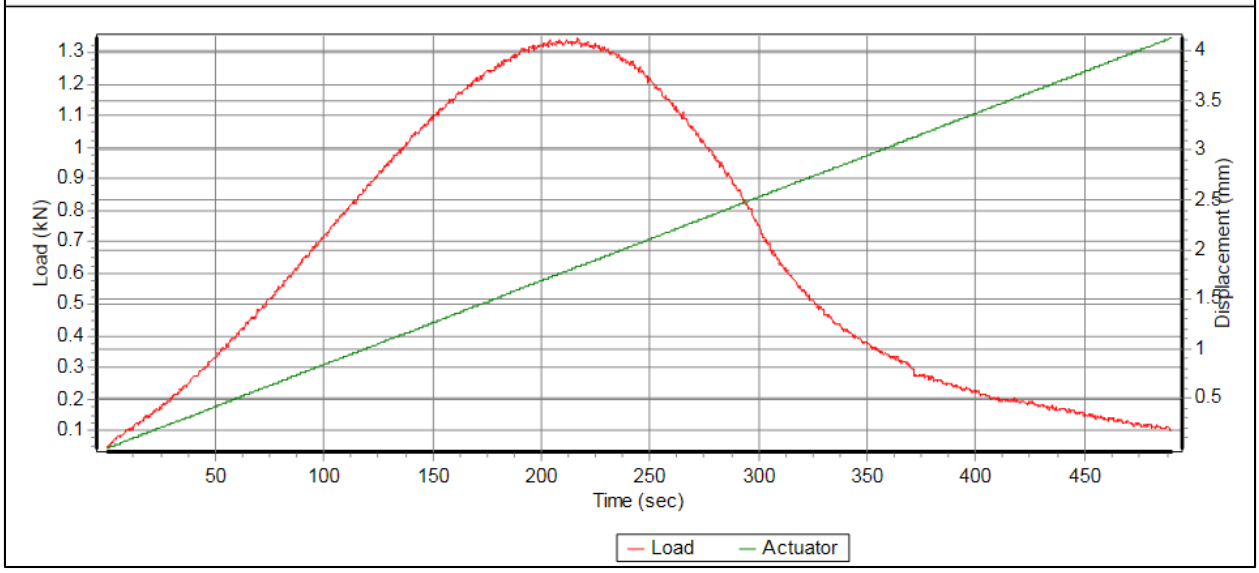

Figure E 1. An example of output SCB test of the sample with 30% RAP content, 6% binder content, and PG 58-34 binder grade

The following tables represent the parameters calculated from the conducted SCB tests on the samples with different combinations of RAP contents, binder contents, and binder grades.

Table E 1. SCB output parameters of the mixtures with RAP contents of 30% and 40%, binder contents of 6%, 6.4%, and 6.8%, and binder grade of PG 58-34

Sample ID	P_{peak}(KN)	G_f(KJ/m)	S(N/mm)	K_{IC} (MPa×m^0.5)	FI
SCB-B1-R30-BC6-N1-R1	1.334739	0.932583	0.747716	0.165827	6.065515
SCB-B1-R30-BC6-N1-R2	1.01861	0.660832	0.665133	0.127035	7.353682
SCB-B1-R30-BC6-N1-R3	1.300811	1.003422	0.752647	0.1626	9.604394
SCB-B1-R30-BC6-N1-R4	0.944208	0.801379	0.540906	0.11969	13.06569
SCB-B1-R30-BC6.4-N1-R1	0.992688	0.882511	0.52462	0.134064	10.85301
SCB-B1-R30-BC6.4-N1-R2	0.884587	0.773015	0.523993	0.11911	13.38828
SCB-B1-R30-BC6.4-N1-R3	0.732918	0.688381	0.451726	0.106011	12.20928
SCB-B1-R30-BC6.4-N1-R4	0.944208	0.801379	0.540906	0.11969	13.06569
SCB-B1-R30-BC6.8-N1-R1	0.554409	0.664644	0.255929	0.075043	21.59776
SCB-B1-R30-BC6.8-N1-R2	0.659996	0.871872	0.282231	0.087932	30.38775
SCB-B1-R30-BC6.8-N1-R3	0.517494	0.510292	0.284172	0.067537	14.95304
SCB-B1-R30-BC6.8-N1-R4	0.680646	0.778366	0.303828	0.089655	15.94785
SCB-B1-R40-BC6-N1-R1	1.713902	0.995252	1.018796	0.233018	3.342299
SCB-B1-R40-BC6-N1-R2	1.7313	1.010353	1.004071	0.224833	3.434897
SCB-B1-R40-BC6-N1-R3	1.578773	1.115036	0.894637	0.213934	6.81095
SCB-B1-R40-BC6-N1-R4	1.43726	0.974227	0.869208	0.186826	6.005766
SCB-B1-R40-BC6.4-N1-R1	1.650921	1.241505	0.8708	0.218231	7.209115
SCB-B1-R40-BC6.4-N1-R2	1.659602	1.26043	0.949409	0.219498	7.879071
SCB-B1-R40-BC6.4-N1-R3	1.316	0.847397	0.88124	0.176959	5.603601
SCB-B1-R40-BC6.4-N1-R4	1.25529	0.853148	0.820595	0.163873	7.067049
SCB-B1-R40-BC6.8-N1-R1	1.377683	1.292614	0.666054	0.18734	14.22936
SCB-B1-R40-BC6.8-N1-R2	1.415205	1.348643	0.722117	0.183784	13.43798
SCB-B1-R40-BC6.8-N1-R3	0.895037	0.769656	0.545391	0.121284	11.37469
SCB-B1-R40-BC6.8-N1-R4	0.925418	0.850085	0.511584	0.120242	11.65955

Note: B1= PG 58-34, B2= PG 64-22, and B3 = PG 76-22.
R30 = 30% RAP, and R40 = 40% RAP.
BC6= 6% binder content, BC6.4 =6.4 % binder content, and BC6.8 = 6.8% binder content.
R1= replicate 1, R2 = replicate 2, R3 = replicate 3, and R4 = replicate 4.

Table E 2. SCB output parameters of the mixtures with RAP contents of 30% and 40%, binder contents of 6%, 6.4%, and 6.8%, and binder grade of PG 64-22

Sample ID	P_{peak}(KN)	G_f(KJ/m)	S(N/mm)	K_{IC} (MPa×m^0.5)	FI
SCB-B2-R30-BC6-N1-R1	1.690027	1.00423	1.092149	0.225821	4.881555
SCB-B2-R30-BC6-N1-R2	2.099718	1.338342	1.286017	0.276906	6.066062
SCB-B2-R30-BC6-N1-R3	2.115344	1.218491	1.317466	0.293268	4.075961
SCB-B2-R30-BC6-N1-R4	1.795603	1.241341	1.054114	0.245573	6.77194
SCB-B2-R30-BC6.4-N1-R1	1.536024	1.178503	0.912176	0.204693	8.741626
SCB-B2-R30-BC6.4-N1-R2	1.589597	1.279484	0.907322	0.21745	9.545497
SCB-B2-R30-BC6.4-N1-R3	2.468214	2.082823	1.310117	0.319166	6.581691
SCB-B2-R30-BC6.4-N1-R4	1.390283	0.986151	0.970261	0.184109	8.190074
SCB-B2-R30-BC6.8-N1-R1	1.789496	1.818763	0.696907	0.243718	11.85493
SCB-B2-R30-BC6.8-N1-R2	1.295952	1.094757	0.688757	0.171199	9.614523
SCB-B2-R30-BC6.8-N1-R3	1.316622	1.637103	0.637763	0.18263	32.56863
SCB-B2-R30-BC6.8-N1-R4	1.399538	1.254098	0.703601	0.192902	11.04857
SCB-B2-R40-BC6-N1-R1	2.063133	1.13688	1.344699	0.286016	4.445504
SCB-B2-R40-BC6-N1-R2	2.543138	1.590926	1.382835	0.345878	3.345155
SCB-B2-R40-BC6-N1-R3	2.070894	1.2	1.038394	0.266025	3.881941
SCB-B2-R40-BC6-N1-R4	3.122043	1.647958	1.692796	0.408557	2.482492
SCB-B2-R40-BC6.4-N1-R1	2.307711	1.708995	1.101531	0.317075	6.128718
SCB-B2-R40-BC6.4-N1-R2	1.910275	1.28316	1.162412	0.257219	6.967571
SCB-B2-R40-BC6.4-N1-R3	2.032226	1.458394	1.235774	0.268286	8.575698
SCB-B2-R40-BC6.4-N1-R4	1.740358	1.3493	1.018307	0.238658	10.06147
SCB-B2-R40-BC6.8-N1-R1	1.838985	1.602558	0.872794	0.240791	11.94607
SCB-B2-R40-BC6.8-N1-R2	1.658912	1.246585	0.968992	0.220448	9.835788
SCB-B2-R40-BC6.8-N1-R3	1.602207	1.428913	0.703132	0.220104	13.78655
SCB-B2-R40-BC6.8-N1-R4	1.726532	1.380802	0.956447	0.237689	9.497141

Note: B1= PG 58-34, B2= PG 64-22, and B3 = PG 76-22.
R30 = 30% RAP, and R40 = 40% RAP.
BC6= 6% binder content, BC6.4 =6.4 % binder content, and BC6.8 = 6.8% binder content.
R1= replicate 1, R2 = replicate 2, R3 = replicate 3, and R4 = replicate 4.

Table E 3. SCB output parameters of the mixtures with RAP contents of 30% and 40%, binder contents of 6%, 6.4%, and 6.8%, and binder grade of PG 76-22

Sample ID	P_{peak}(KN)	G_f(KJ/m)	S(N/mm)	K_{IC} (MPa×m^0.5)	FI
SCB-B3-R30-BC6-N1-R1	2.324836	1.029629	1.704005	0.304545	2.927766
SCB-B3-R30-BC6-N1-R2	2.781805	1.200177	1.858606	0.368451	2.027122
SCB-B3-R30-BC6-N1-R3	1.972	0.857019	1.545747	0.288286	1.98266
SCB-B3-R30-BC6-N1-R4	2.635283	1.308486	1.870414	0.375222	3.28077
SCB-B3-R30-BC6.4-N1-R1	2.423966	1.053417	1.531824	0.282257	3.039504
SCB-B3-R30-BC6.4-N1-R2	2.655942	1.065503	1.848318	0.31404	2.767431
SCB-B3-R30-BC6.4-N1-R3	2.472496	1.443253	1.430282	0.349264	3.10105
SCB-B3-R30-BC6.4-N1-R4	2.924412	1.023371	1.557565	0.289192	2.591482
SCB-B3-R30-BC6.8-N1-R1	1.585272	1.05925	1.054538	0.207382	7.884061
SCB-B3-R30-BC6.8-N1-R2	1.816852	1.252314	1.098874	0.239521	8.224557
SCB-B3-R30-BC6.8-N1-R3	1.537192	1.237848	0.880737	0.215386	9.834032
SCB-B3-R30-BC6.8-N1-R4	1.748545	1.293349	0.943271	0.239379	8.01912
SCB-B3-R40-BC6-N1-R1	2.236957	0.915777	1.651589	0.316687	1.961986
SCB-B3-R40-BC6-N1-R2	3.163744	1.159176	2.382182	0.444139	1.3602
SCB-B3-R40-BC6-N1-R3	2.964227	1.187105	2.178698	0.389669	1.923276
SCB-B3-R40-BC6-N1-R4	2.852603	0.971445	2.171937	0.370327	1.186711
SCB-B3-R40-BC6.4-N1-R1	2.15281	0.929704	1.685622	0.29732	2.164295
SCB-B3-R40-BC6.4-N1-R2	2.833779	1.411908	1.896534	0.396284	3.603897
SCB-B3-R40-BC6.4-N1-R3	2.455876	1.304901	1.747539	0.339116	4.241639
SCB-B3-R40-BC6.4-N1-R4	2.519657	1.243322	1.74455	0.343277	3.07051
SCB-B3-R40-BC6.8-N1-R1	1.705179	1.024928	1.154806	0.231898	4.166839
SCB-B3-R40-BC6.8-N1-R2	2.621298	1.398095	1.603476	0.346566	3.510713
SCB-B3-R40-BC6.8-N1-R3	2.063202	1.255936	1.197876	0.285003	4.52651
SCB-B3-R40-BC6.8-N1-R4	2.518905	1.80119	1.420546	0.35347	8.18842

Note: B1= PG 58-34, B2= PG 64-22, and B3 = PG 76-22.
R30 = 30% RAP, and R40 = 40% RAP.
BC6= 6% binder content, BC6.4 =6.4 % binder content, and BC6.8 = 6.8% binder content.
R1= replicate 1, R2 = replicate 2, R3 = replicate 3, and R4 = replicate 4.

APPENDIX F: EXAMPLE OF DATA GENERATED BY UTM DEVICE FOR DYNAMIC MODULUS TEST AND DEVELOPING THE MASTER CURVES

The following tables show output data from UTM device of dynamic modulus test for the mixture with 30% RAP content, 6% binder content, and PG 58-34 binder grade.

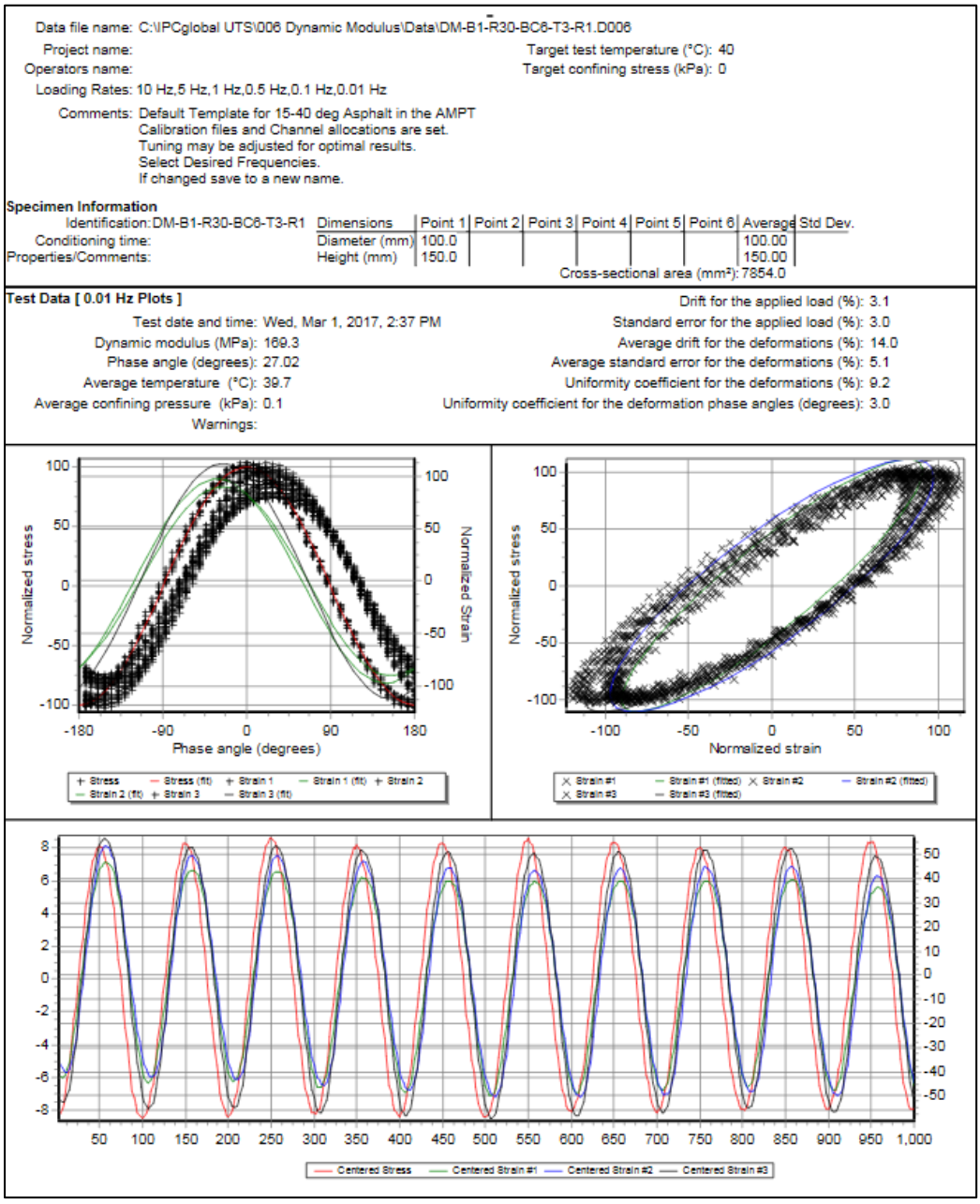

Figure F 1. An example of output dynamic modulus test of mixture with 30% RAP content, 6% binder content, and PG 58-34 binder grade

An example of the data used to make the dynamic modulus and phase angle master curves is shown in the tables below.

Table F 1. VMA and VFA of the mixture with 30% RAP content, 6% binder content, and PG 58-34 binder grade

VMA	Volume, %	15.4
VFA	Volume, %	74.0
Reference Temp		20

Table F 2. Dynamic modulus and phase angles of mixture with 30% RAP content, 6% binder content, and PG 58-34 binder grade at different temperatures and frequencies

Conditions		Specimen 1		Specimen 2		Average	Modulus	Average	Std Dev
Temperature	Frequency	Modulus	Phase Angle	Modulus	Phase Angle	Modulus	CV	Phase	Phase
C	Hz	Ksi	Degree	Ksi	Degree	Ksi	%	Deg	Deg
4	0.1	1165.7	16.0	1222.4	15.7	1194.0	3.4	15.9	0.2
4	0.5	1482.6	13.4	1552.6	13.2	1517.6	3.3	13.3	0.1
4	1	1628.8	12.5	1706.5	12.3	1667.6	3.3	12.4	0.1
4	5	1977.6	10.4	2073.2	10.3	2025.4	3.3	10.3	0.1
4	10	2138.1	9.7	2231.8	9.5	2185.0	3.0	9.6	0.1
20	0.1	363.6	26.6	389.1	27.0	376.4	4.8	26.8	0.3
20	0.5	554.2	23.9	593.6	24.2	573.9	4.9	24.1	0.2
20	1	649.9	23.1	700.4	23.4	675.2	5.3	23.2	0.2
20	5	924.0	20.0	999.0	20.1	961.5	5.5	20.1	0.1
20	10	1055.4	18.8	1150.7	18.9	1103.1	6.1	18.8	0.1
40	0.01	24.6	27.0	33.7	26.2	29.1	22.2	26.6	0.6
40	0.1	53.0	30.6	66.6	29.7	59.8	16.1	30.2	0.6
40	0.5	99.6	31.3	116.5	33.1	108.0	11.0	32.2	1.3
40	1	130.6	31.7	148.2	34.0	139.4	9.0	32.8	1.6
40	5	241.3	30.8	256.3	32.5	248.8	4.2	31.6	1.2
40	10	304.6	31.0	316.8	31.4	310.7	2.8	31.2	0.3

Shift factors and the best-fit curves are presented in the following tables and figures. Dynamic modulus data collected at various temperatures (See Figure F 2) can be shifted with respect to the loading frequencies so that the different curves can be aligned to form a single smooth master curve (See Figure F 4). The shift factor is the mechanism that allows horizontal shifting of the data

on the master curve. Actual loading frequencies at different temperature are shifted with respect to the reference temperature (20 ºC in this thesis) using the shift factors to create the master curves. For example, in Figure F 2 loading frequencies at 4 ºC are shifted to the right and frequencies at 40 ºC are shifted to the left to make the master curve. Shift factors for different temperature are presented in Figure F 5. The same shift factors created for dynamic modulus were used to create the master curves for phase angles (See Figure F 6).

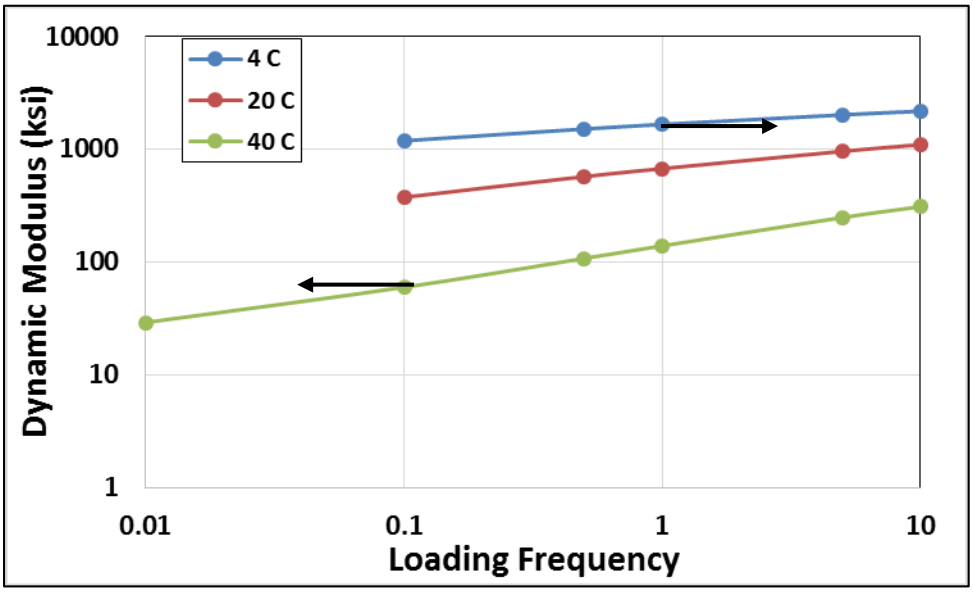

Figure F 2. Dynamic modulus of the mixture with 30% RAP content, 6% binder content, and PG 58-34 binder grade at different temperatures and frequencies

			Pc	E*, ksi	logE*													
Maximum Modulus			0.8769324	3340.413	3.52380015													
			Initial Values															
Log (Min)			0.485108	0.5	Copy Cells C4:C7 to													
Beta			-1.24166	-1	B4:B7 using				R2	0.998293	0.999919							
Gamma			-0.46711	-0.5	Copy/Paste Values				Se	0.016704								
EA			199240.4	200000														
Reference Temp			20															
			Average		Average	Log Average												
Temperature		Frequency	Modulus		Phase Ang	Modulus		Predicted	Error	Error^2		loga(t)	log (wr)	wr		wr	log E*	E*, ksi
C		Hz	Ksi		Degree													
	4	0.1	1194.0	15.9	3.07701264			3.066767	0.010246	0.000105		2.048502	1.048502	11.18154		1000000	3.471475	2961.25
	4	0.5	1517.6	13.3	3.18115788			3.179657	0.001501	2.25E-06		2.048502	1.747472	55.90769		500000	3.463731	2908.916
	4	1	1667.6	12.4	3.22210321			3.220291	0.001812	3.28E-06		2.048502	2.048502	111.8154		100000	3.441169	2761.652
	4	5	2025.4	10.3	3.30650629			3.298568	0.007938	6.3E-05		2.048502	2.747472	559.0769		50000	3.429082	2685.851
	4	10	2185.0	9.6	3.33945004			3.326192	0.013258	0.000176		2.048502	3.048502	1118.154		10000	3.394072	2477.834
	20	0.1	376.4	26.8	2.57561827			2.565106	0.010512	0.000111		0	-1	0.1		1000	3.321965	2098.77
	20	0.5	573.9	24.1	2.75884695			2.765514	-0.00667	4.45E-05		0	-0.30103	0.5		500	3.293798	1966.971
	20	1	675.2	23.2	2.82940059			2.842687	-0.01329	0.000177		0	0	1		100	3.214046	1636.989
	20	5	961.5	20.1	2.98296168			2.99969	-0.01673	0.00028		0	0.69897	5		50	3.172682	1488.272
	20	10	1103.1	18.8	3.04260867			3.0579	-0.01529	0.000234		0	1	10		10	3.0579	1142.615
	40	0.01	29.1	26.6	1.46424461			1.459204	0.00504	2.54E-05		-2.2663	-4.2663	5.42E-05		1	2.842687	696.1253
	40	0.1	59.8	30.2	1.77690486			1.790095	-0.01319	0.000174		-2.2663	-3.2663	0.000542		0.1	2.565106	367.3722
	40	0.5	108.0	32.2	2.03354973			2.036682	-0.00313	9.81E-06		-2.2663	-2.56733	0.002708		0.05	2.470533	295.4831
	40	1	139.4	32.8	2.14424948			2.143122	0.001128	1.27E-06		-2.2663	-2.2663	0.005416		0.01	2.236184	172.2599
	40	5	248.8	31.6	2.39587163			2.383377	0.012495	0.000156		-2.2663	-1.56733	0.027081		0.005	2.130892	135.1737
	40	10	310.7	31.2	2.49230037			2.481668	0.010632	0.000113		-2.2663	-1.2663	0.054162		0.001	1.883411	76.45589
																0.0001	1.543301	34.93822
				Sy	0.57173048					0.001674	Use Solver on this Cell					0.00001	1.24747	17.67949
																0.000001	1.012326	10.28788

Figure F 3. An example of procedure of creating master curve

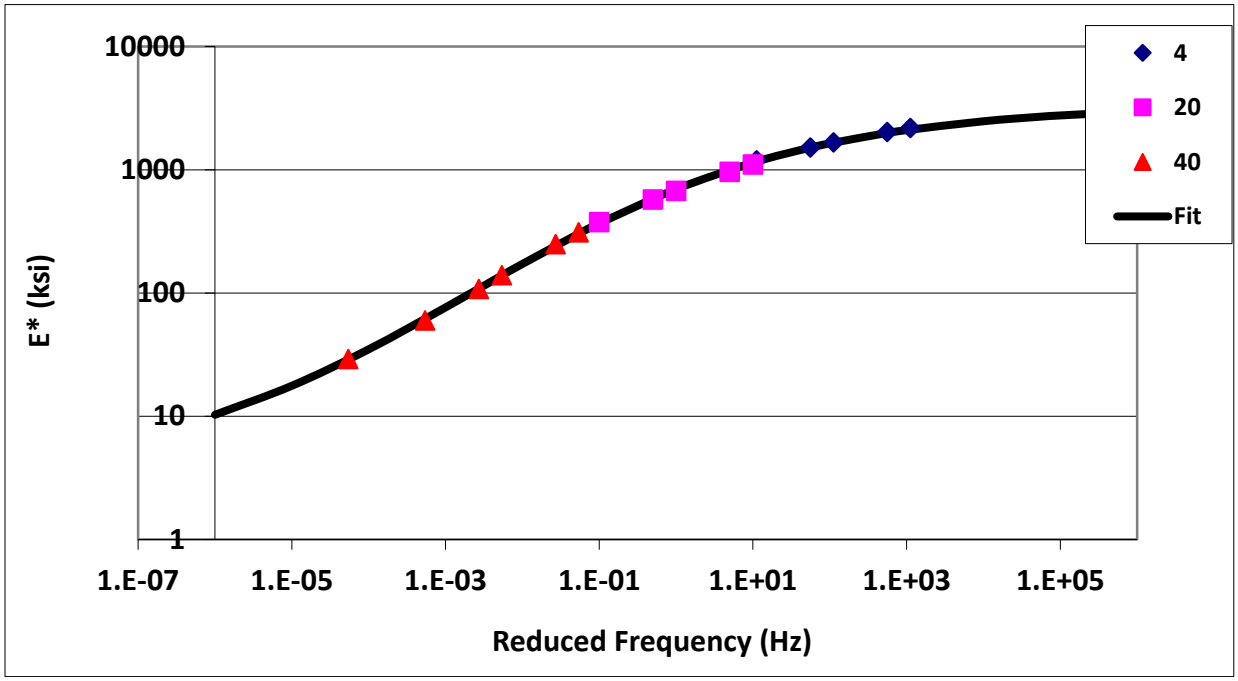

Figure F 4. An example of the master curve of dynamic modulus for the mixture with 30% RAP content, 6% binder content, and PG 58-34 binder grade

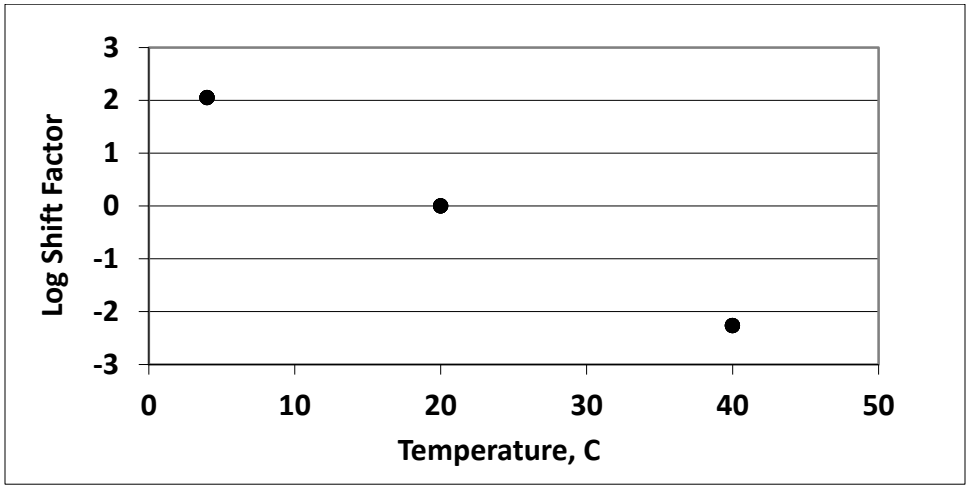

Figure F 5. Shift factor curve of the mixture with 30% RAP content, 6% binder content, and PG 58-34 binder grade

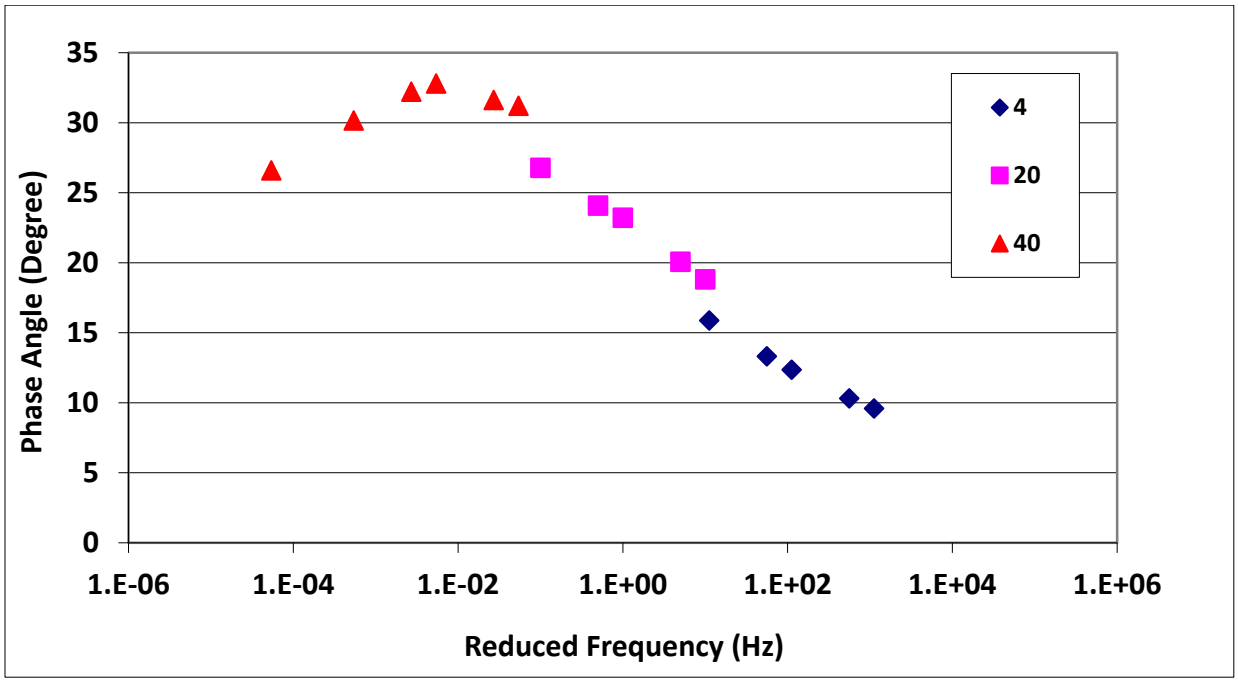

Figure F 6. An example of the master curve of phase angle for the mixture with 30% RAP content, 6% binder content, and PG 58-34 binder grade

APPENDIX G: FLOW NUMBER TEST RESULTS

An example of the data produced by UTM device Flow Number Test for the sample with 30% RAP content, 6% binder content, and PG 58-34 binder grade is presented as follows. This data was used to estimate the flow numbers using Francken Model and compare the rutting resistance of asphalt mixtures with different binder grades, RAP contents, and binder contents.

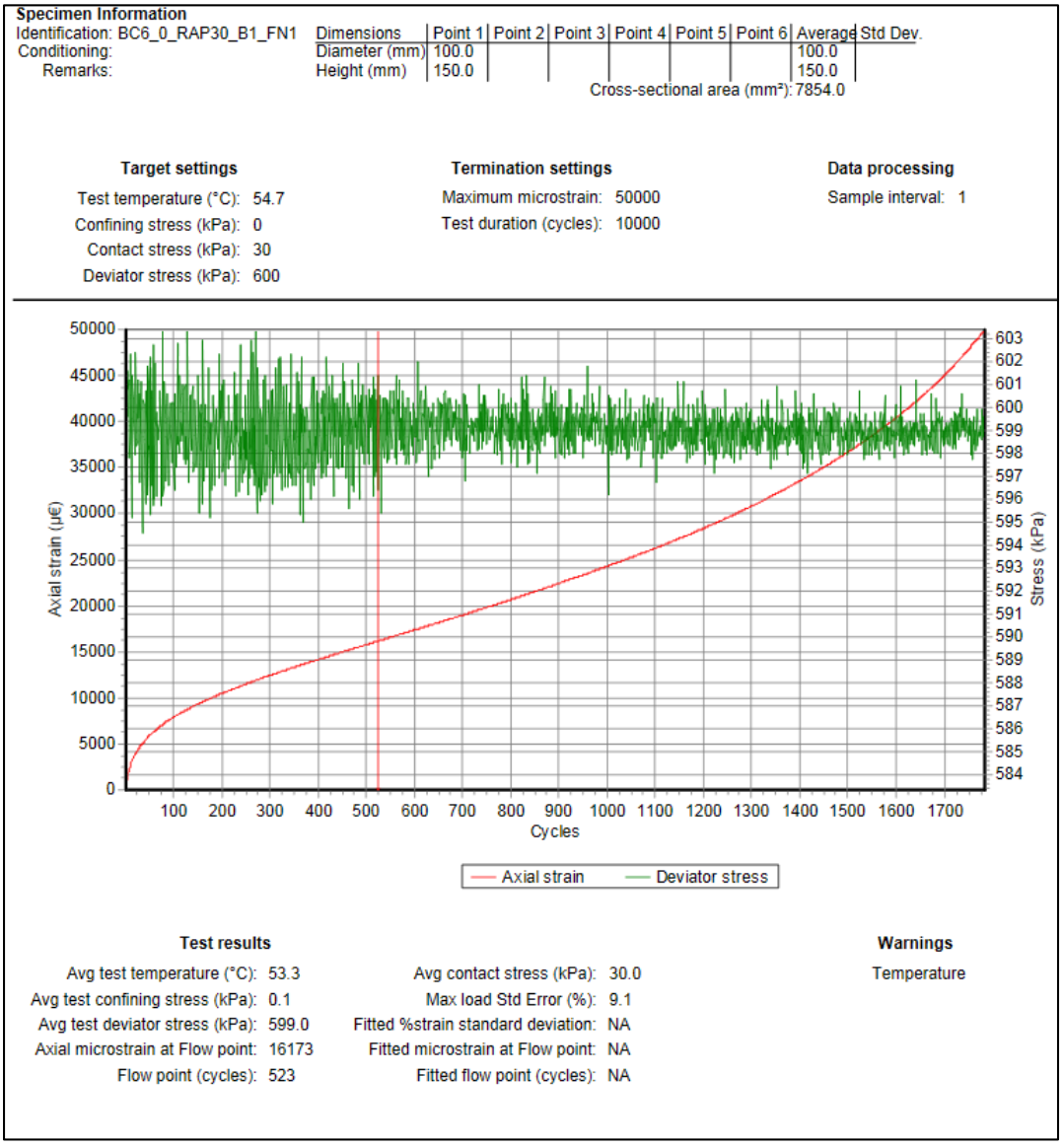

Figure G 1. An example of flow number test output data for the sample with 30% RAP content, 6% binder content, and PG 58-34 binder grade

APPENDIX H: PAVEMENT HISTORY AND STRUCTURES FOR EACH SECTION

Table H 1. Pavement history for all

Section ID	Thickness (inches)	Section ID	Thickness (inches)	Section ID	Thickness (inches)
CA-0501-DGAC-CS	0.3	CA-8149-DGAC	1.9	ID-A320_DGAC_SS	0.2
CA-0502-DGAC-CS	0.2	CA-8150-DGAC	3.3	ID-A330_DGAC_CS	0.2
CA-0503-DGAC-CS	0.2	CA-8153-DGAC-CS	0.3	ID-A350_DGAC_CS	0.2
CA-0504-DGAC	5	CA-8156-DGAC-CS	0.1	ID-C320_DGAC_SS	0.2
CA-0505-DGAC-CS	0.2	CA-8201-DGAC-CS	0.2	ID-C330_DGAC_CS	0.6
CA-0506-DGAC	2.2	CA-8202-DGAC-CS	0.3	ID-C350_DGAC_CS	0.4
CA-0507-DGAC	4.6	CA-8534-OGAC	0.7	OR-2002_DGAC	2.3
CA-0508-RAPHL	4.3	CA-8535-DGAC-CS	0.1	OR-5006_CPR	2
CA-0509-RAPHL	2.1	CA-A310-DGAC	1.3	OR-5008_CPR	2
CA-0559-DGAC-CS	0.3	CA-A311-DGAC	1.4	OR-7018_CP	1.6
CA-0561-DGAC	1.9	CA-A320-DGAC-SS	0.3	OR-7019_CP	2.1
CA-0562-DGAC	2	CA-A321-DGAC-SS	0.2	WA-1005_DGAC	2.1
CA-0563-DGAC	2.2	CA-A330-DGAC-CS	0.2	WA-1006_DGAC_CS	0.1
CA-0565-DGAC	2.7	CA-A340-DGAC-CS	0.2	WA-1007_DGAC	2.3
CA-0566-OGAC	0.6	CA-A350-DGAC-CS	0.3	WA-1008_DGAC	1.7
CA-0567-OGAC	0.8	CA-A351-DGAC-CS	0.2	WA-1501_DGAC	1.9
CA-0568-DGAC	4.4	CA-A352-DGAC-CS	0.4	WA-1801_DGAC	4.5
CA-0569-DGAC	1.7	CA-A353-DGAC-CS	0.3	WA-6020_DGAC	2.7
CA-0570-DGAC-CS	0.4	CA-A361-DGAC	2	WA-6048_RAPHL	2.8
CA-0571-RAPHL	1.8	CA-A362-DGAC	1	WA-6056_RAPCL	1.8
CA-1253-DGAC-CS	0.2	CA-A363-DGAC-CS	0.2	WA-7322_DGAC	1.8
CA-2002-DGAC	3.5	ID-1001_DGAC	1.2	WA-A320-DGAC-SS	0.2
CA-2004-OGAC	0.7	ID-1005_DGAC_CS	0.4	WA-A350-DGAC-SS	0.2
CA-2038-DGAC-CS	0.2	ID-1007_DGAC_CS	0.2	WA-B310-DGAC	1.3
CA-2041-DGAC	3.4	ID-1009_DGAC_CSMB	0.6	WA-B320-DGAC-SS	0.2
CA-2051-DGAC	0.1	ID-1010_DGAC_CS	0.2	WA-B330-DGAC	2
CA-2053-DGAC	4.1	ID-1020_DGAC_CS	0.2	WA-B350-DGAC-CS	0.5
CA-2647-DGAC-CS	0.1	ID-9032_DGAC_CS	0.4	WA-C310-DGAC	1.1
CA-6044-DGAC	4.8	ID-9034_DGAC	2	WA-C320-DGAC-SS	0.2
CA-7452-DGAC	1.4	ID-A310_DGAC	1	WA-C350-DGAC-CS	0.3
CA-7491-DGAC	4				

DGAC: dense graded asphalt concrete.
DGAC_CS: chip-seal on dense graded asphalt concrete overlaid.
DGAC_SS: slurry-seal on dense graded asphalt concrete overlaid.
DGAC_CSMB: chip-seal with modified binder on dense graded asphalt concrete overlaid.
CP: composite pavement.
CPR: composite pavement having RAP.
RAPCL: cold-laid recycled asphalt pavement.
RAPHL: hot-laid recycled asphalt pavement.